Environmental and genetic regulation of mouth-form plasticity in *Pristionchus pacificus*

Dissertation
der Mathematisch-Naturwissenschaftlichen Fakultät
der Eberhard Karls Universität Tübingen
zur Erlangung des Grades eines
Doktors der Naturwissenschaften
(Dr. rer. nat.)

vorgelegt von
Bogdan Sieriebriennikov
aus Bila Tserkva, Ukraine

Tübingen
2020

Gedruckt mit Genehmigung der Mathematisch-Naturwissenschaftlichen Fakultät der Eberhard Karls Universität Tübingen.

Tag der mündlichen Qualifikation:	14.05.2020
Dekan:	Prof. Dr. Wolfgang Rosenstiel
1. Berichterstatter	Prof. Dr. Ralf J. Sommer
2. Berichterstatter	Prof. Dr. Alfred Nordheim
3. Berichterstatter	Prof. Dr. Hinrich Schulenburg

Table of contents

I. Acknowledgments

I would like to thank Dr. Vahan Serobyan and Dr. Manuela Kieninger for teaching me how to do science and providing moral support in the first years of my PhD. I am also grateful to all the current and past members of the lab 17, namely Dr. Eduardo Moreno, Hanh Witte, Shuai Sun, Metta Riebesell, Sandra Mäck, Sara Wighard, Nermin Akduman, Mohannad Dardiry, Mohammad Atighi and Dr. Melanie Mayer, for creating a fun and productive working environment. Special thanks go to Dr. Michael Werner, Dr. Neel Prabh, Dr. Christian Rödelsperger, Dr. Adrian Streit, Dr. Cameron Weadick, Dr. Jan Falcke and Dr. Kohta Yoshida, who regularly provided constructive critique of my ideas. My work would not be possible without the assistance of Hanh Witte, Metta Riebesell and Heike Haussmann. Finally, I am grateful to Prof. Dr. Ralf Sommer for being an inspiring mentor and to German taxpayers for their financial contribution to the functioning of the Max Planck Society.

Cordial thanks go to my parents, Halyna Ishchuk and Andrii Sieriebriennikov, and my sister, Yuliia Horbatii, who tolerated my absence and absent-mindedness during these years and gave me their love and support.

II. Summary

Phenotypic plasticity is the ability of organisms with the same genetic complements to develop different phenotypes in response to environmental influences. This phenomenon is extremely widespread, but evolutionary consequences of phenotypic change in the absence of genetic change are currently unclear. Numerous ideas have been developed to explain the potential significance of phenotypic plasticity for evolution, but the formulation of explicit falsifiable hypotheses requires better mechanistic insight into plastic development. An ideal study system to investigate phenotypic plasticity must combine amenability to experimental genetic research and accessibility of lineages in which one of the alternative phenotypes has been fixed. Plasticity in feeding structures of diplogastrid nematodes satisfies both of these criteria. Isogenic lab populations of the species *Pristionchus pacificus* can develop two discrete alternative phenotypes depending on the rearing conditions. The eurystomatous (Eu) morph has a wide mouth with two hooked teeth and is a facultative predator. The stenostomatous (St) morph has a tube-like mouth with only one tooth and is a non-aggressive microbial grazer. Previous research uncovered the role of pheromones and identified the sulftase EUD-1, the sulfotransferase SULT-1 and the nuclear hormone receptor NHR-40 as regulators of mouth form decision in *P. pacificus*. In my thesis work, I aimed to reveal further environmental factors and genetic players controlling the phenotype. I discovered the effect of food composition and helped identify the effect of a range of solid and liquid media on the ratio between morphs in the population. On the genetic side, I found that *eud-1* is part of a chromosomal cluster of functionally related genes, reminiscent of supergenes. Further, I isolated another transcription factor regulating morph decision, NHR-1, and identified a set of common transcriptional targets between NHR-40 and NHR-1, which may be the genes directly involved in making the alternative phenotypes. In addition, I elucidated the role of heat shock proteins in canalizing the development of discrete alternative morphologies. Finally, I participated in studies that provide a genome-wide description of chromatin states in *P. pacificus* and implicate histone acetylation in specifying the Eu morph.

III. Deutsche Zusammenfassung

Phänotypische Plastizität beschreibt die Fähigkeit von Organismen, von identischem Genotyp, unterschiedliche Phänotypen als Reaktion auf Einflüsse der Umwelt zu entwickeln. Obgleich dieses Phänomen weit verbreitet ist, verbleiben die evolutionären Konsequenzen phänotypischer Veränderungen, ohne zugrunde liegender genetischer Veränderungen, ungeklärt. Eine Vielzahl von Ideen wurde unterbreitet, um die potentielle Relevanz phänotypischer Plastizität für die Evolution aufzuzeigen, jedoch bedarf die Formulierung expliziter und falsifizierbarer Hypothesen eines besseren mechanistischen Verständnisses der plastischen Entwicklung. Ein ideales Modellsystem für Studien zur phänotypischen Plastizität muss experimentelle genetische Untersuchungen erlauben, sowie Zugang zu Taxa gewährleisten, in welchen einer der alternativen Phänotypen fixiert wurde. Der Mundform-Polyphänismus der Nematoden aus der Familie der Diplogastridae erfüllt beide zuvor angeführten Kriterien. Genetisch uniforme Laborpopulationen von *Pristionchus pacificus* sind in der Lage zwei alternative Phänotypen, basierend auf unterschiedlichen Haltungsbedingungen, zu entwickeln. Die eurystomate (Eu) Morphe ist ein fakultativer Prädator mit weiter Mundhöhle und zwei hakenförmigen Zähnen. Bei der stenostomaten (St) Morphe hingegen, handelt es sich um einen nicht-aggressiven Mikrobivoren mit röhrenförmigem Mund und nur einem Zahn. Bisherige Studien demonstrierten eine zentrale Rolle von Pheromonen und identifizierten die Sulfatase EUD-1, die Sulfotransferase SULT-1 und den nukleären Hormonrezeptor NHR-40 als Regulatoren in der Mundformentscheidung von *P. pacificus*. Ziel meiner Dissertation ist es, weitere Umweltfaktoren und genetische Komponenten aufzuzeigen, welche diese Phänotypen kontrollieren. Ich entdeckte den Einfluss der Nahrungszusammensetzung und trug dazu bei, den Effekt einer Reihe von festen und flüssigen Nährmedien auf das Zahlenverhältnis der Morphen in einer Population zu identifizieren. Auf der Seite der Genetik fand ich heraus, dass *eud-1* Teil eines chromosomalen Clusters von funktionell verwandten Genen ist, welcher an Supergene erinnert. Außerdem isolierte ich einen weiteren Transkriptionsfaktor, NHR-1, und identifizierte eine Reihe von gemeinsamen

transkriptionalen Zielgenen von NHR-40 und NHR-1, welche möglicherweise direkt an der Produktion der alternativen Phänotypen beteiligt sind. Weiterhin beschrieb ich die Rolle von Heat Shock Proteinen in der Kanalisierung der Entwicklung alternativer Strukturen. Außerdem beteiligte ich mich an Studien, die eine genomweite Beschreibung der Chromatinzustände in *P. pacificus* bereitstellen und Histon-Acetylierung während der Ausprägung der Eu Morphe implizieren.

IV. List of publications

1. Sommer, R.J., Dardiry, M., Lenuzzi, M., Namdeo, S., Renahan, T., **Sieriebriennikov, B.**, and Werner, M.S. (2017). The genetics of phenotypic plasticity in nematode feeding structures. Open Biol. *7*, 160332.

2. Werner, M.S., **Sieriebriennikov, B.**, Loschko, T., Namdeo, S., Lenuzzi, M., Dardiry, M., Renahan, T., Sharma, D.R., and Sommer, R.J. (2017). Environmental influence on *Pristionchus pacificus* mouth form through different culture methods. Sci. Rep. *7*, 7207.

3. Sanghvi, G.V., Baskaran, P., Röseler, W., **Sieriebriennikov, B.**, Rödelsperger, C., and Sommer, R.J. (2016). Life History Responses and Gene Expression Profiles of the Nematode *Pristionchus pacificus* Cultured on *Cryptococcus* Yeasts. PLoS One *11*, e0164881.

4. **Sieriebriennikov, B.**, Prabh, N., Dardiry, M., Witte, H., Röseler, W., Kieninger, M.R., Rödelsperger, C., and Sommer, R.J. (2018). A Developmental Switch Generating Phenotypic Plasticity Is Part of a Conserved Multi-gene Locus. Cell Rep. *23*, 2835–2843.

5. Serobyan, V., Xiao, H., Namdeo, S., Rödelsperger, C., **Sieriebriennikov, B.**, Witte, H., Röseler, W., and Sommer, R.J. (2016). Chromatin remodelling and antisense-mediated up-regulation of the developmental switch gene *eud-1* control predatory feeding plasticity. Nat. Commun. *7*, 12337.

6. Werner, M.S., **Sieriebriennikov, B.**, Prabh, N., Loschko, T., Lanz, C., and Sommer, R.J. (2018). Young genes have distinct gene structure, epigenetic profiles, and transcriptional regulation. Genome Res. *28*, 1675–1687.

7. **Sieriebriennikov, B.**, Markov, G.V., Witte, H., and Sommer, R.J. (2017). The Role of DAF-21/Hsp90 in Mouth-Form Plasticity in *Pristionchus pacificus*. Mol. Biol. Evol. *34*, 1644–1653.

8. **Sieriebriennikov, B.**, and Sommer, R.J. (2018). Developmental Plasticity and Robustness of a Nematode Mouth-Form Polyphenism. Front. Genet. *9*, 382.

9. **Sieriebriennikov, B.**, Sun, S., Lightfoot, J.W., Witte, H., Moreno, E., Rödelsperger, C., and Sommer, R.J. Conserved nuclear receptors controlling a novel plastic trait in nematodes target rapidly evolving genes. Ready for submission.

V. List of abbreviations

cGMP	:	cyclic guanosine monophosphate
DNA	:	deoxyribonucleic acid
IGF	:	insulin-like growth factor
RNA	:	ribonucleic acid
RNAi	:	ribonucleic acid interference
TGF-β	:	transforming growth factor beta
EGF	:	epidermal growth factor
TOR	:	target of rapamycin

1. General introduction

1.1. Developmental plasticity and its role in evolution

1.1.1. Background

Mendel's famous experiments established that inheritance of organismal traits is underlain by recombination between discrete "factors", later referred to as genes. However, in the early days of genetic research it became abundantly clear that traits are rarely controlled by single genes [1]. By drawing parallels with chemical reactions, whereby different functional groups lend certain properties to molecules but the product of the reaction is made as a result of interaction between different molecules in a specific environmental condition, a view was developed that genes do not determine the traits directly but rather work together to shape the way development will proceed in a specific environment [1–4].

However, practical considerations warranted a more reductionist approach. The elucidation of the basic mechanisms of development required studying developmental sequences that would be devoid of 'noise' caused by sensitivity to environment. Therefore, in the course of the 20th century, the field of developmental biology devoted significant attention to studying invariant patterns, such as the cell lineage of the nematode *Caenorhabditis elegans*, whereby almost every cell division is determined [5]. Thus, *C. elegans*, mouse and *Drosophila* became the models of choice for developmental biology and genetics, as they could be easily kept in laboratory and their development was highly reproducible [6]. In the context of these systems, the effect of environment on development came to be either ignored or viewed as strictly deleterious, such as in the case of teratogens, exposure to which leads to severe developmental abnormalities [7].

Nevertheless, it was always apparent that many developmental processes and genetic correlations between them are influenced by the environment [8]. Furthermore, some non-model organisms produce vastly dissimilar phenotypes in response to different rearing conditions, such as castes in social insects [9]. This calls

for a new paradigm, which would be able to incorporate the influence of environment on development.

1.1.2. Developmental basis of plasticity

An ability to produce different phenotypes under distinct environmental conditions is called developmental plasticity [10]. West-Eberhard [11] draws a distinction between phenotypic plasticity as an ability to form different phenotypes in response to external environmental inputs on one hand and developmental plasticity as a broader concept which includes responses to both external and internal (e.g. hormones or gene products inside the cell) environment on the other hand. I personally prefer to avoid this distinction to steer clear of the semantic debate surrounding the definition of phenotype. At the time when the term was introduced, phenotype was defined based on some single measurable quality of an organism, such as height or color, whereby a phenotype was a typically observed value of the chosen metric in a population or its subset [1]. Later the definition evolved from describing a typical value of a single trait in a population to describing a set of observable qualities of a particular individual [12]. Yet, for practical reasons, working definitions of phenotype still often include only single features of an organism [13]. Depending on whether it is expression of a single gene or a feature of an organismal level, hormones and gene products inside cells may be viewed as factors of either external or internal environment. For this reason, I prefer to treat phenotype as a multi-level concept and to equate phenotypic and developmental plasticity *sensu* West-Eberhard.

On the surface, the ability to generate different phenotypes in different environments may seem restricted to special cases of adaptive responses to changing ambient conditions, such as shade avoidance in plants. However, phenotypic plasticity is an intrinsic feature of organisms, firmly embedded in the process of development itself. In the developing embryo, all the distinct tissues differentiate from a single zygote. The correct differentiation of tissues is dependent on the ability to perceive and react to inputs from the neighboring tissues as well as to other external inputs, such as spermatozoon entry or the presence of maternally deposited factors [14]. This ability is best illustrated by classical experiments with

grafting portions of one embryo onto a different embryo, whereby the transplanted organizer induces the formation of additional embryonic structures [15]. It does so by providing different environmental context for the responding tissue in the absence of any change of the genotype, demonstrating that differentiation and morphogenesis are inherently plastic processes.

Conversely, the principles behind the differentiation of tissues from the same progenitor may be extrapolated to plastic development in general. There is a view that differentiation into multiple discrete entities is controlled by a cascade of environmentally sensitive binary switches [11,16,17]. If this is the case, control by a series of switches has important implications for the evolution of development because the output of a switch can be influenced in two different ways. One way is to manipulate the input and the other way is to make changes to the switch mechanism, similar to rewiring an electric switch. Zuckerkandl and Villet devised an elegant Gedankenexperiment to translate this into the organismal context. They proposed a model consisting of a positive regulator protein akin to a transcription factor and the promoter of a downstream gene. In this simple scenario, the concentration of the regulator can be increased by some external influence, or the regulator protein can be mutated such that its affinity to the promoter increases despite the unaltered concentration. In any of the two cases, the expression of the downstream gene rises [18]. Thus, if development is organized as a series of switches, its phenotypic outcome can be influenced by manipulating either the environment or the underlying genes, whereby both manipulations activate the same stereotypic program.

This theoretically anticipated behavior is reflected in a phenomenon that attracted considerable attention among evolutionary and developmental biologists - phenocopies. These are environmentally induced phenotypes that closely resemble those induced by genetic mutations [19]. Phenocopies were already discussed in the context of one of the earliest described examples of phenotypic plasticity: daphnid water fleas can reduce their chance of being eaten by forming large head “helmets” and a spike at the rear end of the body. The ability to grow these structures depends on many factors, including food supply. At the same time, wild isolates from different lakes (which presumably have a different genetic makeup) have different propensities to form helmets and pointy spikes. However, a well-protected natural

isolate can be made to resemble a poorly protected one by starving the animals, and a reverse effect can be achieved by providing the poorly protected isolate with nutrient-rich food [2].

Some other prominent examples of phenocopies were described by Waddington. For instance, if pupae of *Drosophila melanogaster* are heat-shocked, the posterior cross-vein on the wings of the adult flies may not develop completely. Waddington heat-shocked and selected cross-veinless flies for multiple generation and obtained lines that exhibited the phenotype even in the absence of the original inducing stimulus [20]. When this experiment was recently reproduced, it was discovered that the heat shock increases the rate of DNA deletions and transpositions. Some of these mutations happen to phenocopy the environmentally induced phenotype and can be selected for [21]. Thus, the originally proposed "genetic assimilation" of the environmentally-induced effect is not supported by later experiments and seems generally implausible in the light of modern knowledge. Nonetheless, Waddington's experiments strongly promote the notion of interchangeability between the influence of environment and the effect of genetic mutations [22].

1.1.3. Evolutionary significance of plasticity

While it is intriguing that genetic mutations and environmental influences can induce the same phenotype, the evolutionary consequences of this are still debated. Multiple theories have been developed to predict the potential significance of the phenomenon, and they can be broadly classified into three categories. The first group of theories deal with immediate improvement or decline in fitness as a result of plasticity. For example, it is sometimes argued that increase in fitness without change in allele frequencies, provided by plasticity, renders selection ineffective and slows down evolution [23]. This argument is in principle valid, but it is regarded as unimaginative and leaves little lasting impression [11]. More often, the ability to alter the phenotype without invoking a genotype is viewed as advantageous in rapidly changing environmental conditions, which can be described by a tautology "adaptability is adaptive" [11,24]. Interestingly, a recent study suggests that even non-adaptive plasticity may be advantageous because the presence of less fit

individuals may increase the efficiency of directional selection [25]. The interpretation of the results of this study has been disputed [26,27] but the additional potential role of plasticity in evolution, which it describes, may be a valuable complement to the existing theories.

Furthermore, the ability to phenocopy genetic mutations by environmental influences may have profound evolutionary consequences beyond the short-term fitness effects. The earliest ideas on this date back to the 19th century, when Darwin's and Lamarck's views on inheritance and evolution were being discussed in the light of the recent discovery of the separation between germplasm and soma [4,28]. Incidentally, the most prominent hypotheses about the evolutionary role of adaptive plasticity were developed by psychologists, as they were interested in the evolutionary consequences of higher psychological processes, such as learning, which can be viewed as a form of behavioral plasticity [28,29]. Their ideas can be summarized as follows: in the absence of plasticity, if the environmental conditions change, the organism must rely on a fortuitous occurrence of a mutation that would increase its fitness, otherwise it will be at a disadvantage and may be eliminated. In contrast, if the new environmental condition alone can induce a better adapted phenotype, the population may persist for a large number of generations, long enough for a random mutation fixing the phenotype to occur [28,29]. This hypothesis was also in line with Waddington's experiments, and he further amended it by adding that prior to fixation, the newly expressed phenotype will not be just recurrently induced. It will also undergo stabilizing selection, whereby the developmental modules producing it will co-adapt - a process which he referred to as "canalization" [22]. These early ideas about "genes as followers" in evolution have been recently integrated in "plasticity-first" and "flexible stem" hypotheses. According to them, the evolution of novel traits must proceed through a phase of conditional expression, during which the phenotypic alternatives diversify and undergo stabilizing selection, and one or more alternative pathways are later fixed by mutations that shift the threshold of environmental sensitivity or disable one of the developmental trajectories [11,30–32].

Finally, the last group of theories deal with developmental plasticity in the context of cryptic genetic variation. The latter is defined as genetic variation that

does not affect the phenotypes normally observed in a population, but is able to contribute to phenotypes that occur under novel environmental conditions or after the introduction of a new mutant allele [33]. Cryptic mutations are retained more often than non-cryptic ones, because alleles with low phenotypic expression are selected less efficiently [34]. As a result, accumulated cryptic variation may boost adaptive change by serving as material for selection once it becomes expressed, which may happen in a new environment or once an allele arises that begins to genetically interact with formerly cryptic variants [35]. Since plasticity by definition entails conditional expression of phenotypes, the average long-term expression of genes associated with such phenotypes is lower than it would have been had the expression been constitutive. Thus, plasticity may facilitate the accumulation of cryptic genetic variation and thereby accelerate evolution [36].

In conclusion, developmental plasticity may influence evolution in a variety of ways. Numerous theories have been developed to describe different aspects of this interaction but they all share a unifying theme: selection acts on genes that are expressed, and genes that are expressed together evolve together. It is the role of development to orchestrate the expression of genes in time and space, and inherent conditional sensitivity of development allows environment to influence the strength and direction of selection on genes, in addition to its traditionally considered role as a provider of selective forces [37]. Despite the rationality of this statement, it is hard to deny its conjectural nature. Therefore, mechanistic insight into plastic development must be gained before explicit falsifiable hypotheses about the evolutionary consequences of plasticity can be formulated.

1.2. Model systems for studying phenotypic plasticity

1.2.1. Dauer development in *C. elegans*

An example of developmental plasticity at the organismal level with the best understood underlying molecular mechanism is direct *vs.* dauer development in *C. elegans*. Many nematodes of the order Rhabditida, to which *C. elegans* belongs, are able to differentiate in two alternative morphs as third instar larvae. Some animal

parasites can choose between forming free-living or infective larvae depending on host availability, whereas non-parasitic species may develop directly or choose to go through a persistent stage called “dauer” should the environmental conditions become adverse [38]. In *C. elegans*, entering the dauer diapause entails drastic changes in morphology, physiology and behavior. In comparison to larvae going through the direct cycle, dauer larvae have a more slender body, plugged body openings, reinforced cuticle, constricted pharynx, shrunken intestinal lumen as well as a partially remodeled nervous system [39,40]. They mostly stay immobile on agar plates in the laboratory, but are able to climb onto projections and wave their heads while standing on their tails in an attempt to get attached to a carrier animal [39,41].

The first forward genetic screens revealed more than 30 loci, in which mutations either suppress or lead to constitutive dauer formation [42,43]. Prior to their molecular characterization, these genes were grouped into pathways based on the pattern of their genetic interactions and the similarity of mutant phenotypes [43,44]. After the initial screens approached saturation, several enhancer screens identified additional players in the regulatory network [45,46]. Cloned genes encode components of the intraflagellar transport machinery in the endings of ciliated sensory neurons [47], as well as components of the cGMP signaling pathway [48,49] and proteins involved in serotonergic neurotransmission [50]. Together, these pathways impinge on TGF-β and insulin/IGF-like signaling [51,52]. These two signaling cascades converge to regulate the biosynthetic pathway for a steroid hormone dafachronic acid. The latter serves as the ligand of the nuclear hormone receptor DAF-12 [53]. Upregulation of serotonergic neurotransmission and of hormonal (insulin/IGF-like, TGF-β and steroid) signaling ultimately leads to the activation of DAF-12 by its ligand, which promotes direct development. In turn, in the absence of the ligand, DAF-12 represses direct development and promotes dauer diapause [54].

Thus, decades of molecular genetic research on dauer induction in *C. elegans* provided an unprecedented mechanistic understanding of the process. However, placing these findings into an evolutionary context and using them to evaluate existing hypotheses about the role of plasticity in evolution remains an unresolved challenge. Firstly, only a subset of lineages in the order Rhabditida are able to form dauer larvae and it is not clear when and how many times this ability originated and

how many times it was lost. Specifically, dauer larvae of species that belong to two closely related infraorders Rhabditomorpha and Diplogasteromorpha are regularly found in nature and are well described [38,39,55]. However, formation of dauer larvae by nematodes that belong to a distantly related infraorder Panagrolaimomorpha seems to only be well known to researchers conducting soil biomonitoring [56], but remains largely ignored by other fields. Only recently, analysis of the genome of *Panagrellus redivivus* revealed the presence of many players implicated in the dauer induction pathway in *C. elegans* [57]. Shortly thereafter a first taxonomic description of *Panagrellus* dauer larvae was published [58]. Assuming that all dauer larvae are homologous, the ability of panagrolaimomorph nematodes to form them shifts the timing of the origin of the trait from the base of the suborder Rhabditina closer to the last common ancestor of the complete order. In turn, this has important implications for understanding the evolution of animal parasitism. The commonality of some mechanisms regulating dauer and infective larvae formation has led to a hypothesis that dauer formation may be a step towards evolution of parasitism [38]. Since animal parasitism originated multiple times in Rhabditida and parasitic lineages are interspersed within the order [59], relative timing of origins and losses of the ability to form dauer and infective larvae is absolutely crucial for the validation of this hypothesis.

Furthermore, explicit testing of “plasticity-first” or “flexible stem” hypotheses may not be directly feasible using dauer formation as a model system. These hypotheses make predictions about evolution of traits in transition from the stage of conditional expression to fixation. However, no known species constitutively forms dauer larvae. Only some animal parasitic clades simultaneously contain lineages with obligatory and facultative induction of infective larvae, making these clades candidate systems for testing theories about the evolutionary significance of developmental plasticity. Mechanistic understanding of dauer development in *C. elegans* can be helpful in studying animal parasitic nematodes but the translation of results between these lineages should be approached with caution before the evolutionary relationship between dauer and infective juvenile induction is ascertained.

1.2.2. Vernalization-induced flowering in *A. thaliana*

Plants are rich in traits that exhibit plasticity [60], but the plastic process whose mechanistic underpinning has been dissected in greatest detail is flowering following a prolonged period of cold. Activation of flowering upon extended exposure to low temperatures is referred to as vernalization and is required by many plants to prevent flowering before winter and promote it in spring or summer instead [61]. Natural variation in vernalization requirement in *Arabidopsis thaliana* maps to a single locus dubbed *FRIGIDA*, and genetic modifier screens indicate that the action of *FRIGIDA* is dependent on the genotype of the flowering repressor *Flowering Locus C* (*FLC*) [62–64]. Cloning of the identified loci and subsequent experiments demonstrate that *FRIGIDA* encodes a coiled coil domain containing protein that activates the expression of *FLC* through recruitment of transcription factors, regulation of mRNA capping and recruitment of writers of activating chromatin marks, in particular H3K36me3 [65–67]. Thus, the role of FRIGIDA is to maintain the active transcription of *FLC* before exposure to cold, thereby repressing flowering.

The action of FRIGIDA and the associated protein complex is antagonized by a set of constitutively active *FLC* repressors, together referred to as the autonomous pathway [61]. Components of the pathway include enzymes that erase chromatin marks written by the FRIGIDA complex machinery [68,69]. Other pathway components are RNA-binding proteins that regulate processing of a set of antisense transcripts which are expressed from the *FLC* locus and are collectively referred to as *COOLAIR* [61,69]. Before vernalization, *COOLAIR* transcription is suppressed by a homeodomain protein that stabilizes a complex between the template DNA and the nascent transcript, leading to RNA polymerase stalling [70]. However, immediately upon vernalization, this inhibition is released, and the *COOLAIR* transcription begins to interfere with *FLC* transcription both directly and by recruiting the RNA-binding proteins that indirectly promote removal of activating methylation marks from the locus [69,71,72]. Altogether, the autonomous pathway balances out the activating action of FRIGIDA on *FLC* expression and primes transcriptional shutdown of *FLC* during the first weeks of cold exposure.

Further exposure to cold activates the third set of genes that encode members of Polycomb repressive complex 2, which write repressive H3K27me3 marks in place of erased H3K36me3 marks in a small region overlapping the first exon and the first intron of *FLC*, named nucleation region [73,74]. Upon return to warmth, chromatin silencing spreads from this region to the whole *FLC/COOLAIR* locus, shutting down the expression of both transcripts in a heritable manner [75]. The shutdown of *FLC* allows pathways sensing other environmental factors, such as photoperiod, to activate flowering [61].

In summary, research on vernalization-induced flowering in *A. thaliana* elucidated part of a very complex mechanism of how environmental signals can be integrated over a prolonged period of time to initiate an important life stage transition. Even though this mechanism does not regulate a choice between alternative life histories, like dauer *vs.* direct development in *C. elegans*, and hence cannot be used as a model for testing "plasticity first" hypothesis, it nevertheless provides invaluable insight into environmental control of development. In particular, regulation of *FLC* expression demonstrates the role of antagonistic molecular pathways in maintaining balance between mutually exclusive chromatin states. Additionally, it highlights the importance of some little characterized molecular mechanisms of gene regulation, such as mutually exclusive sense and antisense transcription and stabilized RNA-DNA complexes at the transcription start site. Many of these mechanisms may be wide-spread and research in other system is needed to evaluate their pervasiveness and relative importance.

1.2.3. Emerging models

Research on the mechanisms behind phenotypic plasticity is not limited to well-established model species. Recently, the molecular regulation of plastic phenotypes began to be investigated in an array of newly established lab organisms. In this section, I will briefly summarize the major findings in several emerging animal models, in which research has moved towards experimental genetic manipulation.

The model for plasticity research, which arguably gained the most lasting impression in the evo-devo field, is the horned beetles of the genus *Onthophagus*. Scarab beetles, to which *Onthophagus* belongs, exhibit a striking diversity of horns

on the head, which appear to be an evolutionary innovation independently acquired by several beetle families [76]. In *O. taurus*, only males develop head horns, and the length of the horns is strongly correlated with the body size, whereby larger individuals produce longer horns [77,78]. Head horn length is also correlated with behavior in that horned males engage in fights whereas hornless males rely on non-aggressive opportunistic behavior [78]. Early studies implicated juvenile hormone in the regulation of the head horn length and put forward a complex model of nutrient control of head horn growth through juvenile hormone and ecdysteroids [79–81]. Work done in other insects, such as *Drosophila* and *Tribolium*, demonstrates that the action of juvenile hormone is dependent on the components of the insulin/IGF-like signaling pathway [82,83]. Surprisingly, RNAi knockdown of either of the two insulin receptor genes, or their combination, has no effect on head horn growth in *O. taurus* [84]. In contrast, RNAi knockdown of *Foxo*, encoding the transcription factor traditionally viewed as the downstream target of insulin/IGF-like signaling, makes the relationship between body size and head horn length less sigmoidal, suggesting that Foxo was co-opted from the insulin/IGF-like signaling pathway to inhibit horn growth when nutrients are scarce (and the body is small) and to sensitize responding tissues at high nutrient levels [84]. In small animals, inhibition of head horn growth by Foxo is mediated by Hedgehog signaling [84,85]. In large animals, Foxo primes horn growth to induction by Doublesex, which is a part of the sex determination pathway in insects with a dual function of promoting head horn growth in large males and inhibiting head horn growth in females of *O. taurus* [86,87]. Altogether, research done in *O. taurus* and related species highlights the role of co-option and reshuffling of components of conserved signaling pathways in the evolution of novel traits. Generally speaking, head horn growth in beetles represents an attractive system to study plasticity because of the obvious ecological relevance of the trait and vast natural diversity in the degree of its development, as well as in the mode of the sexual dimorphism. However, the system also has significant drawbacks, such as limited applicability of molecular biological tools and the lack of unbiased studies (e.g. forward genetic screens) to identify less conserved components of the gene network regulating head horn plasticity.

Another notable example of food-related morphological plasticity in insects is wing form. Some crickets, aphids and planthoppers are able to develop either into a long-winged migratory morph when the population density rises and the host plant deteriorates or a short-winged morph, which has limited mobility and heavily invests in reproduction when the environmental conditions are favorable [88,89]. In the brown planthopper *Nilaparvata lugens*, RNAi knockdown of various components of the insulin/IGF-like signaling pathway, including its terminal transcription factor *FOXO*, drastically shifts the frequency of the two morphs in the population [90]. Interestingly, the genome contains two copies of the insulin receptor gene, and they appear to have undergone striking subfunctionalization, whereby the two genes promote opposite morphs [90]. Incidentally, wing wounding, which is accompanied by a change in FOXO expression, also influences the morph frequency [91]. Finally, RNAi knockdown of *JNK* indicates that it acts along the Insulin/IGF-like signaling pathway in regulating morph frequencies, but its action may be non-canonical in that it is not mediated by the transcription factors Jun and Fos, like in some model organisms [92]. In summary, similar to *O. taurus*, wing plasticity in the brown planthopper is regulated by members of conserved signaling pathways, which were reshuffled and at least in one case duplicated and subfunctionalized. Again, similar to *Onthophagus* beetles, wing forms in brown planthoppers represent an attractive and ecologically relevant phenotype, but the system has limited genetic tractability and the studies to date have only focused on candidate genes and pathways.

Ultimately, the example of phenotypic plasticity in insects which is most well known to the general public is castes in social insects, such as bees, ants, wasps and termites. Drastic morphological, behavioral and aging dissimilarities between different castes, multiple origins of sociality and economic importance of several species make social insects extremely attractive organisms to study despite frequent difficulties in maintaining and propagating their colonies in the lab [9,93,94]. While molecular genetic tools have recently been developed for ants [95,96], wasps [97] and termites [98], most of genetic manipulations of the caste status have been done in honeybees. Queen development in honeybees is induced by feeding larvae with royal jelly, which contains Major Royal Jelly Protein 1, or MRJP1, as the main active compound [9,99]. RNAi knockdown of *Egfr*, a gene encoding an EGF receptor,

abolishes the effect of royal jelly and MRJP1 [99]. In addition to EGF pathway, insulin/IGF-like signaling is involved in caste specification in honeybees as RNAi knockdown of insulin-like peptide genes and of insulin receptor substrate gene suppresses the development of queen-associated traits, such as ovariole number [100–102]. Interestingly, two genes encoding insulin-like peptides appear to have subfunctionalized as they influence the traits they control to a different extent [102]. This is broadly reminiscent of the subfunctionalization of insulin receptor genes in brown planthoppers, although it is not as extreme, as the two honeybee duplicates do not have opposing influences on the phenotype. Further experiments implicate TOR signaling in queen induction. Interference with either TOR or insulin/IGF-like signaling pathway reduces the titre of juvenile hormone and ectopic application of juvenile hormone rescues the development of queen-like traits in knockdown lines [101,103]. These results contradict the often-mentioned notion that juvenile hormone has lost its role as a gonadotropin in honeybees [37,104], indicating that more time- and tissue-resolved studies are needed to dissect the function of different hormones in honeybee development. The situation is further complicated by the presence of feedback loops between juvenile hormone and insulin/IGF-like pathway, as well as between juvenile hormone and vitellogenin synthesis [105,106]. Altogether, caste specification in honeybees involves well-known pathways implicated in nutrient sensing and regulation of cell proliferation, which exhibit complex interplay with several pleiotropic hormones. Evidently, dissection of the genetic network behind caste specification is still in its inception. Nevertheless, social insects continue to attract considerable attention of biologists from various fields, in part because of the variety of phenotypes associated with caste status. Nevertheless, lab maintenance of most species is either impossible or challenging, and application of molecular biological tools has limited efficiency because of slow speed of development and the necessity of early developmental stages to be nursed. Finally, as in all model systems described in this section, most studies in social insects focus on candidate genes and pathways, which may conceal the role of less conserved players in regulation and evolution of plastic traits.

1.3. Feeding dimorphism in diplogastrid nematodes

1.3.1. Basic description of the phenotype and its evolutionary dynamics

A brief overview of available models to study phenotypic plasticity demonstrates the need for a system that would combine genetic tractability of traditional model organisms with ecological and evolutionary relevance of emerging models. Plasticity in mouth parts of the nematode *Pristionchus pacificus* may represent a study system that satisfies both of these criteria. *Pristionchus* is a member of the same order as *C. elegans* and shares its hermaphroditic mode of reproduction, short life cycle and amenability to molecular techniques [107]. At the same time, *P. pacificus* has diverged from *C. elegans* approximately 100 million years ago and acquired substantial differences in its life style and morphology [108,109]. *Pristionchus* belongs to the family Diplogastridae, which are predominantly terrestrial nematodes that often occupy saprobic environments, such as dung, compost or other habitats which contain large amounts of organic material [110]. In these environments, diplogastrid nematodes seem to feed opportunistically on any prey items that they are physically able to consume, including bacteria, fungi, unicellular eukaryotes and other nematodes [110,111]. Diplogastrids are often phoretically associated with insects although some lineages evolved into animal parasites [110,112]. Many diplogastrids have buccal cavities armed with moveable teeth and immobile denticles, and a considerable number of species exhibit plasticity in the degree to which this armature develops. Most plastic species can develop one of the two alternative morphologies: a “wide-mouthed” eurystomatous (Eu) phenotype, or “narrow-mouthed” stenostomatous (St) phenotype, although in some lineages the number of discrete phenotypic alternatives can be as high as five [113,114].

Morphological differences between the Eu and St morphs in some lineages appear merely quantitative, i.e. teeth and other cuticularized structures are larger in Eu individuals, whereas in other lineages the distinction is qualitative, like in *P. pacificus*, whose Eu morph has two hooked teeth, while the St morph has only the dorsal tooth, and the right ventrosublateral tooth is reduced to a cuticularized ridge

with a minute denticle [114,115]. Apart from the morphological differences, Eu and St morphs exhibit different behavior. In large species, both morphs can kill other nematodes but Eu individuals are more aggressive and more efficient [116,117]. In smaller species like *P. pacificus*, this difference is exaggerated: St individuals are completely devoid of killing ability and they never attack potential prey items [116,118]. While the adaptive value of developing into the Eu morph is quite obvious, as it allows to expand the range of potential food sources and eliminate competitors, it is still not entirely clear what are the advantages of developing into the St morph. There are indications that St individuals develop more rapidly as the St mouth armature is presumably simpler and can be built faster than the heavily cuticularized Eu mouth [118]. This is corroborated by the fact that some conditions that impair body growth also induce high incidence of St morphs [119,120].

From the evolutionary perspective, mouth part plasticity in the family Diplogastridae is a highly dynamic trait. It was inferred to have originated at the base of the family and has been independently lost multiple times [121]. Intriguingly, the morphology of animals in some secondarily monomorphic lineages resembles the Eu morphology of dimorphic species, whereas the mouth of other secondarily monomorphic lineages is reminiscent of the mouth in St morphs [114,121]. This is a rare situation when various extant lineages conform to different stages of the origin of novel traits predicted by the “flexible stem” hypothesis. In summary, *P. pacificus* combines amenability to lab culture and genetic manipulations with the presence of two ecologically relevant phenotypic alternatives, which appear to have been independently fixed in neighboring lineages. Together, it makes feeding dimorphism in *P. pacificus* an ultimate model to study the mechanisms behind phenotypic plasticity and to test the predictions of existing theories about its evolutionary significance.

1.3.2. Regulation of mouth form plasticity in *P. pacificus*

The choice between the Eu and St development in *P. pacificus* appears to be regulated by multiple environmental factors, whose individual roles are only beginning to be dissected. An early study described the induction of the Eu morph by pheromones [122]. Subsequent research elucidated the role of individual constituents

of the pheromone cocktail, of which the nematode-derived modular metabolite *dasc#1*, a molecule consisting of sugar and fatty acid derivatives, has the strongest Eu-inducing effect [123]. Examination of the pheromone profiles of different age classes reveals that the ability to induce Eu morphs in developing larvae is higher in pheromones produced by late juveniles and adults, concomitant with higher abundance of *dasc#1* in the cocktail at late developmental stages [124]. This hints at a possibility of cross-generational communication, whereby a large number of adults in the habitat may be sensed by developing juveniles to predict upcoming crowding in their generation.

The first forward genetic screen for morph-defective mutants resulted in 17 mutants that have Eu-defective (Eud) phenotype and only develop into the St morphs. The largest complementation group is formed by four completely penetrant alleles of a gene named *eud-1*, located on the chromosome X. Interestingly, heterozygous *loss-of-function* mutants also have a partially penetrant Eud phenotype, which indicates that the gene is haploinsufficient and acts in a dosage-dependent manner. *eud-1* encodes a sulfatase, which is homologous to the *C. elegans* gene *sul-2*, although *P. pacificus* contains three copies of the gene, whereby *eud-1* and *sul-2.2.1* are located next to each other and presumably result from a more recent duplication event. *eud-1* is expressed in neurons, and its overexpression causes a completely penetrant Eu-constitutive (Euc) phenotype, which prompted labeling of *eud-1* as a “master regulator” of mouth form plasticity in *P. pacificus* [125]. This initial genetic screen was followed by a screen for suppressors of *eud-1*, which identified Euc alleles of a sulfotransferase *sult-1/seud-1* and a nuclear hormone receptor *nhr-40* [126–128]. Finally, dafachronic acid is also implicated in the regulation of mouth form plasticity, whereby its ectopic application suppresses the Eu morph [122].

First investigations of mouth form regulation in *P. pacificus* revealed a combination of previously uncharacterized genetic players and a conserved hormonal mechanism involved in *C. elegans* dauer decision. Thus, it may be an ideal system to compare the role of reshuffling the components of the “molecular toolkit” with the role of novel players that were adopted from non-canonical pathways or arose through gene duplications. Before any broad conclusions can be made,

research on mouth-form plasticity in *P. pacificus* must be simultaneously expanded in several directions that include describing other environmental factors influencing the decision, identification of additional genetic players and finding the links between environment and gene regulation.

2. Objectives of the thesis

The overall goal of this thesis work was to elucidate previously uncharacterized environmental factors and genetic players controlling mouth form decision in *P. pacificus*. To achieve this, I simultaneously pursued several lines of research:

1) I made use of alternative culture conditions introduced by my colleagues, such as rearing worms in liquid and solid media of various composition and feeding worms with yeast instead of bacteria. I assessed mouth form ratios in these conditions to find out if other environmental influences besides pheromones also have an effect on mouth form decision.
2) I investigated the functional roles of genes immediately adjacent to *eud-1* through reverse genetics, following an indication that they may act on the same substrate.
3) I conducted a suppressor screen in the *nhr-40* mutant background to uncover further regulators of the dimorphism and to potentially identify a suite of downstream genes that make the alternative phenotypes.
4) I explored whether the robust development of the two alternative morphologies involves canalization by heat-shock proteins, which are known to mask the effects of cryptic mutations and stochastic variation on development in other systems.
5) I participated in studies investigating the roles of chromatin modifications in mouth form regulation.

The results of my work were integrated with the results produced by my colleagues and placed into a general context in two review articles.

3. Results and discussion

3.1. The genetics of phenotypic plasticity in nematode feeding structures

Sommer, R.J., Dardiry, M., Lenuzzi, M., Namdeo, S., Renahan, T., **Sieriebriennikov, B.**, Werner, M.S.

Open Biology **7**, 160332 (2017), doi: 10.1098/rsob.160332

3.1.1. Synopsis

This review article summarizes what was known about the regulation of mouth form plasticity in *P. pacificus* at the time of its publication. It suggests that the first isolated switch gene, *eud-1*, is a central hub that integrates pheromone perception and steroid hormone signaling. This suggestion is based on the fact that mutations or overexpression of *eud-1* abolish the effects of crowding and ectopic application of dafachronic acid on the morph frequency. Additionally, mutations in histone modifiers lead to decreased expression of *eud-1* suggesting a possibility that morph frequency is controlled by altering the chromatin state of the *eud-1* locus. Mutations in *nhr-40* suppress the mutations in *eud-1* warranting the placement of NHR-40 as the terminal transcription factor in the network. Aside from discussing possible topology of the gene regulatory network, the article highlights some puzzling features of *eud-1*, such as haploinsufficiency.

3.1.2. Own contribution

I participated in the group discussions in which the manuscript was conceived. I estimate my contribution at 10%.

3.2. Environmental influence on *Pristionchus pacificus* mouth form through different culture methods

Werner, M.S., **Sieriebriennikov, B.**, Loschko, T., Namdeo, S., Lenuzzi, M., Dardiry, M., Renahan, T., Sharma, D.R., Sommer, R.J.

Scientific Reports **7**, 7207 (2017), doi: 10.1038/s41598-017-07455-7

3.2.1. Synopsis

This study had a dual goal. Firstly, understanding the regulation of plasticity in *P. pacificus* requires knowledge of the environmental factors influencing the phenotype. Secondly, ability to produce a controlled ratio of the alternative morphs in the population through precise environmental manipulation is instrumental in uncovering the genetic regulation of the trait. We achieved both goals thanks to a serendipitous discovery that culturing worm on a shaker in flasks containing liquid S-medium induces a morph ratio that is opposite to the one normally observed on agar plates with Nematode Growth Medium. We show that the change in ratios is caused by a complex interplay between chemical composition of the medium, presence and type of the gelling agent, and shaking speed. By combining these factors in various combinations, we develop a set of condition that can induce any morph ratio in the range between 7% and 99% Eu individuals. We further focus on a particular Eu-repressing condition and demonstrate that its effects are not maternally inherited and it triggers the same molecular changes as the Eu-repressing mutation in the switch gene *eud-1*. Finally, we test whether culturing worms in liquid equally affects other species of the genus *Pristionchus* and uncover an unexpected interspecies variation in the phenotypic response.

3.2.2. Own contribution

I participated in designing and collecting data from most of the experiments. I estimate my contribution at 25%.

3.3. Life history responses and gene expression profiles of the nematode *Pristionchus pacificus* cultured on *Cryptococcus* yeasts

Sanghvi, G.V., Baskaran, P., Röseler, W., **Sieriebriennikov, B.**, Rödelsperger, C., Sommer, R.J.

PLoS One **11**, e0164881 (2016), doi: 10.1371/journal.pone.0164881

3.3.1. Synopsis

Like *C. elegans*, *P. pacificus* is normally cultured on the OP50 strain of *Escherichia coli* in the lab. This bacterial strain is an auxotroph that is used because its growth is impaired and it does not form thick lawns on agar plates, leaving worms well visible. At the same time, worms grown in such an artificial rearing condition may have a very different lifestyle from those grown in a more natural setting. Therefore, feeding nematodes food other than *E. coli* OP50 may elucidate aspects of their physiology and behavior which were previously missed. For this reason, we fed *P. pacificus* two species of yeasts of the genus *Cryptococcus* and conducted a comprehensive survey of their growth, development and survival in these conditions. In comparison to worms grown on *E. coli*, animals grown on both yeast species develop more slowly, lay fewer eggs and begin to senesce earlier. However, they exhibit downregulation in the expression of genes that are upregulated when *P. pacificus* is cultured on pathogenic bacteria, suggesting that impaired growth of *P. pacificus* on *Cryptococcus* yeasts is not caused by the toxicity of the yeasts. Instead, it may result from nutrient limitation because yeast cells are more difficult to ingest and digest, which is corroborated by low pumping and defecation rate. Interestingly, mouth form frequency in animal grown on one of the yeast species was shifted towards higher incidence of St morph. This parallels the trend in liquid cultures, which may also represent a nutrient limited condition.

3.3.2. Own contribution

I screened mouth form frequencies in worms grown on different food sources. I estimate my contribution at 10%.

3.4. A developmental switch generating phenotypic plasticity is part of a conserved multi-gene locus

Sieriebriennikov, B., Prabh, N., Dardiry, M., Witte, H., Röseler, W., Kieninger, M.R., Rödelsperger, C., Sommer, R.J.

Cell Reports **23**, 2835–2843.e4 (2018), doi: 10.1016/j.celrep.2018.05.008

3.4.1. Synopsis

The developmental switch gene *eud-1* and its tandem duplicate *sul-2.2.1* are homologous to the human gene GALNS. They are surrounded by another pair of duplicates encoding α-N-acetylglucosaminidases, which are homologous to the human gene NAGLU and which we named *nag-1* and *nag-2*. Interestingly, GALNS and NAGLU have similar substrates, and mutations in these genes in humans cause similar disorders. This prompted us to test through reverse genetics whether *nag-1* and *nag-2* contribute to the same phenotype as *eud-1*. We used CRISPR/Cas9 to generate lines with mutations in individual genes or in their various combinations, including a deficiency line where all four genes were absent or truncated. By phenotyping these lines in Eu-inducing and Eu-repressing culture conditions we found that *nag-1* and *nag-2* additively repress the Eu morph, thereby influencing the same phenotype as *eud-1* but shifting it in the opposite direction. *eud-1* is epistatic to the *nag* genes and the three genes are expressed in non-overlapping sensory neurons, suggesting a possibility that they may be involved in perception of disparate environmental inputs. Clusters of genes that have different origin but related functions are sometimes referred to as supergenes, and such configurations in other organisms appear to be evolutionarily dynamic. We therefore examined the synteny between *nag* genes, *eud-1* and *sul-2.2.1* in eight species of *Pristionchus* and in two other diplogastrid genera. We found that the synteny is conserved within the genus but breaks down further in the family. Finally, we established that the evolution of

individual genes in the locus is shaped by a balance between divergence and gene conversion between the paralogs, and we observed conversion between *nag-1* and *nag-2* experimentally.

3.4.2. Own contribution

I conceived and designed all the experiments with the help of my colleagues and collected most of the experimental data. I estimate my contribution at 60%.

3.5. Chromatin remodelling and antisense-mediated up-regulation of the developmental switch gene *eud-1* control predatory feeding plasticity

Serobyan, V., Xiao, H., Namdeo, S., Rödelsperger, C., **Sieriebriennikov, B.**, Witte, H., Röseler, W., Sommer, R.J.

Nature Communications **7**, 12337 (2016), doi: 10.1038/ncomms12337

3.5.1. Synopsis

This study describes the results of a pleiotropic screen for mutants that exhibit altered mouth form frequencies in addition to vulva formation defects, by which they were selected in previous forward genetic screens. Two of the examined mutants have a highly penetrant Eu-deficient phenotype. These lines carry mutations in the genes *lsy-12* and *mbd-2*, both of which encode members of protein complexes involved in histone deacetylation and nucleosome remodeling. Accordingly, the genome-wide levels of H3K9ac and H3K27ac, but also H3K4me2 and H3k4me3 are decreased in these mutants. The expression of *eud-1* is also downregulated in both lines suggesting that morph frequency may be controlled by altering the chromatin state at the *eud-1* locus. Additionally, combination of RT-PCR and RNA-seq experiments in wild type and in *lsy-12* mutant backgrounds provides evidence that an antisense transcript may be expressed from the *eud-1* locus. CRISPR/Cas9-induced mutations in an intron of *eud-1*, which corresponds to the exon of the antisense transcript, lead to decreased *eud-1* expression, suggesting a possibility that the antisense transcript may positively regulate *eud-1* expression.

3.5.2. Own contribution

I performed CRISPR/Cas9 mutagenesis and RT-qPCR experiments on the resulting lines, and participated in the discussion of FISH experiments. I estimate my contribution at 10%.

3.6. Young genes have distinct gene structure, epigenetic profiles, and transcriptional regulation

Werner, M.S., **Sieriebriennikov, B.**, Prabh, N., Loschko, T., Lanz, C., Sommer, R.J.

Genome Research **28**, 1675–1687 (2018), doi: 10.1101/gr.234872.118

3.6.1. Synopsis

With the advent of genome sequencing, a surprising discovery was made that 10%-30% genes in eukaryotes exhibit no traceable homology to genes in other lineages. These genes are called orphan, taxonomically restricted, or new. Many of them were shown to have important phenotypic contributions. To be expressed and integrated into gene regulatory networks, new genes must acquire regulatory sequences, and how this happens is currently unknown. One theory predicts that orphan genes may preferentially arise or be translocated into areas of open chromatin, thereby hijacking existing regulatory sequences around such areas. We made use of deep taxon sampling in *Pristionchus* nematodes to identify orphan genes and collected Iso-Seq, RNA-seq, ChIP-seq and ATAC-seq data for adult hermaphrodites of *P. pacificus* to describe their chromatin states. As a general trend, we find that orphan genes have shorter coding sequences and fewer exons than conserved genes, and their expression is lower, which is consistent with previous studies. Surprisingly, those orphan genes that are expressed display distinct chromatin signatures from conserved genes with similar expression. Chromatin states at the transcription start sites of orphan genes more closely resemble enhancers than promoters, as defined by H3K4me1, H3K27ac, and ATAC-seq peaks and the lack of repressive histone marks. Altogether, this corroborates the model of integration or preferential retention of orphan genes in the areas of open chromatin next to enhancers.

3.6.2. Own contribution

I performed Iso-Seq experiments with the help of my colleagues. I estimate my contribution at 10%.

3.7. The role of DAF-21/Hsp90 in mouth-form plasticity in *Pristionchus pacificus*

Sieriebriennikov, B., Markov, G.V., Witte, H., Sommer, R.J.

Molecular Biology and Evolution **34**, 1644–1653 (2017), doi: 10.1093/molbev/msx106

3.7.1. Synopsis

Plasticity can entail both continuous and discrete distributions of environmentally-regulated phenotypes. Examples of discrete alternative morphs are abundant in nature and include castes in social insects and mouth form in *Pristionchus* nematodes. Still, it is unknown which mechanisms enforce the discontinuity between the alternative phenotypic outcomes. In theory, the distributions of alternative morphologies can be limited by the action of mechanisms that enable robust development in the face of stochastic perturbations and cryptic mutations. This function is ascribed to the heat-shock protein family Hsp90. Here, we used discrete mouth morphologies in *P. pacificus* to test the contribution of robustness mechanisms provided by Hsp90 to the development of a plastic trait. We utilized geometric morphometric analysis of 20 landmarks in the mouth to describe the distribution of Eu and St morphologies in reference condition and upon inhibition of the heat-shock machinery. Interfering with heat-shock activity through culturing animals at an elevated temperature shifts the distributions of Eu and St morphologies, whereas pharmacological inhibition of Hsp90 using radicicol increases the morphological variability of both phenotypes. Finally, CRISPR/Cas9-induced mutation in the *daf-21*/Hsp90 gene has a combined effect. Together, these results provide evidence that heat shock proteins buffer the development of discrete mouth morphologies in *P. pacificus*, demonstrating the interplay between plasticity and robustness, two phenomena that are traditionally viewed as contrasting.

3.7.2. Own contribution

I designed and performed all the experiments with the help of my colleagues. I estimate my contribution at 90%.

3.8. Developmental plasticity and robustness of a nematode mouth-form polyphenism

Sieriebriennikov, B., Sommer, R.J.

Frontiers in Genetics **9**, 382 (2018), doi: 10.3389/fgene.2018.00382

3.8.1. Synopsis

Robustness is an important feature of development, which allows reliable generation of identical phenotypes despite mutations and stochastic perturbations of the environment. On the surface, robustness appears opposing to plasticity, as robustness entails environmental insensitivity while plasticity is defined as environmental sensitivity. Intriguingly, both robustness and plasticity are suggested to accelerate evolution by releasing the constraints of selection. We speculate that the relationship between the two phenomena is more nuanced and propose that they may be complementary rather than opposing. We leverage the knowledge about the mechanisms of plastic development and suggest that the interplay between plasticity and robustness must be studied at two levels. First, the network of genes involved in switching between alternative developmental trajectories requires robustness in that it must reproducibly integrate disparate environmental inputs and initiate one of the downstream developmental programs. Second, the final phenotypic output requires robustness to constrain the range of generated phenotypic outcomes. We apply these theoretical considerations to what is known about the regulation of mouth from plasticity in *P. pacificus*. In particular, we discuss apparent stochasticity in mouth form decision in the light of the robustness of the switch mechanism. To exemplify the robustness of the phenotypic outcome, we refer to our findings about buffering of the alternative morphologies by Hsp90.

3.8.2. Own contribution

I conceived and wrote the article together with Ralf J. Sommer. I estimate my contribution at 70%.

3.9. Conserved nuclear receptors controlling a novel plastic trait in nematodes target rapidly evolving genes

3.9.1. Synopsis

Developmental plasticity was shown to act through switch genes, but little is known about the gene regulatory networks on which environmental signals impinge. Knowledge about the composition of these networks is crucial for understanding how novel environments shape development and evolution. Here, we elucidated the gene regulatory network controlling the development of environmentally-induced predatory morphs in the nematode *Pristionchus pacificus* and explored the evolutionary dynamics of associated genes. We found that two conserved nuclear hormone receptors regulate a small set of 24 target genes. These genes have no orthologs in *Caenorhabditis elegans* and likely result from lineage-specific expansions. Furthermore, they show extreme redundancy, as revealed by systematic CRISPR/Cas9 knockouts and expression studies. Strikingly, all tested target genes are expressed in a single cell, the dorsal pharyngeal gland cell, whose morphological remodeling accompanied the evolution of teeth and predation. Our study links rapid gene evolution with morphological innovations associated with plasticity.

3.9.2. Own contribution

I designed and performed all the experiments with the help of my colleagues. I estimate my contribution at 80%.

4. References

1. Johannsen, W. *Elemente der exakten Erblichkeitslehre*. (Verlag von Gustav Fischer, 1913).
2. Woltereck, R. Weitere experimentelle Untersuchungen über Artveränderung, speziell über das Wesen quantitativer Artunterschiede bei Daphniden. *Verhandlungen der Deutschen Zoologischen Gesellschaft* **19**, 110–173 (1909).
3. Schlichting, C. D. & Pigliucci, M. *Phenotypic evolution: a reaction norm perspective*. (Sinauer Associates Incorporated, 1998).
4. Weismann, A. *The effect of external influences upon development*. (H. Frowde, 1894).
5. Sulston, J. E., Schierenberg, E., White, J. G. & Thomson, J. N. The embryonic cell lineage of the nematode *Caenorhabditis elegans*. *Dev. Biol.* **100**, 64–119 (1983).
6. Bolker, J. Model organisms: There's more to life than rats and flies. *Nature* **491**, 31–33 (2012).
7. Holmes, L. B. Teratogen-induced limb defects. *Am. J. Med. Genet.* **112**, 297–303 (2002).
8. Stearns, S., de Jong, G. & Newman, B. The effects of phenotypic plasticity on genetic correlations. *Trends Ecol. Evol.* **6**, 122–126 (1991).
9. Corona, M., Libbrecht, R. & Wheeler, D. E. Molecular mechanisms of phenotypic plasticity in social insects. *Curr Opin Insect Sci* **13**, 55–60 (2016).
10. Pigliucci, M. Developmental phenotypic plasticity: where internal programming meets the external environment. *Curr. Opin. Plant Biol.* **1**, 87–91 (1998).

11. West-Eberhard, M. J. *Developmental plasticity and evolution*. (Oxford University Press, 2003).
12. Lewontin, R. C. Genotype and Phenotype. in *International Encyclopedia of the Social & Behavioral Sciences* (eds. Smelser, N. J. & Baltes, P. B.) 6159–6162 (Pergamon, 2001).
13. Nachtomy, O., Shavit, A. & Yakhini, Z. Gene expression and the concept of the phenotype. *Stud. Hist. Philos. Biol. Biomed. Sci.* **38**, 238–254 (2007).
14. Jacobson, A. G. & Sater, A. K. Features of embryonic induction. *Development* **104**, 341–359 (1988).
15. Spemann, H. & Mangold, H. Über Induktion von Embryonalanlagen durch Implantation artfremder Organisatoren. *Archiv für mikroskopische Anatomie und Entwicklungsmechanik* **100**, 599–638 (1924).
16. Waddington, C. H. *The Strategy of the Genes*. (George Allen & Unwin Ltd., 1957).
17. Mather, K. & de Winton, D. Adaptation and Counter-Adaptation of the Breeding System in *Primula*. *Ann. Bot.* **5**, 297–311 (1941).
18. Zuckerkandl, E. & Villet, R. Concentration-affinity equivalence in gene regulation: convergence of genetic and environmental effects. *Proc. Natl. Acad. Sci. U. S. A.* **85**, 4784–4788 (1988).
19. Goldschmidt, R. Gen und Ausseneigenschaft. *Zeitschrift für Induktive Abstammungs- und Vererbungslehre* **69**, 38–131 (1938).
20. Waddington, C. H. Genetic assimilation of an acquired character. *Evolution* **7**, 118–126 (1953).
21. Fanti, L., Piacentini, L., Cappucci, U., Casale, A. M. & Pimpinelli, S. Canalization

by Selection of de Novo Induced Mutations. *Genetics* **206**, 1995–2006 (2017).

22. Waddington, C. H. Canalization of Development and the Inheritance of Acquired Characters. *Nature* **150**, 563 (1942).
23. Mayley, G. Guiding or hiding: Explorations into the effects of learning on the rate of evolution. in *Proceedings of the Fourth European Conference on Artificial Life* **97**, 135–144 (Bradford Books/MIT Press, 1997).
24. Johnston, T. D. Selective Costs and Benefits in the Evolution of Learning. in *Advances in the Study of Behavior* (eds. Rosenblatt, J. S., Hinde, R. A., Beer, C. & Busnel, M.-C.) **12**, 65–106 (Academic Press, 1982).
25. Ghalambor, C. K. *et al.* Non-adaptive plasticity potentiates rapid adaptive evolution of gene expression in nature. *Nature* **525**, 372–375 (2015).
26. van Gestel, J. & Weissing, F. J. Is plasticity caused by single genes? *Nature* **555**, E19–E20 (2018).
27. Mallard, F., Jakšić, A. M. & Schlötterer, C. Contesting the evidence for non-adaptive plasticity. *Nature* **555**, E21–E22 (2018).
28. Lloyd Morgan, C. On modification and variation. *Science* **4**, 733–740 (1896).
29. Baldwin, J. M. A new factor in evolution. *Science* **4**, 139 (1896).
30. Gibert, J.-M. The flexible stem hypothesis: evidence from genetic data. *Dev. Genes Evol.* **227**, 297–307 (2017).
31. Schneider, R. F. & Meyer, A. How plasticity, genetic assimilation and cryptic genetic variation may contribute to adaptive radiations. *Mol. Ecol.* **26**, 330–350 (2017).
32. Levis, N. A. & Pfennig, D. W. Evaluating 'Plasticity-First' Evolution in Nature: Key Criteria and Empirical Approaches. *Trends Ecol. Evol.* **31**, 563–574 (2016).

33. Gibson, G. & Dworkin, I. Uncovering cryptic genetic variation. *Nat. Rev. Genet.* **5**, 681–690 (2004).
34. Duret, L. & Mouchiroud, D. Determinants of substitution rates in mammalian genes: expression pattern affects selection intensity but not mutation rate. *Mol. Biol. Evol.* **17**, 68–74 (2000).
35. Ledón-Rettig, C. C., Pfennig, D. W., Chunco, A. J. & Dworkin, I. Cryptic genetic variation in natural populations: a predictive framework. *Integr. Comp. Biol.* **54**, 783–793 (2014).
36. David Van Dyken, J. & Wade, M. J. The genetic signature of conditional expression. *Genetics* **184**, 557–570 (2010).
37. West-Eberhard, M. J. Wasp societies as microcosms for the study of development and evolution. in *Natural History and Evolution of Paper-Wasps* (ed. MJ West-Eberhard, S. T.) 290–317 (Oxford University Press, 1996).
38. Ogawa, A., Streit, A., Antebi, A. & Sommer, R. J. A conserved endocrine mechanism controls the formation of dauer and infective larvae in nematodes. *Curr. Biol.* **19**, 67–71 (2009).
39. Riddle, D. L., Blumenthal, T., Meyer, B. J. & Priess, J. R. *The Dauer State*. (Cold Spring Harbor Laboratory Press, 1997).
40. Schroeder, N. E. *et al.* Dauer-specific dendrite arborization in *C. elegans* is regulated by KPC-1/Furin. *Curr. Biol.* **23**, 1527–1535 (2013).
41. Lee, H. *et al.* Nictation, a dispersal behavior of the nematode *Caenorhabditis elegans*, is regulated by IL2 neurons. *Nat. Neurosci.* **15**, 107–112 (2011).
42. Riddle, D. L., Swanson, M. M. & Albert, P. S. Interacting genes in nematode dauer larva formation. *Nature* **290**, 668–671 (1981).

43. Albert, P. S. & Riddle, D. L. Mutants of *Caenorhabditis elegans* that form dauer-like larvae. *Dev. Biol.* **126**, 270–293 (1988).

44. Vowels, J. J. & Thomas, J. H. Genetic analysis of chemosensory control of dauer formation in *Caenorhabditis elegans*. *Genetics* **130**, 105–123 (1992).

45. Yabe, T., Suzuki, N., Furukawa, T., Ishihara, T. & Katsura, I. Multidrug resistance-associated protein MRP-1 regulates dauer diapause by its export activity in *Caenorhabditis elegans*. *Development* **132**, 3197–3207 (2005).

46. Hu, P. J., Xu, J. & Ruvkun, G. Two membrane-associated tyrosine phosphatase homologs potentiate *C. elegans* AKT-1/PKB signaling. *PLoS Genet.* **2**, e99 (2006).

47. Hao, L., Acar, S., Evans, J., Ou, G. & Scholey, J. M. Analysis of intraflagellar transport in *C. elegans* sensory cilia. *Methods Cell Biol.* **93**, 235–266 (2009).

48. Birnby, D. A. *et al.* A transmembrane guanylyl cyclase (DAF-11) and Hsp90 (DAF-21) regulate a common set of chemosensory behaviors in *Caenorhabditis elegans*. *Genetics* **155**, 85–104 (2000).

49. Coburn, C. M. & Bargmann, C. I. A putative cyclic nucleotide-gated channel is required for sensory development and function in *C. elegans*. *Neuron* **17**, 695–706 (1996).

50. Sze, J. Y., Victor, M., Loer, C., Shi, Y. & Ruvkun, G. Food and metabolic signalling defects in a *Caenorhabditis elegans* serotonin-synthesis mutant. *Nature* **403**, 560–564 (2000).

51. Ren, P. *et al.* Control of *C. elegans* larval development by neuronal expression of a TGF-beta homolog. *Science* **274**, 1389–1391 (1996).

52. Kimura, K. D., Tissenbaum, H. A., Liu, Y. & Ruvkun, G. *daf-2*, an insulin

receptor-like gene that regulates longevity and diapause in *Caenorhabditis elegans*. *Science* **277**, 942–946 (1997).

53. Antebi, A., Yeh, W. H., Tait, D., Hedgecock, E. M. & Riddle, D. L. *daf-12* encodes a nuclear receptor that regulates the dauer diapause and developmental age in *C. elegans*. *Genes Dev.* **14**, 1512–1527 (2000).
54. Fielenbach, N. & Antebi, A. *C. elegans* dauer formation and the molecular basis of plasticity. *Genes Dev.* **22**, 2149–2165 (2008).
55. Fuchs, G. Die Naturgeschichte der Nematoden und einiger anderer Parasiten 1. des *Ips typographus* L. 2. des *Hylobius abietis* L. *Zool. Jahrb.* **38**, 109–222 (1915).
56. Bongers, T. The Maturity Index, the evolution of nematode life history traits, adaptive radiation and cp-scaling. *Plant Soil* **212**, 13–22 (1999).
57. Srinivasan, J. *et al.* The draft genome and transcriptome of *Panagrellus redivivus* are shaped by the harsh demands of a free-living lifestyle. *Genetics* **193**, 1279–1295 (2013).
58. Ivanova, E., Perfilieva, K. & Spiridonov, S. *Panagrellus levitatus* sp. n. (Rhabditida: Panagrolaimidae), a nematode suppressing *Drosophila melanogaster* in laboratory cultures. *Nematology* **20**, 285–297 (2018).
59. Holterman, M. *et al.* Phylum-wide analysis of SSU rDNA reveals deep phylogenetic relationships among nematodes and accelerated evolution toward crown clades. *Mol. Biol. Evol.* **23**, 1792–1800 (2006).
60. Sultan, S. E. Phenotypic plasticity for plant development, function and life history. *Trends Plant Sci.* **5**, 537–542 (2000).
61. Whittaker, C. & Dean, C. The *FLC* Locus: A Platform for Discoveries in

Epigenetics and Adaptation. *Annu. Rev. Cell Dev. Biol.* **33**, 555–575 (2017).

62. Koornneef, M., Blankestijn-de Vries, H., Hanhart, C., Soppe, W. & Peeters, T. The phenotype of some late-flowering mutants is enhanced by a locus on chromosome 5 that is not effective in the Landsberg *erecta* wild-type. *Plant J.* **6**, 911–919 (1994).
63. Lee, I., Michaels, S. D., Masshardt, A. S. & Amasino, R. M. The late-flowering phenotype of *FRIGIDA* and mutations in *LUMINIDEPENDENS* is suppressed in the Landsberg *erecta* strain of *Arabidopsis*. *Plant J.* **6**, 903–909 (1994).
64. Napp-Zinn, K. Untersuchungen Zur Genetik Des Kältebedürfnisses Bei *Arabidopsis thaliana*. *Z. Indukt. Abstamm. Vererbungsl.* **88**, 253–285 (1957).
65. Johanson, U. *et al.* Molecular analysis of *FRIGIDA*, a major determinant of natural variation in *Arabidopsis* flowering time. *Science* **290**, 344–347 (2000).
66. Geraldo, N., Bäurle, I., Kidou, S.-I., Hu, X. & Dean, C. FRIGIDA delays flowering in *Arabidopsis* via a cotranscriptional mechanism involving direct interaction with the nuclear cap-binding complex. *Plant Physiol.* **150**, 1611–1618 (2009).
67. Choi, K. *et al.* The FRIGIDA complex activates transcription of *FLC*, a strong flowering repressor in *Arabidopsis*, by recruiting chromatin modification factors. *Plant Cell* **23**, 289–303 (2011).
68. Gu, X. *et al. Arabidopsis* homologs of retinoblastoma-associated protein 46/48 associate with a histone deacetylase to act redundantly in chromatin silencing. *PLoS Genet.* **7**, e1002366 (2011).
69. Liu, F., Marquardt, S., Lister, C., Swiezewski, S. & Dean, C. Targeted 3' processing of antisense transcripts triggers *Arabidopsis FLC* chromatin silencing. *Science* **327**, 94–97 (2010).

70. Sun, Q., Csorba, T., Skourti-Stathaki, K., Proudfoot, N. J. & Dean, C. R-loop stabilization represses antisense transcription at the *Arabidopsis FLC* locus. *Science* **340**, 619–621 (2013).

71. Marquardt, S. *et al.* Functional consequences of splicing of the antisense transcript *COOLAIR* on *FLC* transcription. *Mol. Cell* **54**, 156–165 (2014).

72. Rosa, S., Duncan, S. & Dean, C. Mutually exclusive sense–antisense transcription at *FLC* facilitates environmentally induced gene repression. *Nat. Commun.* **7**, 13031 (2016).

73. Yang, H., Howard, M. & Dean, C. Antagonistic roles for H3K36me3 and H3K27me3 in the cold-induced epigenetic switch at *Arabidopsis FLC*. *Curr. Biol.* **24**, 1793–1797 (2014).

74. De Lucia, F., Crevillen, P., Jones, A. M. E., Greb, T. & Dean, C. A PHD-polycomb repressive complex 2 triggers the epigenetic silencing of *FLC* during vernalization. *Proc. Natl. Acad. Sci. U. S. A.* **105**, 16831–16836 (2008).

75. Sung, S. *et al.* Epigenetic maintenance of the vernalized state in *Arabidopsis thaliana* requires LIKE HETEROCHROMATIN PROTEIN 1. *Nat. Genet.* **38**, 706–710 (2006).

76. Arrow, G. J. *Horned Beetles: A Study of the Fantastic in Nature*. (Springer-Science+Business Media, B.V., 1951).

77. Emlen, D. J. Artificial Selection on Horn Length-Body Size Allometry in the Horned Beetle *Onthophagus acuminatus* (Coleoptera: Scarabaeidae). *Evolution* **50**, 1219–1230 (1996).

78. Moczek, A. P. Integrating micro- and macroevolution of development through the study of horned beetles. *Heredity* **97**, 168–178 (2006).

79. Emlen, D. J. & Nijhout, H. F. Hormonal control of male horn length dimorphism in the dung beetle *Onthophagus taurus* (Coleoptera: Scarabaeidae). *J. Insect Physiol.* **45**, 45–53 (1999).

80. Emlen, D. J. & Nijhout, H. F. Hormonal control of male horn length dimorphism in *Onthophagus taurus* (Coleoptera: Scarabaeidae): a second critical period of sensitivity to juvenile hormone. *J. Insect Physiol.* **47**, 1045–1054 (2001).

81. Moczek, A. P. & Nijhout, H. F. Developmental mechanisms of threshold evolution in a polyphenic beetle. *Evol. Dev.* **4**, 252–264 (2002).

82. Sheng, Z., Xu, J., Bai, H., Zhu, F. & Palli, S. R. Juvenile hormone regulates vitellogenin gene expression through insulin-like peptide signaling pathway in the red flour beetle, *Tribolium castaneum*. *J. Biol. Chem.* **286**, 41924–41936 (2011).

83. Mirth, C. K. *et al.* Juvenile hormone regulates body size and perturbs insulin signaling in *Drosophila*. *Proc. Natl. Acad. Sci. U. S. A.* **111**, 7018–7023 (2014).

84. Casasa, S. & Moczek, A. P. Insulin signalling's role in mediating tissue-specific nutritional plasticity and robustness in the horn-polyphenic beetle *Onthophagus taurus*. *Proceedings of the Royal Society B: Biological Sciences* **285**, 20181631 (2018).

85. Kijimoto, T. & Moczek, A. P. Hedgehog signaling enables nutrition-responsive inhibition of an alternative morph in a polyphenic beetle. *Proc. Natl. Acad. Sci. U. S. A.* **113**, 5982–5987 (2016).

86. Kijimoto, T., Moczek, A. P. & Andrews, J. Diversification of *doublesex* function underlies morph-, sex-, and species-specific development of beetle horns. *Proc. Natl. Acad. Sci. U. S. A.* **109**, 20526–20531 (2012).

87. Ledón-Rettig, C. C., Zattara, E. E. & Moczek, A. P. Asymmetric interactions between *doublesex* and tissue- and sex-specific target genes mediate sexual dimorphism in beetles. *Nat. Commun.* **8**, 14593 (2017).
88. Lin, X. & Lavine, L. C. Endocrine regulation of a dispersal polymorphism in winged insects: a short review. *Curr Opin Insect Sci* **25**, 20–24 (2018).
89. Zera, A. J. & Tiebel, K. C. Brachypterizing effect of group rearing, juvenile hormone III and methoprene in the wing-dimorphic cricket, *Gryllus rubens*. *J. Insect Physiol.* **34**, 489–498 (1988).
90. Xu, H.-J. *et al.* Two insulin receptors determine alternative wing morphs in planthoppers. *Nature* **519**, 464–467 (2015).
91. Lin, X., Yao, Y., Wang, B., Lavine, M. D. & Lavine, L. C. FOXO links wing form polyphenism and wound healing in the brown planthopper, *Nilaparvata lugens*. *Insect Biochem. Mol. Biol.* **70**, 24–31 (2016).
92. Lin, X. *et al.* JNK signaling mediates wing form polymorphism in brown planthoppers (*Nilaparvata lugens*). *Insect Biochem. Mol. Biol.* **73**, 55–61 (2016).
93. Jemielity, S., Chapuisat, M., Parker, J. D. & Keller, L. Long live the queen: studying aging in social insects. *Age* **27**, 241–248 (2005).
94. Berens, A. J., Hunt, J. H. & Toth, A. L. Comparative transcriptomics of convergent evolution: different genes but conserved pathways underlie caste phenotypes across lineages of eusocial insects. *Mol. Biol. Evol.* **32**, 690–703 (2015).
95. Yan, H. *et al.* An Engineered *orco* Mutation Produces Aberrant Social Behavior and Defective Neural Development in Ants. *Cell* **170**, 736–747.e9 (2017).
96. Trible, W. *et al. orco* Mutagenesis Causes Loss of Antennal Lobe Glomeruli and

Impaired Social Behavior in Ants. *Cell* **170**, 727–735.e10 (2017).

97. Hunt, J. H., Mutti, N. S., Havukainen, H., Henshaw, M. T. & Amdam, G. V. Development of an RNA interference tool, characterization of its target, and an ecological test of caste differentiation in the eusocial wasp *Polistes*. *PLoS One* **6**, e26641 (2011).
98. Hattori, A. *et al.* Soldier Morphogenesis in the Damp-Wood Termite Is Regulated by the Insulin Signaling Pathway. *J. Exp. Zool.* **320**, 295–306 (2013).
99. Kamakura, M. Royalactin induces queen differentiation in honeybees. *Nature* **473**, 478–483 (2011).
100. Wolschin, F., Mutti, N. S. & Amdam, G. V. Insulin receptor substrate influences female caste development in honeybees. *Biol. Lett.* **7**, 112–115 (2011).
101. Mutti, N. S. *et al.* IRS and TOR nutrient-signaling pathways act via juvenile hormone to influence honey bee caste fate. *J. Exp. Biol.* **214**, 3977–3984 (2011).
102. Wang, Y., Azevedo, S. V., Hartfelder, K. & Amdam, G. V. Insulin-like peptides (AmILP1 and AmILP2) differentially affect female caste development in the honey bee (*Apis mellifera* L.). *J. Exp. Biol.* **216**, 4347–4357 (2013).
103. Patel, A. *et al.* The making of a queen: TOR pathway is a key player in diphenic caste development. *PLoS One* **2**, e509 (2007).
104. Robinson, G. E. & Vargo, E. L. Juvenile hormone in adult eusocial Hymenoptera: gonadotropin and behavioral pacemaker. *Arch. Insect Biochem. Physiol.* **35**, 559–583 (1997).
105. Corona, M. *et al.* Vitellogenin, juvenile hormone, insulin signaling, and queen honey bee longevity. *Proc. Natl. Acad. Sci. U. S. A.* **104**, 7128–7133 (2007).

106. Guidugli, K. R. *et al.* Vitellogenin regulates hormonal dynamics in the worker caste of a eusocial insect. *FEBS Lett.* **579**, 4961–4965 (2005).
107. Sommer, R. J. & McGaughran, A. The nematode *Pristionchus pacificus* as a model system for integrative studies in evolutionary biology. *Mol. Ecol.* **22**, 2380–2393 (2013).
108. Rota-Stabelli, O., Daley, A. C. & Pisani, D. Molecular timetrees reveal a Cambrian colonization of land and a new scenario for ecdysozoan evolution. *Curr. Biol.* **23**, 392–398 (2013).
109. Prabh, N. *et al.* Deep taxon sampling reveals the evolutionary dynamics of novel gene families in *Pristionchus* nematodes. *Genome Res.* **28**, 1664–1674 (2018).
110. Andrássy, I. *Free-living nematodes of Hungary*. **1**, (Hungarian Natural History Museum, 2005).
111. Yeates, G. W., Bongers, T., de Goede, R. G. M. & Freckman, D. W. Feeding Habits in Soil Nematode Families and Genera - An Outline for Soil Ecologists. *J. Nematol.* **25**, 315–331 (1993).
112. Ragsdale, E. J., Kanzaki, N. & Herrmann, M. Taxonomy and natural history: the genus *Pristionchus*. in *Pristionchus pacificus: A Nematode Model for Comparative and Evolutionary Biology* (ed. Sommer, R. J.) 77–120 (BRILL, 2015).
113. Susoy, V. *et al.* Large-scale diversification without genetic isolation in nematode symbionts of figs. *Sci Adv* **2**, e1501031 (2016).
114. Fürst von Lieven, A. & Sudhaus, W. Comparative and functional morphology of the buccal cavity of Diplogastrina (Nematoda) and a first outline of the phylogeny of this taxon. *J. Zoolog. Syst. Evol. Res.* **38**, 37–63 (2000).

115. Sommer, R. J., Carta, L. K., Seong-Youn, K. & Sternberg, P. W. Morphological, genetic and molecular description of *Pristionchus pacificus* sp. n. (Nematoda: Neodiplogastridae). *Fundam. appl. Nematol.* **19**, 511–521 (1996).

116. Wilecki, M., Lightfoot, J. W., Susoy, V. & Sommer, R. J. Predatory feeding behaviour in *Pristionchus* nematodes is dependent on phenotypic plasticity and induced by serotonin. *J. Exp. Biol.* **218**, 1306–1313 (2015).

117. Fürst von Lieven, A. *Koerneria sudhausi* n. sp. (Nematoda: Diplogastridae); a hermaphroditic diplogastrid with an egg shell formed by zygote and uterine components. *Nematology* **10**, 27–45 (2008).

118. Serobyan, V., Ragsdale, E. J. & Sommer, R. J. Adaptive value of a predatory mouth-form in a dimorphic nematode. *Proc. Biol. Sci.* **281**, 20141334 (2014).

119. Werner, M. S. *et al.* Environmental influence on *Pristionchus pacificus* mouth form through different culture methods. *Sci. Rep.* **7**, 7207 (2017).

120. Sanghvi, G. V. *et al.* Life History Responses and Gene Expression Profiles of the Nematode *Pristionchus pacificus* Cultured on *Cryptococcus* Yeasts. *PLoS One* **11**, e0164881 (2016).

121. Susoy, V., Ragsdale, E. J., Kanzaki, N. & Sommer, R. J. Rapid diversification associated with a macroevolutionary pulse of developmental plasticity. *Elife* **4**, e05463 (2015).

122. Bento, G., Ogawa, A. & Sommer, R. J. Co-option of the hormone-signalling module dafachronic acid-DAF-12 in nematode evolution. *Nature* **466**, 494–499 (2010).

123. Bose, N. *et al.* Complex small-molecule architectures regulate phenotypic plasticity in a nematode. *Angew. Chem. Int. Ed Engl.* **51**, 12438–12443 (2012).

124. Werner, M. S., Claaßen, M. H., Renahan, T., Dardiry, M. & Sommer, R. J. Adult Influence on Juvenile Phenotypes by Stage-Specific Pheromone Production. *iScience* **10**, 123–134 (2018).

125. Ragsdale, E. J., Müller, M. R., Rödelsperger, C. & Sommer, R. J. A Developmental Switch Coupled to the Evolution of Plasticity Acts through a Sulfatase. *Cell* **155**, 922–933 (2013).

126. Kieninger, M. R. *et al.* The Nuclear Hormone Receptor NHR-40 Acts Downstream of the Sulfatase EUD-1 as Part of a Developmental Plasticity Switch in *Pristionchus*. *Curr. Biol.* **26**, 2174–2179 (2016).

127. Bui, L. T., Ivers, N. A. & Ragsdale, E. J. A sulfotransferase dosage-dependently regulates mouthpart polyphenism in the nematode Pristionchus pacificus. *Nat. Commun.* **9**, 4119 (2018).

128. Namdeo, S. *et al.* Two independent sulfation processes regulate mouth-form plasticity in the nematode *Pristionchus pacificus*. *Development* **145**, dev166272 (2018).

5. Appendix

OPEN BIOLOGY

rsob.royalsocietypublishing.org

Review

Cite this article: Sommer RJ, Dardiry M, Lenuzzi M, Namdeo S, Renahan T, Sieriebriennikov B, Werner MS. 2017 The genetics of phenotypic plasticity in nematode feeding structures. *Open Biol.* **7**: 160332. http://dx.doi.org/10.1098/rsob.160332

Received: 12 December 2016
Accepted: 10 February 2017

Subject Area:
developmental biology/genetics

Keywords:
phenotypic plasticity, *Pristionchus pacificus*, switch genes, nuclear hormone receptors, epigenetics

Author for correspondence:
Ralf J. Sommer
e-mail: ralf.sommer@tuebingen.mpg.de

THE ROYAL SOCIETY PUBLISHING

The genetics of phenotypic plasticity in nematode feeding structures

Ralf J. Sommer, Mohannad Dardiry, Masa Lenuzzi, Suryesh Namdeo, Tess Renahan, Bogdan Sieriebriennikov and Michael S. Werner

Department for Integrative Evolutionary Biology, Max-Planck Institute for Developmental Biology, Spemannstrasse 37, 72076 Tübingen, Germany

RJS, 0000-0003-1503-7749

Phenotypic plasticity has been proposed as an ecological and evolutionary concept. Ecologically, it can help study how genes and the environment interact to produce robust phenotypes. Evolutionarily, as a facilitator it might contribute to phenotypic novelty and diversification. However, the discussion of phenotypic plasticity remains contentious in parts due to the absence of model systems and rigorous genetic studies. Here, we summarize recent work on the nematode *Pristionchus pacificus*, which exhibits a feeding plasticity allowing predatory or bacteriovorous feeding. We show feeding plasticity to be controlled by developmental switch genes that are themselves under epigenetic control. Phylogenetic and comparative studies support phenotypic plasticity and its role as a facilitator of morphological novelty and diversity.

1. Introduction

All organisms have to adapt to the environment and to environmental variation. Often, alternative conditions result in different expressions and values of traits, a phenomenon referred to as 'phenotypic plasticity'. Generally, phenotypic (or developmental) plasticity is defined as the property of a given genotype to produce different phenotypes depending on distinct environmental conditions [1,2]. In addition to being an ecological concept that allows studying how organisms respond to environmental variation, phenotypic plasticity also represents an integral part of the evolutionary process. Given these ecological and evolutionary implications, it is not surprising that the concept of phenotypic plasticity has been contentious ever since its introduction at the beginning of the 20th century. For some, plasticity is the major driver and facilitator of phenotypic diversification, and, as such, of greatest importance for understanding evolution and its underlying mechanisms [1–3]. For others, phenotypic plasticity represents environmental noise and is sometimes considered to even hinder evolution because environmentally induced variation may slow down the rate of adaptive processes [4,5]. This controversy largely depends on two limitations. First, there is confusion over the different types of plasticity found in nature. Plasticity can be adaptive or non-adaptive, reversible or irreversible, conditional or stochastic, and continuous or discrete, all of which require careful evaluations of examples of plasticity for their potential evolutionary significance. Second, the absence of plasticity model systems has long hampered the elucidation of potential molecular and genetic mechanisms, the identification of which would provide a framework for theoretical considerations.

In 1965, Bradshaw made one of the most important contributions to the concept of phenotypic plasticity when he proposed that plasticity must have a genetic basis. This idea grew out of the observation that the plasticity of a trait is independent of the phenotype of the plastic trait itself [6]. However, little progress was made to identify underlying mechanisms, largely due to the absence of laboratory model systems of plasticity. Here, we summarize recent studies on phenotypic plasticity of feeding structures in the nematode *Pristionchus pacificus*. The

Table 1. History of phenotypic plasticity.

Date	Scientist(s)	Theory
1909	Woltereck	reaction norm
1913	Johannsen	genotype–phenotype distinction
1940–1950	Waddington Schmalhausen	canalization/assimilation
1965	Bradshaw	genetic basis of plasticity
1998–2003	Schlichting/Pigliucci West-Eberhard	facilitator hypothesis

advantages of this system have allowed unbiased genetic approaches that provide detailed insight into the genetic control of plasticity and a molecular framework for studying the mechanisms of plasticity and genetic–environmental interactions. A model system approach in nematodes might therefore help clarify the role of plasticity in evolution by shedding light on its molecular mechanisms and macro-evolutionary potentials. We will start with a brief historical account of phenotypic plasticity and its role for the evolution of novelty.

2. A historical account

The history of phenotypic plasticity begins at the beginning of the 20th century (table 1) [7]. In 1909, Richard Woltereck carried out the first experiments on plastic characters using the water flea *Daphnia*. He coined the term 'reaction norm' (or norm of reaction) to describe the relationship between the expressions of phenotypes across a range of different environments [3]. However, it was Johannsen (1911) who first distinguished between genotype and phenotype, and thereby introduced the concept of genotype–environment interaction [8]. This concept was only developed further three decades later by the Russian biologist Schmalhausen and the British developmental biologist Waddington. In particular, Waddington, using environmental perturbation of development, provided important conceptual contributions [9]. For example, he introduced the concept of genetic assimilation based on his work with the bithorax and crossveinless phenotypes in *Drosophila*. When fly pupae were exposed to heat shock, some of them developed a crossveinless phenotype. Upon artificial selection for multiple generations, this trait became fixed in some animals even without heat shock. Similarly, when flies were treated with ether vapour, some exhibited a homeotic bithorax phenotype, which again could be fixed even without ether induction after artificial selection for approximately 20 generations. Waddington argued that genetic assimilation allows the environmental response of an organism to be incorporated into the developmental programme of the organism. While it is now known that the fixation of the bithorax phenotype was based on the selection of standing genetic variation at a homeotic gene [10], at the time these findings were controversially discussed and often referred to as Lamarckian mechanisms. Given the missing genetic foundation of development and plasticity in the 1940s, it is not surprising that Waddington's claim for an extended evolutionary synthesis found little support among neo-Darwinists [11].

The major conceptual advancement for plasticity research was in 1965 when Anthony Bradshaw proposed that phenotypic plasticity and the ability to express alternative phenotypes must be genetically controlled [6]. Some plants develop alternative phenotypes in response to extreme environmental conditions. Using a comparative approach, Bradshaw realized that the plasticity of a trait could differ between close relatives of the same genus, independent of the trait itself. From this observation he concluded that the genetic control of a character is independent of the character's plasticity. This remarkable conclusion represents one of the most important testimonies of the power of comparative approaches and the key foundation for modern studies of plasticity.

It is not surprising that botanists have paid detailed attention to reaction norm and plasticity for breeding purposes, and the first modern monographs that advertised the significance of phenotypic plasticity for development and evolution were written by active practitioners in this field [3]. Many examples of plasticity from animals are known as well, often in insects. The migratory locust *Schistocerca gregaria* can form two alternative phenotypes in relation to food availability. Adult *Schistocerca* are dark with large wings when food is abundant, whereas they are green with small wings when food is limited [12]. Similarly, many butterflies are known to form distinct wing patterns in the dry and rainy season in the tropics or in spring and summer in more temperate climates [13]. Perhaps the most spectacular examples of plasticity are those found in hymenopterans forming the basis for eusociality in insects and resulting in the most extreme forms of morphological and behavioural novelties. Mary-Jane West-Eberhard, after a long and active career studying social behaviours in Hymenoptera, proposed an extended evolutionary theory that links development and plasticity to evolution. Her monograph *Developmental plasticity and evolution* provides an exhaustive overview on alternative phenotypes in nature [2]. Building on the now available genetic understanding of developmental processes, she proposed plasticity to represent a major facilitator and driver for the evolution of novelty and the morphological and behavioural diversification in animals and plants.

This long path from Johannsen, Waddington and Bradshaw to current plasticity research has resulted in a strong conceptual framework for the potential significance of plasticity for evolution (table 1). However, scepticism remains, largely due to the near absence of associated genetic and molecular mechanisms of plasticity [14]. To overcome these limitations, plasticity research requires model systems that tie developmental plasticity in response to environmental perturbations to laboratory approaches. Before summarizing the recent inroads obtained in one laboratory model for phenotypic plasticity, the next paragraph will briefly summarize the different forms of plasticity.

3. Some important terminology: the different forms of plasticity

By definition, the concept of phenotypic plasticity incorporates many unrelated phenomena, which has resulted in enormous confusion and debate about its potential for evolutionary adaptations [15]. Three major distinctions are necessary to properly evaluate the potential significance of plasticity for evolution. First, phenotypic plasticity can be adaptive or non-adaptive, and only the former can contribute to adaptive evolution when organisms are faced with a new or altered environment.

In contrast, non-adaptive plasticity in response to extreme and often stressful environments is likely to result in maladaptive traits that are without evolutionary significance [15].

Second, plasticity can be continuous or discrete, the latter resulting in alternative phenotypes often referred to as polyphenisms. Such alternative phenotypes have several advantages for experimental analysis and evaluation in the field. Most importantly, alternative phenotypes can more readily be distinguished from genetic polymorphisms that can also result in phenotypic divergence. Multiple examples of polyphenisms from aerial and subterranean stem and leaf formation in water plants, insect wing and body form dimorphisms and the casts of social insects have been studied in detail to analyse the interaction between the genotype and the environment in the specification of plastic traits [2]. The binary readout of alternative phenotypes provides a major advantage of such experimental analyses.

Third, plasticity might be regulated by conditional and stochastic factors [16]. While the former is more common, additional stochastic elements of regulation are known in some examples of plasticity and such cases have several experimental advantages. Most examples of plasticity have environment *a* inducing phenotype **A** and environment *b* inducing phenotype **B**. However, organisms might form alternative phenotypes **A** and **B** in part due to stochastic factors that are independent of environmental alterations. The potential role of stochastic factors has been largely overlooked in plant and animal systems, but is well known in microbes. Phenotypic heterogeneity or bistability is known in many bacteria to result in phenotypically distinct subpopulations of cells [17,18]. Persister cell formation in *Staphylococcus aureus* and spore formation in *Bacillus subtilis* represent just a few examples of phenotypic heterogeneity that occur to a certain extent in a stochastic manner. Antibiotic resistance seen by persister cells resulted in detailed molecular and mechanistic insight into the stochastic regulation of phenotypic heterogeneity [19].

Adaptive versus non-adaptive, continuous versus discrete, and conditional versus stochastic regulation of plasticity represent important distinctions for the evaluation and significance of plastic traits in development and evolution. However, one additional factor that often complicates a proper evaluation of plasticity is the inherent difficulty to distinguish between genetic polymorphisms and polyphenisms. Genetic polymorphisms are a cornerstone of mainstream evolutionary theory for the generation of phenotypic divergence. Therefore, empirical studies on plasticity would profit from a proper distinction between polymorphisms and polyphenisms. Besides inbred lines in outbreeding species, self-fertilization in hermaphroditic organisms results in isogenic lines. Such isogenic lines can rule out contributions of genetic polymorphisms. Some plants, nematodes and other animals with a hermaphroditic mode of reproduction are therefore ideal for studies of plasticity, mimicking the isogenic advantages of bacteria with phenotypic heterogeneity.

In the following, we summarize recent insight into the genetic regulation of a mouth-form feeding plasticity in the nematode *P. pacificus*. This example of plasticity is adaptive, represents a dimorphic trait with two alternative phenotypes, and contains conditional and stochastic elements of regulation. *Pristionchus pacificus* is a hermaphroditic species with isogenic propagation, and is amenable to forward and reverse genetic analysis [20,21]. We begin with a brief summary of mouth-form polyphenism in this nematode species.

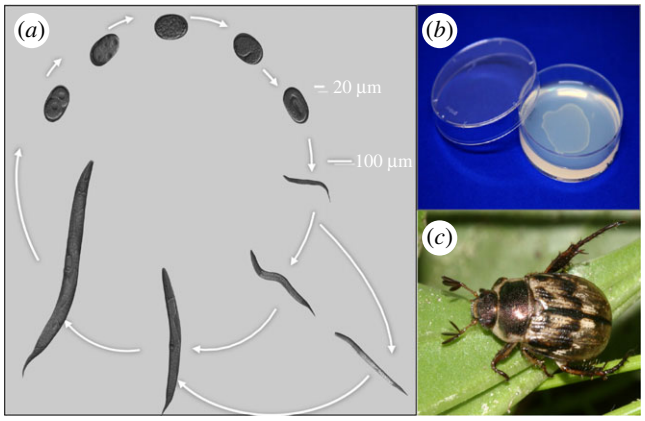

Figure 1. *Pristionchus pacificus* and growth. (*a*) Adult hermaphrodites lay eggs that develop through four larval stages to become adult. The first juvenile stage remains in the eggshell in *P. pacificus*. Under harsh and unfavourable conditions, worms develop into an arrested and long-lived dauer stage. (*b*) In the laboratory, worms are grown on agar plates with *Escherichia coli* as food source. Under these conditions, worms complete their direct life cycle in 4 days (20°). (*c*) The oriental beetle *Exomala orientalis* from Japan and the United States is one of the scarab beetle hosts on which *P. pacificus* is found in the dauer larval stage.

4. Mouth-form polyphenism as a case study

The genus *Pristionchus* belongs to the nematode family Diplogastridae, which shows entomophilic associations (figure 1) and omnivorous feeding strategies, including predation on other nematodes [22]. Usually, nematodes stay in the arrested dauer stage—a nematode-specific form of dormancy—in or on the insect vector (figure 1*a*). Nematode–insect associations represent a continuum between two most extreme forms, with dauer larvae of some species jumping on and off their carriers (phoresy), whereas others wait for the insect to die in order to resume development on the insect carcass (necromeny). Insect carcasses represent heterogeneous environments full of a variety of microbes. Such insect carcasses are best characterized by a boom and bust strategy of many of its inhabitants. While many nematodes, yeasts, protists and bacteria are known to proliferate on insect cadavers, few, if any, of these systems have been fully characterized, in particular with regard to species succession during decomposition.

Pristionchus pacificus and related nematodes live preferentially on scarab beetles (i.e. cockchafers, dung beetles and stag beetles; figure 1*c*) [23]. On living beetles, *P. pacificus* is found exclusively in the arrested dauer stage and decomposition experiments indicate that adult worms are found on the cadaver only 7 days after the beetle's death [24]. *Pristionchus* and other nematodes live on and wait for the beetle to die, resulting in enormous competition for food and survival on the carcass. It was long known that *Pristionchus* and other diplogastrid nematodes form teeth-like denticles in their mouths, which allow predatory feeding (figure 2*a*) [25]. Also, it was long known that many species form two alternative mouth-forms. In the case of *P. pacificus*, animals decide during larval development in an irreversible manner to adopt a eurystomatous (Eu) or a stenostomatous (St) mouth-form (figure 2*a*) [25]. Eu animals form two teeth with a wide buccal cavity, representing predators. In contrast, St animals have a single tooth with a narrow buccal cavity and are strict

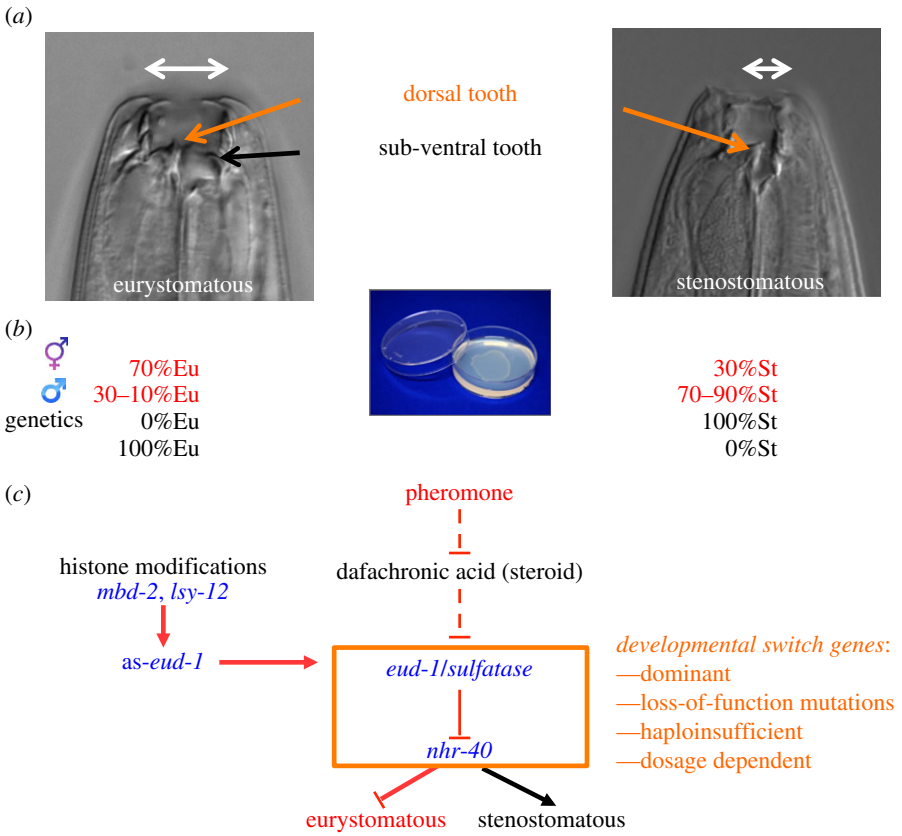

Figure 2. Genetic regulation of phenotypic plasticity of *P. pacificus* feeding structures. (*a*) Mouth dimorphism. During larval development, *P. pacificus* individuals make an irreversible decision to develop a eurystomatous morph with two teeth (orange and black arrows) and a broad buccal cavity (white arrow), or alternatively, a stenostomatous morph with a single dorsal tooth (orange arrow) and a narrow buccal cavity (white arrow). (*b*) Under fixed laboratory conditions, mouth-form plasticity shows stochastic regulation resulting in hermaphrodites having approximately 70% eurystomatous mouth-forms, whereas males have been 10–30% eurystomatous animals. In genetic screens, monomorphic mutants can be isolated that are either 100% stenostomatous or 100% eurystomatous. (*c*) Partial genetic network regulating mouth-form plasticity. The sulfatase-encoding *eud-1* gene and the nuclear hormone receptor are developmental switch mutations, which are dominant, *loss-of-function* and dosage dependent, resulting in all-stenostomatous or all-eurystomatous phenotypes, respectively. Small molecule signalling acts upstream of *eud-1* and involves pheromones and steroid hormone signalling, which are not a subject of this review. Histone modifications are crucial for mouth-form regulation and act through an antisense message at the *eud-1* locus (as-*eud-1*).

microbial feeders. Selection experiments have shown that the mouth-form dimorphism represents an example of phenotypic plasticity because isogenic animals can form both mouth-forms [25]. The dimorphism is discrete and adaptive with strong fitness effects preferring St and Eu animals under bacterial and predatory conditions, respectively [26,27]. Most importantly, mouth-form plasticity is regulated by conditional factors such as starvation and crowding [25], but also contains stochastic elements of regulation. Specifically, a nearly constant ratio of 70–90% Eu : 30–10% St animals is formed under fixed environmental conditions (figure 2*b*). It is this aspect of stochastic regulation resulting in the occurrence of both mouth-forms under standard laboratory conditions that allows manipulation of plasticity by genetic, molecular and chemical tools [16].

5. Genetics of nematode feeding plasticity

Pristionchus pacificus has been developed as a model system in evolutionary biology [20,21]. While only distantly related to *Caenorhabditis elegans*, it shares a number of features: self-fertilization, a short generation time of 4 days and monoxenic growth on *E. coli*. Adopting the functional toolkit of *C. elegans*, forward and reverse genetic tools are available in *P. pacificus*, including CRISPR-Cas9 genetic engineering and genetic transformation [28,29]. In addition, the known beetle association allowed a vast collection of *P. pacificus* strains and genomes to be catalogued [30,31].

Given the stochastic mouth-form dimorphism of wild-type *P. pacificus* animals when grown on bacteria, mutagenesis screens for monomorphic mutants can be performed to isolate strains deficient in the formation of one particular mouth-form (figure 2*b*). The first such unbiased genetic screen resulted in a *eu*rystomatous-form *d*efective mutant, *eud-1*, which turned out to be dominant and represents a developmental switch gene (figure 2*c*) [32]. Mutant *eud-1* animals are all-St, resulting in the complete absence of Eu animals. In contrast, overexpression of *eud-1* in wild-type or *eud-1* mutant animals reverts this phenotype to all-Eu. These and other experiments showed that *eud-1* is haploinsufficient and dosage dependent. *eud-1* alleles are dominant, and their all-St phenotype results from reduction-of-function, but not gain-of-function mutations. Consistently, *eud-1* mutant alleles were rescued with a wild-type copy of *eud-1*, whereas overexpression of a mutant copy of the gene did not result in any phenotype, as would usually be the case for gain-of-function mutations (figure 2*c*) [32].

A suppressor screen for Eu animals in an all-St *eud-1* mutant background resulted in the identification of the nuclear hormone receptor *nhr-40* (figure 2*c*) [33]. Interestingly, *nhr-40* is also part of the developmental switch constituting similar

genetic features but with an opposite phenotype to *eud-1*: *nhr-40* mutants are all-Eu, while overexpression results in all-St lines. *nhr-40* mutants are again dominant as loss-of-function mutants and haplo-insufficient. Thus, two genes regulating mouth-form plasticity show a dominant null or reduction-of-function phenotype. This is in strong contrast to the overall pattern in nematodes. Screens for dominant mutations in *C. elegans* resulted in many gain-of-function alleles, whereas *unc-108* represents the only gene that when mutated results in a dominant null phenotype, indicating haplo-insufficient genes to be rare [34].

Together, the experiments summarized above allow four major conclusions. First, unbiased genetic analysis of *P. pacificus* feeding plasticity indicates that plasticity is indeed under genetic control. *eud-1* and *nhr-40* mutants are monomorphic, being either all-St or all-Eu. Thus, genes affect mouth-form plasticity without affecting the character state itself; in *eud-1* mutants the St mouth-form is properly formed, similar to the Eu form in *nhr-40* mutant animals. Second, both genes are part of a developmental switch with loss-of-function and overexpression, resulting in complete but opposite phenotypes. Developmental switches had long been predicted to play an important role in plasticity regulation [2], but due to the previous absence of genetic models of plasticity, little genetic evidence was obtained. Third, *eud-1* and *nhr-40* are both located on the X chromosome. *Pristionchus pacificus* has an XO karyotype in males, similar to *C. elegans* [35]. Interestingly, males have predominantly a St mouth-form [25] and *eud-1* and *nhr-40* mutant males are all-St and all-Eu, respectively. Thus, *eud-1* and *nhr-40* escape male dosage compensation, a process that is just beginning to be investigated in *P. pacificus* [36]. Finally, it is interesting to note that *eud-1* resulted from a recent duplication [32]. While *C. elegans* contains one *eud-1*/sulfatase copy located on an autosome, *P. pacificus* contains three copies, with the two recently evolved genes being located on the X chromosome. However, CRISPR/Cas9-induced mutations in the two other *eud-1*-like genes in *P. pacificus* suggest that there are no specific phenotypes associated with the knockout of both genes [37].

6. Epigenetic control of switch genes

Two common aspects of *eud-1* and *nhr-40* mutants resulting in monomorphic, plasticity-defective phenotypes are that they show no other obvious phenotypes. In contrast, an unbiased search for mouth-form defects in a collection of mutants previously isolated for their egg-laying- or vulva-defective phenotypes identified *mbd-2* and *lsy-12* mutants to resemble an all-St *eud-1*-like phenotype [38]. *mbd-2* is egg-laying-defective and encodes a member of the methyl-binding protein family that is strongly reduced in *C. elegans* but not in *P. pacificus* [39,40]. *lsy-12* encodes a conserved histone-acetyltransferase, and *mbd-2* and *lsy-12* mutants were shown to result in massive histone modification defects involving multiple gene activation marks, such as H3K4me3, H3K9ac and H3K27ac [38]. Given that *mbd-2*, *lsy-12* and *eud-1* mutants have nearly identical mouth-form monomorphism, *eud-1* was itself a potential target for histone modification, and indeed *eud-1* expression is downregulated in *mbd-2* and *lsy-12* mutants. Interestingly, however, histone modification defects affect an antisense message at the *eud-1* locus, and overexpression experiments with this as-*eud-1* transcript suggest that as-*eud-1* positively regulates *eud-1* expression [38]. Together, these findings strongly suggest that the developmental switch is under epigenetic control. In principle, the epigenetic regulation of a switch mechanism is ideally suited to incorporate environmental information and environmental variation. However, information about associated mechanisms in *P. pacificus* awaits future studies, whereas several studies in insects recently already indicated the involvement of epigenetic mechanisms in gene-environmental interactions [41–43]. In conclusion, the use of forward genetic approaches in a laboratory model system provide strong evidence for the regulation of nematode feeding plasticity by developmental switch genes. Furthermore, epigenetic mechanisms including histone modifications and antisense RNA-mediated regulation might be crucial for gene–environment interactions.

7. Macro-evolutionary potentials

The genetic and epigenetic control of feeding plasticity in *P. pacificus* provides a basis to study how organisms sense and respond to the environment and to environmental variation. But is plasticity also important for evolution? Answering this question requires comparative studies that when performed in a phylogenetic context might provide insight into the significance of plasticity for evolutionary processes. Micro-evolutionary studies, by comparing many different wild isolates of *P. pacificus*, indicated strong differences in Eu : St ratios between isolates that correlated with *eud-1* expression [32]. Two recent studies have moved this analysis to the macro-evolutionary level, suggesting that phenotypic plasticity indeed facilitates rapid diversification. Susoy and co-workers studied the evolution of feeding structures in more than 90 nematode species using geometric morphometrics [44]. These species included dimorphic taxa, such as *P. pacificus*, but also monomorphic species that never evolved feeding plasticity, such as *C. elegans* (primary monomorphic), and those that had secondarily lost it (secondary monomorphic). This study found that feeding dimorphism was indeed associated with a strong increase in complexity of mouth-form structures [44]. At the same time, the subsequent assimilation of a single mouth-form phenotype (secondary monomorphism) coincided with a decrease in morphological complexity, but an increase in evolutionary rates. Thus, the gain and loss of feeding plasticity have led to increased diversity in these nematodes [8].

A second case of mouth-form plasticity increasing morphological diversification came from a striking example of fig-associated *Pristionchus* nematodes. Besides the worldwide branch of the genus that is associated with scarab beetles (currently more than 30 species), a recent study identified *Pristionchus* species, such as *P. borbonicus*, that live in association with fig wasps and figs [16]. These nematodes are extraordinarily diverse in their mouth morphology for two reasons. First, *P. borbonicus* and others form five distinct mouth-forms that occur in succession in developing fig synconia, thereby increasing the polyphenism from two to five distinct morphs. Second, the morphological diversity of these five morphs exceeds that of several higher taxa, although all five morphs are formed by the same species [16]. These findings strongly support the facilitator hypothesis, and they also indicate that ecological diversity can be maintained in the absence of genetic variation as all this diversity is seen within a single species and without associated speciation and radiation events [45].

8. Perspective

Phenotypic plasticity represents a striking phenomenon observed in organisms of all domains of life. It has been a contentious concept and was partially dismissed by mainstream evolutionary theory because many unrelated phenomena have been inappropriately mixed under the same heading. Following and extending previous attempts by Ghalambor *et al*. [15], we have tried to clarify terminology to provide necessary distinctions that will help study and evaluate plasticity, and establish its significance for evolution. Second, the use of a laboratory model system approach has provided strong evidence for the genetic control of feeding plasticity in *P. pacificus*. This genetic framework can serve as a paradigm to study in detail how the same genotype interacts with the environment to control this plastic trait. Besides nematodes, insects and diverse plants are very important multicellular organisms for the study of phenotypic plasticity. In particular, work on butterfly wing patterns and the coloration of caterpillars, but also horn size in different beetles, provide powerful inroads in the proper evaluation of plasticity [46,47]. Together, these studies on plants, insects and nematodes will provide mechanistic insight into this fascinating biological principle and will help provide an extended framework for evolution.

Competing interests. We declare we have no competing interests.

Funding. The work described in this study was funded by the Max-Planck Society to R.J.S.

References

1. Pigliucci M. 2001 *Phenotypic plasticity: beyond nature and nurture: syntheses in ecology and evolution*. Baltimore, MD: Johns Hopkins University Press.
2. West-Eberhard MJ. 2003 *Developmental plasticity and evolution*. Oxford, UK: Oxford University Press.
3. Schlichting CD, Pigliucci M. 1998 *Phenotypic evolution*. Sunderland, MA: Sinauer Associates.
4. de Jong G. 2005 Evolution of phenotypic plasticity: patterns of plasticity and the emergence of ecotypes. *New Phytol.* **166**, 101–117. (doi:10.1111/j.1469-8137.2005.01322.x)
5. Wund MA. 2012 Assessing the impacts of phenotypic plasticity on evolution. *Integr. Comp. Biol.* **52**, 5–15. (doi:10.1093/icb/ics050)
6. Bradshaw AD. 1965 Evolutionary significance of phenotypic plasticity in plants. *Adv. Genet.* **13**, 115–155. (doi:10.1016/S0065-2660(08)60048-6)
7. Nicoglou A. 2015 Phenotypic plasticity: from microevolution to macroevolution. In *Handbook of evolutionary thinking in the sciences* (eds T Heams, P Huneman, G Lecointre, M Silberstein), pp. 285–318. Heidelberg, Germany: Springer.
8. Nijhout HF. 2015 To plasticity and back again. *Elife* **4**, e06995. (doi:10.7554/eLife.06995)
9. Waddington CH. 1959 Canalisation of development and genetic assimilation of acquired characters. *Nature* **183**, 1654–1655. (doi:10.1038/1831654a0)
10. Gibson G, Hogness DS. 1996 Effect of polymorphism in the *Drosophila* regulatory gene *Ultrabithorax* on homeotic stability. *Science* **271**, 200–203. (doi:10.1126/science.271.5246.200)
11. Amundson R. 2005 *The changing role of the embryo in evolutionary thought*. Cambridge, UK: Cambridge University Press.
12. Whitman DW, Ananthakrishnan TN. 2009 *Phenotypic plasticity in insects*. Plymouth, NH: Science Publishers.
13. Nijhout HF. 1991 *The development and evolution of butterfly wing patterns*. Washington, DC: Smithsonian Institution Press.
14. Laland K *et al.* 2014 Does evolutionary theory need a rethink? *Nature* **514**, 161–164. (doi:10.1038/514161a)
15. Ghalambor CK, McKay JK, Carroll SP, Reznick DN. 2007 Adaptive versus non-adaptive phenotypic plasticity and the potential for contemporary adaptation in new environments. *Funct. Ecol.* **21**, 394–407. (doi:10.1111/j.1365-2435.2007.01283.x)
16. Susoy V, Sommer RJ. 2016 Stochastic and conditional regulation of nematode mouth-form dimorphisms. *Front. Ecol. Evol.* **4**, 23. (doi:10.3389/fevo.2016.00023)
17. Dubnau D, Losick R. 2006 Bistability in bacteria. *Mol. Microbiol.* **61**, 564–572. (doi:10.1111/j.1365-2958.2006.05249.x)
18. de Jong IG, Haccou P, Kuipers OP. 2011 Bet hedging or not? A guide to proper classification of microbial survival strategies. *Bioessays* **33**, 215–223. (doi:10.1002/bies.201000127)
19. Smits WK, Kuipers OP, Veening JW. 2006 Phenotypic variation in bacteria: the role of feedback regulation. *Nat. Rev. Microbiol.* **4**, 259–271. (doi:10.1038/nrmicro1381)
20. Sommer RJ, McGaughran A. 2013 The nematode Pristionchus pacificus as a model system for integrative studies in evolutionary biology. *Mol. Ecol.* **22**, 2380–2393. (doi:10.1111/mec.12286)
21. Sommer RJ. 2015 Pristionchus pacificus*: a nematode model for comparative and evolutionary biology*. Leiden, Netherlands: Brill.
22. Kanzaki N, Giblin-Davis RM. 2015 Diplogastrid systematics and phylogeny. In Pristionchus pacificus*: a nematode model for comparative and evolutionary biology* (eds RJ Sommer), pp. 43–76. Leiden, Netherlands: Brill.
23. Ragsdale EJ. 2015 Mouth dimorphis and the evolution of novelty and diversity. In Pristionchus pacificus*: a nematode model for comparative and evolutionary biology* (ed. RJ Sommer), pp. 301–329. Leiden, Netherlands: Brill.
24. Meyer JM, Baskaran P, Quast C, Susoy V, Rödelsperger C, Glöckner FO, Sommer RJ. In press. Succession and dynamics of *Pristionchus* nematodes and their microbiome during decomposition of *Oryctes borbonicus* on La Réunion Islan. *Environ. Microbiol*. (doi:10.1111/1462-2920.13697)
25. Bento G, Ogawa A, Sommer RJ. 2010 Co-option of the hormone-signalling module dafachronic acid-DAF-12 in nematode evolution. *Nature* **466**, 494–497. (doi:10.1038/nature09164)
26. Serobyan V, Ragsdale EJ, Muller MR, Sommer RJ. 2013 Feeding plasticity in the nematode *Pristionchus pacificus* is influenced by sex and social context and is linked to developmental speed. *Evol. Dev.* **15**, 161–170. (10.1111/ede.12030)
27. Serobyan V, Ragsdale EJ, Sommer RJ. 2014 Adaptive value of a predatory mouth-form in a dimorphic nematode. *Proc. R. Soc. B* **281**, 20141334. (doi:10.1098/rspb.2014.1334)
28. Schlager B, Wang X, Braach G, Sommer RJ. 2009 Molecular cloning of a dominant roller mutant and establishment of DNA-mediated transformation in the nematode *Pristionchus pacificus*. *Genesis* **47**, 300–304. (doi:10.1002/dvg.20499)
29. Witte H, Moreno E, Rodelsperger C, Kim J, Kim JS, Streit A, Sommer RJ. 2015 Gene inactivation using the CRISPR/Cas9 system in the nematode *Pristionchus pacificus*. *Dev. Genes Evol.* **225**, 55–62. (doi:10.1007/s00427-014-0486-8)
30. Morgan K, McGaughran A, Villate L, Herrmann M, Witte H, Bartelmes G, Rochat J, Sommer RJ. 2012 Multi locus analysis of *Pristionchus pacificus* on La Reunion Island reveals an evolutionary history shaped by multiple introductions, constrained dispersal events and rare out-crossing. *Mol. Ecol.* **21**, 250–266. (doi:10.1111/j.1365-294X.2011.05382.x)
31. Rodelsperger C, Neher RA, Weller AM, Eberhardt G, Witte H, Mayer WE, Dieterich C, Sommer RJ. 2014 Characterization of genetic diversity in the nematode *Pristionchus pacificus* from population-scale resequencing data. *Genetics* **196**, 1153–1165. (doi:10.1534/genetics.113.159855)
32. Ragsdale EJ, Muller MR, Rodelsperger C, Sommer RJ. 2013 A developmental switch coupled to the evolution of plasticity acts through a sulfatase. *Cell* **155**, 922–933. (doi:10.1016/j.cell.2013.09.054)

33. Kieninger MR, Ivers NA, Rodelsperger C, Markov GV, Sommer RJ, Ragsdale EJ. 2016 The nuclear hormone receptor NHR-40 acts downstream of the sulfatase EUD-1 as part of a developmental plasticity switch in *Pristionchus*. *Curr. Biol.* **26**, 2174–2179. (doi:10.1016/j.cub.2016.06.018)
34. Park EC, Horvitz HR. 1986 Mutations with dominant effects on the behavior and morphology of the nematode *Caenorhabditis elegans*. *Genetics* **113**, 821–852.
35. Pires-daSilva A, Sommer RJ. 2004 Conservation of the global sex determination gene tra-1 in distantly related nematodes. *Genes Dev.* **18**, 1198–1208. (doi:10.1101/gad.293504)
36. Lo TW, Pickle CS, Lin S, Ralston EJ, Gurling M, Schartner CM, Bian Q, Doudna JA, Meyer BJ. 2013 Precise and heritable genome editing in evolutionarily diverse nematodes using TALENs and CRISPR/Cas9 to engineer insertions and deletions. *Genetics* **195**, 331–348. (doi:10.1534/genetics.113.155382)
37. Ragsdale EJ, Ivers NA. 2016 Specialization of a polyphenism switch gene following serial duplications in *Pristionchus* nematodes. *Evolution* **70**, 2155–2166. (doi:10.1111/evo.13011)
38. Serobyan V, Xiao H, Namdeo S, Rodelsperger C, Sieriebriennikov B, Witte H, Roseler W, Sommer RJ. 2016 Chromatin remodelling and antisense-mediated up-regulation of the developmental switch gene *eud-1* control predatory feeding plasticity. *Nat. Commun.* **7**, 12337. (doi:10.1038/ncomms12337)
39. Gutierrez A, Sommer RJ. 2004 Evolution of *dnmt-2* and *mbd-2*-like genes in the free-living nematodes *Pristionchus pacificus, Caenorhabditis elegans* and *Caenorhabditis briggsae*. *Nucleic Acids Res.* **32**, 6388–6396. (doi:10.1093/nar/gkh982)
40. Gutierrez A, Sommer RJ. 2007 Functional diversification of the nematode *mbd2/3* gene between *Pristionchus pacificus* and *Caenorhabditis elegans*. *BMC Genet.* **8**, 57. (doi:10.1186/1471-2156-8-57)
41. Simola DF *et al.* 2016 Epigenetic re(programming) of caste-specific behavior in the ant *Camponotus floridanus*. *Science* **351**, 37–39. (doi:10.1126/science.aac6633)
42. Gibert JM, Mouchel-Vielh E, De Castro S, Peronnet F. 2016 Phenotypic plasticity through transcriptional regulation of the evolutionary hotspot gene tan in *Drosophila melanogaster*. *PLoS Genet.* **12**, e1006218. (doi:10.1371/journal.pgen.1006218)
43. Kucharski R, Maleszka J, Foret S, Maleszka R. 2008 Nutritional control of reproductive status in honeybees via DNA methylation. *Science* **319**, 1827–1830. (doi:10.1126/science.1153069)
44. Susoy V, Ragsdale EJ, Kanzaki N, Sommer RJ. 2015 Rapid diversification associated with a macroevolutionary pulse of developmental plasticity. *Elife* **4**, e05463. (doi:10.7554/eLife.05463)
45. Phillips PC. 2016 Evolution: five heads are better than one. *Curr. Biol.* **26**, R283–R285. (doi:10.1016/j.cub.2016.02.048)
46. Emlen DJ, Hunt J, Simmons LW. 2005 Evolution of sexual dimorphism and male dimorphism in the expression of beetle horns: phylogenetic evidence for modularity, evolutionary lability, and constraint. *Am. Nat.* **166**(Suppl. 4), S42–S68. (doi:10.1086/444599)
47. Moczek AP, Sultan S, Foster S, Ledon-Rettig C, Dworkin I, Nijhout HF, Abouheif E, Pfennig DW. 2011 The role of developmental plasticity in evolutionary innovation. *Proc. R. Soc. B* **278**, 2705–2713. (doi:10.1098/rspb.2011.0971)

SCIENTIFIC REPORTS

OPEN

Environmental influence on *Pristionchus pacificus* mouth form through different culture methods

Received: 8 May 2017
Accepted: 28 June 2017
Published online: 03 August 2017

Michael S. Werner, Bogdan Sieriebriennikov, Tobias Loschko, Suryesh Namdeo, Masa Lenuzzi, Mohannad Dardiry, Tess Renahan, Devansh Raj Sharma & Ralf J. Sommer

Environmental cues can impact development to elicit distinct phenotypes in the adult. The consequences of phenotypic plasticity can have profound effects on morphology, life cycle, and behavior to increase the fitness of the organism. The molecular mechanisms governing these interactions are beginning to be elucidated in a few cases, such as social insects. Nevertheless, there is a paucity of systems that are amenable to rigorous experimentation, preventing both detailed mechanistic insight and the establishment of a generalizable conceptual framework. The mouth dimorphism of the model nematode *Pristionchus pacificus* offers the rare opportunity to examine the genetics, genomics, and epigenetics of environmental influence on developmental plasticity. Yet there are currently no easily tunable environmental factors that affect mouth-form ratios and are scalable to large cultures required for molecular biology. Here we present a suite of culture conditions to toggle the mouth-form phenotype of *P. pacificus*. The effects are reversible, do not require the costly or labor-intensive synthesis of chemicals, and proceed through the same pathways previously examined from forward genetic screens. Different species of *Pristionchus* exhibit different responses to culture conditions, demonstrating unique gene-environment interactions, and providing an opportunity to study environmental influence on a macroevolutionary scale.

Phenotypes can be dramatically influenced by environmental conditions experienced during development, a phenomenon referred to as developmental plasticity[1–3]. Examples of plastic phenotypes have been studied for nearly a century, including differences in morphology[4], sex and caste determination[5–7], and innate immunity[8]. However, despite long-held interest in the field, and decade's worth of progress linking genotype to phenotype, relatively little is known about the mechanisms connecting environment to phenotype. To study the mechanisms of environmental influence on phenotype, easily tunable methods to induce phenotypic changes and model organisms amenable to molecular biology techniques are required. For example, temperature and diet have been utilized to explore plasticity in insects and nematodes[9–14], some of which have revealed fundamental principles of dynamic gene regulation. In particular, investigating life cycle plasticity in *C. elegans* contributed to our understanding of nutrition and endocrine signaling[15–18], and the discovery of regulatory RNAs[19]. However, the number of case studies remains small, and heuristic insight of ecologically relevant phenotypes within an evolutionary framework is still lacking.

The model organism *P. pacificus* exhibits an environmentally sensitive developmental switch of its feeding structures[20]. In the wild *P. pacificus* exists in a dormant state (dauer) on beetles. When beetles die *Pristionchus* exits the dauer state to feed on decomposition bacteria, and proceeds to reproductive maturity[21,22] (Fig. 1A). While developing under crowded conditions a "wide-mouthed" eurystomatous (Eu) morph with two teeth is built, which allows adults to prey on other nematodes (Fig. 1B). Alternatively, a "narrow-mouthed" stenostomatous (St) morph with one tooth relegates diet exclusively to microorganisms (Fig. 1C). While Eu animals can exploit additional food sources[23] and attack and kill competitors[24], St animals mature slightly faster[25], creating a tradeoff of strategies depending on the environment perceived during development. Under monoxenic growth conditions in the laboratory using *Escherichia coli* OP50 bacteria as a food source on NGM-agar plates, 70–90% of the reference *P. pacificus* strain PS312 develop the Eu morph. Metabolic studies have elucidated compounds that affect this mouth-form decision. For example, the steroid hormone dafachronic acid shifts mouth-form frequencies to St[20]. Conversely, the pheromone dasc#1 shifts the frequency to Eu[26]. Recent mutant screens

Department of Evolutionary Biology, Max Planck Institute for Developmental Biology, 72076, Tübingen, Germany. Correspondence and requests for materials should be addressed to R.J.S. (email: ralf.sommer@tuebingen.mpg.de)

Figure 1. Life cycle and phenotypic plasticity of *Pristionchus pacificus*. (**A**) *P. pacificus* exist in a necromenic relationship with host beetles (i.e. shown here *Lucanus cervus*), and upon decomposition of the beetles the worms exit the dormant (dauer) state. Photo taken by M Herrmann and R Sommer. Depending on environmental conditions experienced during this period, adults develop either (**B**) a wide-mouth "eurystomatous" (Eu) morph with an additional tooth allowing them to prey on other nematodes, or (**C**) a microbivorous narrow mouth "stenostomatous" (St) morph. (**D**) Diagram integrating the environment into known gene-phenotype interactions of the *P. pacificus* mouth-form pathway.

have established several genes in the mouth-form regulatory pathway[27–29]. The sulfatase *eud-1* (*eu*rystomatous *d*efective) is a dosage-dependent "switch" gene[30]: *eud-1* mutants are 100% St, while overexpression of a *eud-1*

transgene confers 100% Eu[27]. The nuclear-hormone-receptor *Ppa-nhr-40* was identified as a suppressor of *eud-1*, and regulates downstream genes[28]. *C. elegans* homologs of the epigenetic enzymes acetyltransferase *lsy-12* and methyl-binding protein *mbd-2* have also been identified to control mouth-form plasticity, and are attractive factors for channeling environmental cues to changes in gene regulation. Both mutants led to global losses of activating-histone modifications, and decreased expression of *eud-1*[29].

Identification of these switch genes affords the opportunity to track regulatory mechanisms that respond to environmental cues[31,32]. Unfortunately, the application of small molecules to affect mouth-form ratios in large enough quantities for biochemical fractionation or epigenetic profiling (e.g. ChIP) is impractical given the labor and expense of chemical synthesis or purification. Moreover, it is difficult to obtain consistent mouth-form ratios with pharmacological compounds as they are in constant competition with endogenous hormones and pheromones[20]. Finally, while crowding/starvation can also induce the Eu morph, it is technically challenging to compare different population densities, or to synchronize starved vs. un-starved larvae. To adequately study environmental effects on phenotypic plasticity, cheap, consistent, and simple methods are needed that can tune mouth-form ratios in synchronized populations. Here, we establish a set of culture conditions to affect environmental influence on mouth form. These methods are fast, reproducible, and only require the differential application of buffer, and culturing state (solid vs. liquid). Intriguingly, different species of *Pristionchus* exhibit different response regimes, suggesting evolutionary divergence of gene-environment interactions.

Results

Liquid culture affects *Pristionchus pacificus* mouth-form. In order to accumulate large amounts of biological material for molecular and biochemical experiments we grew the laboratory California strain (PS312) of *P. pacificus* in liquid culture. To our surprise, this culture condition reversed the mouth-form phenotype from preferentially Eu to preferentially St. To better examine this observation we screened mouth-forms of adults representing a parental generation (P), and obtained[33] and split eggs evenly to either agar plates or liquid culture, and screened adults of the next generation (G1) (Fig. 2A). Reproducibly, this simple difference in culturing method led to a dramatic shift in mouth-form ratio (> 95% Eu on agar compared to ~10% Eu in liquid culture, $p < 0.001$, *paired t-test*) (Fig. 2B). Importantly, *P. pacificus* developed at similar rates in agar and liquid culture, allowing facile comparisons between conditions (Fig. 2C), and arguing against nutritional deprivation inducing the mouth-form shift. St animals have a slightly faster development than Eu animals when grown on agar[25], however we found developmental speed to be indistinguishable between morphs in liquid culture (Supplementary Fig. 1). The different environmental conditions present distinct energy requirements (eg. swimming and feeding on motile bacteria in 3-dimensional liquid culture) that might offset potential tradeoffs in resource allocation.

Next, we investigated whether the change in mouth-form ratio induced by liquid culture was capable of being inherited. The mouth-from ratio of adults was consistent with the culture method they developed in regardless of the culture method of the parental generation, suggesting the effect is not transgenerational (Fig. 2D). These results also demonstrate the immediate and robust nature of this plasticity, and similar experiments coupled to mutagenesis may be useful for identifying genes involved in the ability to sense and respond to changing environments.

Buffer components and culture state affect mouth form. To investigate the potential influence of culture conditions on mouth form we examined differences in buffer composition, and solid vs. liquid culturing state. In our previous experiments we had used standard liquid culture protocols for *C. elegans*[33], which utilize S media (S), whereas we normally grow *P. pacificus* on Nematode Growth Media (NGM) agar plates[33]. To assess the contribution of the chemical composition of the medium, as opposed to solid vs. liquid environments (hereafter referred to as 'culture state'), we performed reciprocal culture experiments. Nematodes that were grown on either S-agar or NGM-liquid exhibited intermediate mouth-form ratios ($51 \pm 5\%$ Eu and $38 \pm 13\%$ Eu, respectively, $p < 0.001$ relative to solid or liquid states of the same medium, *paired t-test*) (Table 1d,h,i,p), revealing a growth-medium composition effect. However, as these mouth-form ratios were in-between the extremes of NGM-agar and S-liquid, it also suggests other environmental factors are operating.

S medium contains phosphate (50 mM) and sulfate (14 mM) - both of which have previously been shown to affect mouth-form ratios at 120 mM[27]. To test whether this concentration of phosphate was causing the S-medium effect we made alternative formulations by replacing phosphate with 50 mM Tris ("T-Medium") or Hepes ("H-Medium"), pH 7.5. Liquid culture in T- and H-medium yielded reproducibly higher Eu ratios ($35 \pm 8\%$ and $28 \pm 10\%$, respectively, $p < 0.05$, *paired t-test*) (Table 1d–f), demonstrating a specific, albeit subtle contribution from phosphate. Furthermore, *P. pacificus* grown in axenic (without bacteria)[34], M9[33], or PBS (which does not contain sulfate) -based liquid cultures were all highly St (Table 1a–c). Although nematode survival rate was poor in PBS, and development was slowed in axenic culture (9–10 days for sexual maturation, rather than 3–4).

Rotation speed of liquid culture affects mouth form. Further exploration of liquid culture methodology revealed that decreasing the rotation per minute (rpm) also affected mouth-form ratios. Previous experiments that led to high St ratios had been performed at 180 rpm, but when shifted to "slow" speeds of 70 or 50 rpm, the mouth-form ratio shifted to an intermediate Eu bias ($55 \pm 11\%$ and $66 \pm 9\%$, respectively, $p < 0.05$, *t-test*) (Table 1j,l). The simplicity of changing rpm shaking-speed to affect mouth-form ratios is an intriguing environmental perturbation as other factors like food source, buffer, and culturing state are identical. When examined without bacteria, it became evident that at slow speeds (<90 rpm) nematodes aggregated in the center of the liquid column, whereas at higher speeds they were dispersed. When combined with conditions that exhibited intermediate St ratios the effects were additive, yielding up to $87 \pm 3\%$ Eu with NGM-liquid culture (Table 1k,m,n). The higher density of nematodes at slow speeds suggests that pheromones may be responsible. Consistent with this hypothesis, we passed multiple *P. pacificus* generations from one liquid culture to another,

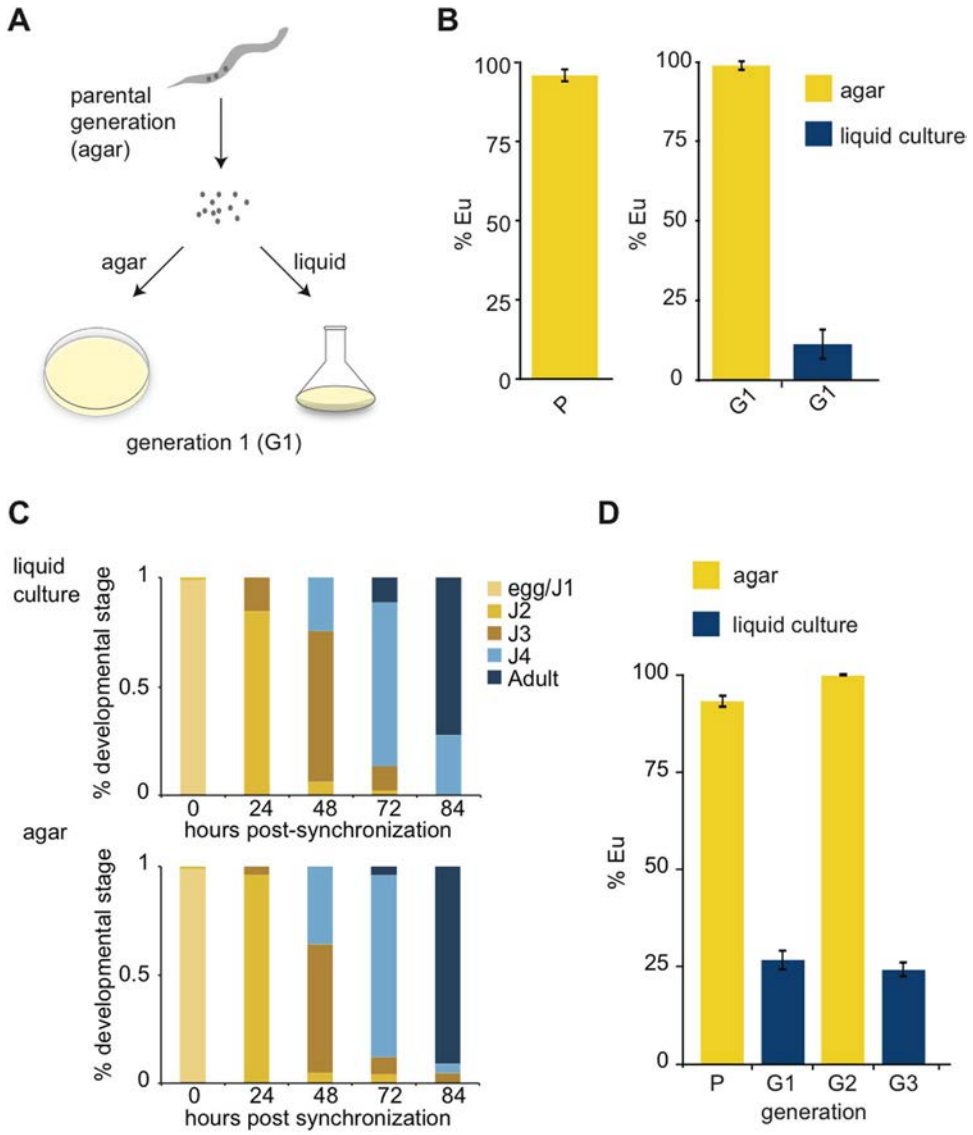

Figure 2. Different culture methods affect mouth-form phenotypic plasticity. (**A**) Diagram of experimental design to compare culture conditions from the same population after bleach synchronization. (**B**) Mouth-form ratios presented as percent eurystomatous (% Eu) from the parental generation (P) and the next generation (G1) grown in either liquid culture or agar plates, $n = 18$ biological replicates, $p < 0.05$, *students two-tailed t-test*, error bars represent SEM. (**C**) Developmental stages of bleach-synchronized *P. pacificus* in either agar plates or liquid culture. Bar graphs represent a typical experiment measuring >30 animals at the indicated time-points. (**D**) Mouth-form ratios of switching experiments between agar and liquid cultures. Nematodes were bleached between generations (P, G1, G2), and eggs-J1 larvae were passed to the next condition, $n = 3$, error bars represent SEM.

either by a 1:10 dilution, or by bleaching and washing. When passed by bleaching the next generation remained highly St ($8 \pm 4\%$). However when passed by dilution the next generation of worms exhibited intermediate Eu ratios ($51 \pm 16\%$, $p < 0.05$, *unpaired t-test*), perhaps because pheromones from the first generation were passed on to the second.

Liquid culture affects body morphology. We also observed morphological differences of body length and width between agar and liquid culture, demonstrating an additional plastic response (Supplementary Figure 2). Worms that develop in liquid culture exhibit longer, narrower bodies compared to worms that develop in agar, a phenomenon that has also been observed in *C. elegans*[33]. To disentangle whether the effect on mouth form is discrete or connected to the change in body shape we grew worms in NGG culture, which is intermediate between liquid and solid states[35]. Similar to liquid culture, adult worms grown in NGG exhibited a more slender body morphology than on agar plates ($p < 0.05$, Mann-Whitney), but they exhibited the highly Eu mouth-form ratio of worms grown in agar culture (Supplementary Fig. 2, Table 1d,o,p). While it is difficult to completely exclude the possibility that they are connected, there is no obvious correlation between the St mouth form and

	Condition	% Eu	S.E.M.
A	LC PBS, 180 rpm	7	3.2
B	LC Axenic Culture, 180 rpm	8.8	8.8
C	LC M9, 180 rpm	11.5	6.2
D	LC S-medium, 180 rpm	12.8	3.2
E	LC H-medium, 180 rpm	28	10.1
F	LC T-medium, 180 rpm	35	7.6
G	LC S-medium, 100 rpm	35.2	3
H	LC NGM, 180 rpm	37.8	12.9
I	AG S-medium	51.4	5.4
J	LC S-medium, 70 rpm	55.1	10.9
K	LC T-medium, 50 rpm	61.5	16.9
L	LC S-medium, 50 rpm	65.9	9
M	LC H-medium, 50 rpm	70.6	15
N	LC NGM, 50 rpm	87.3	3.3
O	NGG	97.1	2.5
P	AG NGM	98.7	0.7

Table 1. Buffer/ions and physical culture state affect mouth-form phenotype. A panel of culturing methods covers phenotypic ratios from ~10–99% Eu. LC = liquid culture, AG = agar, T and H medium = S-medium with phosphate replaced with 50 mM Tris or HEPES, pH 7.5, respectively, NGG = NGM with agar replaced with Gelrite/Gelzan CM (Sigma)[35]. $N \geq 3$ biological replicates per condition, and standard error mean (SEM) is presented in the last column. Mouth-form phenotypes were assessed 4–5 days after bleach-synchronization (see Methods).

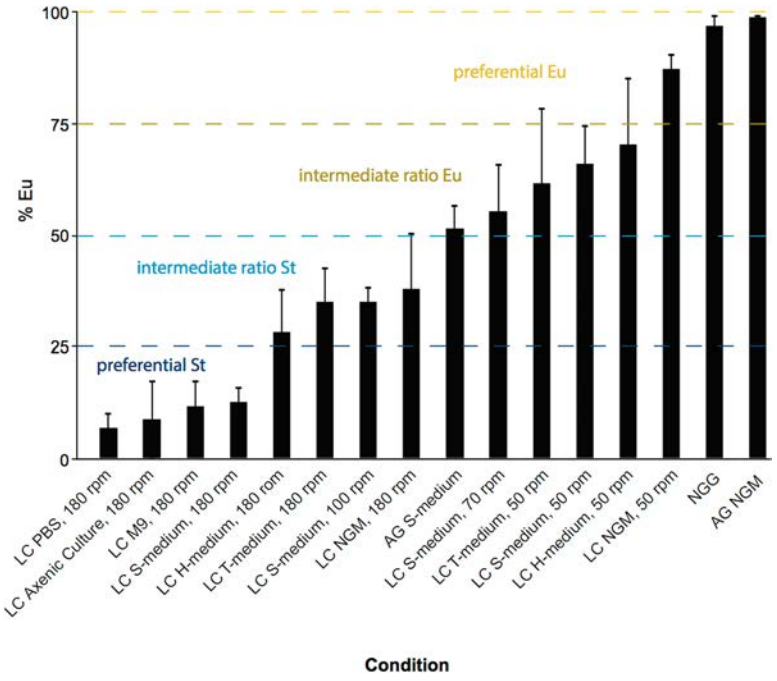

Figure 3. Comprehensive evaluation of culture method on mouth-form ratio in *P. pacificus*. Same data as in Table 1, but presented according to gradation of effect on mouth-form phenotype, from low to high % eurystomatous. LC = liquid culture, AG = agar, T and H medium = S-medium with phosphate replaced with 50 mM Tris or HEPES, pH 7.5, respectively, NGG = NGM with agar replaced with Gelrite/Gelzan CM (Sigma)[35]. Error bars represent standard error mean (SEM) for different biological replicates ($n \geq 3$, Methods).

slender morphology observed in liquid culture. Therefore, it seems these two instances of phenotypic plasticity are under distinct regulation.

Collectively, we have established a broad range of culturing methods that allow the acquisition of almost any mouth-form ratio from an isogenic strain (Fig. 3). A variety of liquid culture conditions, including buffers without phosphates or sulfates, exhibited an effect on mouth form, suggesting an unknown environmental effect that is perhaps specific to solid or liquid states.

Liquid culture acts upstream of known switch genes. Next, we sought to place the environmental effects of liquid culture relative to known genetic and environmental factors. First, we examined whether liquid culture had an effect on mutants that are 100% Eu on agar plates[27,28]. Animals from a *eud-1* overexpression line and *Ppa-nhr-40* mutant line remained 100% Eu in liquid culture, arguing that these genes act downstream of the environmental effect of liquid culture (Fig. 4A). Next, we assessed whether the dasc#1 pheromone was capable of inducing the Eu mouth-form in liquid culture, as it does on agar. dasc#1 experiments demonstrate a large variability in phenotypic ratio (Fig. 4B), however they typically exhibited a higher Eu proportion than control worms without dasc#1 treatment ($p = 0.068$, *paired t-test*). This intermediate and variable effect suggests that liquid culture and the dasc#1 pheromone act in parallel and antagonistically to each other. Finally, we also compared the expression of four genes in different culturing conditions that are up-or down-regulated in *eud-1* mutants (100% St) vs. wild-type (70–100% Eu)[27]. There was a strong correspondence between *eud-1* vs. wild-type RNA-seq data, and liquid vs. agar culture RT-qPCR (Fig. 4C,D). These results provide further evidence that the environmental effect of liquid culture is upstream of *eud-1*, and that this method is suitable for studying genetic pathways that have been determined through mutational experiments[27–29].

Liquid culture effect is dependent on genetic background. Finally, we explored whether there was a macro-evolutionary difference in responses to culture conditions. We chose four *Pristionchus* species that flank *P. pacificus* phylogenetically; three are highly Eu on agar (>95%), and one is highly St (>95%) (Fig. 5A,B). Remarkably, each species exhibited distinct phenotypic responses to liquid culture. For example, *P. maupasi* was highly Eu in both conditions, while *P. entomophagus* shifted to almost 100% St (Fig. 5C) in liquid culture. Meanwhile *P. mayeri* was St in both culture conditions. Taken together, these data show a genetic basis to environmental effects on phenotypic plasticity, which can be exploited for evolutionary, genetic, and molecular exploration of plasticity mechanisms. Whether these differences in response reflect adaptive changes to different environments, or are a result of drift remains to be seen in future investigations.

Discussion

We describe multiple methods for the culture of preferentially St (<25% Eu), intermediate St (25–50% Eu), intermediate Eu (50–75 Eu%), and preferentially Eu (>75% Eu) *P. pacificus* (Fig. 3, Methods). Growth rates are similar between conditions, allowing the generation of developmentally synchronized populations. The effects are immediate, and immediately reversible when switching between liquid and agar, suggesting they are not transgenerational. Importantly, the genetic pathways towards building each respective mouth form are consistent with pathways established from prior forward genetics[27,28]. Finally, the environmental response is unique in four species of *Pristionchus* tested, arguing that evolution has acted, passively or actively, on gene-environment interactions. The ability to toggle between mouth forms with simple culturing conditions provides powerful new tools to study the genetic and molecular mechanisms of phenotypic plasticity.

Perturbation of environmental factors such as salt concentration[15,36–38], pathogen[8,39–42], temperature[7,10,13,43–45], and diet[46,47] have been exploited for decades to study adaptive responses. More recent genome-wide profiling of epigenetic information carriers has revealed potential mechanisms for communicating stimuli to changes in gene expression. So called 'poised' or 'permissive' chromatin states can respond to external signals, leading to changes in transcription that ultimately affect tissue differentiation[48–55]. The time is now ripe to test whether similar processes affect phenotypic plasticity, a critical link between ecology and molecular mechanism that has just begun to be explored[56–60].

Our panel of *P. pacificus* culture conditions saturates the mouth-form frequency space (Fig. 3). The ability to shift ratios by rpm shaking-speed provides perhaps the cleanest method because of its simplicity. In shaking speeds greater than 90 rpm nematodes are dispersed, while below 90 rpm they are concentrated in the center of the liquid vortex. Since different buffer formulations also affected mouth-form ratios, and the combination with slow rpm yielded an additive effect, it seems that alterations in the abundance, diffusion, and local concentration of pheromones and ions (i.e. phosphate and sulfate) contribute to the observed differences between liquid and agar culture conditions. However, we note that densely packed nematodes at slow rpm (much denser than on a plate) in NGM-liquid media are still insufficient to recapitulate the >95% Eu phenotype seen on NGM-agar plates. While it remains possible that these are the only contributing factors, we speculate an additional unknown factor is extant related to bacterial density, metabolism, or the liquid environment itself.

Whether liquid culture is a direct stimulator of the St mouth form is currently unknown. Field observations and competition experiments are required to (1) assess if *Pristionchus* experiences wet-enough conditions in the wild to mimic liquid culture conditions as with other lotic, lentic or marine nematodes[61–63], and (2) determine whether the St mouth form provides an advantage in this environment. Both *C. elegans* and *P. pacificus* exhibit a slender morphology in liquid culture, suggesting a conserved plastic response to this environment. It is conceivable that a liquid culture-dependent signaling pathway related to mouth form also exists, although it could be mediated indirectly through other factors. Seemingly unrelated stimuli are capable of inducing the same developmental pathway by eventually descending on a downstream switch or "evocator"[64–66]. Regardless of the ultimate environmental factor, our analysis of gene expression in liquid culture reflects patterns observed in constitutive St mutants, suggesting that similar downstream pathways are utilized (Fig. 1D). Importantly however, we did not observe faster St development in liquid culture as has been observed on agar, and which is predicted to be the tradeoff advantage of the St morph[25]. It is formally possible that we did not have enough temporal resolution to identify the small but significant differences previously observed (55 hours for St and 61 hours for Eu). It is also worth noting that laboratory culture conditions are highly artificial, and it is perhaps not surprising that they could affect ecological strategies. Nevertheless, our results suggest that caution should be taken when studying *P. pacificus* ecology across different environments, as it may be context dependent. Going forward, it will be

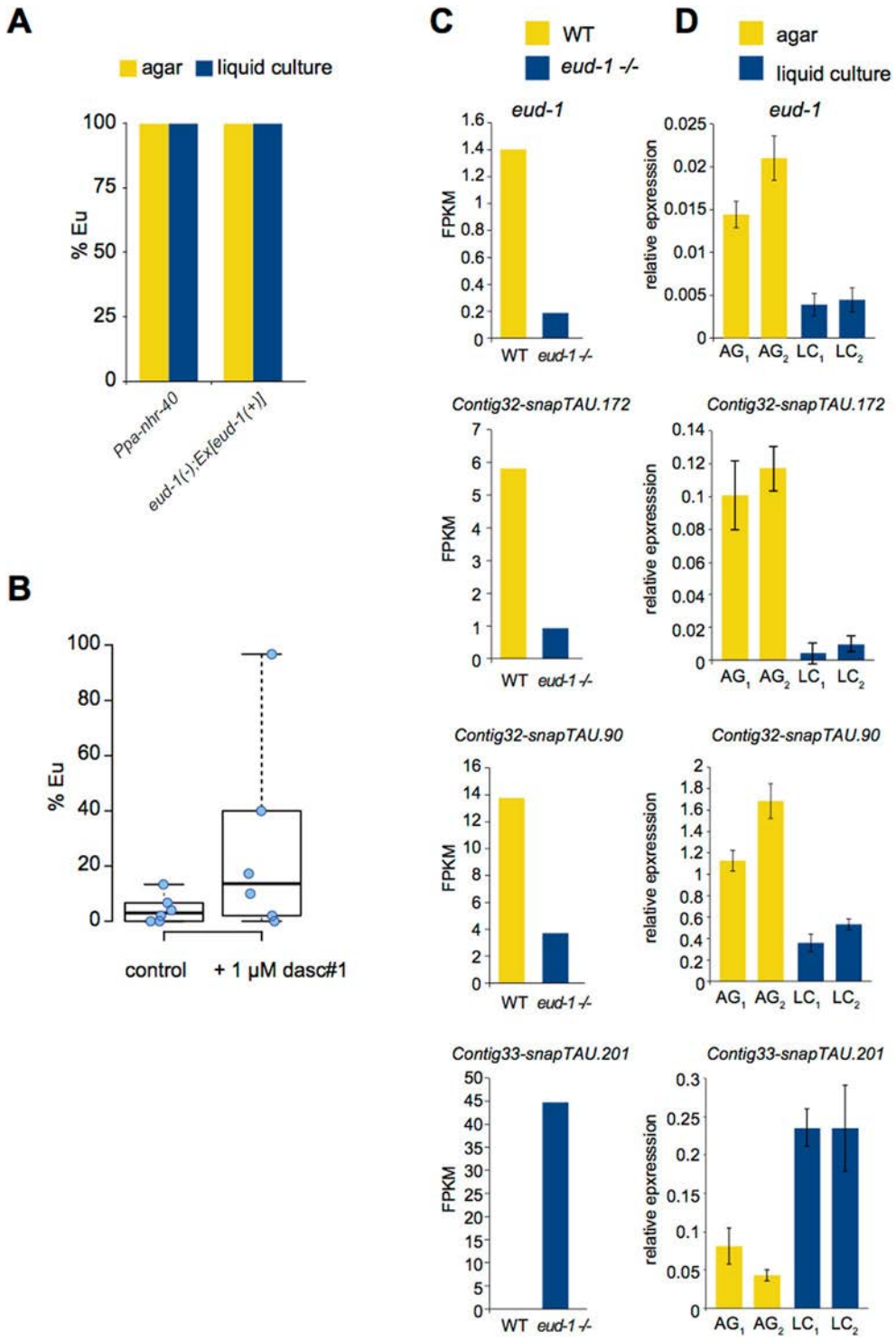

Figure 4. The environmental effect of liquid culture is upstream of known genetic components and induces similar pathways. (**A**) Mouth-form ratios of *eud-1* overexpression[27] and a *Ppa-nhr-40*[28] mutant in liquid culture reveals no effects, suggesting these genes are downstream, $n = 3$ biological replicates. (**B**) Addition of 1 µM dasc#1 exhibits a variable response that appears to induce Eu, although it is not statistically significant ($p = 0.068$). (**C**) Expression analysis of four genes by RNA-seq from *eud-1* mutants (the average of 4 homozygous mutant alleles is represented)[27] (100% St) compared to the RS2333 California strain (70–100% Eu), y-axis = fpkm (relative expression). (**D**) Reverse transcription-quantitative PCR (RT-qPCR) of *P. pacificus* PS312 grown in liquid culture/S-medium (LC) vs. NGM-agar plates (AG) for the two biological replicates displayed, with four technical replicates each. The y-axis represents $2^{\Delta Ct}$ (relative expression) compared to the housekeeping gene *Ppa-Y45F10D.4* (iron binding protein)[69], error bars represent standard deviation of n = 4 technical replicates.

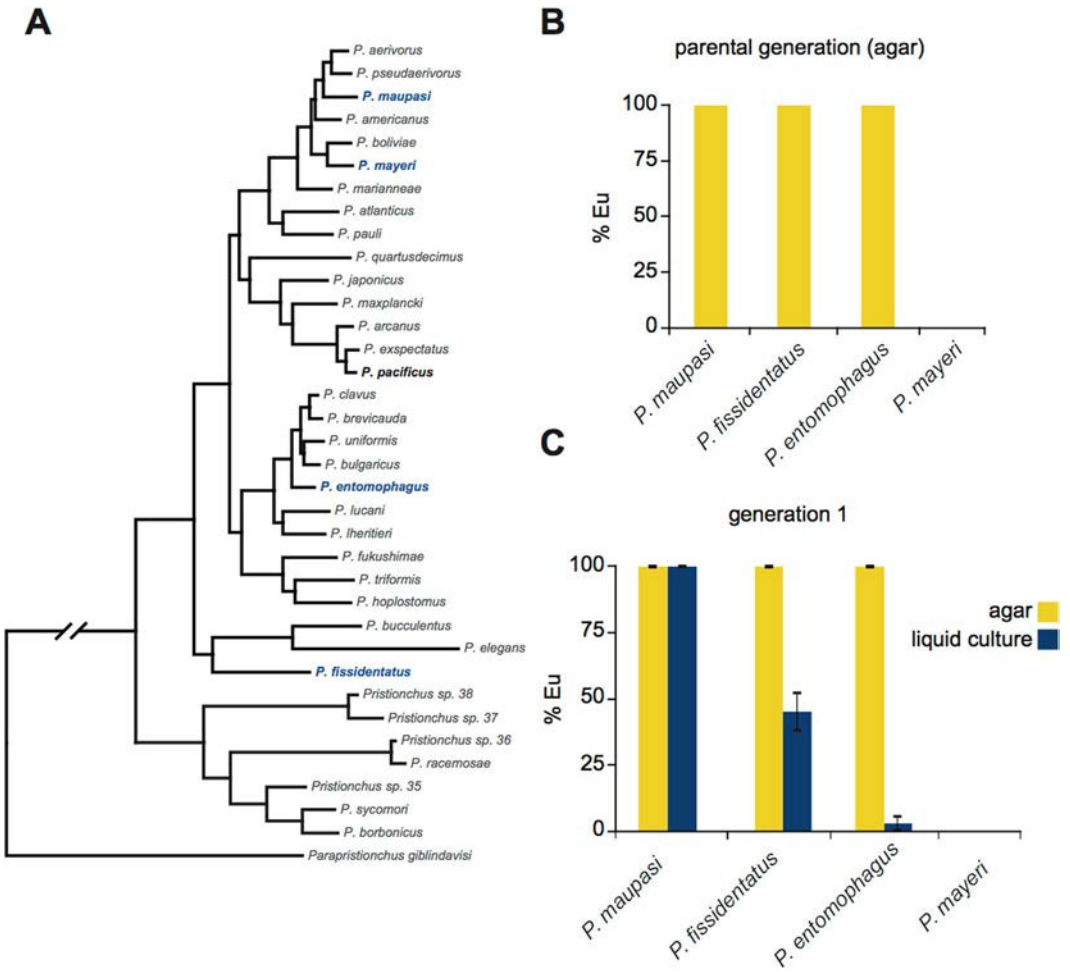

Figure 5. Macro-evolutionary view of liquid culture environmental influence. (**A**) Phylogeny of *Pristionchus* species[70] highlighting *P. pacificus* (bold), *P. fissidentatus*, *P. mayeri*, *and P. entomophagus* (blue). (**B**) Mouth-form ratio of parental generations ($n = 3$) of indicated species on NGM-agar after three consecutive healthy generations on OP50. (**C**) Mouth-form ratios of indicated species in either NGM-agar or liquid culture/S-medium ($n = 3$), error bars represent SEM.

informative to assess if the developmental speed of different species correlates with their response to liquid culture, and the aqueous content in which they are found in nature.

Which culture method is utilized will depend on the purpose of the experiment. Exploiting intermediate ratio conditions may be useful to study genes or other environmental factors predicated to effect mouth form but in an unknown direction (Eu or St). For experiments that require the greatest separation in mouth-form frequencies we recommend S-medium at 180 rpm (St) vs. NGM agar plates (Eu). We also frequently observed a modest degree of variation, which is expected for a stochastic phenotypic trait[67]. As such, every measurement utilizing these culturing methods should be performed side-by-side with control samples. It is our hope that these methods will be a contribution to the study of environmental effects on *P. pacificus* mouth form, and phenotypic plasticity in general.

Methods

Strains and species. For all *P. pacificus* experiments the California strain PS312 was used, except comparisons to RNA-seq data, which used a more grown-out version of the same strain (RS2333). For experiments with different species (Fig. 5) *P. maupasi*, *P. fissidenatus*, and *P. mayeri* were compared to *P. pacificus*. Epistasis experiments (Fig. 4A) were performed with *Ppa-nhr-40*(*tu505*) and *eud-1*(*tu445*);*tuEx[eud-1*(+)*]*.

Culture methods. Five young adult *Pristionchus* nematodes were passed every 4–6 days on 10 ml NGM-agar, 60 mm plates at 20 °C seeded with 300 µl of overnight cultures of *Escherichia coli* OP50 (grown in LB at 37 °C) and covered with parafilm to avoid experiencing starvation for three consecutive generations[33]. The mouth-form phenotype of 4th generation adults represents the parental (P) generation (Fig. 2A,C, and D). Prior to all subsequent phenotyping experiments adults were synchronized by washing off of plates with M9 using plastic Pasteur pipettes into 15 ml conical tubes, and adding 30% final volume NaOH/bleach (0.5 ml NaOH, 1 ml bleach/3.5 ml washed worms) for 9 minutes with gentle agitation every few minutes. Carcasses were filtered through a 120 µm

nylon net (Millipore) fixed between two rubber gaskets in a plastic funnel, washed by applying 3 ml M9 drop-wise on the filter, then pelleted 500 × g, 1 minute, room temperature. Eggs-J1 were washed by gentle re-suspension in 3 ml M9, and re-centrifuged 500 × g, 1 minute, room temperature. It is important not to wash worms with S-medium before or directly after bleach because it will start to precipitate. M9 wash was removed by pipette, and then eggs-J1s were ready for re-suspension in the appropriate buffer depending on the experiment.

For the majority of experiments, eggs-J1 larvae were re-suspended in 100 µl M9 × the number of test conditions (i.e. 200 µl for comparing one agar vs. one liquid culture condition). For re-culturing on agar, eggs-J1 were pipetted in the center of the OP50 lawn on 60 mm agar plates (NGM or S-medium), then the plate was tilted in 360° to spread and dry the eggs. Afterwards the plates were stored at 20° and adults were phenotyped 4–5 days later (see below for details of phenotyping). For culturing in liquid formats, 100 µl of eggs-J1 were pipetted into 10 ml of medium in 50 ml-volume autoclaved Erlenmeyer flasks. To prepare monoxenic liquid cultures the amount of OP50 *E. coli* was empirically determined. For all liquid cultures described (except axenic culture) 100 ml of overnight OP50 *E. coli* (grown in LB) to an optical density (OD_{600}) of 0.5, was pelleted 30 minutes, 4 °C at 3,000 × g in an SLA-3000 rotor and re-suspended in 10 ml filter-sterilized (0.22 µm, Millipore) S-medium[33] unless otherwise noted (e.g. M9 or PBS, Fig. 2). The concentration of bacteria is a critical parameter. The procedure described above led to healthy cultures of *P. pacificus* at the normal developmental rate observed on agar plates (3–4 days[21]), while adding less (50 ml or 10 ml) OP50 led to slower rates, or even the inability to develop beyond the J2 larval stage when significantly less was added. Liquid cultures were incubated 180 rpm, 20–22 °C unless otherwise noted for "slow" rpm experiments (50 and 70 rpm).

For experiments with "H" or "T" medium, S-medium was prepared as before[33] except that phosphates were replaced with 50 mM of HEPES or Tris, pH 7.5, respectively. Axenic culture was prepared according to Samuel *et al.*[34] with the exception that flavin-mononucleotide was replaced with riboflavin (Sigma) at the same amount, and cultures were shaken at 180 rpm instead of 70. As previously noted[34] with *C. elegans*, *P. pacificus* also develops slower in axenic culture, reaching maturity (adults) at 9–10 days after adding eggs. Culture in NGG was performed similar to Muschiol and Traunspurger 2007[35]. In short, 3 ml of NGM was prepared with agar replaced with Gelrite/Gelzan CM (Sigma) at 0.75 g/L and seeded with 300 µl of OP50 and bleached eggs, then incubated at 20 °C.

To collect nematodes from liquid cultures for tracking developmental stages or mouth-form phenotyping we developed a filtering method using removable 5 µm filters (Millipore) combined with the Sterifil aseptic system (47 mm, Millipore). Filters are applied to the Sterifil apparatus and a small amount of M9 is added and vacuumed through to ensure a tight and continuous seal. Then liquid cultures are decanted into the funnel and slowly vacuumed. All *P. pacificus* developmental stages are large enough to be blocked by the 5 µm filter, while bacteria pass through. However when attempting to isolate J2s we recommend applying 2 × 5 µm filters. After all liquid has passed through the filter, nematodes were washed with ~25 ml of M9 by decanting directly on to the filter and applying vacuum pressure. Then the funnel was removed, and forceps were used to transfer the filter to an open 50 ml conical tube in a curved shape to fit into the opening. Nematodes were then washed from the filter by repeatedly applying the same 1 ml of M9 over the filter. Then this 1 ml was transferred to 1.5 ml microcentrifuge tube, and incubated at room temperature for 5 minutes to allow adults to swim to the bottom. Adults were pelleted by a quick (2–3 seconds) centrifugation, and the supernatant was removed. If juveniles are desired, the tube, now free of bacteria after filtering, can also be centrifuged at max speed >5 minutes to pellet. Nematode pellets were then phenotyped, or flash-frozen in liquid N2 and stored −80 °C for subsequent processing (e.g. RT-qPCR).

Developmental rate determination. Worms were grown in liquid culture after bleach synchronization then filtered through a 20 µM filter 2 hours post bleach to isolate synchronous J2 animals, and then returned to liquid culture. Individual aliquots from the same flasks were monitored at regular intervals, and mouth-forms of adults were recorded at the J4-adult transition ($n = 2$). Flasks were rotated at 50 rpm to obtain large quantities of both St and Eu animals. Although not shown, several J4 were present at the earlier time points of 59 and 62 hours, which verified that we were observing the J4-adult transition.

Mouth-form phenotyping. For phenotyping nematodes grown on agar plates or NGG[35], adults were selected with a wire pick and transferred to 3–5 µl of M9 spotted on 4% agar pads (containing 10 mM sodium azide) on a standard microscope slide, then covered with a cover slip. For nematodes grown in liquid culture, after gently pelleting adults, they were re-suspended in the remaining M9 and 3–5 µl were directly pipetted onto the agar pad. When comparing mouth-forms of different conditions, we often performed 'blind' comparisons by writing the identity of the sample (i.e. "agar" or "liquid") on the slide, and then using laboratory tape to cover the identity, and blindly selecting a slide before placing it in the microscope holder. After counting, the identity of the sample was revealed by removing the tape. Phenotyping was performed at 40–100x/1.4 oil objective on a Differential Interference Contrast (DIC) microscope (Zeiss) according to buccal landmarks previously described[20]. In short, Eu were determined by the presence of a wide-mouth, a hooked dorsal tooth, and an additional subventral tooth. Conversely St animals were determined by a narrow-mouth, flint-like dorsal tooth, and absence of a subventral tooth (Fig. 1B,C). The number of biological replicates (n) was ≥3 for all conditions, and as high as 18 for liquid culture/S-medium, with each replicate including ≥50 animals with the exception that PBS and NGM-liquid cultures yielded significantly fewer animals, and included ≥20 animals per replicate. Mouth-forms were assessed 4–5 days after bleach-synchronization. Error bars represent standard error means (SEM), and statistical significance was assessed by *paired 2-tailed t-tests* unless otherwise indicated in the text.

dasc#1 experiments. dasc#1 was added at 1 µM final concentration according to previous methods[26] to eggs-J1 larvae in liquid culture. Mouth-forms were phenotyped as described above after 4 days and compared to

control liquid cultures without dasc#1. The p-value was determined by a 1-tailed, paired *t-test* for $n = 6$ biological replicates.

Morphology measurements. Length and width measurements were performed on synchronized adult animals four days after bleaching. Measurements were made of 12 animals grown on agar, 13 grown on NGG, and 10 in liquid culture using the ImageJ plug-in WormSizer[68]. Box plots in Supplementary Figure 2 show quartile edges (25% and 75%) of the distribution and medians (black bars), made in R {boxplot(shape~Condition, data = worm_sizes, horizontal = TRUE, notch = FALSE)}.

Expression analysis. RNA-seq data was obtained from Ragsdale, Müller *et al.*[27], and average fpkms from 4 mutant alleles of *eud-1* vs. one wild-type California RS2333 were plotted. For RT-qPCR, RNA was first extracted from either 1 agar plate or 1 liquid culture of synchronized young adults (4 days post-bleaching) of the California strain PS312 (same as RS2333 but an earlier frozen stock) by Trizole extraction followed by purification with Zymo RNA-Clean & Concentrator-25 columns following manufacturers instructions from Zymo. 500–1,000 ng of purified RNA was converted to cDNA using SuperScript II (Invitrogen) for 1 hour with $Oligo(dT)_{18}$ primer in 20 µl reactions, and then heat-inactivated with 40 µl of 150 mM KOH/20 mM Tris-base for 10 minutes at 99 °C followed by 40 µl of 150 mM HCl, and 100 µl of TE. 4 µl of cDNA was used for each technical replicate in 10 µl qPCR reactions with 1x LightCycler® 480 SYBR Green I Master Mix (Roche) and 0.25 µM of each primer on a Light-Cycler 480, 384 well format. All primer sets were validated for single amplicon production with Tm melt-curve analysis, and efficiency with a 5-log titration of cDNA. Relative expression ($2^{\Delta Ct}$) was measured relative to *Ppa-Y45F10D.4* (iron binding protein)[69] for each gene.

Data availability. All data generated or analyzed during this study are included in this article and its Supplementary Information files.

References

1. West-Eberhard, M. J. Developmental Plasticity and Evolution. (2003).
2. Bradshaw, A. D. Evolutionary Significance of Phenotypic Plasticity in Plants. *Adv. in Genetics* **13**, 115–155 (1965).
3. Gauze, G. F. *Problems of evolution*. **37**, part 2 (1947).
4. Huxley, J. Problems of relative growth. (1932).
5. Weaver, N. Rearing Honeybee Larvae on Royal Jelly in the Laboratory. *Bee World* (1955).
6. Charnov, E. L. & Bull, J. When is sex environmentally determined? *Nature* **266**, 828–830 (1977).
7. Ferguson, M. W. & Joanen, T. Temperature of egg incubation determines sex in Alligator mississippiensis. *Nature* **296**, 850–853 (1982).
8. Palacios, M. G., Sparkman, A. M. & Bronikowski, A. M. Developmental plasticity of immune defence in two life-history ecotypes of the garter snake, Thamnophis elegans - a common-environment experiment. *J Anim Ecol* **80**, 431–437 (2011).
9. Waddington, C. H. Genetic Assimilation of an Acquired Character. *Evolution* **7**, 118 (1953).
10. Gibert, J.-M., Peronnet, F. & Schlötterer, C. Phenotypic Plasticity in Drosophila Pigmentation Caused by Temperature Sensitivity of a Chromatin Regulator Network. *PLoS Genet* **3**, e30 (2007).
11. Golden, J. W. & Riddle, D. L. The Caenorhabditis elegans dauer larva: Developmental effects of pheromone, food, and temperature. *Developmental Biology* **102**, 368–378 (1984).
12. Sikkink, K. L., Reynolds, R. M. & Ituarte, C. M. Rapid evolution of phenotypic plasticity and shifting thresholds of genetic assimilation in the nematode Caenorhabditis remanei. *G3:* (2014).
13. Powsner, L. The effects of temperature on the durations of the developmental stages of Drosophila melanogaster. *Physiological Zoology* (1935).
14. Brakefield, P. M., Gates, J., Keys, D. & Kesbeke, F. Development, plasticity and evolution of butterfly eyespot patterns. *Nature* (1996).
15. Fielenbach, N. & Antebi, A. C. elegans dauer formation and the molecular basis of plasticity. *Genes & Development* **22**, 2149–2165 (2008).
16. Riddle, D. L., Swanson, M. M. & Albert, P. S. Interacting genes in nematode dauer larva formation. *Nature* **290**, 668–671 (1981).
17. Albert, P. S. & Riddle, D. L. Mutants of Caenorhabditis elegans that form dauer-like larvae. *Developmental Biology* **126**, 270–293 (1988).
18. Gottlieb, S. & Ruvkun, G. daf-2, daf-16 and daf-23: genetically interacting genes controlling Dauer formation in Caenorhabditis elegans. *Genetics* **137**, 107–120 (1994).
19. Lee, R. C., Feinbaum, R. L. & Ambros, V. The C. elegans heterochronic gene lin-4 encodes small RNAs with antisense complementarity to lin-14. **75**, 843–854 (1993).
20. Bento, G., Ogawa, A. & Sommer, R. J. Co-option of the hormone-signalling module dafachronic acid–DAF-12 in nematode evolution. *Nature* **466**, 494–497 (2010).
21. Sommer, R. J. & McGaughran, A. The nematode Pristionchus pacificus as a model system for integrative studies in evolutionary biology. *Molecular Ecology* **22**, 2380–2393 (2013).
22. Meyer, J. M. *et al*. Succession and dynamics of Pristionchus nematodes and their microbiome during decomposition of Oryctes borbonicus on La Réunion Island. *Environmental Microbiology* **19**, 1476–1489 (2017).
23. Serobyan, V., Ragsdale, E. J. & Sommer, R. J. Adaptive value of a predatory mouth-form in a dimorphic nematode. *Proceedings of the Royal Society of London B: Biological Sciences* **281**, 20141334–989 (2014).
24. Wilecki, M., Lightfoot, J. W., Susoy, V. & Sommer, R. J. Predatory feeding behaviour in Pristionchus nematodes is dependent on phenotypic plasticity and induced by serotonin. *J. Exp. Biol.* **218**, 1306–1313 (2015).
25. Serobyan, V., Ragsdale, E. J., Müller, M. R. & Sommer, R. J. Feeding plasticity in the nematode Pristionchus pacificus is influenced by sex and social context and is linked to developmental speed. *Evolution & Development* **15**, 161–170 (2013).
26. Bose, N. *et al*. Complex Small-Molecule Architectures Regulate Phenotypic Plasticity in a Nematode. *Angewandte Chemie International Edition* **51**, 12438–12443 (2012).
27. Ragsdale, E. J., Müller, M. R., Rödelsperger, C. & Sommer, R. J. A Developmental Switch Coupled to the Evolution of Plasticity Acts through a Sulfatase. **155**, 922–933 (2013).
28. Kieninger, M. R. *et al*. The Nuclear Hormone Receptor NHR-40 Acts Downstream of the Sulfatase EUD-1 as Part of a Developmental Plasticity Switch in Pristionchus. *Curr. Biol.* (2016).
29. Serobyan, V. *et al*. Chromatin remodelling and antisense-mediated up-regulation of the developmental switch gene eud-1 control predatory feeding plasticity. *Nat Commun* **7**, 12337 (2016).
30. Mather, K. & De Winton, D. Adaptation and counter-adaptation of the breeding system in Primula. *Annals of Botany* (1941).
31. Sommer, R. J. *et al*. The genetics of phenotypic plasticity in nematode feeding structures. *Open Biology* **7**, 160332–118 (2017).

32. Serobyan, V. & Sommer, R. J. Developmental systems of plasticity and trans-generational epigenetic inheritance in nematodes. *Current Opinion in Genetics & Development* **45**, 51–57 (2017).
33. Stiernagle, T. *Maintenance of C. elegans*, *WormBook*, *ed. The C. elegans Research Community*. (WormBook, 2006).
34. Samuel, T. K., Sinclair, J. W., Pinter, K. L. & Hamza, I. Culturing Caenorhabditis elegans in Axenic Liquid Media and Creation of Transgenic Worms by Microparticle Bombardment. *Journal of Visualized Experiments: JoVE* e51796 (2014).
35. Muschiol, D. & Traunspurger, W. Life cycle and calculation of the intrinsic rate of natural increase of two bacterivorous nematodes from chemoautotrophic Movile Cave, Romania. *Nematology* **9**, 271–284 (2007).
36. Barberon, M. *et al*. Adaptation of Root Function by Nutrient-Induced Plasticity of Endodermal Differentiation. *Cell* **164**, 447–459 (2016).
37. Abbruzzese, G. *et al*. Leaf morphological plasticity and stomatal conductance in three Populus alba L. genotypes subjected to salt stress. *Environmental and Experimental Botany* **66**, 381–388 (2009).
38. Wang, Y. *et al*. Salt-induced plasticity of root hair development is caused by ion disequilibrium in Arabidopsis thaliana. *J Plant Res* **121**, 87–96 (2008).
39. Touchon, J. C. T. C., Gomez-Mestre, I. G.-M. & Warkentin, K. M. W. M. Hatching plasticity in two temperate anurans: responses to a pathogen and predation cues. *Canadian Journal of Zoology* **84**, 556–563 (2006).
40. Hong, J. K. & Hwang, B. K. Induction by pathogen, salt and drought of a basic class II chitinase mRNA and its *in situ* localization in pepper (Capsicum annuum). *Physiologia Plantarum* **114**, 549–558 (2002).
41. Pulendran, B., Palucka, K. & Banchereau, J. Sensing Pathogens and Tuning Immune Responses. *Science* **293**, 253–256 (2001).
42. Huang, Q. *et al*. The Plasticity of Dendritic Cell Responses to Pathogens and Their Components. *Science* **294**, 870–875 (2001).
43. Plunkett, C. R. Temperature as a tool of research in phenogenetics: methods and results (1932).
44. Woodward, D. E. & Murray, J. D. On the Effect of Temperature-Dependent Sex Determination on Sex Ratio and Survivorship in Crocodilians. *Proceedings of the Royal Society of London B: Biological Sciences* **252**, 149–155 (1993).
45. Manenti, T., Loeschcke, V., Moghadam, N. N. & Sørensen, J. G. Phenotypic plasticity is not affected by experimental evolution in constant, predictable or unpredictable fluctuating thermal environments. *Journal of Evolutionary Biology* **28**, 2078–2087 (2015).
46. Brzek, P., Kohl, K., Caviedes-Vidal, E. & Karasov, W. H. Developmental adjustments of house sparrow (Passer domesticus) nestlings to diet composition. *J. Exp. Biol.* **212**, 1284–1293 (2009).
47. Watson, E., MacNeil, L. T., Arda, H. E., Zhu, L. J. & Walhout, A. J. M. Integration of Metabolic and Gene Regulatory Networks Modulates the C. elegans Dietary Response. *Cell* **153**, 253–266 (2013).
48. Bernstein, B. E. *et al*. A Bivalent Chromatin Structure Marks Key Developmental Genes in Embryonic. *Stem Cells.* **125**, 315–326 (2006).
49. Rougvie, A. E. & Lis, J. T. Postinitiation transcriptional control in Drosophila melanogaster. *Mol. Cell. Biol.* **10**, 6041–6045 (1990).
50. Rada-Iglesias, A. *et al*. A unique chromatin signature uncovers early developmental enhancers in humans. *Nature* **470**, 279–283 (2011).
51. Zentner, G. E., Tesar, P. J. & Scacheri, P. C. Epigenetic signatures distinguish multiple classes of enhancers with distinct cellular functions. *Genome Res.* **21**, 1273–1283 (2011).
52. Maxwell, C. S. *et al*. Pol II Docking and Pausing at Growth and Stress Genes in C. elegans. *Cell Rep* **6**, 455–466 (2014).
53. Gaertner, B. *et al*. Poised RNA Polymerase II Changes over Developmental Time and Prepares Genes for Future Expression. *Cell Rep* **2**, 1670–1683 (2012).
54. Ernst, J. *et al*. Mapping and analysis of chromatin state dynamics in nine human cell types. *Nature* **473**, 43–49 (2011).
55. Hsu, H. T. *et al*. Recruitment of RNA polymerase II by the pioneer transcription factor PHA-4. *Science* **384**, 1372–1376 (2015).
56. Ozawa, T. *et al*. Histone deacetylases control module-specific phenotypic plasticity in beetle weapons. *Proc. Natl. Acad. Sci. USA* **113**, 15042–15047 (2016).
57. Kucharski, R., Maleszka, J., Foret, S. & Maleszka, R. Nutritional Control of Reproductive Status in Honeybees via DNA Methylation. *Science* **319**, 1827–1830 (2008).
58. Simola, D. F. *et al*. Epigenetic (re)programming of caste-specific behavior in the ant Camponotus floridanus. *Science* **351**, aac6633–aac6633 (2016).
59. Kooke, R. *et al*. Epigenetic basis of morphological variation and phenotypic plasticity in Arabidopsis thaliana. *Plant Cell* **27**, 337–348 (2015).
60. Zhang, Y. Y., Fischer, M., Colot, V. & Bossdorf, O. Epigenetic variation creates potential for evolution of plant phenotypic plasticity. *New Phytologist* **197**, 314–322 (2013).
61. Traunspurger, W. The biology and ecology of lotic nematodes. *Freshwater Biology* **44**, 29–45 (2000).
62. Tietjen, J. H. & Lee, J. J. Life history and feeding habits of the marine nematode, Chromadora macrolaimoides steiner. *Oecologia* **12**, 303–314 (1973).
63. Herman, P. M. J. & Vranken, G. Studies of the life-history and energetics of marine and brackish-water nematodes. *Oecologia* **77**, 457–463 (1988).
64. Waddington, C. H. *Organisers and Genes by C. H. Waddington*. (The University Press, 1940).
65. Waddington, C. H. Canalization of development and the inheritance of acquired characters. *Nature* (1942).
66. Baeuerle, P. A. & Baltimore, D. IkappaB: a specific inhibitor of the NF-kappaB transcription factor. *Science* (1988).
67. Susoy, V. & Sommer, R. J. Stochastic and Conditional Regulation of Nematode Mouth-Form Dimorphisms. *Front. Ecol. Evol.* **4**, 6706 (2016).
68. Moore, B. T., Jordan, J. M. & Baugh, L. R. WormSizer: high-throughput analysis of nematode size and shape. *PLoS ONE* **8**, e57142 (2013).
69. Schuster, L. N. & Sommer, R. J. Expressional and functional variation of horizontally acquired cellulases in the nematode Pristionchus pacificus. *Gene* **506**, 274–282 (2012).
70. Susoy, V. *et al*. Large-scale diversification without genetic isolation in nematode symbionts of figs. *Science Advances* **2**, e1501031–e1501031 (2016).

Acknowledgements

We are thankful to current members of the Sommer laboratory for thoughtful critique of experiments, results, and interpretations, and Dr. Matthias Herrmann for assistance with the photo in Figure 1A. This study was funded by the Max Planck Society.

Author Contributions

M.S.W., B.S. and R.J.S. conceived and designed the experiments. M.S.W. and T.L. performed mouth-form experiments with help from B.S. in making axenic culture, RNA-seq analysis (also with assistance from S.N.), and rpm experiments. M.S.W., B.S., S.N., M.L., M.D., T.R. and D.R.S. all contributed to RT-qPCR experiments. M.S.W. wrote the manuscript with edits and assistance from R.J.S., and with contribution and approval from all other authors.

Additional Information

Supplementary information accompanies this paper at doi:10.1038/s41598-017-07455-7

Competing Interests: The authors declare that they have no competing interests.

Publisher's note: Springer Nature remains neutral with regard to jurisdictional claims in published maps and institutional affiliations.

Supplementary Information

Environmental influence on *Pristionchus pacificus* mouth form through different culture methods

Michael S. Werner, Bogdan Sieriebriennikov, Tobias Loschko, Suryesh Namdeo, Masa Lenuzzi, Mohannad Dardiry, Tess Renahan, Devansh Raj Sharma and Ralf J. Sommer*

[1]Department of Evolutionary Biology, Max Planck Institute for Developmental Biology, 72076 Tübingen, Germany

*Correspondence: ralf.sommer@tuebingen.mpg.de

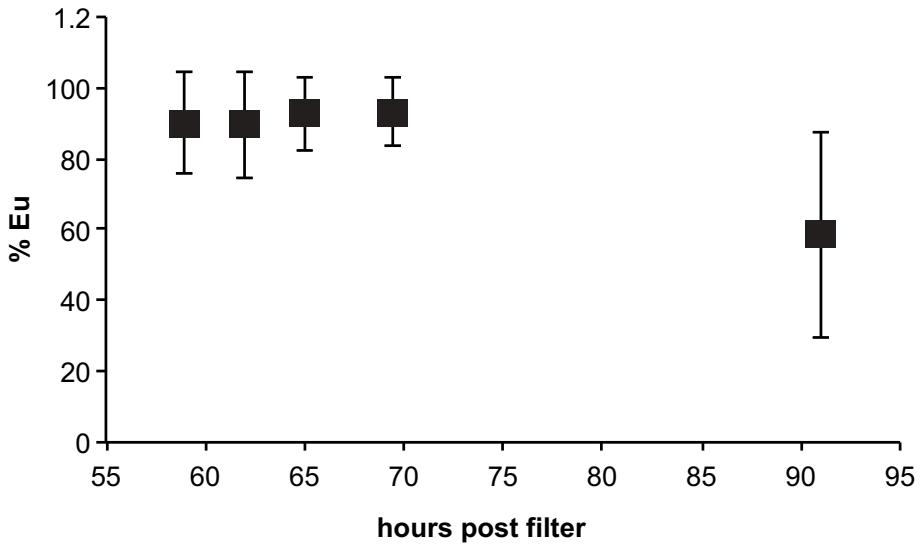

Supplementary Figure 1. Growth rate of morphs in liquid culture. Percent Eu of adult hermaphrodites grown in liquid at the J4-adult transition (59-70 hours post filter), and at 91 hours, a time point at which we normally collect and phenotype animals (n = 2). Worms were incubated at 22° C in S-Medium with 50 rpm shaking to induce sufficient numbers of both, St and Eu animals, allowing statistical significance testing ($p > 0.05$ between any two time-points arguing against slower development of Eu animals, two-tailed t-test).

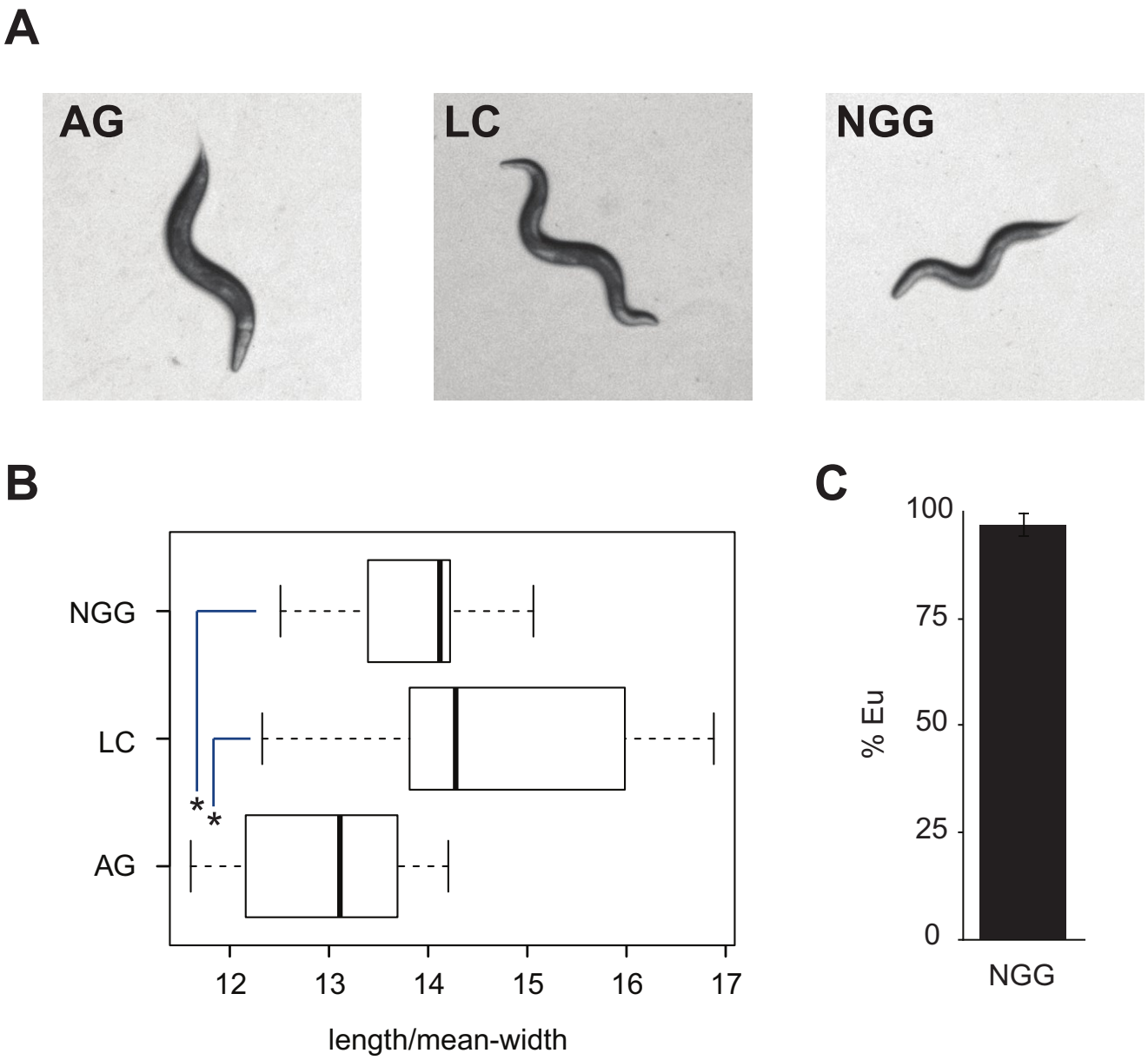

Supplementary Figure 2. Slender morphology does not correlate with mouth-form. (A) Images of *P. pacificus* grown in liquid culture and NGG display more slender morphology than on agar plates, quantified in (**B**). Measurements of adults from the same synchronized population were made with Wormsizer[68], n = 12 (agar), 13 (NGG), and 10 (liquid culture = 'LC'). Statistical significance was measured with a nonparametric Mann-Whitney U test in R. (**C**) Same as in Figure 2, mouth-form ratio of adult PS312 grown in NGG, n = 3.

PLOS ONE

RESEARCH ARTICLE

Life History Responses and Gene Expression Profiles of the Nematode *Pristionchus pacificus* Cultured on *Cryptococcus* Yeasts

Gaurav V. Sanghvi, Praveen Baskaran, Waltraud Röseler, Bogdan Sieriebriennikov, Christian Rödelsperger, Ralf J. Sommer*

Max Planck Institute for Developmental Biology, Department of Evolutionary Biology, Spemannstraße 37, Tübingen, Germany

* ralf.sommer@tuebingen.mpg.de

Citation: Sanghvi GV, Baskaran P, Röseler W, Sieriebriennikov B, Rödelsperger C, Sommer RJ (2016) Life History Responses and Gene Expression Profiles of the Nematode *Pristionchus pacificus* Cultured on *Cryptococcus* Yeasts. PLoS ONE 11(10): e0164881. doi:10.1371/journal.pone.0164881

Editor: Read Pukkila-Worley, University of Massachusetts Medical School, UNITED STATES

Received: June 13, 2016

Accepted: October 3, 2016

Published: October 14, 2016

Data Availability Statement: Raw reads have been submitted to the NCBI short read archive database under the accession number SRP081198.

Funding: This work was supported by the core funding of the Max-Planck Society to RJS. The funder had no role in study design, data collection and analysis, decision to publish, or preparation of the manuscript.

Competing Interests: The authors have declared that no competing interests exist.

Abstract

Nematodes, the earth's most abundant metazoa are found in all ecosystems. In order to survive in diverse environments, they have evolved distinct feeding strategies and they can use different food sources. While some nematodes are specialists, including parasites of plants and animals, others such as *Pristionchus pacificus* are omnivorous feeders, which can live on a diet of bacteria, protozoans, fungi or yeast. In the wild, *P. pacificus* is often found in a necromenic association with beetles and is known to be able to feed on a variety of microbes as well as on nematode prey. However, in laboratory studies *Escherichia coli* OP50 has been used as standard food source, similar to investigations in *Caenorhabditis elegans* and it is unclear to what extent this biases the obtained results and how relevant findings are in real nature. To gain first insight into the variation in traits induced by a non-bacterial food source, we study *Pristionchus*-fungi interactions under laboratory conditions. After screening different yeast strains, we were able to maintain *P. pacificus* for at least 50–60 generations on *Cryptococcus albidus* and *Cryptococcus curvatus*. We describe life history traits of *P. pacificus* on both yeast strains, including developmental timing, survival and brood size. Despite a slight developmental delay and problems to digest yeast cells, which are both reflected at a transcriptomic level, all analyses support the potential of *Cryptococcus* strains as food source for *P. pacificus*. In summary, our work establishes two *Cryptococcus* strains as alternative food source for *P. pacificus* and shows change in various developmental, physiological and morphological traits, including the transcriptomic profiles.

Introduction

The phylum Nematoda (roundworms) is one of the most diverse groups of animals, whose members occupy almost every ecological niche on earth [1]. Their numerical abundance and omnipresence, and the existence of a diversity of life cycles point towards an important role of nematodes in many ecosystems with functions at various trophic levels [2]. As a result, nematodes

show an enormous range of feeding strategies [3] with many of the estimated 1–10 million species being specialists that cannot be cultured under laboratory conditions. In contrast, some nematode species are easily cultured using *Escherichia coli* or other bacteria as food and have been developed as model organisms in basic biology, the best studied example being *Caenorhabditis elegans* (www.wormbook.org). Similarly, its distant cousin *Pristionchus pacificus* has been established as a second laboratory model with similar molecular and genetic tools available [4, 5].

P. pacificus is a self-fertilizing hermaphrodite and belongs to the family Diplogastridae [6]. It has first been established as a satellite model organism in evolutionary developmental biology (evo-devo) due to several technical features that allow functional and mechanistic studies under laboratory conditions. These technical features include i) a short generation time of four days at 20°C, ii) a large brood size, and iii) the ability to be cryopreserved [7]. Further, an annotated genome, whole genome re-sequencing data of 104 *P. pacificus* strains and the mapping of the pharyngeal connectome have complemented large-scale efforts in developmental genetics based on forward and reverse genetic tools, all of which allowed detailed comparisons of developmental processes between *P. pacificus* and *C. elegans* [8–12]. More recently, *P. pacificus* has been developed as a model organism for integrative studies in evolutionary biology that try to link laboratory-based, mechanistic studies with field work in ecology and population genetics [13]. In the wild, *P. pacificus* is often found in association with scarab beetles in an interaction that is described as entomophilic or necromenic [14,15]. Necromeny is the phenomenon where a nematode associates with a living insect or other invertebrate in the growth-arrested dauer stage, an alternative, third larval stage [16]. After the death of the vector, nematodes resume development and feed on microbes, including bacteria, fungi, protozoans, which come together to decompose the carcass.

Additionally, *P. pacificus* has more recently been used as a model to study phenotypic plasticity, the ability of a genotype to produce distinct phenotypes in different environmental conditions [17]. Specifically, *P. pacificus* shows a mouth dimorphism and individual animals irreversibly develop either a narrow-mouthed "stenostomatous" (St) or a wide-mouthed "eurystomatous" (Eu) form [18]. Eu animals have two teeth allowing predatory feeding on other nematodes, whereas St animals with only one tooth are strict microbial feeders. *P. pacificus* mouth-form development is controlled by various conditional (i.e. starvation, crowding) and stochastic factors, making *P. pacificus* a model system to study the genetic, molecular and environmental control of phenotypic plasticity [17] For example, detailed studies revealed the involvement of small molecules in mouth-form development and they identified the sulfatase-encoding *eud-1* gene as a developmental switch controlling Eu *vs*. St development [19, 20].

Microbial communities present in ecological niches play a critical role in nematode ecology, behavior and physiology. However, while behavioral, neurobiological and physiological studies for food selection were reported in many animal species, like rats (*Rattus norvegicus*), mink (*Mustela vison*), moth caterpillars (e.g. *Heliothis zea*) and predatory beetles (*Agonum dorsale*) [21–24], little is known about omnivorous nematodes and their behavioral and physiological responses to different food sources. Only recent studies in *C. elegans* have started to investigate the influence of different bacteria and yeast on this model organisms physiology [25, 26]. For *P. pacificus*, beetle-associated bacteria [27, 28] have been isolated, but they have largely been characterized with regard to their potential pathogenicity. Furthermore, yeast or other fungi have never been investigated as potential food source for *P. pacificus*.

Given that most research on *C. elegans* and *P. pacificus* is performed in the background of *E. coli* as food, it is unclear to what extent this precondition influences the investigated traits and how important the underlying molecular mechanisms are in controlling a given trait in real nature. In this study we ask the question, how variable various life-history traits and transcriptomic profiles are between worms that are grown on different food sources. We chose yeast

strains for comparison because we anticipated that a comparison with a non-bacterial organism would maximize the observed differences relative to *E. coli* and would be the best starting point to estimate the overall magnitude of expected variation when comparing different bacteria as food sources. We therefore first tried to find yeast strains of the *Cryptococcus* genus, on which *P. pacificus* can complete its life cycle for multiple generations and characterize life history traits, such as development time, brood size, mouth-form ratio, and defecation time of *P. pacificus* in order to confirm that these traits are comparable to worms that are grown on *E. coli*. Furthermore, we measured gene expression profiles of *P. pacificus* grown on *Cryptococcus* to estimate the amount of transcriptomic changes on different food sources and to find novel candidates for previously un-described genes that might be important under specific environmental conditions.

Materials and Methods

Nematode and yeast strains

P. pacificus PS312 was grown and maintained on nematode growing media (NGM) plates seeded with *E. coli* OP50 at 20°C. Different *Cryptococcus* yeast strains viz. *C. flavus*, *C. humicola*, *C. curvatus*, *C. tephrensis* and *C. terreus* were purchased from Deutsche Sammlung von Mikroorganismen und Zellkulturen (DSMZ), Braunschweig, Germany. Yeast strains were maintained on Potato dextrose agar media (Sigma-Aldrich Chemie GmbH, Germany) and on media 186 as prescribed by DSMZ for culture maintenance of some yeast strains. All yeast strains were maintained at 30°C. In order to minimize differences for media composition, pH and temperature, the activated broth cultures of yeast were seeded on NGM media similar to *E. coli* OP50.

Selection of yeast strains suitable for culturing *P. pacificus*

Among the tested strains, the two yeast strains *C. albidus* (C3) and *C. curvatus* (C5) were facilitating the growth of *P. pacificus*. Furthermore, both the strains form transparent lawns on NGM facilitating the observations for life span assays. *P. pacificus* strains were cultivated on *Cryptococcus* strains for multiple generations (~ 50–60 generations). These two strains were used for further experimentation. To avoid any bacterial contamination, unseeded plates were inoculated with a mixture of chloramphenicol and streptomycin antibiotic solutions. The same procedure was done for control OP50 plates.

Life history and physiological traits of yeast-fed worms

1. Development Time. For studying developmental time, 20–50 young adults were transferred to agar plates seeded with yeast at 20°C. Eggs hatched within 1–2 hours from young adults were transferred to new plates and observed till new eggs of the next generation appeared after self-fertilization. Eggs were transferred by a metal pick to new plates. In all protocols, NGM media plates with *E. coli* OP50 were kept as control and the same procedure was followed for *E. coli* OP50 at 20°C. Ten plates were used per replicate and experiments were repeated two times.

2. Survival and brood size assay. Yeast cultures were activated in Potato dextrose broth by overnight culture in a shaking incubator at 30°C. 500 μl of cultures were seeded on 6 cm NGM plates and incubated overnight. Assays were performed with 20 J4 *P. pacificus* animals at 20°C. Survival was monitored for 10 days. After every two days, *P. pacificus* was transferred onto fresh yeast plates. Individuals, which did not respond to a touch by a metal pick were considered dead. For brood size, 10 J4 larvae were transferred to agar plates with yeast or *E. coli* OP50. Hatched progeny were counted as J2 or J3 larvae.

3. Mouth-form phenotyping. For mouth-form phenotyping, *P. pacificus* was grown for four generations on both yeasts as well as *E. coli* OP50 plates in order to exclude transgenerational effects induced by the transfer. Hundred individuals were randomly picked from plates to score Eu and St mouth-form frequencies. The mouth-form was observed by Differential Interference Contrast microscopy (DIC) and screened in five biological replicates as previously described [29].

4. Defecation time and Pharyngeal pumping rate. For defecation assays, overnight-activated liquid cultures were seeded on NGM plates and incubated overnight. Nematodes feeding on yeast and *E. coli* OP50 were starved for five hours on NGM plates. Starved worms were transferred on yeast and OP50 containing plates. Plates were not disturbed for 15–20 minutes so that nematode could adjust to the culture medium. Defecation rate was defined as the number of defecation recorded in a 10-minute time interval by a single nematode. Defecation was observed using a Carl Zeiss Discovery microscope (Germany). In order to examine the nature of yeast clumps in the nematode intestine, 10 adults feeding on yeast cultures were photographed using DIC microscope. To verify that altered defecation rate was not linked to permanent attachment of potentially pathogenic yeast cells to the walls of intestinal lumen, the same individuals were put on empty plates and were allowed to defecate for 15–20 minutes. After that, nematodes were removed and plates were incubated for two days to test if yeast cells could still grow after passing through digestive system of the worm.

For counting pharyngeal pumping rate, 10 young adults were transferred on 10 seeded yeast strain plates. Worms were kept undisturbed for 10 min for recovery and initiating regular pumping. Pharyngeal pumping rates were observed via the Zeiss Axio imager a1 microscope for 15 seconds under both *Cryptococcus* species and *E. coli* OP50 strains. For each worm, pumps were counted for 15 seconds and then multiplied its mean by four to derive the mean pumps per minute.

Statistical Analysis

Mouth-form phenotyping, brood size, chemotaxis scores, defecation time were compared using student t-test for means. The survival of *P. pacificus* (10 days) grown on *Cryptococcus* species was analyzed using Kaplan–Meier tests. For testing for differences in developmental timing (egg to egg), brood size, pumping rate, defecation rate, and mouth-form differences, we applied Kruskal-Wallis test with posthoc chi-squared tests.

Gene expression profiling

For gene expression profiling, adult worms were picked and frozen at -80°C. Frozen worms were homogenized by multiple freeze—thaw cycles. Total RNA was isolated using standard Trizol extraction following the manufacturers' instructions (Ambion, CA, USA). RNA concentration was quantified using Qubit and Nanodrop measurements (Invitrogen Life technologies, CA, USA). RNAseq libraries were prepared using TruSeq RNA library preparation kit v2 (Illumina Inc, CA, USA) according to the manufacturer's instructions from 1 μg of total RNA in each sample. Libraries were quantified using Qubit and Bioanalyzer measurements (Agilent Technologies, CA, USA) and normalized to 2.5 nM. Samples were sequenced as 150bp paired end reads in one multiplexed lane using the HiSeq2000 platform (Illumina Inc, CA, USA).

Analysis of RNA-seq data

Raw reads were aligned to the *P. pacificus* reference genome (version Hybrid1) using TopHat (version 2.0.14) [30]. We downloaded the TAU2011 annotation of *P. pacificus* genes from pristionchus.org and estimated expression levels for each data set separately using cufflinks

(version 2.0.1) [31]. Principal component analysis was done using R. Differential expression analysis was done using cuffdiff (version 2.0.1) [31]. For all programs, default parameters were used. Sets of differentially expressed genes were compared with previous expression profiling studies [32–34] and enrichment was tested using Fisher's exact test. Similarly metabolic pathway annotations for *C. elegans* were downloaded from http://www.genome.jp and *P. pacificus* genes were annotated with a given pathway if they fell into an orthologous cluster as defined by the orthoMCL software [35].

Results

After screening several *Cryptococcus* strains for their potential to serve as alternative food source for *P. pacificus*, we were able to maintain nematode cultures for multiple generations (~ 50–60 generations) on the two yeast strains *C. albidus* (C3) and *C. curvatus* (C5). Furthermore, both strains form transparent lawns on NGM, which facilitates the observation in life span assays. We therefore decided to use these two strains for further experiments.

Developmental Timing

Food source is known to be one of the primary factors influencing generation time (from egg to egg) in nematodes. We compared development rate of *P. pacificus* cultured on *E. coli* OP50, *C. albidus* (C3) and *C. curvatus* (C5) (Fig 1A). We found no significant differences in the speed of embryonic development between nematodes grown on OP50 and both yeast strains (Fig 1A). However, significant differences ($P<0.01$) were observed during larval development (Fig 1A). Specifically, starting from the J3 larval stage, *P. pacificus* grew slower on both yeast strains than on OP50 (Fig 1A).

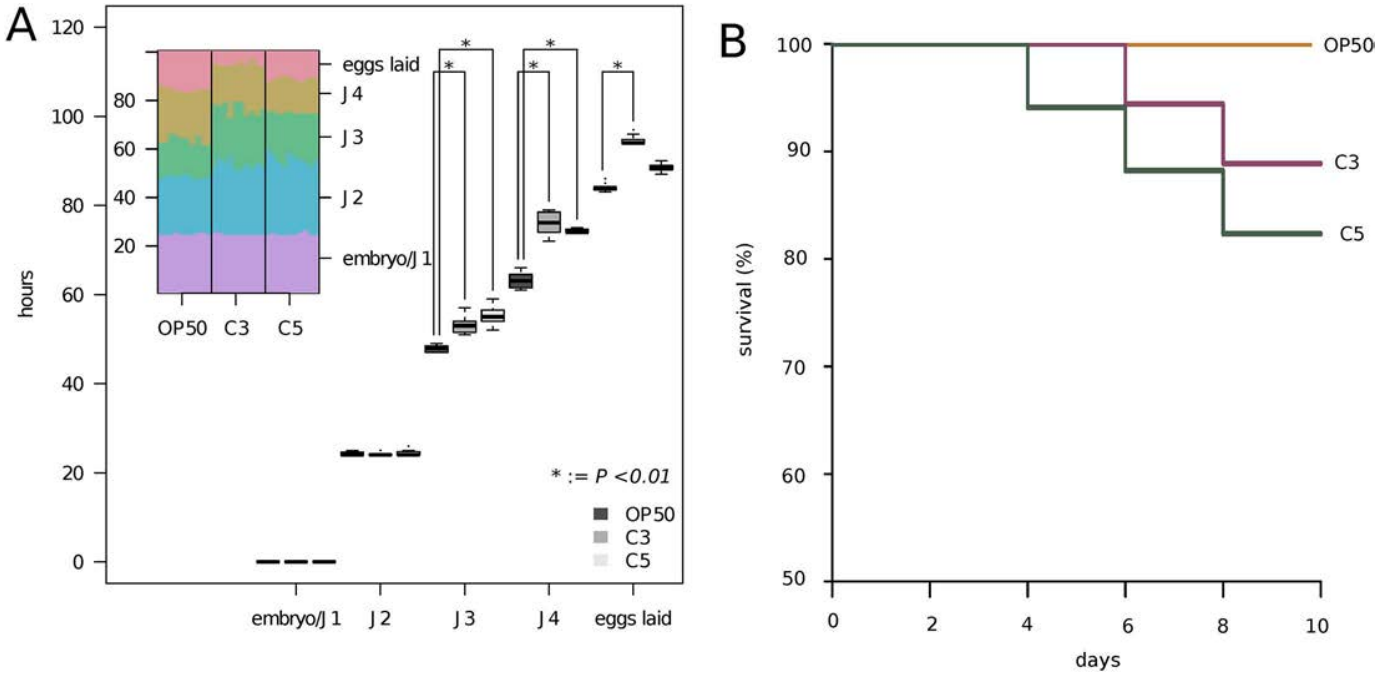

Fig 1. Developmental timing and survival curves of *P. pacificus* after exposure to *C. albidus* and *C. curvatus*. A) The boxplots show the time needed for *P. pacificus* nematodes to enter different developmental stage when growing on *E. coli* OP50 or *Cryptococcus* strains. The inlay shows the individual data points representing ten plates per food source. B) Survival of *P. pacificus* exposed to *C. albidus* (C3) and *C. curvatus* (C5) for 10 days. Standard lab food *E. coli* OP50 was used as a control.

doi:10.1371/journal.pone.0164881.g001

Survival and Brood size assay. We assessed survival of *P. pacificus* on both *Cryptococcus* strains. On *C. albidus*, a more than 90% survival rate was observed after eight days of incubation, close to the survival seen for *E. coli*-fed worms. Survival on th *C. curvatus* was somewhat lower, but still 80% of animals were alive after 10 days of incubation (Fig 1B). These data demonstrate that all yeast-fed worms are alive at the onset of reproduction and a sufficient proportion of individuals survive during the early reproductive period, which permits indefinite propagation of *P. pacificus* on *C. albidus* and *C. curvatus*.

Brood size measurements revealed similar differences between *C. albidus* and *C. curvatus*, and *E. coli* OP50 (Fig 2A). Specifically, self-fertilizing hermaphrodites laid 140 (median) eggs on *E. coli* OP50 seeded plates and 130 (median) eggs were laid on *C. albidus* plates. In contrast, on *C. curvatus* plates only 100 (median) eggs were observed. This number is significantly different in comparison to the number of eggs laid on *E.coli* OP50 and *C. albidus* ($P<0.05$) (Fig 2A). These results suggest that *C. albidus* can be considered to represent a comparable food source for maintaining the reproductive life cycle of *P. pacificus*. In contrast, culturing *P. pacificus* on *C. curvatus* results in reduced survival rates and brood sizes.

Pharyngeal puming rate and Defecation Assays. Pharyngeal pumping rate was observed via Zeiss Axio imager a1 microscope for 15 seconds for both *Cryptococcus* and *E. coli* OP50. When *P. pacificus* was fed on *E. coli* OP50 the median pumping rate was 170 compared to median pumping rate of 70 on *C. albidus* and 140 on *C. curvatus*. Thus, a significant difference in the mean ($P<0.05$) was observed on both yeast strains when compared to *E. coli* OP50 (Fig 2B).

When *P. pacificus* was fed on *E. coli* OP50 the defecation rate (10 min) was 5.5 compared to 3 on *C. albidus* and 4 on *C. curvatus*. Thus, a significant difference in the mean defecation rate ($P<0.05$) was observed on both yeast strains when compared to *E. coli* OP50 (Fig 2C). Also, clumps of yeast cells were observed in the intestine of the nematodes. To test if these clumps were due to indigestibility of yeast cells, yeast-feeding nematodes were transferred to unseeded NGM plates and were allowed to defecate. After three hours on unseeded plates, yeast clumps were no longer present in the intestine of worms suggesting that yeasts cells can be digested or excreted by *P. pacificus*. Furthermore, these findings suggest that the larger cell size slows down defecation time (Fig 3).

Mouth-form plasticity. Next, we tested the influence of continuous culturing of *P. pacificus* on *C. albidus* and *C. curvatus* on the mouth-form ratio. On *E. coli* OP50, the *P. pacificus* reference strain RS2333 has a 90–70%Eu:10–30%St ratio [17]. In the culturing conditions used in our experiments, we observed a Eu mouth-form frequency of median 89% (Fig 2D). In contrast, worms grown on *C. albidus* and *C. curvatus* formed 50% and 84% Eu animals, respectively (Fig 2D). Thus, feeding *P. pacificus* on *C. albidus* increases the St mouth-form frequency ($P<0.05$).

Yeast diet induces substantial transcriptomic responses. The experiments described above show that a *Cryptococcus* diet influences several physiological characteristics of *P. pacificus* relative to an *E. coli* diet. To study the influence of diet on gene expression profiles, we sequenced the transcriptomes of hand picked young adult *P. pacificus* worms that were grown on the two yeast strains and used worms grown on *E. coli* OP50 as reference. For each strain, two biological replicates were sequenced resulting in a total of 49–70 million reads (2x150bp). Despite substantial variation between the two control samples grown on *E. coli*, principal component analysis of expression values shows a clear separation between transcriptome profiles of worms grown on different food sources (Fig 4A). We identified 716 (319 up, 397 down) genes significantly differentially expressed in response to exposure to *C. curvatus* (FDR corrected $P<0.05$). In contrast, 2518 (1431 up, 1087 down) genes were differentially expressed in response to exposure to *C. albidus* (C3).

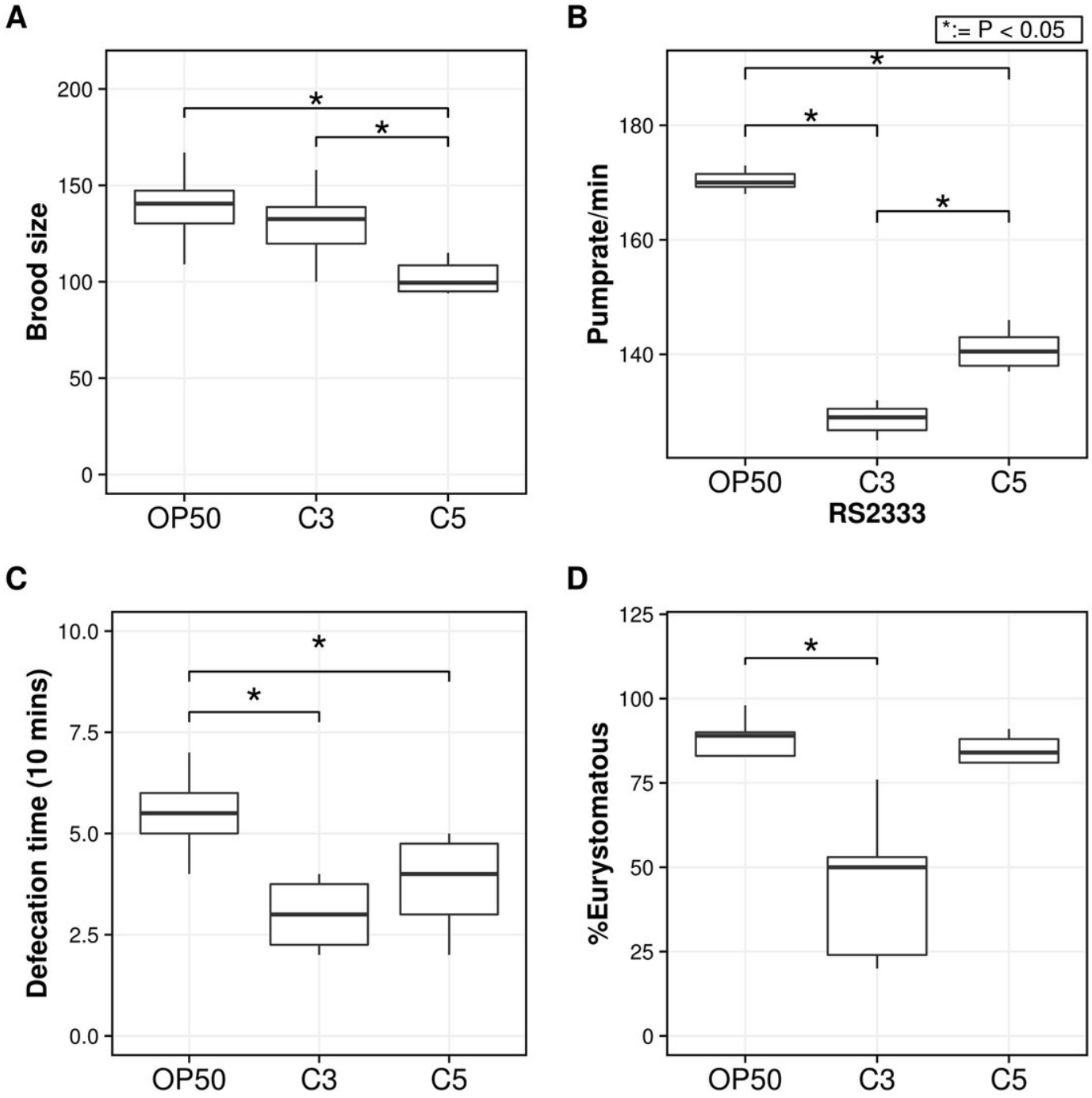

Fig 2. Life history traits of *P. pacificus* cultured on the yeasts *C. albidus* and C. *curvatus*. The boxplots show the median, first and third quartile values from different life history traits experiments. A) Brood size of *P. pacificus* grown on *C. albidus* (C3), *C. curvatus* (C5) and *E. coli* OP50. Brood size was calculated as average number of progeny of 10 J4 larvae. B) Pharyngeal pumping rate results of *P. pacificus* exposed to *Cryptococcus* species. Assay was performed using *E. coli* OP50 as control. C) Defecation time (10 mins) of *P. pacificus* exposed to *C. albidus* (C3) and *C. curvatus* (C5) using *E. coli* OP50 as control. D) Eurystomatous (Eu) ratio of *P. pacificus* adults grown on *C. albidus* (C3) and *C. curvatus* (C5). Eu ratio was calculated from five biological replicates. Statistical significance was calculated using student t-test.

doi:10.1371/journal.pone.0164881.g002

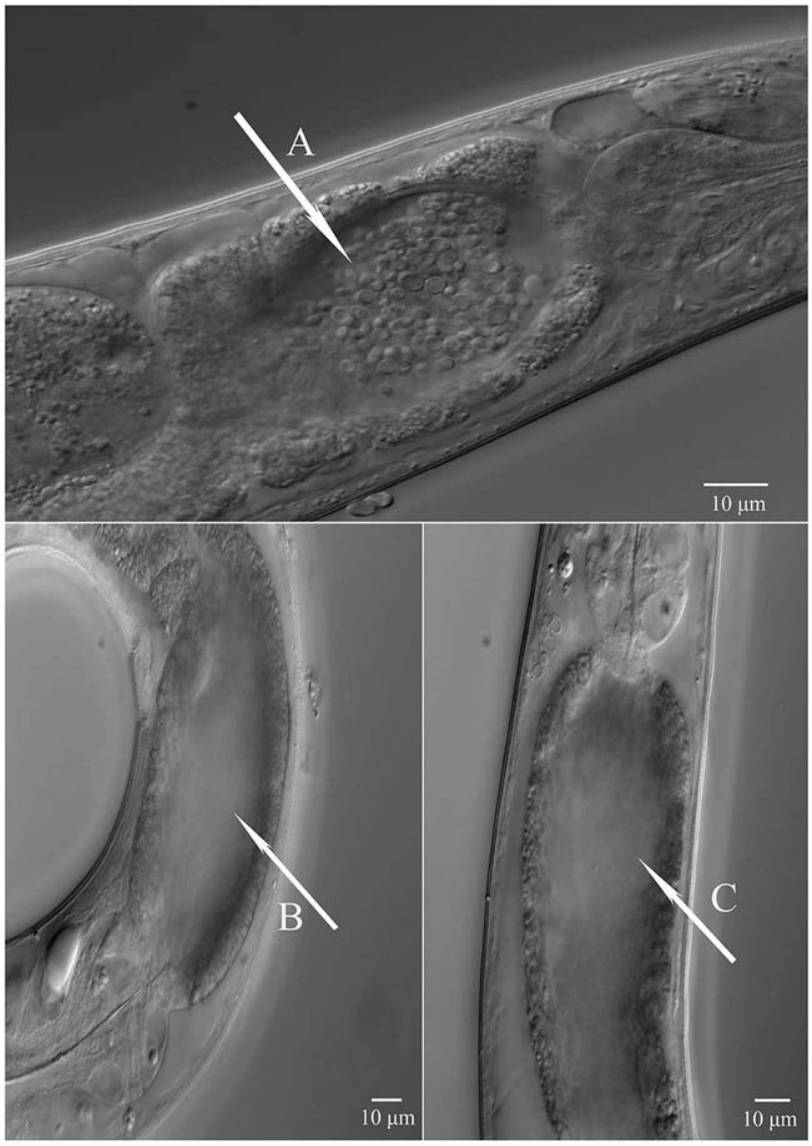

Fig 3. Differential Interference Contrast microscopy (DIC) to study nature of yeast clumps. A) Yeast cells clumps of *C. albidus (C3)* in intestine of *P. pacificus*. B), C) Absence of yeast clumps in defecated worms after 3 hours off food, suggesting that yeasts cells can be fully digested or excreted by *P. pacificus*.

doi:10.1371/journal.pone.0164881.g003

To characterize the identified gene sets in greater detail, we compared our findings with results from previous gene expression profiling studies in *P. pacificus*. Interestingly, despite the fact that only adult worms were picked for RNA extraction, in both transcriptomes significantly differentially expressed genes exhibited a strong overlap with genes, previously identified as developmentally regulated [33]. More precisely, 786 (57%, $P<10^{-250}$) of genes that are up-regulated in response to exposure to *C. albidus* were previously described as developmentally regulated. Similarly 168 (53% $P<10^{-50}$) of up-regulated genes in response to *C. curvatus* are also developmentally regulated. To illustrate these trends, we plotted the mean expression level of all significantly differentially expressed genes (yeasts *vs*. *E. coli*) across the developmental transcriptomesshowing that up regulation in response to both yeast strains seem to correlate

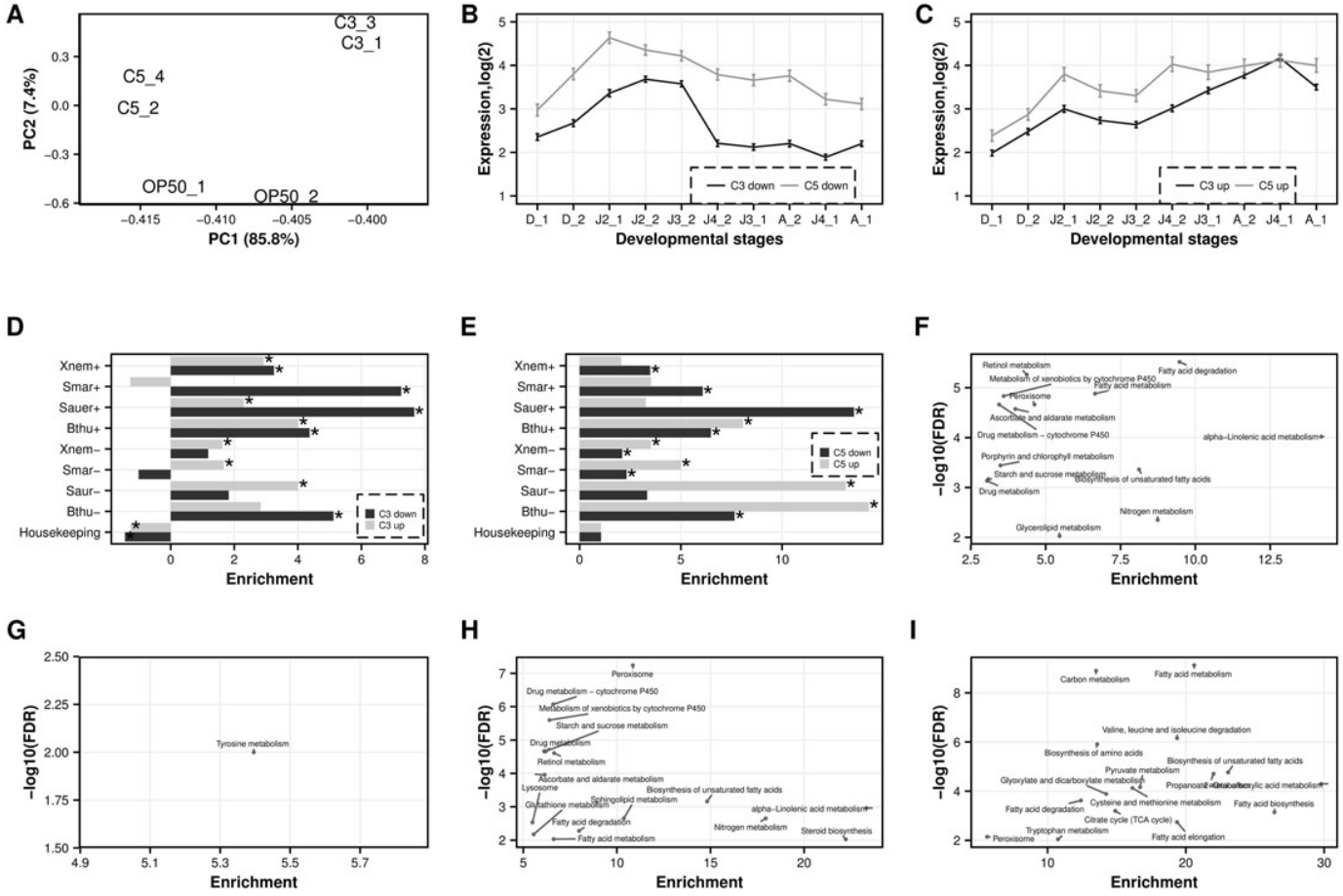

Fig 4. Gene expressions profiling of *P. pacificus* after a *Cryptoccocus* or *E. coli* diet. A) PCA of transcriptomes obtained from *P. pacificus* adult worms growing on *C. albidus* (C3), *C. curvatus* (C5) and *E. coli* OP50. Despite substantial variation in the control samples grown on *E. coli* OP50, different samples cluster together according to their food source indicating robust expression changes under different environments. B) Genes that are down-regulated upon *Cryptococcus* diet show a bias towards higher expression at early developmental stages. The graph shows mean expression and standard error of down-regulated genes in 10 developmental transcriptomes representing dauer, J2, J3, J4, and adult worms. C) Genes that are up regulated upon *Cryptococcus* tend to reflect transcriptomes from later developmental stages. D) Enrichment of significantly differentially expressed genes upon exposure to *C. albidus (C3)* in previous gene expression profiling studies. E) Enrichment of significantly differentially expressed genes upon exposure to *C. curvatus (C5)* in previous gene expression profiling studies. F) KEGG pathway enrichment of down-regulated genes under exposure to *C. albidus (C3)*. The x-axis shows the enrichment score indicating how much more genes of a given pathway are found as differentially expressed when compared to random gene sets. The y-axis shows the negative logarithm of the p-value indicating the significance of the overrepresentation. G) KEGG pathway enrichment of up-regulated genes under exposure to *C. albidus* (C3). H) Enrichment of KEGG pathways among down-regulated genes when fed with *C. curvatus* (C5). I) Enrichment of KEGG pathways among up-regulated genes after exposure to *C. curvatus* (C5).

doi:10.1371/journal.pone.0164881.g004

with expression at later developmental stages (Fig 4B and 4C) [33]. Similarly, genes that are up-regulated in response to *E. coli* are biased towards transcriptomes of earlier developmental stages. This finding might suggest that genes whose expression is food source dependent are in addition also developmentally regulated. Alternatively, it is also possible that the observed pattern is a secondary effect of slower development (Fig 1A).

Housekeeping functions can still be maintained. Based on the comparison of the differentially expressed genes to previous gene expression profiling studies in *P. pacificus* [32–34], we found that exposure to both yeast strains only showed a mild effect on housekeeping functions (Fig 4D and 4E). These findings are clearly different from the response to bacterial pathogens, such as *Serratia marcescens* and *Xenorhabdus nematophila* that kill *P. pacificus* within

five days [32], which is reflected in a massive breakdown of housekeeping function at the transcriptomic level [33]. These findings suggest that both yeast strains are not toxic or pathogenic to *P. pacificus*. Moreover, known pathogen-induced genes show a tendency to be significantly down regulated when worms are grown on the both yeast strains as opposed to *E. coli* OP50 (Fig 4D and 4E).

General activation of protein, sugar, and fatty acid metabolism. We complemented the characterization of the transcriptomes by overrepresentation analysis of gene families (as defined by PFAM domains) and metabolic pathways (KEGG). Similar to the analysis of previous expression profiling studies, we found that in response to both yeasts, Cytochrome P450 genes, which are associated with the detoxification of xenobiotics, are significantly down regulated in response to both yeast strains (Fig 4F and 4H). Again, this observation could potentially suggest that *E. coli* OP50 is actually more toxic than *Cryptococcus*. In addition, genes upregulated in response to exposure to *C. curvatus* (Fig 4I) showed enrichments in protein ('Biosynthesis of amino acids', $P<10^{-7}$, Fisher's exact test), sugar ('Gylcoslyis/Glucogenesis', $P<10^{-2}$), and fatty acid metabolism ('Fatty acid metabolism', $P<10^{-2}$). The only significantly enriched pathway for *C. albidus* was 'Tyrosine metabolism' (Fig 4G). Given that both yeast strains lead to a developmental delay, these results could potentially suggest that yeast cells are either more difficult to digest or are less nutritious. We speculate that worms have to invest more energy in synthesize essential molecules and therefore, develop slower.

Discussion

Several studies in the recent past have investigated the tritrophic interactions of bacteria, beetles and *Pristionchus* nematodes [27], whereas the potential interaction of *Pristionchus* with fungi or yeast was never specifically investigated under *in vitro* conditions. Therefore, the present study is the first of its kind and aims to investigate the interaction of yeast with *Pristionchus* by investigating the effects of *C. albidus* and *C. curvatus* on life history traits and gene expression profiles of *P. pacificus*. Our study results in four major conclusions.

First, *P. pacificus* is able to grow and reproduce on *C. albidus* and *C. curvatus* yeast strains. Despite the relatively large size of yeast cells, *P. pacificus* was able to complete its life cycle in 3.9 days and 3.7 days on *C. albidus* and *C. curvatus* at 20°C, respectively. These values are comparable to the generation time of 3.5 days on *E. coli* OP50. In addition, our data on survival and brood size of *P. pacificus* on both yeast strains indicate that *P. pacificus* can survive and finish its self-fertilizing reproductive cycle when feeding on *C. albidus* or *C. curvatus* although the latter reduces survival and brood size.

Second, we found a significant change in mouth-form ratios of *P. pacificus* when fed on *C. albidus*. Specifically, 50% Eu animals were observed on *C. albidus*, whereas 89% Eu animals were found on *E. coli* (Fig 3D). This change in mouth-form frequency might be influenced by several factors. For example, the relatively large size and density of yeast cells will influence nematode metabolism and energy consumption, which eventually may lead to a metabolic cost of plasticity. We speculate that the on average faster larval development of St animals [29] is favored when the nematode metabolizes yeast cells. The gene expression profiles of *P. pacificus* cultures on yeast cells suggest that young adults are more similar to later adult stages grown on *E. coli* OP50. This finding (see below for a more detailed discussion) would support a potential metabolic cost hypothesis. However, it should be noted that it is inherently difficult to estimate metabolic and other costs for plastic traits [36].

Third, survival, brood size and generation time assays, nor the defecation studies showed extreme effects of both *Cryptococcus* strains. While effects of *C. albidus* and/or *C. curvatus* on various life history traits were observed, none of them resulted in growth arrest or a heavily

increased mortality. The precise fitness effect was strongest for *C. curvatus* reducing brood size. However, it should be noted that in the wild, nematodes are not exposed to monoxenic cultures of microbes as those used in laboratory studies. Consistently, nematodes recovered from decomposed beetle carcasses usually have a diversity of microbes in their intestine [27](Meyer and Sommer, manuscript in preparation).

Finally, our analysis of transcriptomic changes in response to yeast exposure overlapped significantly ($P<10^{-250}$) with gene sets that were previously known as developmentally regulated [33]. Currently it is unclear, whether this strong association is truly a yeast-induced response or represents a secondary effect of slower development. If the latter explanation were correct, this would suggest that the transcriptomic age of a worm might not necessarily correspond to its morphological stage. However, to decide on this question requires much more detailed expression profiling studies. The transcriptomic signal of the remaining genes basically support the two previous findings as general housekeeping functions can still be maintained and pathogen related genes tend to be down-regulated.

In conclusion, the present study establishes two *Cryptococcus* strains as alternative food source for *P. pacificus* and shows for the first time in a systematic manner the interactions of *P. pacificus* with yeast. We found that *Pristionchus* was able to continue its life cycle on two yeast strains and had developmental time, brood size and survival rate comparable to worms grown on the common lab food *E. coli* OP50. *Pristionchus* shows considerable mouth form dimorphism when fed on yeasts indicating an important role of feeding plasticity when *Pristionchus* is exposed to different food sources in nature. Future studies should aim to understand the genetic regulation involved in different food choices.

Acknowledgments

We thank Dr. Matthias Herrmann for critical comments on the manuscript and the Sommer lab for discussions. This work was funded by the Max-Planck Society to RJS.

Author Contributions

Conceptualization: GVS BS CR RJS.

Data curation: PB CR.

Formal analysis: PB CR.

Funding acquisition: RJS.

Investigation: GVS BS WR.

Methodology: GVS PB WR BS.

Project administration: RJS.

Supervision: CR RJS.

Validation: GVS PB CR.

Visualization: GVS PB.

Writing – original draft: GVS PB CR RJS.

Writing – review & editing: GVS PB CR RJS.

References

1. Hugot J-P, Baujard P, Morand S. Biodiversity in helminths and nematodes as a field of study: an overview. Nematology. 2001; 3: 199–208. doi: 10.1163/156854101750413270
2. Platt HM. "Foreword". In: Lorenzen S, Lorenzen SA, editor. The phylogenetic systematics of free-living nematodes. London: The Ray Society; 1994.
3. Munn E. A. & Munn PD. Feeding and digestion. In: Lee DH, editor. London: Taylor & Francis; 2002. pp. 211–232.
4. Sommer RJ, McGaughran A. The nematode Pristionchus pacificus as a model system for integrative studies in evolutionary biology. Mol Ecol. 2013; 22: 2380–2393. doi: 10.1111/mec.12286 PMID: 23530614
5. Sommer RJ. Integrative evolutionary biology and mechanistic approaches in comparative biology. In: Sommer RJ, editor. Pristionchus pacificus—a nematode model for comparative and evolutionary biology. leiden: Brill; 2015. pp. 19–41.
6. Sommer R, Carta L, Kim S, Sternberg PW. Morphological, genetic and molecular description of Pristionchus pacificus sp. n. (Nematoda:Neodiplogastridae) [Internet]. Fundamental and applied Nematology. 1996. pp. 511–521. Available: http://www.usmarc.usda.gov/SP2UserFiles/person/897/2aSommeretal1996.pdf
7. Hong RL, Sommer RJ. Pristionchus pacificus: A well-rounded nematode. BioEssays. 2006; 28: 651–659. doi: 10.1002/bies.20404 PMID: 16700067
8. Tian H, Schlager B, Xiao H, Sommer RJ. Wnt Signaling Induces Vulva Development in the Nematode Pristionchus pacificus. Curr Biol. 2008; 18: 142–146. doi: 10.1016/j.cub.2007.12.048 PMID: 18207741
9. Dieterich C, Clifton SW, Schuster LN, Chinwalla A, Delehaunty K, Dinkelacker I, et al. The Pristionchus pacificus genome provides a unique perspective on nematode lifestyle and parasitism. Nat Genet. 2008; 40: 1193–1198. doi: 10.1038/ng.227 PMID: 18806794
10. Rödelsperger C, Neher RA, Weller AM, Eberhardt G, Witte H, Mayer WE, et al. Characterization of genetic diversity in the nematode Pristionchus pacificus from population-scale resequencing data. Genetics. 2014; 196: 1153–1165. doi: 10.1534/genetics.113.159855 PMID: 24443445
11. Bumbarger DJ, Riebesell M, Rödelsperger C, Sommer RJ. System-wide rewiring underlies behavioral differences in predatory and bacterial-feeding nematodes. Cell. 2013; 152: 109–119. doi: 10.1016/j.cell.2012.12.013 PMID: 23332749
12. Witte H, Moreno E, Rödelsperger C, Kim J, Kim JS, Streit A, et al. Gene inactivation using the CRISPR/Cas9 systemin the nematode Pristionchus pacificus. Dev Genes Evol. 2015; 225: 55–62. doi: 10.1007/s00427-014-0486-8 PMID: 25548084
13. Sommer RJ. The future of evo-devo: model systems and evolutionary theory. Nat Rev Genet. 2009; 10: 416–422. doi: 10.1038/nrg2567 PMID: 19369972
14. Herrmann M, Mayer WE, Hong RL, Kienle S, Minasaki R, Sommer RJ. The nematode Pristionchus pacificus (Nematoda: Diplogastridae) is associated with the oriental beetle Exomala orientalis (Coleoptera: Scarabaeidae) in Japan. Zoolog Sci. 2007; 24: 883–9. doi: 10.2108/zsj.24.883 PMID: 17960992
15. Herrmann M, Kienle S, Rochat J, Mayer WE, Sommer RJ. Haplotype diversity of the nematode Pristionchus pacificus on R??union in the Indian Ocean suggests multiple independent invasions. Biol J Linn Soc. 2010; 100: 170–179. doi: 10.1111/j.1095-8312.2010.01410.x
16. Sudhaus W. Preadaptive plateau in Rhabditida (Nematoda) allowed the repeated evolution of zooparasites, with an outlook on evolution of life cycles within Spiroascarida. Paleodiversity. 2010;Supplement: : 117–130.
17. Susoy V, Sommer RJ. Stochastic and Conditional Regulation of Nematode Mouth-Form Dimorphisms. Front Ecol Evol. 2016; 4: 1–7. doi: 10.3389/fevo.2016.00023
18. Bento G, Ogawa A, Sommer RJ. Co-option of the hormone-signalling module dafachronic acid-DAF-12 in nematode evolution. Nature. Nature Publishing Group; 2010; 466: 494–497. doi: 10.1038/nature09164 PMID: 20592728
19. Bose N, Ogawa A, Von Reuss SH, Yim JJ, Ragsdale EJ, Sommer RJ, et al. Complex small-molecule architectures regulate phenotypic plasticity in a nematode. Angew Chemie—Int Ed. 2012; 51: 12438–12443. doi: 10.1002/anie.201206797 PMID: 23161728
20. Ragsdale EJ, Muller MR, Rodelsperger C, Sommer RJ. A developmental switch coupled to the evolution of plasticity acts through a sulfatase. Cell. 2013;155. doi: 10.1016/j.cell.2013.09.054 PMID: 24209628
21. Walbauer G.P. and Friedman S.. Self-Selection of Optimal Diets by Insects. Annu Rev Entomol. 1991; 36: 43–63.
22. Stephen J. Simpson DR. The Hungry Locust. Adv Study Behav. 2000; 29: 1–44.

23. Koehnle TJ, Russell MC, Gietzen DW. Rats rapidly reject diets deficient in essential amino acids. J Nutr. 2003; 133: 2331–2335. PMID: 12840202

24. Mayntz D., Nielsen V. H., Sorensen A., Toft S., Raubenheimer D., Hejlesen C., & Simpson SJ. Balancing of protein and lipid intake by a mammalian carnivore, the mink, Mustela vison. Anim Behav. 2009; 77: 349–355.

25. Mylonakis E, Ausubel FM, Perfect JR, Heitman J, Calderwood SB. Killing of Caenorhabditis elegans by Cryptococcus neoformans as a model of yeast pathogenesis. Proc Natl Acad Sci U S A. 2002; 99: 15675–15680. doi: 10.1073/pnas.232568599 PMID: 12438649

26. Watson E, MacNeil LT, Ritter AD, Yilmaz LS, Rosebrock AP, Caudy AA, et al. Interspecies systems biology uncovers metabolites affecting *C. elegans* gene expression and life history traits. Cell. 2014; 156: 759–70. doi: 10.1016/j.cell.2014.01.047 PMID: 24529378

27. Rae R, Riebesell M, Dinkelacker I, Wang Q, Herrmann M, Weller AM, et al. Isolation of naturally associated bacteria of necromenic Pristionchus nematodes and fitness consequences. J Exp Biol. 2008; 211: 1927–36. doi: 10.1242/jeb.014944 PMID: 18515723

28. Rae R, Iatsenko I, Witte H, Sommer RJ. A subset of naturally isolated Bacillus strains show extreme virulence to the free-living nematodes Caenorhabditis elegans and Pristionchus pacificus. Environ Microbiol. 2010; 12: 3007–3021. doi: 10.1111/j.1462-2920.2010.02278.x PMID: 20626457

29. Serobyan V, Ragsdale EJ, Müller MR, Sommer RJ. Feeding plasticity in the nematode pristionchus pacificus is influenced by sex and social context and is linked to developmental speed. Evol Dev. 2013; 15: 161–170. doi: 10.1111/ede.12030 PMID: 23607300

30. Trapnell C, Pachter L, Salzberg SL. TopHat: Discovering splice junctions with RNA-Seq. Bioinformatics. 2009; 25: 1105–1111. doi: 10.1093/bioinformatics/btp120 PMID: 19289445

31. Ding X, Boney-montoya J, Owen BM, Bookout AL, Coate C, Mangelsdorf DJ, et al. Differential analysis of gene regulation at transcript resolution with RNA-seq. Nat Biotechnol. 2013; 16: 387–393.

32. Sinha A, Rae R, Iatsenko I, Sommer RJ. System Wide Analysis of the Evolution of Innate Immunity in the Nematode Model Species Caenorhabditis elegans and Pristionchus pacificus. PLoS One. 2012; 7. doi: 10.1371/journal.pone.0044255 PMID: 23028509

33. Baskaran P, Rödelsperger C. Microevolution of Duplications and Deletions and Their Impact on Gene Expression in the Nematode Pristionchus pacificus. PLoS One. 2015; 10: e0131136. doi: 10.1371/journal.pone.0131136 PMID: 26125626

34. Lightfoot JW, Chauhan VM, Aylott JW, Rödelsperger C. Comparative transcriptomics of the nematode gut identifies global shifts in feeding mode and pathogen susceptibility. BMC Res Notes. BioMed Central; 2016; 9: 142. doi: 10.1186/s13104-016-1886-9 PMID: 26944260

35. Markov G V., Baskaran P, Sommer RJ. The Same or Not the Same: Lineage-Specific Gene Expansions and Homology Relationships in Multigene Families in Nematodes. J Mol Evol. 2014; 80: 18–36. doi: 10.1007/s00239-014-9651-y PMID: 25323991

36. Pigliucci M. Phenotypic Plasticity: Beyond Nature and Nurture. Baltimore, MD: Johns Hopkins University Press.; 2001.

Cell Reports

Report

A Developmental Switch Generating Phenotypic Plasticity Is Part of a Conserved Multi-gene Locus

Graphical Abstract

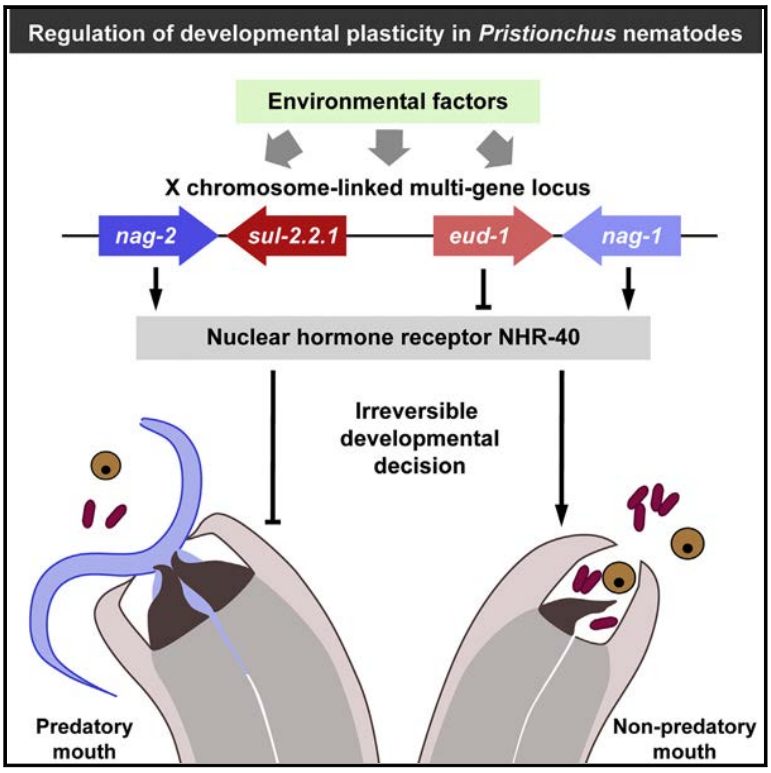

Highlights

- The *eud-1* switch induces the development of predatory morphology in *P. pacificus*
- *nag-1* and *nag-2* surround *eud-1* and have opposite effects on the same phenotype
- The locus architecture is conserved in *Pristionchus*, but not in other dimorphic genera
- Gene conversion counteracts divergence between paralogs within the locus

Authors

Bogdan Sieriebriennikov, Neel Prabh, Mohannad Dardiry, ..., Manuela R. Kieninger, Christian Rödelsperger, Ralf J. Sommer

Correspondence

ralf.sommer@tuebingen.mpg.de

In Brief

The clonally reproducing roundworm *Pristionchus pacificus* can develop either as a toothed predator or as a narrow-mouthed microbe feeder depending on environmental conditions. Sieriebriennikov et al. show that the switch gene controlling this developmental decision is physically linked with two other genes having opposing influence on the same phenotype.

Sieriebriennikov et al., 2018, Cell Reports *23*, 2835–2843
June 5, 2018
https://doi.org/10.1016/j.celrep.2018.05.008

CellPress

Cell Reports
Report

A Developmental Switch Generating Phenotypic Plasticity Is Part of a Conserved Multi-gene Locus

Bogdan Sieriebriennikov,[1] Neel Prabh,[1,2] Mohannad Dardiry,[1,2] Hanh Witte,[1] Waltraud Röseler,[1] Manuela R. Kieninger,[1,3] Christian Rödelsperger,[1] and Ralf J. Sommer[1,4,*]
[1]Department for Integrative Evolutionary Biology, Max Planck Institute for Developmental Biology, Max-Planck-Ring 9, 72076 Tübingen, Germany
[2]These authors contributed equally
[3]Present address: Wellcome Trust/Cancer Research UK Gurdon Institute, University of Cambridge, Cambridge CB2 1QN, England, UK
[4]Lead Contact
*Correspondence: ralf.sommer@tuebingen.mpg.de
https://doi.org/10.1016/j.celrep.2018.05.008

SUMMARY

Switching between alternative complex phenotypes is often regulated by "supergenes," polymorphic clusters of linked genes such as in butterfly mimicry. In contrast, phenotypic plasticity results in alternative complex phenotypes controlled by environmental influences rather than polymorphisms. Here, we show that the developmental switch gene regulating predatory versus non-predatory mouth-form plasticity in the nematode *Pristionchus pacificus* is part of a multi-gene locus containing two sulfatases and two α-N-acetylglucosaminidases (*nag*). We provide functional characterization of all four genes, using CRISPR-Cas9-based reverse genetics, and show that *nag* genes and the previously identified *eud-1*/sulfatase have opposing influences. Members of the multi-gene locus show non-overlapping neuronal expression and epistatic relationships. The locus architecture is conserved in the entire genus *Pristionchus*. Interestingly, divergence between paralogs is counteracted by gene conversion, as inferred from phylogenies and genotypes of CRISPR-Cas9-induced mutants. Thus, we found that physical linkage accompanies regulatory linkage between switch genes controlling plasticity in *P. pacificus*.

INTRODUCTION

Many animals and plants exhibit complex traits that occur as discrete alternative morphs. In general, two mechanisms are known to underlie the formation of alternative phenotypes: genetic polymorphism and plasticity (polyphenism). Examples of adaptive alternative phenotypes are butterfly wing patterns involved in mimicking unsavory species, long- and short-styled flowers in primroses shaped to promote cross-fertilization, and single-queen versus multiple-queen colonies in fire ants (Charlesworth, 2015; Schwander et al., 2014). These phenotypes are inherited as single genetic polymorphisms—a phenomenon referred to as "supergenes"—which presumably contain multiple physically linked genes associated with the phenotype (Joron et al., 2011; Kim et al., 2017; Kunte et al., 2014; Li et al., 2016; Wang et al., 2013). While the identities of the causal genes are, in some cases, yet to be determined, the evolutionary turnover of supergene loci is believed to be rapid. For example, in *Papilio* butterflies, the *doublesex* haplotype associated with the mimetic morph is restricted to three species, and its origin dates back to 2 million years ago, while mimicry in other species of the same genus is controlled by different loci (Timmermans et al., 2014; Zhang et al., 2017).

Physical linkage of functionally related genes is not restricted to examples traditionally considered within the supergene concept. For example, the major histocompatibility complex (MHC) in chordates and the Y chromosome also contain functionally related genes specifying alternative phenotypes (Edwards and Hedrick, 1998; Schwander et al., 2014). Studies on these loci and other loci that contain linked genes but are not associated with alternative phenotypes, such as clusters of tandem duplicates and imprinted clusters, revealed that physical proximity facilitates coordinated regulation of gene expression (Hallast et al., 2005; Trowsdale, 2002; Zakharova et al., 2009). Arguably, concerted transcription of the linked genes is also important for loci associated with complex traits, with an additional advantage of facilitating co-adaptation between the genes through the reduction of recombination.

Complex alternative phenotypes may also develop under environmental influence rather than polymorphisms. This phenomenon is known as developmental or phenotypic plasticity, with the genes responsible for both phenotypes present in the same organism (West-Eberhard, 2003). Additionally, genomes of species that exhibit plasticity contain a set of regulatory genes that switch between the developmental trajectories upon perception of relevant environmental inputs. Conceptually, plasticity and genetic polymorphism represent different mechanisms of generating alternative phenotypes. However, the differences and similarities remain largely unexplored,

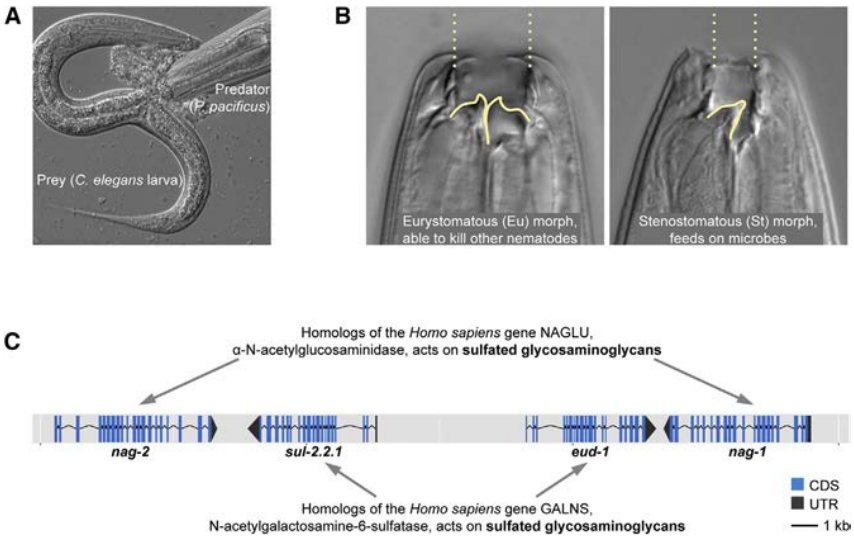

Figure 1. Developmental Plasticity of Predatory Morphology in *Pristionchus pacificus*

(A) Adult *P. pacificus* devouring a larva of *Caenorhabditis elegans*.

(B) Mouths of eurystomatous (Eu) and stenostomatous (St) morphs. The omnivorous Eu morph has a wide mouth with two teeth, whereas the microbivorous St morph has a narrow mouth with a dorsal tooth only.

(C) Genomic locus containing the previously identified developmental switch gene *eud-1* consists of two pairs of duplicated genes in an inverse tandem arrangement. Both pairs encode proteins that potentially have sulfated glycosaminoglycans as their substrate.

because knowledge about the mechanisms and evolution of plastic traits is scarce.

Nonetheless, recent findings provided first insight into the mechanisms associated with developmental plasticity (Projecto-Garcia et al., 2017). Studies on plasticity between predatory and microbe-feeding morphs in the nematode *Pristionchus pacificus* identified the sulfatase-encoding gene *eud-1* as a developmental switch and also implicated the chromatin modifiers *lsy-12* and *mbd-2* and the nuclear hormone receptor *nhr-40* in the same pathway (Figures 1A, 1B, and 2D) (Kieninger et al., 2016; Ragsdale et al., 2013; Serobyan et al., 2016). While wild-type populations show a mixture of two morphs (Bento et al., 2010), mutations in *eud-1* lead to the absence of "wide-mouthed" eurystomatous (Eu) animals, which have two hooked teeth and are facultative predators (Wilecki et al., 2015). Instead, all animals in the mutant lines develop into "narrow-mouthed" stenostomatous (St) morphs, which have one flint-like tooth and only feed on microbes (Figure 1B). These phenotypes and additional genetic experiments indicated that *eud-1* acts as a developmental switch (Ragsdale et al., 2013), confirming long-standing theoretical predictions that plasticity requires developmental reprogramming and new input by developmental switch genes (West-Eberhard, 2003, 2005). Also, the functional characterization of *eud-1* revealed that it operates in phenotypically divergent populations of *P. pacificus* and in the closely related species *P. exspectatus*, with which *P. pacificus* can form viable but sterile hybrids (Ragsdale et al., 2013). Thus, the *eud-1* switch gene is an important regulator of mouth-form plasticity and its evolution.

Here, we expand the investigation of *eud-1* to the neighboring genomic regions. Interestingly, *eud-1* belongs to an inverted tandem duplication containing two sulfatase and two α-N-acetylglucosaminidase (*nag*)-encoding genes. The main finding of this study is that the *nag-1* and *nag-2* genes have an opposing effect on the morph frequencies in comparison to *eud-1*. Thus, plasticity in *P. pacificus* is controlled by a set of genes that display physical linkage in addition to regulatory linkage. We further explore the expression pattern and evolutionary history of the multi-gene locus and discuss functional and evolutionary implications of physical linkage between the genes it contains.

RESULTS

The Switch Gene *eud-1* and Its Tandem Paralog Are Surrounded by a Pair of NAGLU Genes

eud-1 is located on the left arm of the X chromosome of *P. pacificus*. It belongs to an ~30-kb region that contains four genes in an inverted tandem configuration (Figure 1C). Specifically, *eud-1* and its paralog *sul-2.2.1* are in the center of this cluster in a head-to-head orientation, and they are separated by an ~7-kb intergenic region that contains a promoter driving the expression of *eud-1* (Ragsdale et al., 2013). Both genes are homologous to the *Caenorhabditis elegans* gene *sul-2* and to the human gene GALNS coding for an N-acetylgalactosamine-6-sulfatase. *Cel-sul-2* is a single autosomal gene, whereas *P. pacificus* has three *sul-2*-like genes, one on the same autosome as in *C. elegans* and the X chromosome *eud-1* and *sul-2.2.1* genes, which most likely result from lineage-specific duplication and translocation events (Ragsdale et al., 2013).

Interestingly, the two neighboring genes of *eud-1* and *sul-2.2.1* are also inverted duplicates, homologous to an uncharacterized *C. elegans* autosomal gene *K09E4.4* and the human gene NAGLU encoding an α-N-acetylglucosaminidase. In humans, both GALNS and NAGLU have sulfated glycosaminoglycans as their substrates, and mutations in these genes cause different types of mucopolysaccharidosis, a disorder characterized by disrupted formation of extracellular matrix (Beesley et al., 2005; Rivera-Colón et al., 2012). This offers the possibility that the homologs of GALNS and NAGLU in *P. pacificus* play a role in similar biochemical pathways. This potential relationship and the peculiar genomic arrangement of the locus prompted us to test the function of the NAGLU homologs in *P. pacificus*, which we named *nag-1* and *nag-2*.

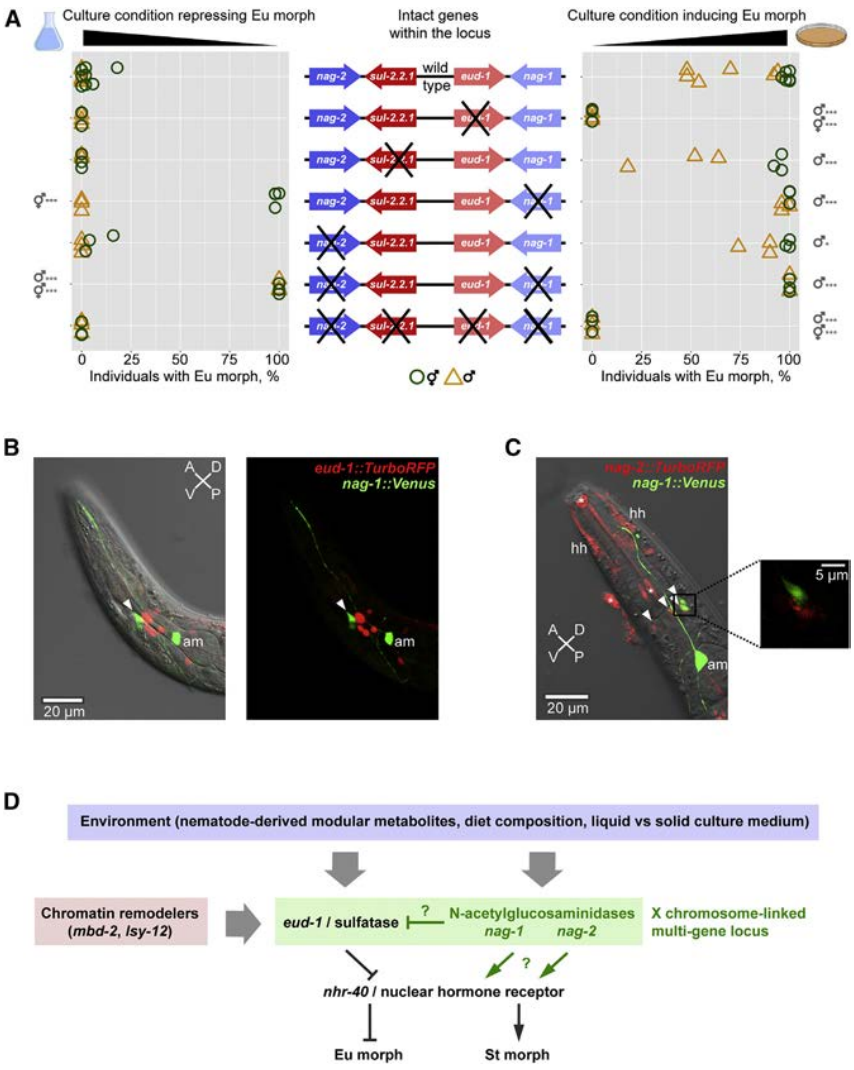

Figure 2. *eud-1* Locus Organization, Functions, and Expression of Individual Genes

(A) Morph frequencies in wild-type and mutant lines in both sexes and two culture conditions. Triangles represent males, and circles represent hermaphrodites. The cartoon illustrates the genotype of every examined line. Arrows represent genes, and arrowheads point toward the 3′ ends. Crosses indicate inactivated genes. Strains from top to bottom: PS312 wild-type, *eud-1(tu445)*, *sul-2.2.1(iub2)*, *nag-1(tu1137)*, *nag-2(tu1138)*, *nag-1(tu1142) nag-2(tu1143)*, and *tuDf1[nag-1 sul-2.2.1 eud-1 nag-2]*. *p < 0.05; ***p < 0.001; all the comparisons are to wild-type, and only statistically significant comparisons are shown.

(B) *nag-1* and *eud-1* do not co-localize. Head region of an animal carrying *nag-1* and *eud-1* reporters. Left: overlay of a differential interference contrast (DIC) image, maximum-intensity Z-projection of the Venus channel, and sum-of-slices projection of the TurboRFP channel. Right: the same without DIC.

(C) *nag-1* and *nag-2* do not co-localize. Head of an animal carrying *nag-1* and *nag-2* reporters. Main frame: overlay of a DIC image, maximum-intensity Z-projection of the Venus channel, and maximum-intensity projection of the TurboRFP channel. Inset: overlay of Venus and TurboRFP channels in the same plane.

In (B) and (C), arrowheads indicate cell bodies of labial sensilla. am, amphid neuron; hh, head hypodermis; A, anterior end; P, posterior end; D, dorsal side; V, ventral side. In (C), asterisks indicate auto-fluorescent regions.

(D) Updated model of the regulation of mouth-form plasticity.

See also Figures S1 and S2.

nag-1 and *nag-2* Regulate the Same Phenotype as *eud-1*

To study the function of *nag-1* and *nag-2* in *P. pacificus*, we knocked out both genes using CRISPR-Cas9 technology (Witte et al., 2015). We isolated *nag-1(tu1137)* and *nag-2(tu1138)* single mutants and a double-knockout line *nag-1(tu1142) nag-2(tu1143)* (Figure S1A). Additionally, we obtained a line with a deletion *tuDf1[nag-1 sul-2.2.1 eud-1 nag-2]* that affects all four genes in the locus (Figure S1B). In the absence of an *a priori* expectation as to whether the knockout phenotype of the *nag* genes will be Eu constitutive (Euc) or Eu deficient (Eud), mouth form was assessed under two culture conditions (Figure 2A). One of them (liquid S-medium) is Eu repressing for wild-type worms (Werner et al., 2017), thus facilitating identification of the Euc phenotype. Another condition (agar plates with nematode growth medium) is Eu inducing, which aids detection of the Eud phenotype. For the same reason, we phenotyped both sexes, as wild-type males are more prone to becoming St than wild-type hermaphrodites on agar plates (Serobyan et al., 2013). Knockout of *nag-1* resulted in a partially penetrant Euc phenotype, observable in hermaphrodites in liquid culture and in males on agar plates (Figure 2A). Mutation in its paralog, *nag-2*, also resulted in a Euc phenotype, although it was weaker and only manifested in a slight shift toward Eu in males on agar plates. When *nag-1* and *nag-2* were inactivated, the Euc phenotype became completely penetrant and evident in both sexes and in both culture conditions, demonstrating additive action of the two paralogous genes (Figure 2A). As the *nag-1 nag-2* phenotype is opposite that of *eud-1*, we scored mouth-form frequency in the line where all four genes were deleted. The quadruple mutant had a completely penetrant Eud phenotype identical to that of the *eud-1* single knockout, demonstrating that *eud-1* is epistatic over *nag-1* and *nag-2* (Figures 2A and 2D). These experiments indicate that, first, both *nag* genes and *eud-1* control the same developmentally plastic trait and, second, *nag-1* and *nag-2* have opposing effects on mouth-form frequencies to *eud-1*, because they promote the formation of St morphs. Given the clustering of these genes and the X chromosome position, which reduces recombination in nematodes with their XO sex determination system (Pires-daSilva and Sommer, 2004), these findings demonstrate that the multi-gene locus controlling developmental plasticity in *P. pacificus* has at

least some supergene characteristics. Therefore, we continued to study the development, expression, and evolution of this multi-gene locus.

The *eud-1* Paralog *sul-2.2.1* Has Only a Minor Role in Mouth-Form Specification

Since both the *nag-1* and *nag-2* mutants had mouth-form defects, we re-analyzed the already existing *sul-2.2.1* mutant. Previous studies had not found any significant effect of *sul-2.2.1* on mouth-form plasticity, but these experiments were only performed in hermaphrodites and in one culture condition (Ragsdale and Ivers, 2016). We observed only a weak but significant shift toward St morphs in males on agar plates (Figure 2A). Similarly, when we overexpressed both genes in a *eud-1* mutant background, we observed a much stronger rescue with *eud-1* compared to *sul-2.2.1* (Figure S2B). Thus, *nag-1*, *nag-2*, and *eud-1* play major roles in the regulation of mouth-form plasticity, whereas *sul-2.2.1* appears to have only a minor contribution.

nag-1, *nag-2*, and *eud-1* Are Expressed in Different Sensory Neurons and Interneurons

Next, we investigated in which tissues *nag-1* and *nag-2* are expressed and whether they co-localize with each other and with *eud-1*, which is expressed in several head neurons (Ragsdale et al., 2013). We created transcriptional reporter constructs for both genes and generated transgenic animals. *nag-1* was expressed in 1 pair of head neurons, with the wiring pattern and cell body position resembling those of amphid neurons in *C. elegans* (Altun and Hall, 2017), and in 1–3 pairs of head neurons bearing semblance to labial sensilla (Figures 2B, 2C, and S2C). *nag-2* localized to 1–3 pairs of different labial sensilla but also to hypodermal cells at the head tip (Figure 2C; Figures S2D and S2E). Importantly, *nag-1* and *nag-2* did not co-localize (Figure 2C), which is consistent with their additive contributions to the phenotype suggesting that the paralogs underwent subfunctionalization. Also, *nag-1* and *eud-1* were expressed in different cells (Figure 2B), which, taken together with *eud-1* being epistatic to *nag-1*, indicates that *eud-1* is expressed in downstream interneurons and/or in sensory neurons perceiving an environmental input that can override the input perceived through cells expressing *nag-1*. Thus, the multi-gene locus regulating plasticity in *P. pacificus* consists of genes that are expressed in non-overlapping sensory and interneurons.

Synteny in the Locus Is Preserved throughout the Genus *Pristionchus*

To examine the evolution of the multi-gene locus, we investigated the architecture of the *eud-1* locus in seven other species of *Pristionchus*, which represent the taxonomic distribution of the genus (N.P. W.R., H.W., G. Eberhardt, R.J.S., C.R., unpublished data) and all of which exhibit mouth-form plasticity. Performing a BLASTP search for homologs of *nag-1* and *eud-1* in the selected genomes, we found at least two homologs of *nag-1* and at least three homologs of *eud-1* in every species (Data S1). A pair of sulfatase genes and a pair of *nag* genes always adjoined each other, and their order and orientation were conserved across all tested species of *Pristionchus* (Figure 3A). Similarly, homologs of *C. elegans dpy-23* and *F40E10.6*, which are adjacent to *nag-2* and *nag-1* in *P. pacificus*, respectively, were found to surround the plasticity locus in all *Pristionchus* species (Figure 3A). Importantly, *dpy-23* and *F40E10.6* are not part of the locus regulating plasticity, as knockout mutants of these genes do not have mouth-form-defective phenotypes (Table S1). Thus, genes constituting the plasticity multi-gene locus in *P. pacificus* are syntenic throughout the genus *Pristionchus*, which represents an evolutionary diversification of more than 30 species (Ragsdale et al., 2015).

The Locus Architecture Is Different in Other Dimorphic Genera

Having established that the locus architecture is preserved in *Pristionchus* spp., we inspected the genomes of two more dimorphic species of the same family: a close relative, *Micoletzkya japonica* (N.P. et al., unpublished data), and a basal species, *Allodiplogaster sudhausi*, sequenced in this study. We found that *M. japonica* had three NAGLU homologs in the same locus and that the sulfatase genes were exterior to a pair of NAGLU homologs, opposite to what is found in *Pristionchus* (Figure 3A; Data S1). In contrast, all NAGLU homologs and all sulfatase genes were on different contigs and never adjoined each other in *A. sudhausi*, although contigs were large enough and contained several BLAST hits with other *Pristionchus* genes in the neighboring regions (Figures 3A and S3A; Data S1). These findings result in several conclusions. First, synteny within the locus is restricted to the *Pristionchus* genus, implying that its architecture, as observed in *P. pacificus*, has evolved at the base of or in the genus. Second, a tandem arrangement is also found in *M. japonica,* while the order and orientation of genes are different. Finally, the clustering of *eud-1* and *nag-1* homologs is absent in the basal *A. sudhausi*, indicating that the physical linkage between NAGLU homologs and sulfatases is not essential for mouth-form plasticity and may have evolved after the origin of plasticity or, alternatively, has been lost in *A. sudhausi*.

Evolutionary History of Paralogs in the Locus Is Shaped by Gene Conversion

To investigate the evolutionary forces acting on the individual genes, we reconstructed maximum-likelihood phylogenies for all sulfatase and NAGLU homologs within the syntenic block (Figure 3B; Figures S3B and S3C). Interestingly, neither the NAGLU nor the sulfatase gene tree recapitulated the species tree, the latter of which is shown in Figure 3A. Specifically, paralogs clustered with each other in the basal clades, whereas orthologous clusters were formed only in the terminal clades, albeit of different depths in the sulfatase and the NAGLU tree (Figure 3B; Figures S3B and S3C). For example, EUD-1 and SUL-2.2.1, of the closely related species *P. pacificus*, *P. exspectatus*, and *P. arcanus*, recapitulate the species phylogeny. In contrast, in all the more basal species (*P. maxplancki*, *P. japonicus*, *P. fissidentatus*, *P. mayeri*, and *P. entomophagus*), the two paralogous sequences of each species group together. Similarly, NAG-1 and NAG-2 sequences of *P. mayeri* and *P. fissidentatus* group together (Figure S3C). Given the conserved structure of the *Pristionchus* plasticity multi-gene locus, these patterns are unlikely to result from independent gene duplications. Therefore, we explored an alternative mechanism—namely, the involvement of gene conversion.

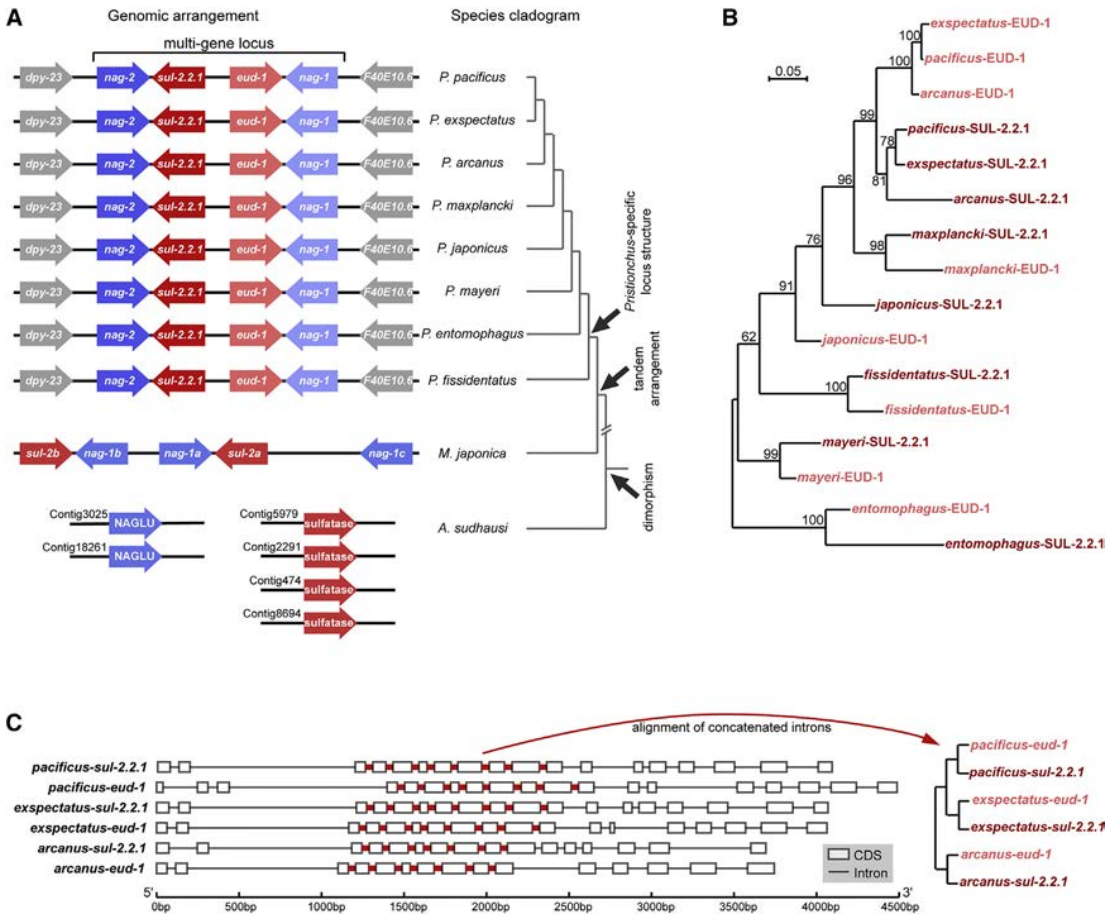

Figure 3. Evolution of the Multi-gene Locus in the Family Diplogastridae

(A) Cartoon representation of synteny of the genes in the locus in eight species of *Pristionchus*; a closely related species, *Micoletzkya japonica*; and a basal but already dimorphic species, *Allodiplogaster sudhausi*. Colored arrows represent gene predictions, and tips point toward the 3′ ends. Gene predictions connected with a black line are located in the same scaffold and adjoin each other. In *Pristionchus* spp., gene names are assigned based on proximity to homologs of the *C. elegans* genes *dpy-23* and *F40E10.6*.

(B) Maximum-likelihood tree of amino acid sequences of EUD-1 homologs in the genus *Pristionchus*. Numbers indicate values of bootstrap support.

(C) Exon-intron structure of *eud-1* and *sul-2.2.1* in *P. pacificus*, *P. exspectatus*, and *P. arcanus*. Introns that align in all six sequences are indicated in red. On the right, a cladogram built from the intron alignment.

See also Figure S3 and Table S1.

For this, we scrutinized the nucleotide sequences of sulfatases in *P. pacificus*, *P. exspectatus*, and *P. arcanus*, those species in which sulfatase homologs still formed orthologous clusters (Figure 3C). Given that species-specific codon bias may lead to convergence of coding sequences, we focused on intronic sequences instead. We aligned the intronic regions and removed all unreliable columns. The resultant alignment broke down into two blocks: a region where introns of either one or the other orthologous group were aligned and a region where all sequences were aligned but variants at the informative sites matched between paralogs (Figure S4). These two regions yielded conflicting phylogenetic trees in which, correspondingly, either orthologs or paralogs clustered together (Figure 3C; Figure S4). Thus, we observe not only that the two gene pairs in the locus, i.e., sulfatases and the NAGLU homologs, show incongruence between their tree topologies but also that even the different parts of the two sulfatases genes show contrasting phylogenetic signals. Considering that we have established that the locus synteny originated in the common ancestor of the *Pristionchus* nematodes, we propose that gene conversion is the most likely mechanism that can explain the complex phylogeny we observe at this locus. Gene conversion has been inferred in other gene families, including opsin genes in fish and humans (Cortesi et al., 2015; Zhao et al., 1998), but direct experimental support for gene conversion is generally scarce (Lynch, 2007).

Experimental Demonstration of Gene Conversion between *nag-1* and *nag-2*

Strikingly, we obtained what seems a direct evidence for gene conversion between *nag-1* and *nag-2* under experimental, laboratory conditions. After CRISPR-Cas9-induced double-strand

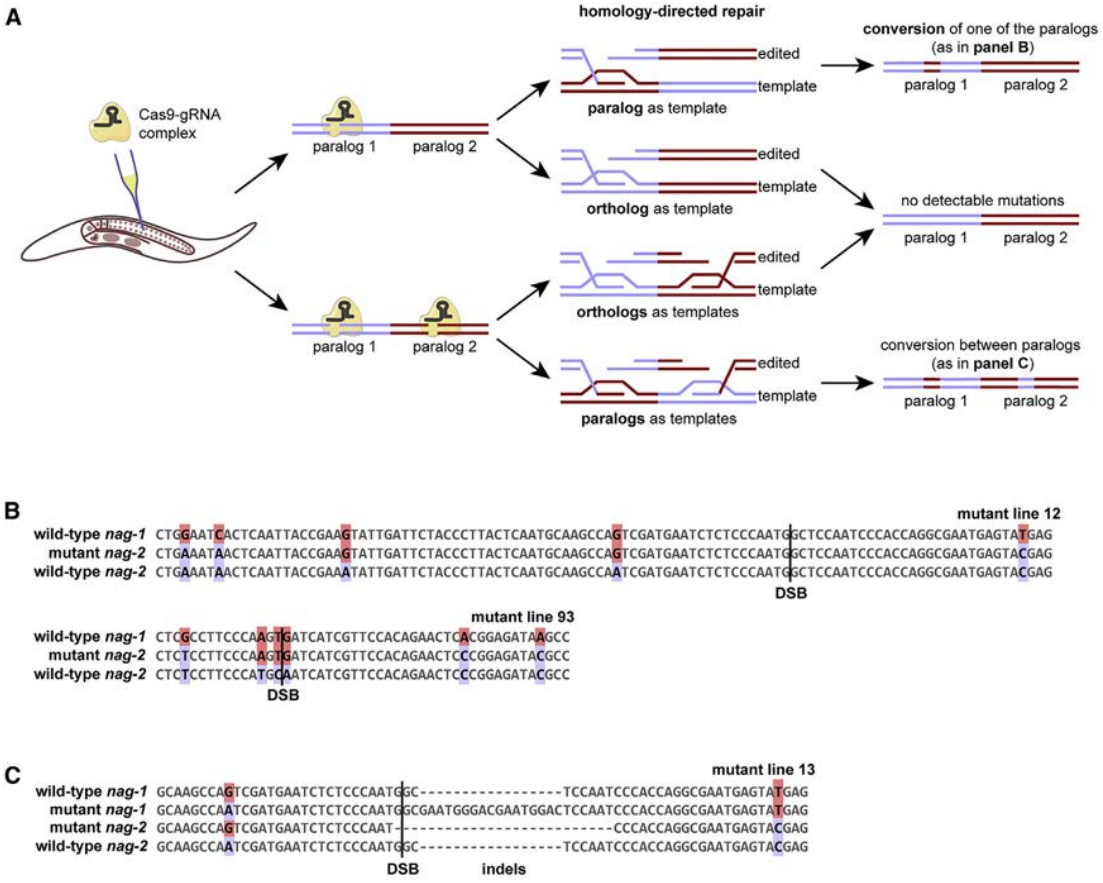

Figure 4. Gene Conversion between Paralogs in the Multi-gene Locus

(A) Hypothetical mechanism of gene conversion that occurred in CRISPR-Cas9-induced mutants and resulted in sequence similarity patterns shown in (B) and (C). In all drawn scenarios, sister chromatids are used as repair templates; however, intra-chromatid conversion may also be possible.

(B and C) Alignment of wild-type and mutant *nag-1* and *nag-2* sequences that underwent gene conversion in either one (B) or both paralogs (C) following CRISPR-Cas9-induced double-strand breaks (DSBs). Colored nucleotides mark informative sites.

See also Figure S4.

break (DSB), we found three independent mutants, in which some informative positions were exchanged between *nag-1* and *nag-2* (Figure 4). Specifically, in two experiments, we targeted exon 5 of both *nag-1* and *nag-2* (Figure S1A) and genotyped a total of 192 F1 progeny of injected animals, 18 of which carried molecular lesions in one or both genes. Interestingly, two mutant lines had genotypes that were best explained by gene conversion (Figure 4). We then repeated an experiment with a different guide RNA (gRNA) targeting exon 4 of *nag-2* (Figure S1A). Here, we genotyped 96 F1 animals and isolated 8 mutants, one of which had a genotype that is consistent with gene conversion (Figures 4A and 4B). Thus, we observed gene conversion at the multi-gene locus under experimental conditions with a relatively high frequency (3 out of 26 mutants in 288 tested animals). Even though CRISPR-Cas9-mediated DSB-induction is clearly not part of normal cell physiology, the fact that the paralogs of affected genes could be used as repair templates demonstrates the propensity of paralogous sequences in the locus to be interconverted.

DISCUSSION

This study has established that the predatory mouth-form dimorphism in *P. pacificus* is controlled by a multi-gene locus, which includes the switch gene *eud-1*. The region contains two pairs of duplicated genes in an inverted tandem configuration. The paralogs *nag-1* and *nag-2*, which code for α-N-acetylglucosaminidases, additively promote the microbivorous St morph, while the *eud-1*/sulfatase promotes the omnivorous Eu morph. The deletion of the complete locus shows that *eud-1* is epistatic over *nag-1* and *nag-2*. We show that *nag* genes and *eud-1* are all expressed in neurons, suggesting their role in environmental perception, a hallmark of developmental plasticity. We speculate that the opposing effects of *eud-1* and the *nag* genes and their non-overlapping expression are linked to the perception of disparate environmental input, which may have necessitated their co-adaptation maintained by physical linkage. Additionally, such genomic organization may facilitate coordinated expression during the time window when the developmental decision is taken.

The multi-gene locus controlling plasticity in *P. pacificus* has multiple similarities to, but also important differences from, other gene clusters that regulate complex traits, which include, but are not limited to, supergenes. We compared our system to other known examples with regard to its relationship with alternative phenotypes, its physical size, and its evolutionary history and reached five major conclusions. First, the multi-gene locus characterized in this study regulates developmental plasticity, in contrast to supergenes and other clusters of linked genes, which represent genetic polymorphisms specifying alternative phenotypes. This demonstrates that the concept of coordinated expression and evolution of structural genes associated with polymorphic phenotypes can be extended to signaling genes associated with plastic phenotypes.

Second, we compared the size of the plasticity multi-gene locus in *P. pacificus* with those of similar loci in other organisms. While the smallest known supergene contains one coding sequence with several associated non-coding genetic elements, and the largest known MHC complex contains several thousand genes (Delarbre et al., 1992; Nishikawa et al., 2015), the plasticity locus in *P. pacificus* consists of four enzyme-encoding genes, three of which are functionally important for dimorphism. Thus, according to the current knowledge, the size of the plasticity multi-gene locus in *P. pacificus* is at the lower end of the range typically found in other known clusters of functionally related genes.

The third conclusion of our study is that the architecture of the *eud-1* locus has been conserved over millions of years and a diversification of more than 30 species. In contrast, traits controlled by supergenes are believed to have multiple origins, and the evolution of supergenes is thought to be rapid, based on comparisons between species of butterflies and ants in well-resolved phylogenetic context (Joron et al., 2011; Purcell et al., 2014; Timmermans et al., 2014; Zhang et al., 2017). Similarly, the number of MHC clusters and their exact gene composition are highly variable between and within different species of primates (Adams and Parham, 2001; Norman et al., 2017). In *Pristionchus*, all eight species with recently sequenced genomes—which cover the complete phylogeny of the genus and were collected in different geographic locations, in different years, and from different host beetles—have the same locus architecture.

Fourth, our outgroup comparison allows insight into the long-term evolutionary stability of the locus organization and its correlation with the trait it controls. Phylogenetic reconstructions in Diplogastridae, the family to which the genus *Pristionchus* belongs, date the evolution of the dimorphism and mouth-form plasticity to the last common ancestor of the entire family (Susoy et al., 2015). The genus *Allodiplogaster* is one of the basal taxa, and sequencing and genome analysis in *A. sudhausi* revealed the absence of clustering of *eud-1* and *nag-1* homologs in this species. These results indicate that the evolution of the trait—alternative mouth forms and plasticity—and the structure of the locus are uncoupled. It is possible that such patterns simply reflect structural turnover in these genomes, and selection for linkage is not always sufficiently strong to counteract it. Alternatively, mouth-form control may be subject to developmental systems drift in Diplogastridae, whereby different loci may control predatory plasticity in *Pristionchus* and in *Allodiplogaster*.

The final conclusion from our study is to provide sequence-based and experimental support for the involvement of gene conversion in shaping the architecture of the plasticity locus in *P. pacificus* and for limiting the divergence of linked genes. Gene conversion was previously observed between paralogs in segmentally duplicated clusters (Hallast et al., 2005; Sharon et al., 1999), in MHC loci in vertebrates (Chen et al., 2007; Goebel et al., 2017), and between odorant-binding proteins in the fire ant supergene (Pracana et al., 2017). Similarly, we inferred from phylogenies that gene conversion has occurred within both pairs of paralogs in the *Pristionchus* multi-gene locus. At the same time, however, the additive phenotypic effects and the non-overlapping expression of *nag-1* and *nag-2*, as well as the drastic difference in the phenotypic contribution between *eud-1* and *sul-2.2.1*, clearly demonstrate that both pairs of paralogs have functionally diverged. Thus, evolution of individual genes is likely shaped by a balance between gene conversion and divergence.

Generally, it is thought that gene conversion constraints divergence and contributes to the neo- or sub-functionalization after gene duplication by preventing newly formed paralogs from pseudogenization (Cortesi et al., 2015; Lynch et al., 2001; Walsh, 1987). Similarly, gene conversion between paralogs can disrupt chromosome structure by enabling non-homologous crossovers (Connallon and Clark, 2010). Such an event may have created the different arrangements of NAGLU and sulfatase homologs in *Pristionchus* and *Micoletzkya*. However, direct evidence for gene conversion is generally scarce, largely due to limited functional tools that would permit the visualization of gene conversion in action. Despite this, in our CRISPR-Cas9 experiments targeting *nag-1* and *nag-2*, we observed molecular lesions that can best be explained by gene conversion. While CRISPR-Cas9-mediated DSB induction represents an un-physiological perturbation, the very fact that paralogs can be used as repair templates demonstrates the propensity of paralogous sequences in the multi-gene locus regulating plasticity to be interconverted.

Taken together, our study shows that physical linkage of functionally related genes occurs between signaling genes associated with phenotypic plasticity. Future investigations will focus on two questions. First, comparisons between wild isolates of *P. pacificus* are necessary to explore the haplotype composition and patterns of selection in the region. It is possible that genetic polymorphisms in the plasticity locus exist and that they correspond to different frequencies of the alternative phenotypes. Second, studying chromatin states and genetic regulatory elements in the locus will elucidate how transcription from the multi-gene locus is regulated.

STAR★METHODS

Detailed methods are provided in the online version of this paper and include the following:

- KEY RESOURCES TABLE
- CONTACT FOR REAGENT AND RESOURCE SHARING
- EXPERIMENTAL MODEL AND SUBJECT DETAILS
- METHOD DETAILS

SUPPLEMENTAL INFORMATION

Supplemental Information includes four figures, one table, and one data file and can be found with this article online at https://doi.org/10.1016/j.celrep.2018.05.008.

ACKNOWLEDGMENTS

We would like to thank Drs. Hernán Burbano and Talia Karasov for discussion. We are also grateful to Drs. Michael Werner, James Lightfoot, Adrian Streit, and Ms. Tess Renahan for giving their comments on the manuscript. The *sul-2.2.1* mutant line was kindly provided by Dr. Erik Ragsdale. The work was funded by the Max Planck Society.

AUTHOR CONTRIBUTIONS

Conceptualization, B.S., N.P., M.R.K., and R.J.S.; Methodology, B.S., N.P., M.D., C.R., M.R.K., and R.J.S.; Formal Analysis, B.S. and N.P.; Investigation, B.S., N.P., M.D., H.W., and W.R.; Resources, H.W. and W.R.; Writing – Original Draft, B.S. and R.J.S.; Writing – Review & Editing, B.S., N.P., M.D., and R.J.S.; Visualization, B.S. and N.P.; Supervision, C.R. and R.J.S.

DECLARATION OF INTERESTS

The authors declare no competing interests.

Received: February 6, 2018
Revised: April 4, 2018
Accepted: May 2, 2018
Published: June 5, 2018

REFERENCES

Adams, E.J., and Parham, P. (2001). Species-specific evolution of *MHC* class I genes in the higher primates. Immunol. Rev. *183*, 41–64.

Altun, Z.F., and Hall, D.H. (2017). Handbook of *C. elegans* anatomy. In WormAtlas. http://www.wormatlas.org/hermaphrodite/hermaphroditehomepage.htm.

Beesley, C.E., Jackson, M., Young, E.P., Vellodi, A., and Winchester, B.G. (2005). Molecular defects in Sanfilippo syndrome type B (mucopolysaccharidosis IIIB). J. Inherit. Metab. Dis. *28*, 759–767.

Bento, G., Ogawa, A., and Sommer, R.J. (2010). Co-option of the hormone-signalling module dafachronic acid-DAF-12 in nematode evolution. Nature *466*, 494–497.

Charlesworth, D. (2015). The status of supergenes in the 21st century: recombination suppression in Batesian mimicry and sex chromosomes and other complex adaptations. Evol. Appl. *9*, 74–90.

Chen, J.-M., Cooper, D.N., Chuzhanova, N., Férec, C., and Patrinos, G.P. (2007). Gene conversion: mechanisms, evolution and human disease. Nat. Rev. Genet. *8*, 762–775.

Connallon, T., and Clark, A.G. (2010). Gene duplication, gene conversion and the evolution of the Y chromosome. Genetics *186*, 277–286.

Cortesi, F., Musilová, Z., Stieb, S.M., Hart, N.S., Siebeck, U.E., Malmstrøm, M., Tørresen, O.K., Jentoft, S., Cheney, K.L., Marshall, N.J., et al. (2015). Ancestral duplications and highly dynamic opsin gene evolution in percomorph fishes. Proc. Natl. Acad. Sci. USA *112*, 1493–1498.

Cribari-Neto, F., and Zeileis, A. (2010). Beta regression in R. J. Stat. Softw. *34*, 1–24.

Delarbre, C., Jaulin, C., Kourilsky, P., and Gachelin, G. (1992). Evolution of the major histocompatibility complex: a hundred-fold amplification of MHC class I genes in the African pigmy mouse *Nannomys setulosus*. Immunogenetics *37*, 29–38.

Edwards, S.V., and Hedrick, P.W. (1998). Evolution and ecology of MHC molecules: from genomics to sexual selection. Trends Ecol. Evol. *13*, 305–311.

Goebel, J., Promerová, M., Bonadonna, F., McCoy, K.D., Serbielle, C., Strandh, M., Yannic, G., Burri, R., and Fumagalli, L. (2017). 100 million years of multigene family evolution: origin and evolution of the avian MHC class IIB. BMC Genomics *18*, 460.

Hallast, P., Nagirnaja, L., Margus, T., and Laan, M. (2005). Segmental duplications and gene conversion: Human luteinizing hormone/chorionic gonadotropin beta gene cluster. Genome Res. *15*, 1535–1546.

Joron, M., Frezal, L., Jones, R.T., Chamberlain, N.L., Lee, S.F., Haag, C.R., Whibley, A., Becuwe, M., Baxter, S.W., Ferguson, L., et al. (2011). Chromosomal rearrangements maintain a polymorphic supergene controlling butterfly mimicry. Nature *477*, 203–206.

Katoh, K., and Standley, D.M. (2013). MAFFT multiple sequence alignment software version 7: improvements in performance and usability. Mol. Biol. Evol. *30*, 772–780.

Kieninger, M.R., Ivers, N.A., Rödelsperger, C., Markov, G.V., Sommer, R.J., and Ragsdale, E.J. (2016). The nuclear hormone receptor NHR-40 acts downstream of the sulfatase EUD-1 as part of a developmental plasticity switch in *Pristionchus*. Curr. Biol. *26*, 2174–2179.

Kim, K.-W., Bennison, C., Hemmings, N., Brookes, L., Hurley, L.L., Griffith, S.C., Burke, T., Birkhead, T.R., and Slate, J. (2017). A sex-linked supergene controls sperm morphology and swimming speed in a songbird. Nat. Ecol. Evol. *1*, 1168–1176.

Kunte, K., Zhang, W., Tenger-Trolander, A., Palmer, D.H., Martin, A., Reed, R.D., Mullen, S.P., and Kronforst, M.R. (2014). *doublesex* is a mimicry supergene. Nature *507*, 229–232.

Langmead, B., and Salzberg, S.L. (2012). Fast gapped-read alignment with Bowtie 2. Nat. Methods *9*, 357–359.

Lenth, R. (2016). Least-squares means: the R package lsmeans. J. Stat. Softw. *69*, 1–33.

Li, J., Cocker, J.M., Wright, J., Webster, M.A., McMullan, M., Dyer, S., Swarbreck, D., Caccamo, M., Oosterhout, C.V., and Gilmartin, P.M. (2016). Genetic architecture and evolution of the S locus supergene in *Primula vulgaris*. Nat. Plants *2*, 16188.

Lynch, M. (2007). The Origins of Genome Architecture (Sinauer Associates).

Lynch, M., O'Hely, M., Walsh, B., and Force, A. (2001). The probability of preservation of a newly arisen gene duplicate. Genetics *159*, 1789–1804.

Nishikawa, H., Iijima, T., Kajitani, R., Yamaguchi, J., Ando, T., Suzuki, Y., Sugano, S., Fujiyama, A., Kosugi, S., Hirakawa, H., et al. (2015). A genetic mechanism for female-limited Batesian mimicry in *Papilio* butterfly. Nat. Genet. *47*, 405–409.

Norman, P.J., Norberg, S.J., Guethlein, L.A., Nemat-Gorgani, N., Royce, T., Wroblewski, E.E., Dunn, T., Mann, T., Alicata, C., Hollenbach, J.A., et al. (2017). Sequences of 95 human *MHC* haplotypes reveal extreme coding variation in genes other than highly polymorphic *HLA class I* and *II*. Genome Res. *27*, 813–823.

Pires-daSilva, A., and Sommer, R.J. (2004). Conservation of the global sex determination gene *tra-1* in distantly related nematodes. Genes Dev. *18*, 1198–1208.

Pracana, R., Levantis, I., Martínez-Ruiz, C., Stolle, E., Priyam, A., and Wurm, Y. (2017). Fire ant social chromosomes: Differences in number, sequence and expression of odorant binding proteins. Evol. Lett. *1*, 199–210.

Projecto-Garcia, J., Biddle, J.F., and Ragsdale, E.J. (2017). Decoding the architecture and origins of mechanisms for developmental polyphenism. Curr. Opin. Genet. Dev. *47*, 1–8.

Purcell, J., Brelsford, A., Wurm, Y., Perrin, N., and Chapuisat, M. (2014). Convergent genetic architecture underlies social organization in ants. Curr. Biol. *24*, 2728–2732.

Ragsdale, E.J., and Ivers, N.A. (2016). Specialization of a polyphenism switch gene following serial duplications in *Pristionchus* nematodes. Evolution *70*, 2155–2166.

Ragsdale, E.J., Müller, M.R., Rödelsperger, C., and Sommer, R.J. (2013). A developmental switch coupled to the evolution of plasticity acts through a sulfatase. Cell *155*, 922–933.

Ragsdale, E.J., Kanzaki, N., and Herrmann, M. (2015). Taxonomy and natural history: the genus *Pristionchus*. In *Pristionchus Pacificus*: A Nematode Model for Comparative and Evolutionary Biology, R.J. Sommer, ed. (BRILL), pp. 77–120.

Rivera-Colón, Y., Schutsky, E.K., Kita, A.Z., and Garman, S.C. (2012). The structure of human GALNS reveals the molecular basis for mucopolysaccharidosis IV A. J. Mol. Biol. *423*, 736–751.

Rödelsperger, C., Meyer, J.M., Prabh, N., Lanz, C., Bemm, F., and Sommer, R.J. (2017). Single-molecule sequencing reveals the chromosome-scale genomic architecture of the nematode model organism *Pristionchus pacificus*. Cell Rep. *21*, 834–844.

Schindelin, J., Arganda-Carreras, I., Frise, E., Kaynig, V., Longair, M., Pietzsch, T., Preibisch, S., Rueden, C., Saalfeld, S., Schmid, B., et al. (2012). Fiji: an open-source platform for biological-image analysis. Nat. Methods *9*, 676–682.

Schlager, B., Wang, X., Braach, G., and Sommer, R.J. (2009). Molecular cloning of a dominant roller mutant and establishment of DNA-mediated transformation in the nematode *Pristionchus pacificus*. Genesis *47*, 300–304.

Schwander, T., Libbrecht, R., and Keller, L. (2014). Supergenes and complex phenotypes. Curr. Biol. *24*, R288–R294.

Sela, I., Ashkenazy, H., Katoh, K., and Pupko, T. (2015). GUIDANCE2: accurate detection of unreliable alignment regions accounting for the uncertainty of multiple parameters. Nucleic Acids Res. *43* (*W1*), W7–W14.

Serobyan, V., Ragsdale, E.J., Müller, M.R., and Sommer, R.J. (2013). Feeding plasticity in the nematode *Pristionchus pacificus* is influenced by sex and social context and is linked to developmental speed. Evol. Dev. *15*, 161–170.

Serobyan, V., Xiao, H., Namdeo, S., Rödelsperger, C., Sieriebriennikov, B., Witte, H., Röseler, W., and Sommer, R.J. (2016). Chromatin remodelling and antisense-mediated up-regulation of the developmental switch gene *eud-1* control predatory feeding plasticity. Nat. Commun. *7*, 12337.

Sharon, D., Glusman, G., Pilpel, Y., Khen, M., Gruetzner, F., Haaf, T., and Lancet, D. (1999). Primate evolution of an olfactory receptor cluster: diversification by gene conversion and recent emergence of pseudogenes. Genomics *61*, 24–36.

Smithson, M., and Verkuilen, J. (2006). A better lemon squeezer? Maximum-likelihood regression with beta-distributed dependent variables. Psychol. Methods *11*, 54–71.

Stamatakis, A. (2014). RAxML version 8: a tool for phylogenetic analysis and post-analysis of large phylogenies. Bioinformatics *30*, 1312–1313.

Stiernagle, T. (2016). Maintenance of *C. elegans*. WormBook, 1–11.

Susoy, V., Ragsdale, E.J., Kanzaki, N., and Sommer, R.J. (2015). Rapid diversification associated with a macroevolutionary pulse of developmental plasticity. eLife *4*, e05463.

Timmermans, M.J.T.N., Baxter, S.W., Clark, R., Heckel, D.G., Vogel, H., Collins, S., Papanicolaou, A., Fukova, I., Joron, M., Thompson, M.J., et al. (2014). Comparative genomics of the mimicry switch in *Papilio dardanus*. Proc. Biol. Sci. *281*, 20140465.

Trowsdale, J. (2002). The gentle art of gene arrangement: the meaning of gene clusters. Genome Biol. *3*, comment2002.1–comment2002.5.

Walsh, J.B. (1987). Sequence-dependent gene conversion: can duplicated genes diverge fast enough to escape conversion? Genetics *117*, 543–557.

Wang, J., Wurm, Y., Nipitwattanaphon, M., Riba-Grognuz, O., Huang, Y.-C., Shoemaker, D., and Keller, L. (2013). A Y-like social chromosome causes alternative colony organization in fire ants. Nature *493*, 664–668.

Werner, M.S., Sieriebriennikov, B., Loschko, T., Namdeo, S., Lenuzzi, M., Dardiry, M., Renahan, T., Sharma, D.R., and Sommer, R.J. (2017). Environmental influence on *Pristionchus pacificus* mouth form through different culture methods. Sci. Rep. *7*, 7207.

West-Eberhard, M.J. (2003). Developmental Plasticity and Evolution (Oxford University Press).

West-Eberhard, M.J. (2005). Developmental plasticity and the origin of species differences. Proc. Natl. Acad. Sci. USA *102* (*Suppl 1*), 6543–6549.

Wilecki, M., Lightfoot, J.W., Susoy, V., and Sommer, R.J. (2015). Predatory feeding behaviour in *Pristionchus* nematodes is dependent on phenotypic plasticity and induced by serotonin. J. Exp. Biol. *218*, 1306–1313.

Witte, H., Moreno, E., Rödelsperger, C., Kim, J., Kim, J.S., Streit, A., and Sommer, R.J. (2015). Gene inactivation using the CRISPR/Cas9 system in the nematode *Pristionchus pacificus*. Dev. Genes Evol. *225*, 55–62.

Zakharova, I.S., Shevchenko, A.I., and Zakian, S.M. (2009). Monoallelic gene expression in mammals. Chromosoma *118*, 279–290.

Zhang, W., Westerman, E., Nitzany, E., Palmer, S., and Kronforst, M.R. (2017). Tracing the origin and evolution of supergene mimicry in butterflies. Nat. Commun. *8*, 1269.

Zhao, Z., Hewett-Emmett, D., and Li, W.H. (1998). Frequent gene conversion between human red and green opsin genes. J. Mol. Evol. *46*, 494–496.

STAR★METHODS

KEY RESOURCES TABLE

REAGENT or RESOURCE	SOURCE	IDENTIFIER
Bacterial and Virus Strains		
Escherichia coli: Strain OP50	*Caenorhabditis* genetics center	RRID:WB-STRAIN:OP50
Chemicals, Peptides, and Recombinant Proteins		
Alt-R CRISPR-Cas9 tracrRNA	Integrated DNA Technologies	Cat#1072534
EnGen Cas9 NLS, *S. pyogenes*	New England Biolabs	Cat#M0646M
Deposited Data		
Whole-genome sequences of *Allodiplogaster sudhausi*	This paper	ENA: ERS2028649
Whole-genome sequences of *Allodiplogaster sudhausi*	This paper	ENA: ERS2028650
Experimental Models: Organisms/Strains		
Pristionchus pacificus: strain PS312	Stock of Dep. IV, MPI Developmental Biology Tuebingen	RRID:WB-STRAIN:PS312
Pristionchus pacificus: strain RS2561: *eud-1(tu445)*	Ragsdale et al., 2013	N/A
Pristionchus pacificus: strain EJR1033: *sul-2.2.1(iub2)*	Ragsdale and Ivers, 2016	N/A
Pristionchus pacificus: strain RS3191: *nag-1(tu1137)*	This paper	N/A
Pristionchus pacificus: strain RS3192: *nag-2(tu1138)*	This paper	N/A
Pristionchus pacificus: strain RS3195: *nag-1(tu1142) nag-2(tu1143)*	This paper	N/A
Pristionchus pacificus: strain RS3198: *tuDf1[nag-1 sul-2.2.1 eud-1 nag-2]*	This paper	N/A
Pristionchus pacificus: strain RS2653: *tuEx177 [eud-1p::TurboRFP::rpl-23utr]*	Ragsdale et al., 2013	N/A
Pristionchus pacificus: strain RS3250: *tuEx275 [nag-1p::Venus::rpl-23utr]*	This paper	N/A
Pristionchus pacificus: strain RS3381: *tuEx280 [nag-2p::TurboRFP::rpl-23utr]*	This paper	N/A
Pristionchus pacificus: strain RS3200: *eud-1(tu445); tuEx271[eud-1p::eud-1(+)cds::rpl-23utr]*	This paper	N/A
Pristionchus pacificus: strain RS3201: *eud-1(tu445); tuEx272[eud-1p::eud-1(+)cds::rpl-23utr]*	This paper	N/A
Pristionchus pacificus: strain RS3268: *eud-1(tu445); tuEx276[eud-1p::sul-2.2.1cds::rpl-23utr]*	This paper	N/A
Pristionchus pacificus: strain RS3272: *eud-1(tu445); tuEx278[eud-1p::sul-2.2.1cds::rpl-23utr]*	This paper	N/A
Allodiplogaster sudhausi: strain SB413	Stock of Dep. IV, MPI Developmental Biology Tuebingen	N/A
Oligonucleotides		
sgRNA target sequence: exon 5 of *nag-1* and *nag-2*: CCTGGTGGGATTGGAGCCAT	This paper	N/A
crRNA target sequence: exon 4 of *nag-2*: TCTGTGGAACGATGATTGCA	This paper	N/A
crRNA target sequence: *dpy-23*: CAACGACAAATTGACGTTAG	This paper	N/A
crRNA target sequence: *F40E10.6*: AGGGTGAGCAGAGACATGAT	This paper	N/A
Recombinant DNA		
Plasmid: pUC19-*egl-20p::TurboRFP::rpl-23utr*	Schlager et al., 2009	N/A
Plasmid: pUC19-*eud-1p::eud-1cds::rpl-23utr*	This paper	N/A

(*Continued on next page*)

Continued

REAGENT or RESOURCE	SOURCE	IDENTIFIER
Plasmid: pUC19-*eud-1p::sul-2.2.1cds::rpl-23utr*	This paper	N/A
Plasmid: pUC19-*nag-1p::Venus::rpl-23utr*	This paper	N/A
Plasmid: pUC19-*nag-2p::TurboRFP::rpl-23utr*	This paper	N/A
Software and Algorithms		
Bowtie 2	Langmead and Salzberg, 2012	N/A
FIJI	Schindelin et al., 2012	RRID:SCR_002285
DISCOVAR *de novo*	https://software.broadinstitute.org/software/discovar/blog/	N/A
MAFFT	Katoh and Standley, 2013	RRID:SCR_011811
GUIDANCE2	Sela et al., 2015	N/A
RAxML	Stamatakis, 2014	RRID:SCR_006086
R	http://www.r-project.org/	RRID:SCR_001905

CONTACT FOR REAGENT AND RESOURCE SHARING

Further information and requests for resources and reagents should be directed to and will be fulfilled by the Lead Contact, Ralf J. Sommer (ralf.sommer@tuebingen.mpg.de).

EXPERIMENTAL MODEL AND SUBJECT DETAILS

Stock cultures of *P. pacificus* wild-type strain PS312, all the mutant and transgenic strains used in this study and *A. sudhausi* SB413 were maintained following standard protocols for *C. elegans* (Stiernagle, 2016). Specifically, worms were kept at room temperature (20-25°C) on 6 cm plates with nematode growth medium (NGM) consisting of 1.7% agar, 3 g/L NaCl, 2.5 g/L tryptone, 1 mM $CaCl_2$, 1 mM $MgSO_4$, 5 mg/L cholesterol and 25 mM KPO_4 buffer (diluted from a 1 M stock solution of 108.3 g/L KH_2PO_4 and 35.6 g/L K_2HPO_4 with pH adjusted to 6.0). *Escherichia coli* OP50 was used as the food source. Bacteria were grown overnight at 37°C in L Broth consisting of 10 g/L tryptone, 5 g/L yeast extract and 5 g/L NaCl with pH adjusted to 7.0. Bacterial lawns were grown from 250-400 uL of the overnight culture on NGM agar plates at room temperature, and nematodes were transferred to the lawns. For maintenance, *P. pacificus* cultures were propagated clonally by passing self-fertilizing hermaphrodites only. For the experiments where presence of males was required, males spontaneously formed in stock cultures were allowed to breed and thus increase the male proportion in the population. These mixed-sex cultures were propagated by passing multiple animals of both sexes and different developmental stages to new plates.

METHOD DETAILS

CRISPR-Cas9 mutagenesis

Procedure for CRISPR-Cas9 mutagenesis was based on the existing protocol for *P. pacificus* (Witte et al., 2015) and included several modifications described below. Single guide RNA (sgRNA) obtained from Toolgen was used to target exon 5 in *nag-1* and *nag-2*, whereas the rest of the loci were targeted using hybridized target-specific CRISPR RNAs (crRNAs) and universal *trans*-activating CRISPR RNA (tracrRNA) obtained from Integrated DNA Technologies (Alt-R product line). To hybridize crRNA and tracrRNA, 10 uL of the 100 uM stock of each molecule were combined, denatured at 95°C for 5 min and allowed to cool down and anneal at room temperature for 5 min. 5 uL of the hybridization product or 2 uL of 3 ug/uL sgRNA was combined with 2 uL of 20 uM Cas9 protein (New England Biolabs) and incubated at room temperature for 5 min. The mixture was diluted with Tris-EDTA buffer to the total volume of 25 uL and injected in the gonad rachis in 1 day old hermaphrodites. The sgRNA and all the crRNAs were designed to target 20 bp upstream of protospacer adjacent motifs (PAMs) marked in Figure S1A. Molecular lesions were detected in F1 progeny by high-resolution melting curve analysis of PCR amplicons using LightCycler 480 High Resolution Melting Master on a LightCycler 480 Instrument II (Roche). Presence of mutations in candidate amplicons was verified by Sanger sequencing. To detect large rearrangements that affected multiple genes in the locus (Figure S1B), genomic DNA was extracted from worms, for which no PCR amplicon containing the sgRNA or crRNA target site could be obtained. Next generation sequencing libraries were prepared using TruSeq DNA PCR-Free Low Throughput Library Prep Kit and sequenced on a HiSeq 3000 machine (Illumina). Reads were mapped to the El Paco assembly of the *P. pacificus* genome (Rödelsperger et al., 2017) using Bowtie 2 (Langmead and Salzberg, 2012). Consequently, read coverage in the locus of interest was visually inspected to detect any deviations from the pattern in the surrounding regions.

Mouth form phenotyping

Phenotyping was done in two culture conditions. Culturing *P. pacificus* on NGM agar plates (as stock cultures are maintained, see above) induces the Eu morph and thus enables identification of Eu-deficient (Eud) phenotype, whereas culturing the worms in liquid S-medium represses the Eu morph and facilitates identification of the Eu-constitutive (Euc) mutant phenotype (Werner et al., 2017). S-medium consists of 5.85 g/L NaCl, 1 g/L K_2HPO_4, 6 g/L KH_2PO_4, 5 mg/L cholesterol, 3 mM $CaCl_2$, 3 mM $MgSO_4$, 18.6 mg/L disodium EDTA, 6.9 mg/L $FeSO_4 \cdot 7H_2O$, 2 mg/L $MnCl_2 \cdot 4H_2O$, 2.9 mg/L $ZnSO_4 \cdot 7H_2O$, 0.25 mg/L $CuSO_4 \cdot 5H_2O$ and 10 mM Potassium citrate buffer (diluted from a 1 M stock solution of 20 g/L citric acid monohydrate and 293.5 g/L tri-potassium citrate monohydrate with pH adjusted to 6.0) (Stiernagle, 2016). Liquid cultures were started with nematode eggs extracted by bleaching animals collected from stock cultures (Stiernagle, 2016; Werner et al., 2017). For this, worms were washed from plates with water and incubated for 10 min in a mixture of household bleach at 1:5 final dilution and NaOH at the final concentration of 0.5 M. Extracted eggs were pelleted down, washed with water and added to 10 mL of S-medium that contained re-suspended *E. coli* OP50 in the amount corresponding to 100 mL of an overnight bacterial culture (see above) with OD_{600} of 0.5. Flasks with liquid cultures were incubated on a shaking platform at 180 rpm. Only adults were phenotyped for mouth form. Animals were immobilized on agar pads containing 0.3% NaN_3 and examined using differential interference contrast (DIC) microscopy. The Eu morph was distinguished from the St morph based on the presence of the right ventrosublateral tooth, the shape of the dorsal tooth and the width of the mouth (buccal cavity).

Genetic rescue of *eud-1* mutants

Constructs for the genetic rescue of *eud-1(tu445)* mutants were made by fusing 2 kb of sequence upstream of the first ATG codon of the *eud-1* gene with wild-type coding DNA sequence (CDS) of either *eud-1* or *sul-2.2.1* and 3′ untranslated region (UTR) of a ribosomal gene *rpl-23* (Data S1; Figure S2A). Previously published CDS sequence of *eud-1* was used (Ragsdale et al., 2013) and CDS sequence of *sul-2.2.1* was identified based on the available gene prediction (Rödelsperger et al., 2017) and verified with rapid amplification of cDNA ends (RACE). Synthetic gBlocks fragments containing the CDS sequences were obtained from Integrated DNA Technologies. pUC19-based plasmids carrying the rescue constructs were assembled using NEBuilder HiFi DNA Assembly Master Mix (New England Biolabs). For transformation, complex arrays were made by digesting the rescue construct, a tail-specific transformation marker (*egl-20p::TurboRFP*) and *eud-1* mutant genomic DNA with the restriction enzyme FastDigest PstI (Thermo Fisher Scientific), followed by a clean-up using Wizard SV Gel and PCR Clean-Up System (Promega), and mixing the digested components. Final concentrations in the mix were 10 ng/uL for each plasmid and 60 ng/uL for gDNA. Transformation arrays were injected in the gonad rachis in 1 day old hermaphrodites (Schlager et al., 2009). F1 progeny were examined under a fluorescent dissecting microscope and animals expressing transformation marker were isolated and allowed to self-fertilize.

Co-localization experiments

Reporter constructs for *nag-1* and *nag-2* were made by cloning a sequence upstream of the first ATG codon of the respective gene (5.1 kb for *nag-1* and 3.9 kb for *nag-2*) into a pUC19-based plasmid containing a fluorescent protein (Venus for *nag-1* and TurboRFP for *nag-2*) and the 3′ UTR of the ribosomal gene *rpl-23* (Data S1). Cloning was done using NEBuilder HiFi DNA Assembly Master Mix (New England Biolabs). Complex arrays were prepared and transgenic lines were created as described above for the *eud-1* rescue experiments with the exception that wild-type gDNA was used in the transformation arrays instead of mutant gDNA. To establish co-localization of expression of different genes, animals carrying the *tuEx275[nag-1p::Venus]* reporter were crossed either with *tuEx280 [nag-2p::TurboRFP]* or with previously available *tuEx177[eud-1p::TurboRFP]*, and F1 progeny were microscopically examined. For crossing, small bacterial lawns were grown from 10-50 uL of bacterial culture. Up to six adult males of one strain were transferred to a plate containing one or two hermaphrodites of the other strain. Hermaphrodites used for mating were visually older and had no visible eggs inside the uteri, which indicated that most of self-produced sperm had been used and thus the probability of self-fertilization was reduced. Mating success was verified by observing sex ratio in the progeny. Cross progeny were immobilized on agar pads containing 0.3% NaN_3 and imaged using a Leica TCS SP8 confocal microscope. Post-processing of images was done using FIJI [version 1.0] (Schindelin et al., 2012). The main figures contain expression patterns in the head region. Additionally, *nag-1* was expressed in the oviduct and *nag-2* was expressed in the vulva and, occasionally, in pharyngeal gland cells (Figure S2C-E).

Whole-genome sequencing

A. sudhausi worms from nutrient depleted plates were rinsed with M9 buffer (3 g/L KH_2PO_4, 6 g/L Na_2HPO_4, 5 g/L NaCl, 1 mM $MgSO_4$) and the worm pellet was collected by centrifugation at 1300 rpm for 3 minutes at 4°C. The pellet was immediately frozen by pouring liquid nitrogen onto it and then ground to a fine powder using mortar and pestle. The powder was transferred to the lysis buffer from Genomic DNA Buffer Set (QIAGEN) and Genomic-tip 100/G columns (QIAGEN) were used for DNA extraction as per the manufacturer's protocol. We used Qubit 2.0 Fluorometer (Thermo Fisher Scientific) and NanoDrop ND 1000 spectrometer (Peqlab) for DNA quality and quantity determination.

Library preparation for the whole genome sequencing was done with TruSeq DNA PCR-Free Library Prep kit following the manufacturer's protocol and the prepared libraries were run on Illumina MiSeq. The intial assembly was generated with DISCOVAR *de novo* assembler (https://software.broadinstitute.org/software/discovar/blog/). Then, we checked for *E. coli* contamination by BLASTN searches against the NCBI nt database and removed contaminated contigs after manual inspection to create the final assembly.

Phylogenetic reconstructions

Multiple sequence alignments were created by MAFFT (version 7.271) (Katoh and Standley, 2013) and unreliable alignment positions were identified and removed through GUIDANCE2 (version 2.02) (Sela et al., 2015). After manual inspection, each alignment was passed to RAxML (version 8.2.4) (Stamatakis, 2014) for making maximum likelihood trees with 100 bootstrap replicates.

QUANTIFICATION AND STATISTICAL ANALYSIS

Morph frequencies were compared by fitting beta regression using the R package betareg (Cribari-Neto and Zeileis, 2010). Since morph ratios in some strains included the extremes 0 and 1, we followed the guidelines outlined by Smithson and Verkuilen and applied a (y*(n-1)+0.5)/n transformation, where y is the response variable and n is the sample size (Smithson and Verkuilen, 2006). Post hoc pairwise comparison was done using the R package lsmeans with false discovery rate correction of the p values (Lenth, 2016). All p values < 0.05 are summarized with asterisks in corresponding figures. For strains carrying mutations in *nag-2, sul-2.2.1, eud-1, nag-1* or in any combination of these genes, at least three biological replicates with at least 50 individuals per replicate were counted for each sex. For strains in which genes outside of the supergene were altered, only one biological replicate was collected and only hermaphrodites were phenotyped. For transgenic *eud-1* rescue lines, at least three biological replicates with at least 30 transgenic individuals per replicate were counted and only hermaphrodites were phenotyped.

DATA AND SOFTWARE AVAILABILITY

The whole-genome sequencing data for *A. sudhausi* are deposited in the European Nucleotide Archive at https://www.ebi.ac.uk/ena with sample accession numbers ENA: ERS2028649 and ERS2028650.

FASTA files containing all the gene predictions used in this study are provided in the supplemental file Data S1.

Cell Reports, Volume *23*

Supplemental Information

A Developmental Switch Generating Phenotypic Plasticity Is Part of a Conserved Multi-gene Locus

Bogdan Sieriebriennikov, Neel Prabh, Mohannad Dardiry, Hanh Witte, Waltraud Röseler, Manuela R. Kieninger, Christian Rödelsperger, and Ralf J. Sommer

Supplemental information

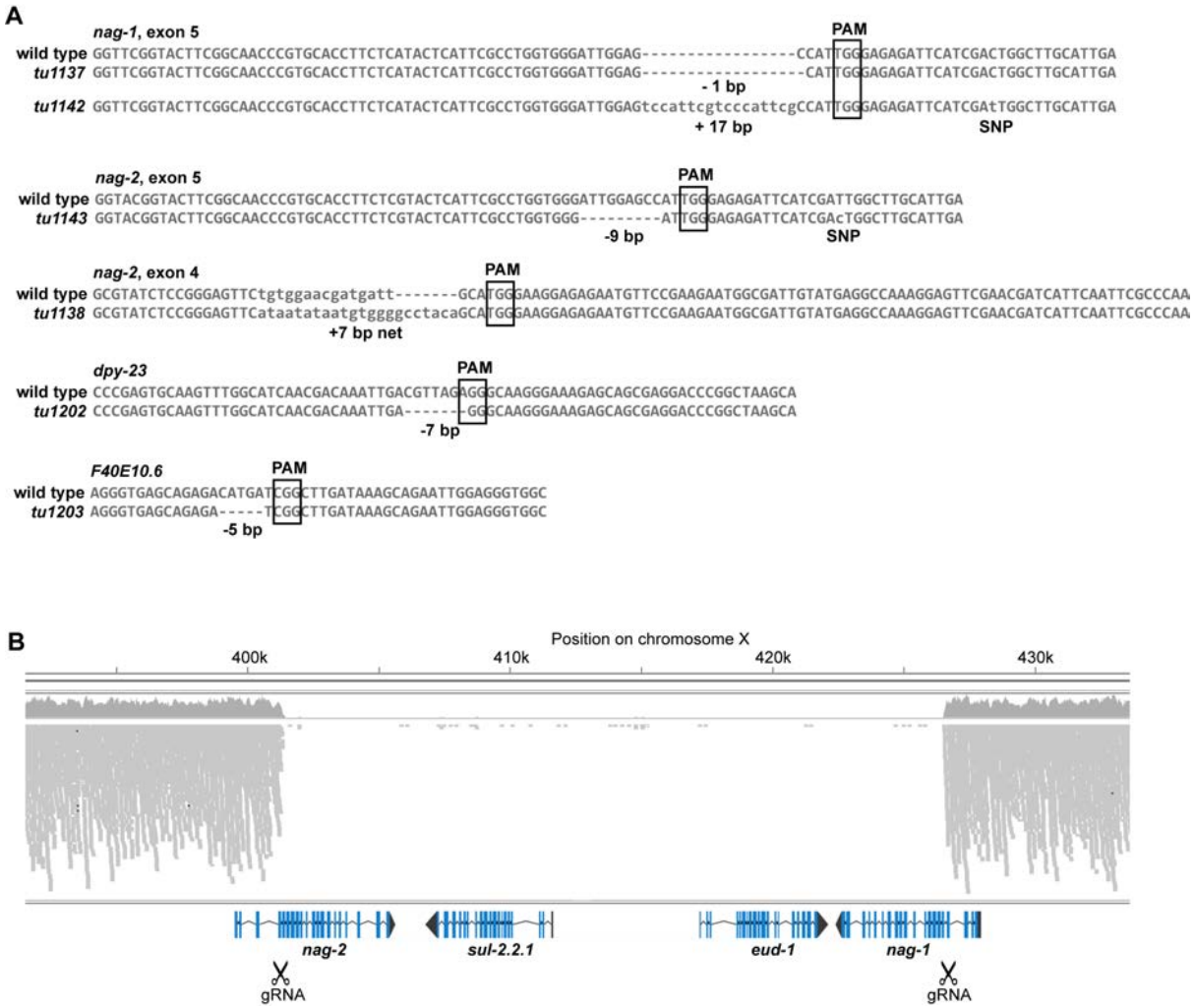

Figure S1. Molecular lesions in CRISPR/Cas9 mutants. Related to Figure 2. (**A**) Alignment of wild type and *nag-1* and *nag-2* mutant sequences. PAM = protospacer adjacent motif. All sgRNA/crRNAs were designed to target 20 bp upstream of PAMs. SNP = single nucleotide polymorphism. (**B**) Whole-genome resequencing reads mapping to the plasticity multi-gene locus in the quadruple mutant *tuDf1[nag-1 sul-2.2.1 eud-1 nag-2].*

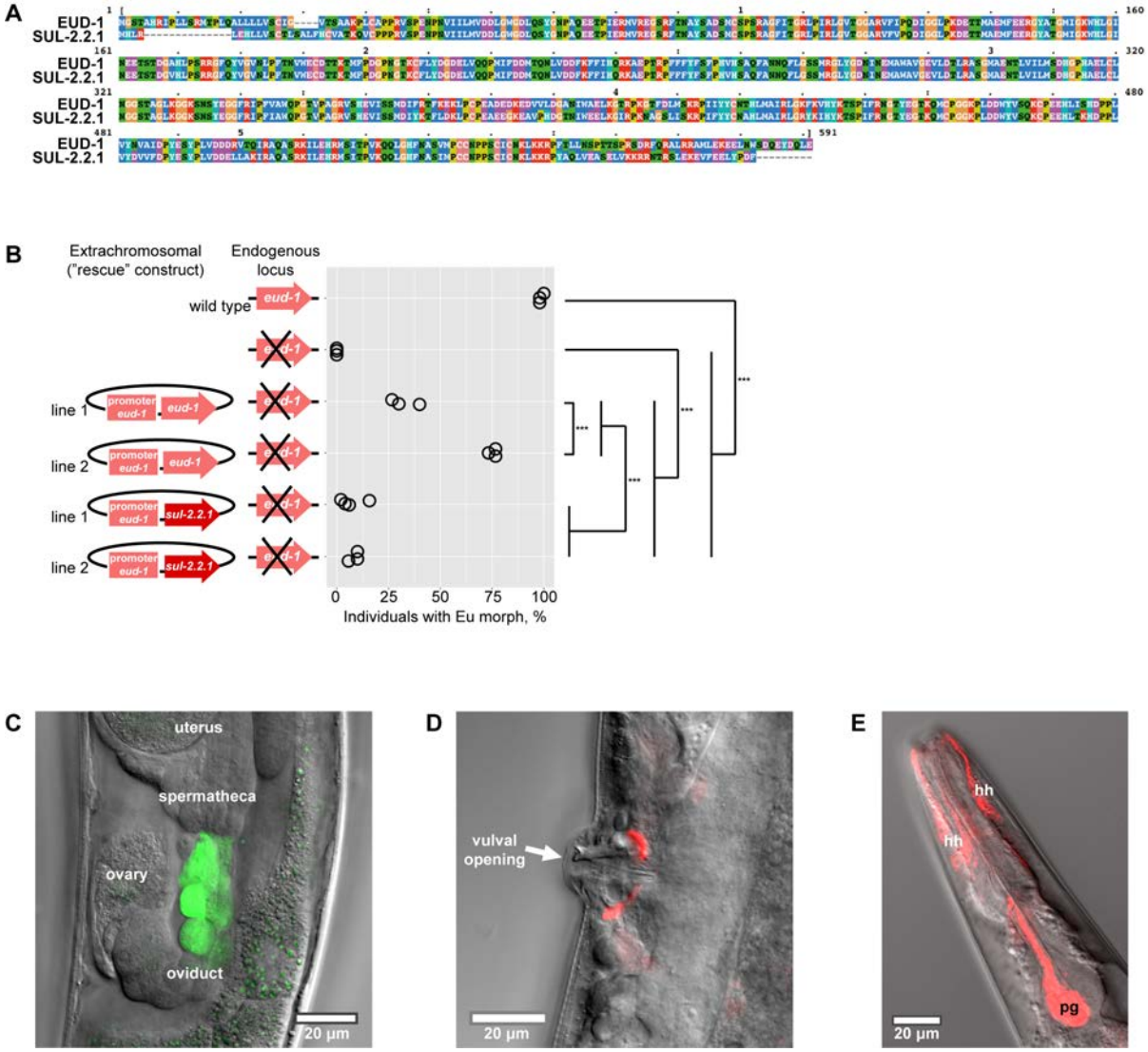

Figure S2. Rescue experiments with sulfatase CDS and expression patterns of *nag* genes. Related to Figure 2. (**A**) Alignment of amino acid sequences of EUD-1 and SUL-2.2.1 in *P. pacificus*. (**B**) Overexpression of *sul-2.2.1* can only partially rescue the *eud-1* mutant phenotype. Shown are morph frequencies in wild type PS312 hermaphrodites, the *eud-1(tu445)* mutant and the 'rescue' lines (top to bottom) *eud-1(tu445);tuEx271[eud-1p::eud-1(+)], eud-1(tu445);tuEx272[eud-1p::eud-1(+)], eud-1(tu445);tuEx278[eud-1p::sul-2.2.1(+)]* and *eud-1(tu445);tuEx276[eud-1p::sul-2.2.1(+)]*. *** = p<0.001. (**C**) Fragment of the reproductive system in a *P. pacificus* hermaphrodite of the *tuEx275[nag-1p::Venus]* reporter line. Overlay of DIC image and standard deviation Z-projection of the Venus channel. (**D**) Vulva region of a hermaphrodite carrying the *tuEx280[nag-2p::TurboRFP]* reporter. Overlay of DIC image and standard deviation Z-projection of the TurboRFP channel. (**E**) Head region of an animal of the *tuEx280[nag-2p::TurboRFP]* reporter line. Overlay of DIC image and maximal intensity Z-projection of the TurboRFP channel. hh = head hypodermis, pg = pharyngeal gland.

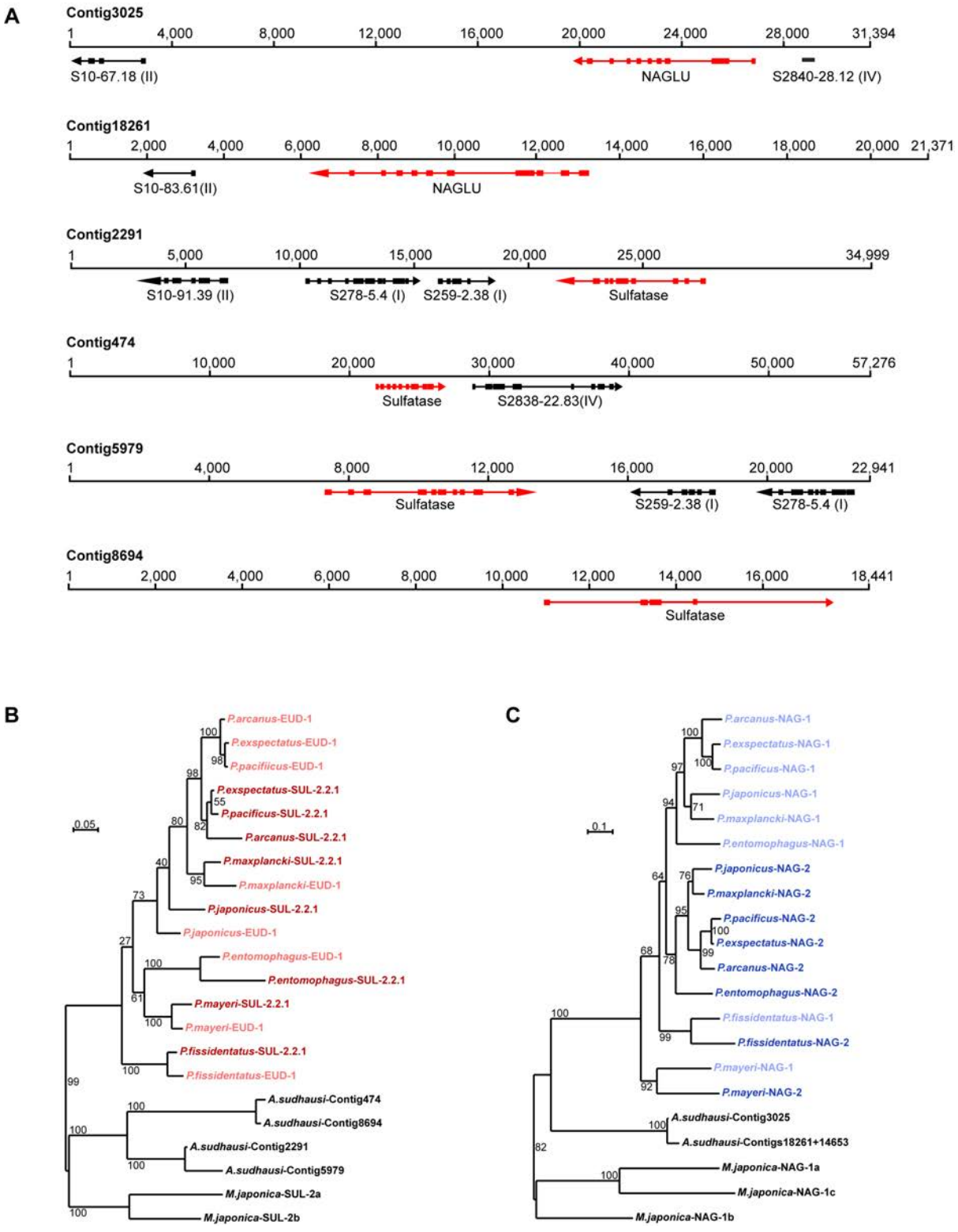

Figure S3. Genomic location of EUD-1 and NAG-1 homologs in newly sequenced *A. sudhausi* and maximum likelihood tree of EUD-1 and NAG-1 homologs in all studied genomes. Related to Figure 3. (**A**) Contigs of the *A. sudhausi* genome containing EUD-1 and NAG-1 homologs. Neighboring *P. pacificus* homologs are labelled with their chromosome numbers in parenthesis. The scale bar indicates the base position

on each contig. (**B**) Maximum likelihood tree of amino acid sequences of EUD-1 homologs in all studied genomes. (**C**) Maximum likelihood tree of amino acid sequences of NAG-1 homologs in all studied genomes. In B and C, numbers show values of bootstrap support. Only genes shown in Fig. 3A are included.

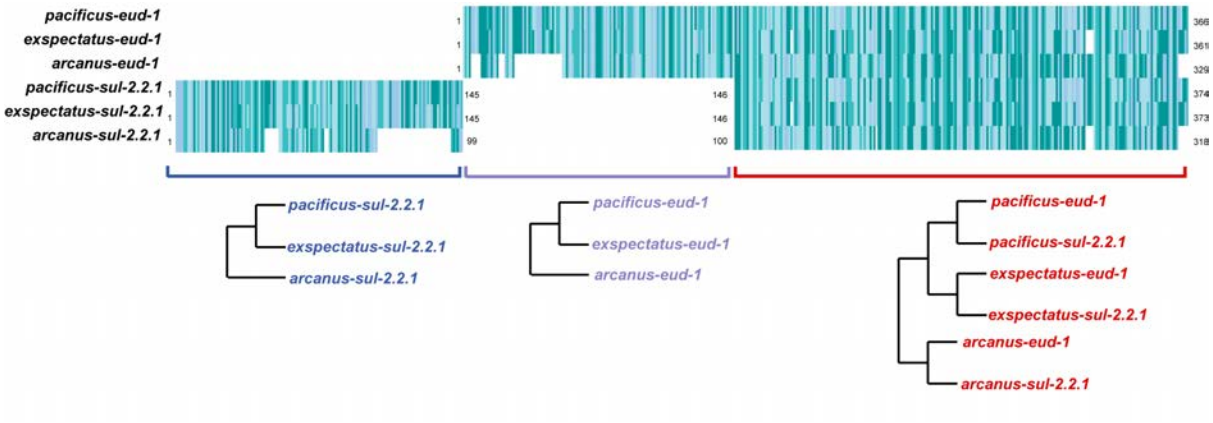

Figure S4. Visual representation of the reliable columns extracted from the alignment of intronic region of *eud-1* and *sul-2.2.1*, and cladograms generated from different parts of the alignment. Related to Figures 3 and 4. Each column is color-coded by the corresponding nucleotide composition for each gene. Absence of color indicates gap at the given alignment position for the given gene. Unrooted tree placed below the alignments were generated based on the parts of the alignment directly above them.

Table S1. Phenotypes of strains with CRISPR/Cas9-induced mutations in genes adjacent to the multi-gene locus in *P. pacificus*. Related to Figure 3.

Culture condition	Strain	Eu	St
Liquid culture	Wild-type PS312	1	49
Liquid culture	*dpy-23(tu1202)*	2	48
Liquid culture	*F40E10.6(tu1203)*	1	49
Agar plates	Wild-type PS312	50	0
Agar plates	*dpy-23(tu1202)*	50	0
Agar plates	*F40E10.6(tu1203)*	50	0

nature COMMUNICATIONS

ARTICLE

Received 4 May 2016 | Accepted 23 Jun 2016 | Published 4 Aug 2016

DOI: 10.1038/ncomms12337 OPEN

Chromatin remodelling and antisense-mediated up-regulation of the developmental switch gene *eud-1* control predatory feeding plasticity

Vahan Serobyan[1], Hua Xiao[1,†], Suryesh Namdeo[1], Christian Rödelsperger[1], Bogdan Sieriebriennikov[1], Hanh Witte[1], Waltraud Röseler[1] & Ralf J. Sommer[1]

Phenotypic plasticity has been suggested to act through developmental switches, but little is known about associated molecular mechanisms. In the nematode *Pristionchus pacificus*, the sulfatase *eud-1* was identified as part of a developmental switch controlling mouth-form plasticity governing a predatory versus bacteriovorous mouth-form decision. Here we show that mutations in the conserved histone-acetyltransferase *Ppa-lsy-12* and the methyl-binding-protein *Ppa-mbd-2* mimic the *eud-1* phenotype, resulting in the absence of one mouth-form. Mutations in both genes cause histone modification defects and reduced *eud-1* expression. Surprisingly, *Ppa-lsy-12* mutants also result in the down-regulation of an antisense-*eud-1* RNA. *eud-1* and antisense-*eud-1* are co-expressed and further experiments suggest that antisense-*eud-1* acts through *eud-1* itself. Indeed, overexpression of the antisense-*eud-1* RNA increases the *eud-1*-sensitive mouth-form and extends *eud-1* expression. In contrast, this effect is absent in *eud-1* mutants indicating that antisense-*eud-1* positively regulates *eud-1*. Thus, chromatin remodelling and antisense-mediated up-regulation of *eud-1* control feeding plasticity in *Pristionchus*.

[1] Department for Evolutionary Biology, Max-Planck-Institute for Developmental Biology, Spemannstrasse 35, 72076 Tübingen, Germany. [†] Present address: University of Missouri-Columbia, Division of Biological Sciences 103 Tucker Hall, Columbia, Missouri 65211 USA. Correspondence and requests for materials should be addressed to R.J.S. (email: ralf.sommer@tuebingen.mpg.de).

Developmental (phenotypic) plasticity has been suggested to facilitate morphological novelty and diversity[1–5], but little is known about the molecular aspects of developmental switch mechanisms that underlie plasticity. The nematode *Pristionchus pacificus* is a potential model system to study the molecular and mechanistic details of developmental plasticity because it can be easily cultured in the laboratory by feeding on bacteria, but in the wild it lives in a necromenic interaction with beetles[6,7]. Specifically, the necromenic life style of *P. pacificus* and related nematodes is facilitated by dynamic feeding mode switching between bacterial grazing and the predation of other nematodes (Fig. 1a,b; ref. 7). This feeding diversity relies on the presence of moveable teeth and *Pristionchus* nematodes exhibit two distinct morphs—stenostomatous (St, narrow-mouthed) or eurystomatous (Eu, wide-mouthed) —that differ in the number and shape of associated teeth and the size and form of the buccal cavity[8] (Fig. 1c,d). When fed on *Escherichia coli* OP50 bacteria under lab conditions, *P. pacificus* California reference strain RS2333 hermaphrodites have a stable 70:30% Eu:St ratio, but this can be influenced by starvation, crowding and pheromone signalling[8–10]. Because *P. pacificus* hermaphrodites reproduce primarily by selfing, strains are genetically homogeneous, and the presence of two distinct morphs thus represents an example of developmental plasticity, which was also demonstrated experimentally[8].

The existence of developmental switch mechanisms is essential for the irreversible control of plasticity and has long been anticipated by evolutionary theory[1], but associated mechanisms are largely unknown. We have recently identified the sulfatase *eud-1* as part of a genetic network that constitutes the developmental switch for the *P. pacificus* mouth-form decision[6]. In *eud-1* mutants, the Eu form is absent (*eud*, *eu*rystomatous-form-*d*efective), whereas overexpression from transgenes fixes the Eu form, thus confirming that EUD-1 acts as a developmental switch[6]. *eud-1* is X-linked and dosage-dependent, and it regulates differences in mouth-form frequency between hermaphrodites and males, among *P. pacificus* strains, and between *Pristionchus* species[6]. Interestingly, *P. pacificus eud-1* derives from a recent duplication that resulted in two neighbouring gene copies arranged in a head-to-head orientation (Fig. 1e). *eud-1* is expressed in a small number of *P. pacificus* head neurons, where its expression is sufficient to induce the execution of the Eu mouth-form[6]. However, while *eud-1* expression is highly regulated, the underlying mechanisms that control this developmental switch gene remain unknown.

Here we show that mutations in the conserved histone acetyltransferase *Ppa-lsy-12* and the methyl-binding-protein *Ppa-mbd-2* result in the absence of the Eu mouth-form similar to mutants in *Ppa-eud-1*. Mutations in both genes cause histone modification defects that result among others, in reduced *eud-1* expression. In addition, in *Ppa-lsy-12* mutants an antisense-*eud-1* RNA is also down-regulated. Overexpression of the antisense-*eud-1* RNA from transgenes increases the *eud-1*-sensitive mouth-form and results in increased *eud-1* expression. In contrast, this effect is absent in *eud-1* mutants indicating that antisense-*eud-1* positively regulates *eud-1*. These epigenetic mechanisms provide a theoretical framework for linking genetic regulation to environmental input.

Results

Two pleiotropic mutants with mouth-form defects. To study the regulation of *eud-1,* we searched for pleiotropic mutants with a Eud phenotype in hermaphrodites, similar to *eud-1*. By screening more than 30 already-established mutant strains with egg laying- or vulva defects, we identified two mutants, *tu319* and *tu365,* with a nearly complete loss of the Eu form (Fig. 2a). While *tu319* was previously molecularly uncharacterized, *tu365* represents a deletion allele in the methyl-binding protein family member *Ppa-mbd-2* (ref. 11). *Ppa-mbd-2(tu365)* is recessive, homozygous viable, and displays both a fully penetrant egg-laying defect and a complete absence of the Eu mouth-form (Fig. 2a). *Ppa-mbd-2(tu365)* contains a 1.7 kb deletion that removes four of six exons, suggesting that the absence of the Eu form results from a strong reduction-of-function or even null mutation in this gene. Thus, the phenotype of *mbd-2* in *P. pacificus* reveals the existence of pleiotropic regulators of mouth-form plasticity.

A conserved histone-acetyltransferase regulates plasticity. In *tu319* mutants, only 2% of hermaphrodites have a Eu mouth-form (Fig. 2a). *tu319* was isolated in a screen for vulva-defective mutants and represents one of three alleles of the previously genetically characterized *vul-2* (*vul*valess) locus[12]. Interestingly, only *tu319* but not the two other alleles, *tu18* and *tu30,* show mouth-form defects indicating that the effect of *vul-2* on mouth-form regulation is allele-specific. We mapped *tu319* to the tip of chromosome IV in proximity to the marker S210 (Supplementary Fig. 1a). Sequencing of fosmid clones of this gene poor region resulted in the identification of a histone-acetyltransferase orthologous to the *Caenorhabditis elegans* gene *lsy-12* (Supplementary Fig. 1b,c; ref. 13. Sequencing of *lsy-12* identified mutations in all three alleles; *tu319* and *tu30* have splice-site mutations, whereas *tu18* contains a 598 bp deletion in the putative 3′-end of the gene (Supplementary Fig. 1b). *Ppa-lsy-12* is a complex gene with more than 30 predicted exons, and rapid amplification of cloned/cDNA ends (RACE) and RNA seq experiments provide strong evidence for extensive alternative splicing (Supplementary Fig. 1b). *Ppa-lsy-12* has a typical MYST domain in the 5′ part of the gene encoded by exons 5–13 (Supplementary Fig. 1b), which is present in the majority of transcripts. Interestingly, *tu319* affects the splice site of exon 7, whereas the two other alleles affect the 3′ part of the gene, which is not associated with known protein domains and is not present in the majority of transcripts.

To attempt phenotypic rescue, we generated a construct of *Ppa-lsy-12* containing exons 1–20 (see Methods) and obtained three independently transformed lines carrying the *Ppa-lsy-12* construct alongside an *egl-20::rfp* (red fluorescent protein) reporter. All three transgenic lines rescued both the vulvaless defect and the mouth-form defect of *tu319* (Supplementary Fig. 1c,d). Specifically, in transgenic animals the mouth-form was 71% Eu (versus 2% Eu in *tu319* worms) and, in one line studied in greater detail, 90% of the vulva precursor cells were induced to form vulval tissue (versus 33% in *tu319* worms). These results indicate that *vul-2* is indeed identical to *Ppa-lsy-12* and we renamed the gene accordingly. Taken together, two evolutionarily conserved genes, *Ppa-lsy-12* and *Ppa-mbd-2*, are pleiotropic regulators of mouth-form plasticity and mutations in these genes result in a strong reduction or absence of the Eu mouth-form.

***mbd-2 and lsy-12* mutants cause histone modification defects**. The molecular nature of *Ppa-lsy-12* suggests that chromatin remodelling may control the developmental switch mechanism that underlies the *P. pacificus* mouth dimorphism. Chromatin remodelling proteins regulate numerous developmental processes[14], but nothing is known of a potential role for chromatin remodelling in the regulation of developmental plasticity. Therefore, we first asked if histone modifications are indeed altered in *lsy-12* and *mbd-2* mutants. We isolated proteins from mixed stage cultures of wild-type, *mbd-2,* and *lsy-12* mutant

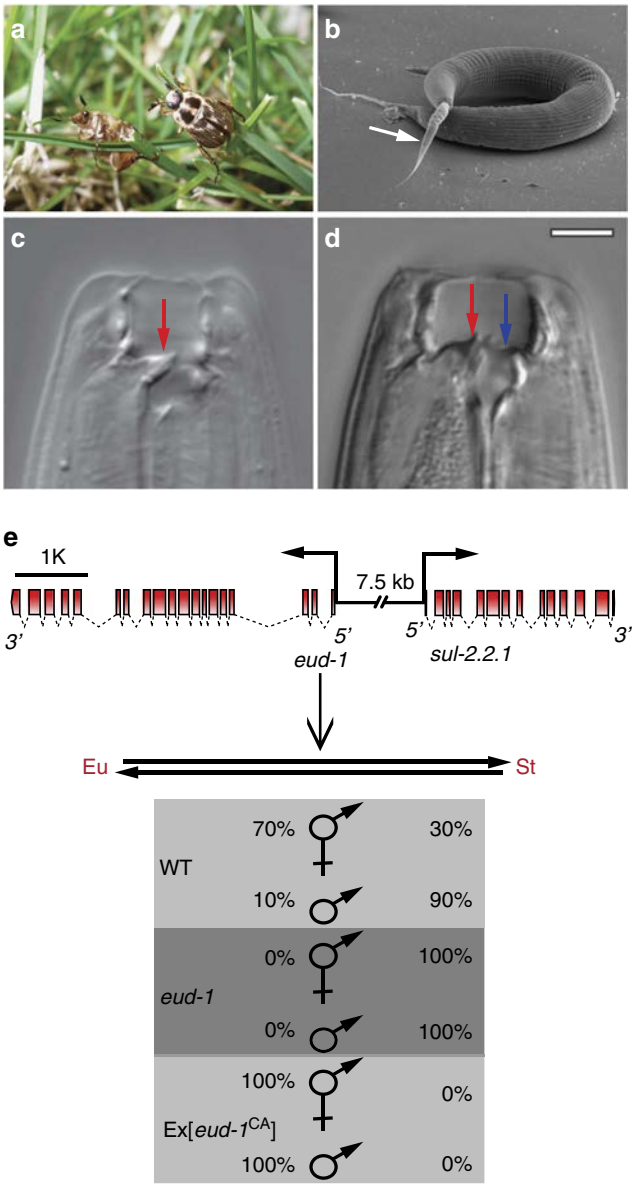

Figure 1 | Developmental plasticity in *P. pacificus* and its regulation by the developmental switch gene *eud-1*. (**a**) The oriental beetle *Exomala orientalis* is one of the beetle hosts with which *P. pacificus* lives in a necromenic association. (**b**) Scanning electron micrograph showing *P. pacificus* predatory feeding on a small larva of *C. elegans* (white arrow). (**c**,**d**) Mouth dimorphism of *P. pacificus* enabling a switch between bacterial grazing and predatory feeding. Stenostomatous (St) animals (**c**) have a narrow buccal cavity and a flint-like dorsal tooth (red arrow), but miss the subventral tooth. In contrast, eurystomatous (Eu) animals (**d**) have a wide buccal cavity, a claw-like dorsal tooth (red arrow) and an additional subventral tooth (blue arrow). Scale bars, 10 µm. (**e**) Molecular organization of the *eud-1* locus and effect of *eud-1* function on mouth-form ratios. *eud-1* derives from a recent gene duplication, with the neighbouring sulfatase *sul-2.2.1* arranged in a head-to-head orientation. The two genes are separated by a 7.5 kb intergenic region that when used as promoter drives the expression of *eud-1* in various head neurons. In wild-type animals, hermaphrodites and males form ~70% and 10% Eu animals, respectively. In *eud-1* mutants, both sexes are completely St, whereas *eud-1* overexpression causes both genders to form only Eu animals indicating that EUD-1 functions as developmental switch.

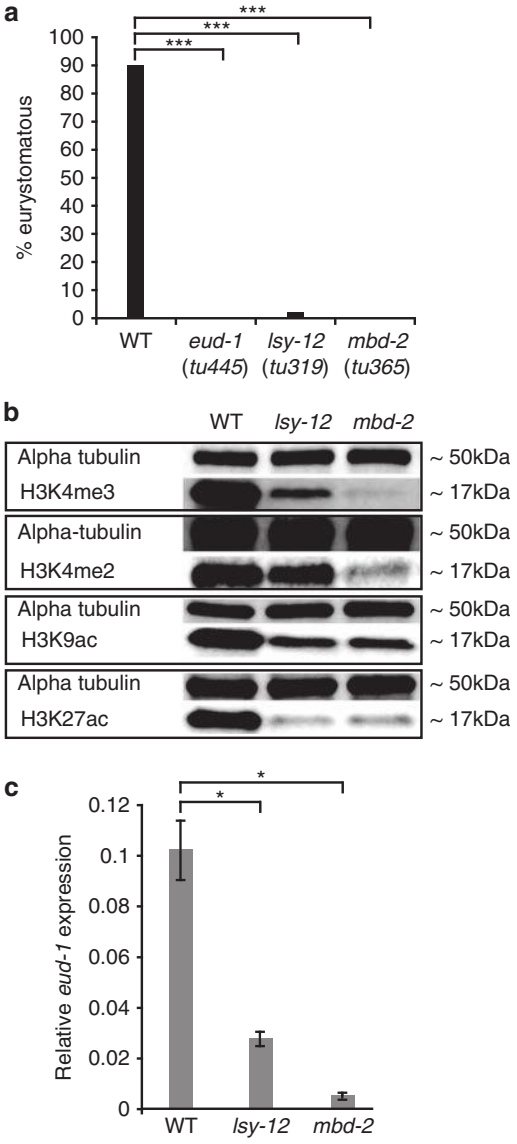

Figure 2 | Mouth-form defects of two pleiotropic mutants and their effect on histone modification and *eud-1* expression. (**a**) *Ppa-lsy-12(tu319)* and *Ppa-mbd-2(tu365)* result in the (nearly) complete absence of Eu hermaphrodites, similar to *eud-1* mutants. Data are presented as the total Eu frequency, $n>100$ for all strains. (**b**) *Ppa-lsy-12* and *Ppa-mbd-2* mutants result in severe histone modification defects. This experiment has been replicated three times. (**c**) qRT-PCR experiments reveal down-regulation of *eud-1* expression in *Ppa-lsy-12* and *Ppa-mbd-2* mutants relative to wild type in J2 larvae. This experiment has been replicated three times. Error bars are defined as s.e.m. $^{*}P<0.05$ and $^{***}P<10^{-5}$, Kruskal–Wallis test.

animals and found changes of four histone marks using antibody staining (Fig. 2b). H3K4me3 is strongly reduced in both *mbd-2* and *lsy-12* mutant animals, whereas H3K4me2 is reduced only in *mbd-2* mutants (Fig. 2b). In contrast, H3K4me1 and several other histone marks are not affected (Supplementary Fig. 2a). In addition to H3K4 methylation, the acetylation of H3K27 is strongly, and that of H3K9 moderately, reduced in both mutants (Fig. 2b). These findings demonstrate a genome-wide role for MBD-2 and LSY-12 in histone modifications in *P. pacificus*. Furthermore, because H3K4 methylation and acetylation of various H3 lysines are often found as gene activation marks[14], these results suggest that the effects of *mbd-2* and *lsy-12*

on mouth-form developmental plasticity is a consequence of chromatin remodelling-mediated transcriptional regulation.

***eud-1* expression is down-regulated in *lsy-12* mutants**. Next, we tested the developmental switch gene *eud-1* as a potential candidate target of chromatin remodelling by LSY-12 and MBD-2. First, we studied *eud-1* expression by performing quantitative reverse transcription (qRT)–PCR experiments in wild-type and mutant hermaphrodites in different developmental stages. Indeed, *eud-1* is significantly down-regulated in *mbd-2* and *lsy-12* mutants, in J2 worms, the larval stage at which the mouth-form is determined (Fig. 2c). In addition, we also observed *eud-1* down-regulation in adult stages, suggesting that *eud-1* expression is similarly controlled throughout development (Supplementary Fig. 2b). These results suggest that the mouth-form defects of *mbd-2* and *lsy-12* mutants result from down-regulation of *eud-1*. Interestingly, these effects of *mbd-2* and *lsy-12* mutants on *eud-1* expression levels and the mouth-form frequency qualitatively match the patterns seen in *P. pacificus* males and highly St wild isolates[6]. Altogether, our findings indicate that reduction-of-function or loss-of-function mutations in *mbd-2* and *lsy-12* cause genome-wide changes in histone modifications, which alter, among other target genes, the expression of *eud-1* throughout development.

An antisense RNA associated with the *eud-1* locus. To further explore the function of chromatin remodelling on the regulatory network controlling the developmental switch, we used ultra-directional RNAseq to compare the transcriptomes of wild-type and *Ppa-lsy-12* mutant animals (Fig. 3a). In total, we found 309 genes to be differentially expressed (Supplementary Data 1). This includes, consistent with our qRT–PCR results *eud-1* expression, which was heavily down-regulated in *Ppa-lsy-12* worms ($P<10^{-8}$, Fisher exact test). Surprisingly, however, we also found a strong effect on previously uncharacterized antisense reads at the *eud-1* locus (Fig. 3a). Indeed, additional RT–PCR experiments identified an antisense *eud-1* transcript, termed as-*eud-1*. The as-*eud-1* RNA consists of three exons with a total size of 863 nucleotides, some of which cover *eud-1* exons, such as exons 7–10 and exon 19 (Fig. 3a). When we searched for short open reading frames we did not observe any evidence for coding potentials and putative micropeptides longer than 10 amino acids. Thus, as-*eud-1* has no obvious open reading frame suggesting that as-*eud-1* encodes a long non-coding (lnc) RNA (Supplementary Fig. 3).

***eud-1* and as-*eud-1* are co-expressed**. Next, we tried to determine the expression pattern of as-*eud-1*. First, we used various constructs containing a putative 3.5 kb as-*eud-1* promoter fragment fused to turbo-RFP but they did not reveal specific expression. Therefore, we established RNA fluorescent *in-situ* hybridization (FISH) protocols. Indeed, we were able to detect *eud-1* RNA in the same head neurons as previously reported for a 7 kb *eud-1* promoter fragment driving RFP expression (Fig. 4a, Supplementary Fig. 4a; ref. 6). FISH of the as-*eud-1* RNA and *eud-1* RNA revealed that both transcripts are indeed expressed at the same site (Fig. 4b, Supplementary Fig. 4b; Supplementary Movie). Thus, our experiments suggest that *eud-1* and as-*eud-1* are co-expressed.

Overexpression of as-*eud-1* increases the Eu mouth-form. To study the functional significance of this lnc RNA for the mouth-form decision, we performed overexpression experiments of as-*eud-1*. Specifically, we generated transgenic animals in which the as-*eud-1* complementary DNA (cDNA) is placed under the *eud-1* promoter, because the putative as-*eud-1* promoter region itself does not drive specific expression of the antisense transcript (see above). Given that *eud-1* and as-*eud-1* are co-expressed the use of the *eud-1* promoter presumably results in overexpression of as-*eud-1*. We generated transgenic animals in a wild-type background in order to be able to score the potential effects of as-*eud-1*. We obtained three independent transgenic lines, all of which showed a strong masculinization phenotype resulting in more than 95% of animals being males. These transgenic lines showed no embryonic lethality and transgenic males were successfully mated indicating that the high incidence of males result from as-*eud-1*-induced X chromosome-specific non-disjunction, a phenomenon known from various *C. elegans* mutants such as *him-8* (ref. 15). We, therefore, used the male mouth-form frequency to study the influence of as-*eud-1*. In contrast to hermaphrodites, spontaneous wild-type males are only 10–20% Eu because *eud-1* is X-linked and dosage-sensitive (Fig. 1e; refs 6,10). The male mouth-form phenotype should be shifted towards more St animals in case of a negative effect and towards higher Eu frequencies in case of a positive function of the as-*eud-1*RNA.

We made the remarkable finding that as-*eud-1* has a positive function on the Eu versus St mouth-form decision and *eud-1* expression (Fig. 3b,c), whereas most cases of antisense-mediated regulation results in transcriptional down-regulation[16]. Four observations result in this conclusion. First, the frequency of the *eud-1*-sensitive mouth-form was dramatically increased in transgenic lines carrying as-*eud-1* in a wild-type background (from 20 to 64% Eu males) (Fig. 3b). Second, qRT–PCR experiments revealed a strong up-regulation of *eud-1* in as-*eud-1* transgenic males (Fig. 3c). Third, *eud-1* RNA can be detected in the J1 stage in *eud-1*::as-*eud-1* transgenic animals, an early expression that is never seen in wild-type animals (Fig. 4c). Finally, as-*eud-1* transgenes in a *eud-1* mutant background also caused a high incidence of males, but without affecting male mouth-form. Specifically, *eud-1(tu445)*;Ex(as-*eud-1*) males were completely St (Fig. 3b), indicating that as-*eud-1* acts through *eud-1*. Taken together, these experiments suggest that chromatin remodelling acts through antisense-mediated up-regulation of *eud-1*.

Finally, we used the recently developed CRISPR/Cas9 technology in *P. pacificus* (ref. 17) to generate mutations that would specifically affect as-*eud-1*, but not *eud-1*. Therefore, we targeted the small exon 2 of as-*eud-1*, but were unable to generate a deletion/insertion in this 26 bp exon (Fig. 3a). In contrast, we succeeded in generating two mutations in the putative promoter of as-*eud-1* (Fig. 3a). Specifically, *tu520* eliminates a 4 bp fragment, whereas *tu522* contains a 44 bp insertion. Both mutant lines show a wild-type mouth-form ratio. However, the *tu522* mutant shows significantly reduced *eud-1* expression as observed by qRT–PCR experiments (Fig. 3d). In contrast, qRT–PCR experiments with as-*eud-1* failed to reveal transcripts above background level, a phenomenon known from other lnc RNAs[18]. Altogether, these experiments provide further evidence that as-*eud-1* up-regulates *eud-1* expression and additionally, they suggest that as-*eud-1* expression is itself driven by distal regulatory elements that are unaffected in the *tu520* and *tu522* mutants.

Discussion

Developmental switching represents an appealing concept to link genetic and environmental influences on phenotypically plastic traits. Our studies of the sulfatase *eud-1* —its function as a developmental switch, its role in micro- and macroevolutionary divergence and, here its regulation—provide such mechanistic insights. Previous characterization of *eud-1* resulted in several surprising findings, that is its recent origin by gene duplication and its epistasis to other factors controlling feeding plasticity[6].

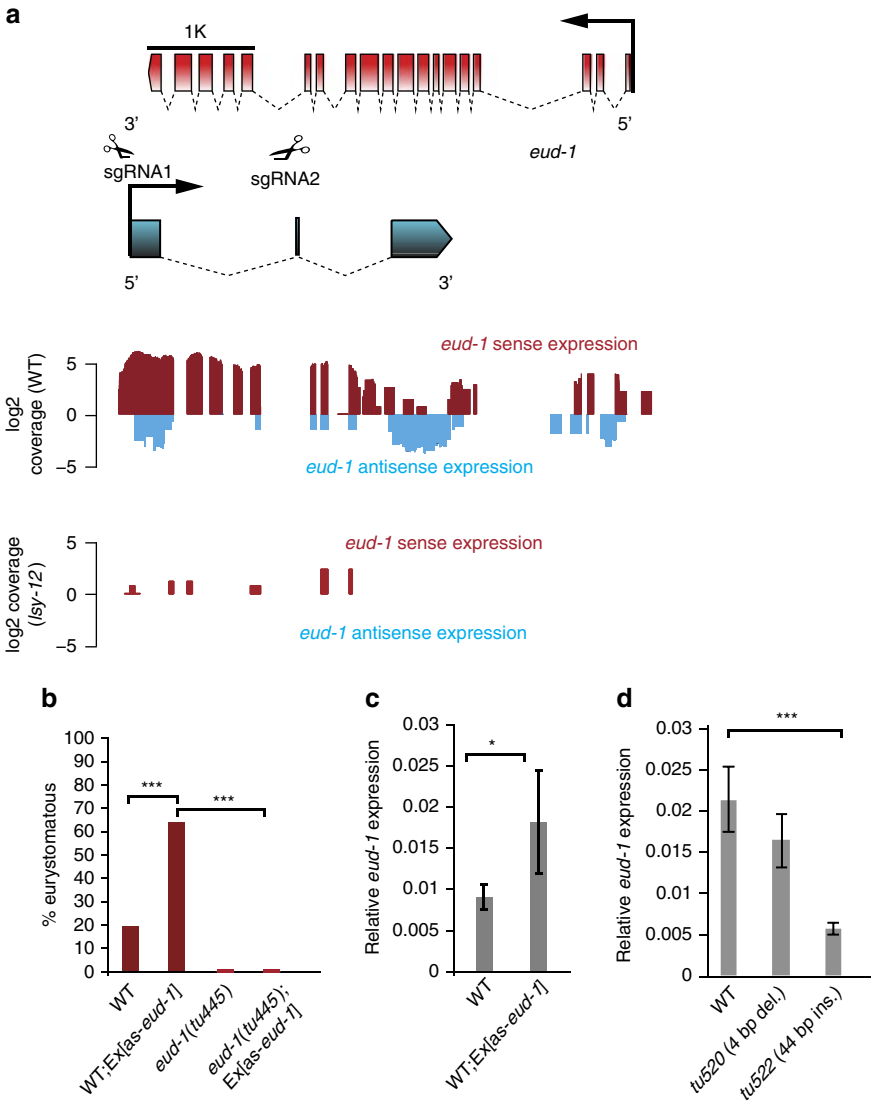

Figure 3 | Molecular organization and function of as-*eud-1*. (**a**) Organization of the *eud-1* and antisense *eud-1* (as-*eud-1*) locus and RNAseq experiments of wild-type and *Ppa-lsy-12* mutant animals. The long noncoding RNA as-*eud-1* consists of three exons that span large parts of the *eud-1* coding region. The structure of as-*eud-1* was identified in RT–PCR experiments and revealed the existence of a short exon, which went undetected in RNAseq. Other antisense reads obtained at lower frequency in the RNAseq experiment, were not confirmed to be part of as-*eud-1* in RT–PCR experiments with mixed stage wild-type animals. Subsequent panels show sense and antisense expression as measured for wild-type (wt) and *Ppa-lsy-12* mutant animals. Note that nearly no reads of *eud-1* and as-*eud-1* were observed in *Ppa-lsy-12* mutants. sgRNA1 and sgRNA2 in the 5′ untranslated region (UTR) and exon 2 of as-*eud-1*, respectively, were used to induce mutations by CRISPR. (**b**) Transformation of wild-type hermaphrodites with as-*eud-1* cDNA induced a high incidence of males and a Eud phenotype in male progeny. In contrast, transformation of *eud-1(tu445)* mutant animals with as-*eud-1* did not result in a Eud phenotype, although the high incidence of males was similar to the transformation of wild-type animals. Two independent transgenic lines were generated each, $n>100$ for all strains. (**c**) qRT–PCR experiments reveal an up-regulation of *eud-1* in as-*eud-1* transgenic males relative to wild-type males. This experiment has been replicated three times. Error bars are defined as s.e.m. (**d**) qRT–PCR experiments reveal that *eud-1* is significantly down-regulated in the as-*eud-1* promoter mutant *tu522* that contains a 44 bp insertion. This experiment has been replicated three times. Error bars are defined as s.e.m. $^{*}P<0.05$ and $^{***}P<10^{-5}$, Kruskal–Wallis test.

We have now shown that two evolutionarily conserved genes, *mbd-2* and *lsy-12*, are involved in genome-wide histone modifications that also influence transcription of *eud-1*, providing first insight into the molecular mechanisms underlying the regulation of developmental switches. In particular, the involvement of antisense-mediated up-regulation of *eud-1* indicates an unexpected complexity and results in three major conclusions. First, our findings demonstrate that the role of *eud-1* involves complex regulation of its own transcription. We previously observed that the coding region of *eud-1* is subject to strong purifying selection, and our new findings support and extend these conclusions regarding the importance of regulatory versus structural changes. Second, we demonstrate the involvement of chromatin remodelling in the developmental switch mechanism regulating mouth-form plasticity in *P. pacificus*. We speculate that chromatin remodelling represents a powerful epigenetic mechanism that might link environmental signals to transcriptional regulation of plasticity. Third, we provide evidence for an antisense RNA in up-regulation. Transcriptional surveys of many eukaryotes have uncovered hundreds of noncoding transcripts[19] and though many of these function as transcriptional regulators, most do so

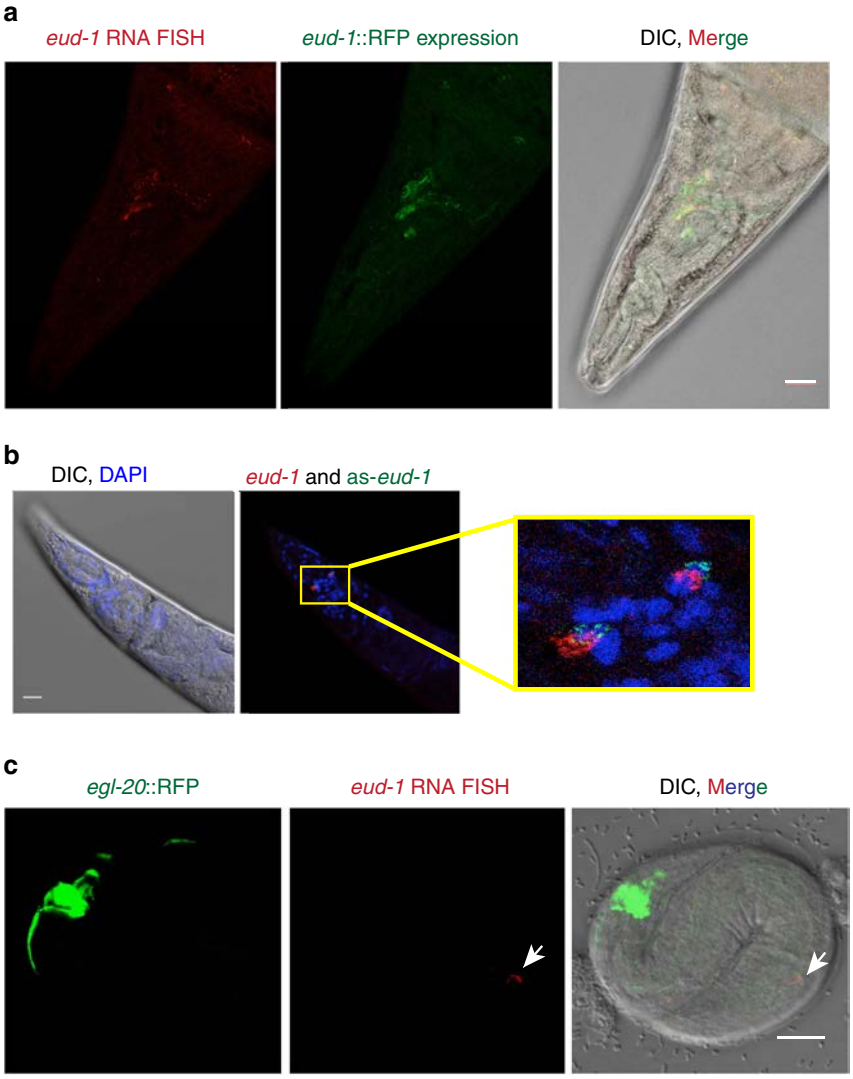

Figure 4 | Fluorescent *in situ* hybridization (FISH) of *eud-1* and as-*eud-1* reveals co-expression of both transcripts. FISH probes were designed as described in the Methods section. Photographs in **a** and **b** show adult animals, photographs in **c** show a J1 stage larvae, which in *P. pacificus* is still in the egg shell. (**a**) *eud-1* FISH (red, left image) and an *eud-1*::RFP reporter construct (green, central image) show the same expression pattern in several head neurons. The image at the right represents a merger of both and differential interference contrast (DIC) microscopy. Note that not all *eud-1*-expressing cells are visible in this plane of focus. (**b**) Head area of an adult worm with DIC and 4,6-diamidino-2-phenylindole staining (left image) and co-expression of *eud-1* (red) and as-*eud-1* (green) as revealed by FISH probes. Both transcripts are expressed at multiple foci, two of which are shown in this plane of focus (inset). Overlapping fluorescence (yellow) was seen in all animals observed, but not in all cells. The expression pattern was highly consistent among multiple adults ($n > 20$). See Supplementary Movie for additional details of the partially overlapping expression of both transcripts. (**c**) Transgenic animals carrying an *eud-1*::as-*eud-1* construct show *eud-1* expression in head neurons already in the J1 stage, which is never seen in wild-type animals. *egl-20*::RFP (green, left image) is used as transformation marker. The same *eud-1* FISH probe (red, central image) was used as above. The image at the right represents a merger and DIC microscopy. Supplementary Fig. 4 provides additional photographs for **a** and **b**. Scale bars, 10 μm.

as inhibitors. Conversely, antisense-mediated transcriptional activation or maintenance has only rarely been described[18,20]. Thus, the example of as-*eud-1* regulation of *eud-1* reveals complex regulatory mechanisms that can serve as model to link genetic and environmental control of developmental plasticity in future studies.

Methods

Culture conditions. All wild-type worms were *P. pacificus* reference strain RS2333. All *Pristionchus* strains were kept on 6-cm plates with nematode growth medium agar and were fed with a lawn of *E. coli* OP50 grown in 400 μl L-broth. Cultures were maintained at 20 °C. Because the mouth-form ratio is sensitive to unknown environmental factors[6], all experiments include their own controls for the wild-type Eu frequency. Also, to minimize the potential for laboratory evolution of the trait, a new culture of the California (RS2333) strain was revived annually from a frozen voucher.

Phenotype scoring. The mouth-form phenotype was scored using the following characters to discriminate between Eu and St individuals, respectively, (i) the presence versus absence of a subventral tooth, (ii) a claw-like versus flint-like or triangular dorsal tooth, and (iii) a wide versus narrow stoma (mouth). Characters (i) and (ii) were discrete, non-overlapping, and sufficient to distinguish the two forms. Apparent intermediates between the two forms were rare ($< 0.1\%$) and were not included in counts. Phenotypes could be scored using Zeiss Discovery V.12 stereomicroscopes and were supplemented where necessary with differential interference contrast (DIC) microscopy on a Zeiss Axioskop.

Mapping of *vul-2(tu319)* and mutant identification. For genetic mapping, mutants in the California background were crossed to the Washington strain

(PS1843). F2 progeny were cloned and screened for two generations to confirm the mutant phenotype and the homozygosity of mutations. Genomic DNA of outcrossed mutant lines was extracted for genetic mapping. Simple-sequence conformation polymorphism markers were tested against 30–40 outcrossed mutant lines and detected as previously described[21,22]. *vul-2* was mapped to the tip of chromosome IV close to the marker S210. Further mapping localized *vul-2* to the bacterial-artificial-chromosome clone BACPP16-M16 and the fosmid subclones 525-J06, 543-P16 and 558-O23. Light shotgun sequencing of these fosmid clones resulted in the identification of *Ppa-lsy-12* as candidate gene for *vul-2*. To prepare samples for whole-genomic sequencing, DNA was extracted from all three alleles *tu18*, *tu30* and *tu319* and mutations were identified in all three alleles.

Alternative splicing of *Ppa-lsy-12*. Following preparation of mixed-stage RNA libraries for *P. pacificus* RS2333, coding DNA (cDNA) was amplified by reverse transcription PCR and sequenced. 5′ and 3′ RACE experiments were performed by SMARTer RACE cDNA Amplification Kit following the manufacturer's protocol (Life Technologies). The full list of gene-specific primers that were designed according to the available genomic sequence for *Ppa-lsy-12* is provided in Supplementary Table 1.

RNA-sequencing experiments. The presence and levels of gene expression were measured by whole-transcriptome sequencing (RNA-Seq) of *Ppa-lsy-12(tu319)* mutants and *P. pacificus* wild type. Culture populations were allowed to grow until their food was exhausted, immediately after which the cultures were processed for sequencing. Five mixed-stage plates were washed with 40 ml M9, centrifuged immediately at 1300 *g* for 4 min, rinsed with 40 ml 0.9% NaCl treated with 40 µl ampicillin and 40 µl chloramphenicol and shaken gently for 2 h, and finally concentrated into a pellet by centrifugation and immediately frozen in liquid nitrogen. NEBNext Ultradirectional RNA Library Kit (Cat # E7420L) was used to prepare libraries. RNA-Seq libraries were sequenced as 2 × 100-bp paired-end reads on an Illumina HiSeq 2000, yielding 30.6 million reads for the wild type and 31.6 million reads for the *lsy-12* sample. Raw reads were aligned to the reference genomes of *P. pacificus* (Hybrid1) (www.pristionchus.org), using the software Tophat v.2.0.3 (ref. 23). Expression levels were estimated and tested for differential expression using the programs Cufflinks and Cuffdiff v.2.0.1 (ref. 23) resulting in 95 significantly differentially expressed genes including *eud-1* (FDR corrected P value < 0.01). The equivalent test for down-regulation of as-*eud-1* was not significant despite no evidence of as-*eud-1* expression in *Ppa-lsy-12* animals, which is probably due to the reduced statistical power for differential expression detection resulting from the low expression of as-*eud-1* even in wild-type animals.

qRT-PCR. Total RNA from synchronized cultures was isolated using TRIzol (ambion by life technologies). For reverse transcription Superscript II reverse transcriptase (Invitrogen, Cat. No: 18064) was used following the manufacturer's instructions. We used 1 µg total RNA. The qRT–PCR experiments were performed on a LightCycler 480 system; using SybrGreen (Roche Diagnostics) with a reaction set up described elsewhere[24]. To detect *eud-1* expression we used VSe13F GATGATCGAGTCACACAGATCCG forward and VSe13R ATGTAGTAGGAGA GTTGAGCAGCG reverse primers. *Ppa-cdc-42* and *Ppa-Y45F10D.4* were used as reference genes as previously described[25]. PCR efficiencies were determined using external standards on plasmid mini-preparation of cloned PCR-products. Expression levels were analysed by basic relative quantification. We performed 3–6 biological replicates for different experiments.

as-*eud-1* transcript analysis. RNAseq reads of wild-type worms cover the majority of *eud-1* exons to a similar extent. In addition, we observed antisense readsat the *eud-1* locus that were previously uncharacterized. These antisense reads are expressed at very low levels and cannot be detected in qRT–PCR experiments, which otherwise are used as a standard procedure in *P. pacificus* (see above). We used many different PCR primer combinations (Supplementary Table 2) in a variety of nested PCR experiments to study which of the antisense reads if any are present in a potential as-*eud-1* cDNA. These experiments revealed the existence of one transcript of 863 nucleotides that consists of three exons (Fig. 3, Supplementary Fig. 5). The two larger exons cover exactly those reads that were most abundantly found in the RNAseq experiment of wild-type worms. However, exon 2 consists of only 26 nucleotides and went unnoticed at the RNAseq level. Similar to noncoding (nc) RNA (ncRNA) in other systems[18], as-*eud-1* is expressed at very low levels.

Genetic transformation. For phenotypic rescue of *vul-2*, the germ line of *vul-2(tu319)* mutant animals was injected with a 17 kb genomic construct containing exons 1-20 of *Ppa-lsy-12* and 4.5 kb of flanking regulatory region (2 ng ul^{-1}), the marker *Ppa-egl-20*::*TurboRFP* (10 ng ul^{-1}) and genomic carrier DNA (60 ng ul^{-1} from the recipient strain[26]. To study the as-*eud-1* lnc RNA, we generated a 7.5 kb construct consisting of ~6.5 kb promoter element and the 860 bp cDNA fragment of as-*eud-1*. This construct was injected (2 ng ul^{-1}) with the *Ppa-egl-20*::*TurboRFP* (10 ng ul^{-1}) marker and genomic carrier DNA (60 ng ul^{-1}) of *P. pacificus* RS2333 and *Ppa-eud-1(tu445)*, respectively. For all constructs, at least two independent transgenic lines were generated and transgenic animals were scored over multiple generations involving at least 100 transgenic animals per line. Transgenic lines containing the as-*eud-1* lnc RNA yielded more than 90% male progeny and all lines were kept at least until the tenth generation. No embryonic lethality was observed in association with these transgenes. Transgenic males were crossed with *Ppa-pdl-1* and wild-type hermaphrodites and cross-progeny was readily observed.

CRISPR/Cas9 induced mutations. To generate CRISPR/Cas9 induced mutations, sgRNAs were co-injected with Cas9 protein[17]. We used the following sites for single-guided (sg) RNAs (sgRNA):
sgRNA1: 5′CAGTTGAAGAACAAAACACACGG3′.
sgRNA2: 5′GTCGTAATCAAGCTAACAGCTGG3′.

Statistical analyses. All phenotypic data show Eu frequency calculated from total individuals screened. Total sample size is illustrated on graphs. Significant differences were tested by Fisher's exact test. For the expression data we performed Kruskal–Wallis test. All statistical analyses were implemented in the program Statistica v. 9 (Statsoft).

Western blotting and antibodies. Proteins were extracted from mixed stage cultures. Concentration was determined by Neuhoff's Dot-Blot assay[24]. Proteins were equally loaded and separated in polyacrylamid gels. Proteins were transferred to polyvinylidene difluoride transfer membrane and incubated overnight with primary antibodies (Supplementary Table 3), and were then incubated for an hour in secondary antibodies (Anti-rabbit IgG, horseradish peroxidase-linked antibody, Cell Signaling Technology, Cat. #7074S and Anti-mouse IgG, horseradish peroxidase-linked antibody, Cell Signaling Technology, Cat. #7076S). For dilution of primary antibodies see Supplementary Table 3. The secondary antibody was diluted 1:1,000. The detection was done by Bio-Rad Clarity western enhanced chemiluminescent (ECL) substrate using Peqlab FUSION Xpress multi-imaging system. We provide an uncropped scan of the most important blot as Supplementary Fig. 5.

Single molecule RNA FISH. Single molecule RNA FISH was performed using a protocol described earlier for *C. elegans*[25]. Biosearch Technologies Stellaris FISH online platform was used to design and order *eud-s* and *as-eud-1* probes. They were coupled with Quasar 670 and TAMRA fluorescent dyes, respectively. Image acquisition was performed on Leica SP8 confocal system using settings to maximize detection of fluorescent dyes. Image J software was used for Image analysis.

Data availability. All relevant data, including mutant and transgenic lines, constructs and plasmids are available upon request from the corresponding author[26].

References

1. West-Eberhard, M.-J. *Developmental Plasticity and Evolution* (Oxford University Press, 2003).
2. Moczek, A. P. *et al.* The role of developmental plasticity in evolutionary innovation. *Proc. R. Soc. B* **278,** 2705–2713 (2011).
3. Nijhout, H. F. *Insect Hormones* (Princeton University Press, 2003).
4. Schlichting, C. D. Origins of differentiation via phenotypic plasticity. *Evol. Dev.* **5,** 98–105 (2003).
5. Pigliucci, M. *Phenotypic Plasticity: Beyond Nature and Nurture* (John Hopkins University, 2001).
6. Ragsdale, E., Müller, M., Roedelsperger, C. & Sommer, R. J. A developmental switch coupled to the evolution of plasticity acts through a sulfatase. *Cell* **155,** 922–933 (2013).
7. Herrmann, M. *et al.* The nematode *Pristionchus pacificus* (Nematoda: Diplogastridae) is associated with the Oriental beetle *Exomala orientalis* (Coleoptera: Scarabaeidae) in Japan. *Zool. Sci.* **24,** 883–889 (2007).
8. Bento, G., Ogawa, A. & Sommer, R. J. Co-option of the endocrine signaling module Dafachronic Acid-DAF-12 in nematode evolution. *Nature* **466,** 494–497 (2010).
9. Bose, N. *et al.* Complex small molecular architectures regulate phenotypic plasticity in a nematode. *Angew. Chemie.* **51,** 12438–12443 (2012).
10. Serobyan, V., Ragsdale, E., Müller, M. & Sommer, R. J. Feeding plasticity in the nematode *Pristionchus pacificus* is influenced by gender and social context and is linked to developmental speed. *Evol. Dev.* **15,** 173–182 (2013).
11. Gutierrez, A. & Sommer, R. J. Functional diversification of the *mbd-2* gene between *Pristionchus pacificus* and *Caenorhabditis elegans*. *BMC. Genet.* **8,** 57 (2007).
12. Sigrist, C. & Sommer, R. J. Vulva formation in *Pristionchus pacificus* relies on continuous gonadal induction. *Dev. Genes Evol* **209,** 451–459 (1999).

13. Sarin, S. *et al.* Analysis of multiple ethyl methanesulfonate-mutagenized *Caenorhabditis elegans* strains by whole-genome sequencing. *Genetics* **185,** 417–430 (2010).
14. Musselman, C. A., Lalonde, M.-E., Cote, J. & Kutateladze, T. G. Perceiving the epigenetic landscape through histone readers. *Nat. Struct. Mol. Biol.* **19,** 1218–1227 (2012).
15. Hodgkin, J. A., Horvitz, H. R. & Brenner, S. Nondisjunction mutants on the nematode *Caenorhabditis elegans*. *Genetics* **91,** 67–94 (1979).
16. Rinn, J. L. & Chang, H. Y. Genome regulation by long noncoding RNAs. *Annu. Rev. Biochem.* **81,** 145–166 (2012).
17. Witte, H. *et al.* Gene inactivation using the CRISPR/Cas9 system in the nematode *Pristionchus pacificus*. *Dev. Genes Evol.* **225,** 55–62 (2015).
18. Dimitrova, N. *et al. LincRNA-p21* activates *p21* in *cis* to promote polycompb target gene expression and to enforce the G1/S checkpoint. *Mol. Cell* **54,** 1–14 (2014).
19. Guttman, M. *et al.* Chromatin signature reveals over a thousand highly conserved large non-coding RNAs in mammals. *Nature* **458,** 223–227 (2009).
20. Sakurai, I. *et al.* Positive regulation of *psbA* gene expression by cis-encoded antisense RNAs in *Synechocystis* sp. PCC6803. *Plant. Physiol.* **160,** 1000–1010 (2012).
21. Srinivasan, J. *et al.* A bacterial artificial chromosome-based genetic linkage map of the nematode *Pristionchus pacificus*. *Genetics* **162,** 129–134 (2002).
22. Srinivasan, J. *et al.* An integrated physical and genetic map of the nematode *Pristionchus pacificus*. *Mol. Genet. Genomics* **269,** 715–722 (2003).
23. Trapnell, C. *et al.* Differential gene and transcript expression analysis of RNA-Seq experiments with TopHat and Cufflinks. *Nat. Protoc.* **7,** 562–578 (2012).
24. Neuhoff, V., Philipp, K., Zimmer, H.-G. & Mesecke, S. A simple, versatile, sensitive and volume-independent method for quantitative protein determination which is independent of other external influences. *Hoppe-Seyler's Z. Physiol. Chem.* **360,** 1657–1670 (1979).
25. Ji, N. & van Oudenaarden, A. *Single Molecule Fluorescent In Situ Hybridization (smFISH) of C. elegans Worms and Embryos*. The *C. elegans* Research Community. Wormbook, ed. (2012).
26. Schlager, B., Wang, X., Braach, G. & Sommer, R. J. Molecular cloning of a dominant Roller mutant and establishment of DNA-mediated transformation in the nematode model *Pristionchus pacificus*. *Genesis* **47,** 300–304 (2009).

Acknowledgements

We thank Drs C. Weadick, J. Lightfoot and A. Streit for comments on the manuscript and members of the Sommer lab for discussion.

Author contributions

V.S. performed mouth-form and transgenic experiments, histone modification assays and RT–PCR experiments. H.X. physically cloned *vul-2*, S.N. and B.S. performed FISH experiments, B.S. performed CRISPR and qRT-PCR experiments and C.R. performed all computational studies. W.R. and H.W. were involved in the molecular parts of the project and R.J.S. led the overall project and wrote the manuscript with assistance from V.S. and C.R.

Additional information

Accession Codes: The RNA-seq data are available at the NCBI sequence read archive under accession codes SRX1609204, SRX1858662, SRX1858663.

Supplementary Information accompanies this paper at http://www.nature.com/naturecommunications

Competing financial interests: The authors declare no conflict of interest.

Reprints and permission information is available online at http://npg.nature.com/reprintsandpermissions/

How to cite this article: Serobyan, V. *et al.* Chromatin remodelling and antisense-mediated up-regulation of the developmental switch gene *eud-1* control predatory feeding plasticity. *Nat. Commun.* 7:12337 doi: 10.1038/ncomms12337 (2016).

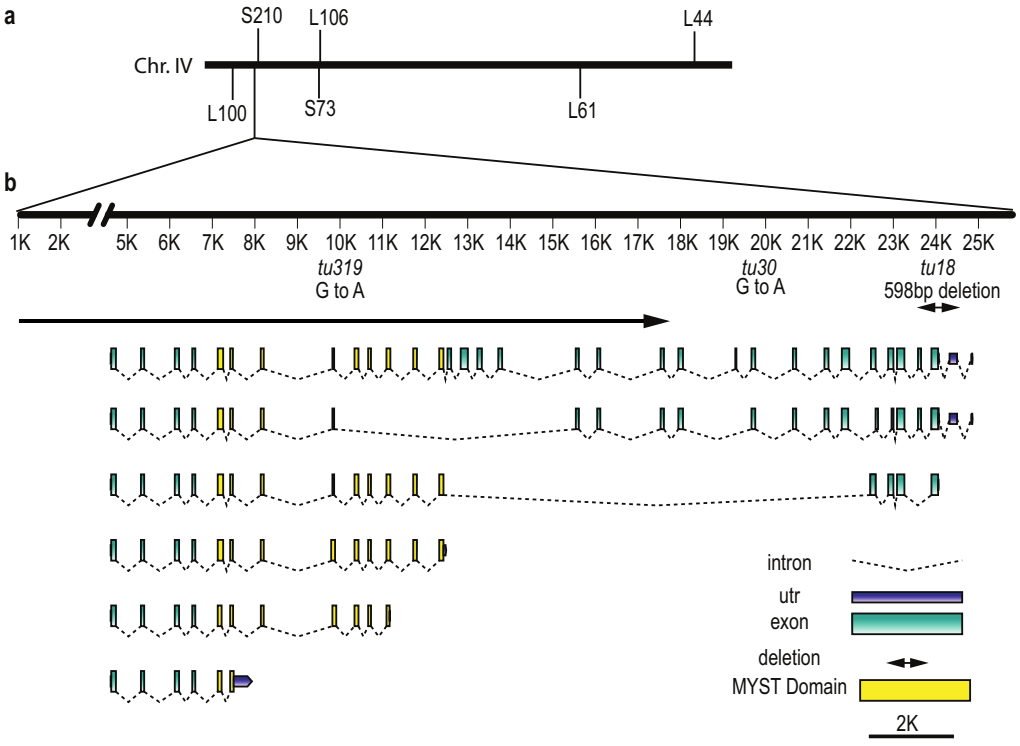

c

	WT	*lsy-12 (tu319)*	*tu319* Ex[*lsy-12*]
induction index	3	0.97	2.7
number of animals	many	72	10

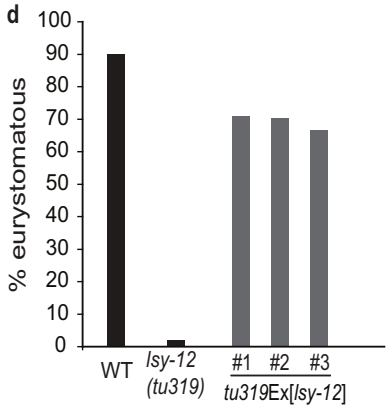

Supplementary Figure 1: Mapping, gene structure and rescue of *P. pacificus lsy-12*. (**a**) Genetic map showing the tip region of chromosome IV. (**b**) Exon – intron structure of *Ppa-lsy-12* deduced from cDNA cloning and sequencing and molecular nature of mutations. The various shown isoforms

are ordered by length. Note, that this list represents just a subset of the observed isoforms. Like in *C. elegans*, multiple isoforms exist and more than 30 exons are predicted for the *Ppa-lsy-12* gene. The successful rescue experiment indicated below were carried with a genomic fragment of approximately 17 kb covering 20 predicted exons as indicated by the arrow above the isoforms. (**c**) Rescue experiment of the vulva defect of *tu319*. In wild type hermaphrodites, three vulval precursor cells are induced to form vulval tissue as indicated by an induction index of 3. *tu319* mutant animals have an average induction of 0.97 cells that is rescued to an average induction of 2.7 cells by an array carrying multiple copies of *Ppa-lsy-12*. Only one transgenic line was tested for the rescue of the vulval defect. (**d**) Rescue experiment of the mouth-form defect of *tu319*. *tu319* animals are 2% Eu, whereas wild type hermaphrodites are 90% Eu under the same cultural conditions. Three independent transgenic lines (#1-#3) carrying multiple copies of *Ppa-lsy-12*, show 60-70% Eu animals as indicated by the analysis of more than 100 animals. Data are represented as the total Eu frequency.

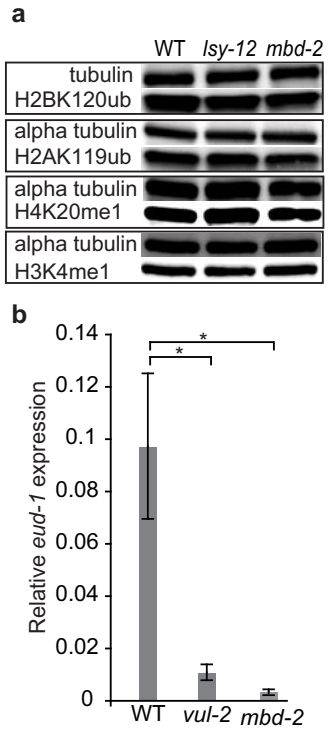

Supplementary Figure 2: Histone modification of additional histone markers and *eud-1* expression in adult animals. (**a**) *Ppa-lsy-12* and *Ppa-mbd-2* mutants do not result in obvious histone modification defects in several other tested histone marks. Here we show four representatives for ubiquitination (ub) and mono-methylation (me1). (**b**) qRT-PCR experiments reveal down regulation of *eud-1* expression in *Ppa-lsy-12* and *Ppa-mbd-2* mutants relative to wild type in adult worms. Error bars are s.e.m. *p<0.05 and ***p<10^{-5}, Kruskal-Wallis test.

ggaagacttccgcaagaagcatgcaaacactacattctaaatgatacaagagatttaacaatttactataataaatgtccagtt
gaagaacaaaacacacggagaaggttgtgaagggtttgcgaaagaactgatggaagcgagataaatcgttaggtatatttta
ttcttattcaagctgatcgtattcttgatcactccagttgagttcttccttctcgagcatggctcttcgaagcgcgcgctggaatc
gatcactgcgtggagatgtagtagggtcgtaaaacaacgctaggtgggaccagggccgagtgggctacaagggaatcat
tatttgggattttaatactagcaaattagtacctcggcttttctctggtgaatgaagaacttaaaatcatcaaccaaattctgagtc
atatcgtcgaatatcatgggttgttgcaccaactcatcaccgtcatacaagaagcacttggttccattgggaccatcagggaa
cattgtctaaacaatctcgaaaattggtgttggtagatttttcagtaccttagtggtatcgcactcccatacatttgtgaagggaa
ggttgactcccacgtattgaaaaccacgacgggaaggcaaatgtactccgtcagtactggttctgaagcataaccatttaaa
gtgctgataattacaatttactaactcttcattgattccgagatgccatttgccgatcattcctgttgcgtaacctgaatttgcaatt
atttagatgtattcaatttcaattcccacctcgttcttcgaacatctcggccattgtagtctcatctttcggtagtcctccaatgtcct
gaggaacgaacactcgag

Supplementary Figure 3: Nucleotide sequence of the as-*eud-1* transcript as obtained in RT-PCR experiments.

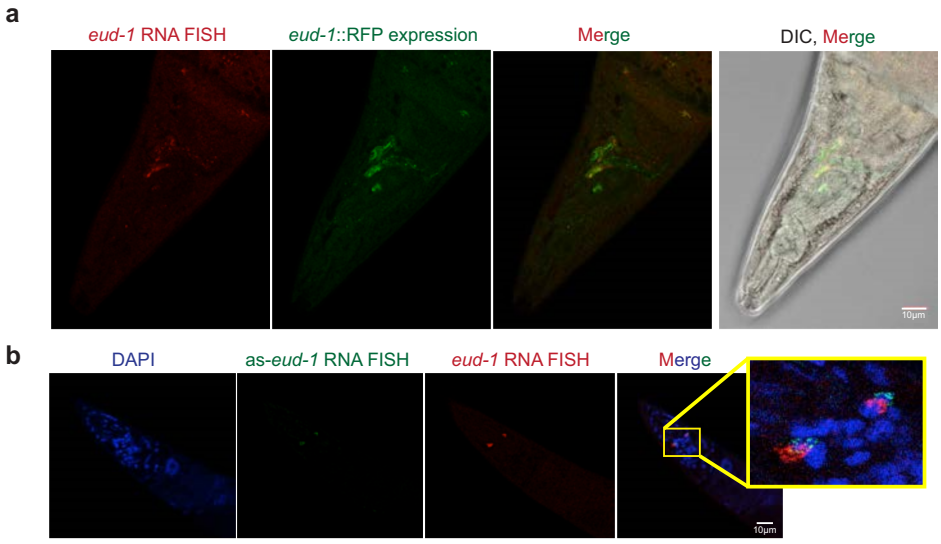

Supplementary Figure 4: Fluorescent *in situ* hybridization (FISH) of *eud-1* and as-*eud-1*. Photographs show adult animals and provide the same and additional photographs to those shown in Figure 4. (**a**) from left to right: i) *eud-1* FISH (red); ii) *eud-1*::RFP reporter construct (green); iii) merger of *eud-1* RNA FISH and *eud-1*::RFP expression showing overlap in yellow; iv) merger of both expressions with differential interference contrast (DIC) microscopy. (**b**) from left to right: i) DAPI staining; ii) as-*eud-1* RNA FISH (green); iii) as-*eud-1* (red); iv) co-expression of *eud-1* (red), as-*eud-1* (green) and DAPI.

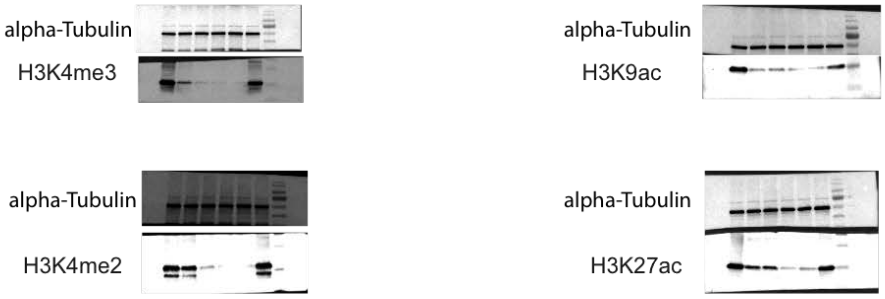

Supplementary Figure 5: Histone modification of *Ppa-lsy-12* and *Ppa-mbd-2* mutants result in severe histone modification defects. Un-cropped scans of blots provided in Figure 2b. Note that the original gels and blots contain additional lanes unrelated to this study. In each graph, the lanes relevant to this study are lanes 1-3 from the left, presenting wild type, *lsy-12* and *mbd-2* as shown in Figure 2b.

Supplementary Table 1: Differentially expressed genes between wild type and *Ppa-lsy-12* mutant animals (blue, up-regulated; green, down regulated).

P. pacificus Gene ID (version Hybrid1)	Expression foldchange	P (FDR corrected)
Contig41-snap.23	13,29000737	1,84319E-07
Contig22-snap.173	9,101661929	9,63592E-05
Contig11-snap.172	6,027375725	0,000110313
Contig70-snap.1	12,39485939	0,000128043
Contig12-snap.157	3,697320223	0,000149273
Contig106-snap.25	4,775295463	0,000300751
Contig10-snap.353	11,18109827	0,000317931
Contig41-snap.82	7,096117999	0,000919555
Contig77-snap.8	65,96916778	0,00100054
Contig143-snap.16	16,83556227	0,00105018
Contig4-snap.53	37,7475211	0,00123591
Contig22-snap.106	3,599433838	0,00179514
Contig52-snap.11	4,42065455	0,00284796
Contig29-snap.5	61,43291773	0,00333557
Contig30-snap.191	11,6756422	0,00333557
Contig65-snap.25	inf	0,00409407
Contig80-snap.15	3,577619607	0,0046836
Contig81-snap.24	14,3205004	0,00530466
Contig11-snap.371	2,536642133	0,00549032
Contig60-snap.86	87,23891972	0,00709599
Contig43-snap.76	5,296245508	0,00714069
Contig41-snap.5	4,873269472	0,00780334
Contig70-snap.59	3,294820797	0,00829626
Contig5-snap.322	79,30225582	0,00843321
Contig14-snap.271	3,385760678	0,00917801
Contig50-snap.180	2,637900229	0,00969665
Contig18-snap.207	78,60504474	0,0103225
Contig21-snap.203	5,691977662	0,0107445
Contig114-snap.47	3,607451503	0,01173
Contig70-snap.44	21,23570353	0,011961
Contig5-snap.109	73,6753447	0,0122673
Contig15-snap.100	26,78809343	0,012506
Contig2-snap.143	39,36795862	0,0133108
Contig43-snap.100	2,800452581	0,0143238
Contig122-snap.33	12,62892558	0,0143824
Contig11-snap.54	8,836162803	0,0170202
Contig45-snap.65	10,71500041	0,0205952
Contig0-snap.107	4,994949181	0,0206185
Contig45-snap.142	inf	0,0206552
Contig1-snap.244	4,337248188	0,0221536
Contig45-snap.89	12,50765998	0,0224134
Contig125-snap.20	3,921566323	0,0224164
Contig13-snap.199	2,791498924	0,0228273
Contig165-snap.14	inf	0,0268869
Contig91-snap.44	3,577669204	0,0272269
Contig13-snap.239	7,533132996	0,0280861
Contig36-snap.166	2,722458392	0,0282879
Contig93-snap.38	inf	0,0301426

Contig65-snap.26	8,275520184	0,0314173
Contig23-snap.131	9,258317253	0,0328285
Contig7-snap.59	3,557761992	0,0328329
Contig49-snap.90	3,471285437	0,0335256
Contig0-snap.498	2,38574525	0,03497
Contig5-snap.298	2,253129132	0,0364589
Contig29-snap.28	4,126704113	0,0379509
Contig12-snap.10	inf	0,0391579
Contig99-snap.10	2,124995815	0,039204
Contig155-snap.3	47,83915494	0,0394386
Contig12-snap.416	3,1659753	0,0409838
Contig3-snap.167	2,16899992	0,0409838
Contig125-snap.78	2,846699088	0,0411583
Contig11-snap.380	2,20643921	0,0434612
Contig43-snap.120	2,218062472	0,0438765
Contig78-snap.48	inf	0,0451409
Contig23-snap.197	54,92039132	0,0451409
Contig111-snap.8	45,22943284	0,0451409
Contig106-snap.1	18,20698332	0,0487759
Contig0-snap.648	3,022369399	0,0490452
Contig116-snap.30	3,456471428	0,0491213
Contig1-snap.120	inf	0,0493838
Contig28-snap.265	0,129880793	0
Contig97-snap.101	0,076369479	1,7466E-12
Contig56-snap.93	0,038545333	7,33573E-11
Contig14-snap.170	0,090279986	1,83393E-10
Contig10-snap.464	0,165198215	2,7573E-09
Contig56-snap.97	0,040389945	2,7573E-09
Contig36-snap.191	0,221967444	2,2105E-08
Contig63-snap.66	0,226367696	2,68968E-08
Contig97-snap.102	0,149884178	6,34591E-08
Contig14-snap.131	0,178311295	9,9724E-08
Contig77-snap.99	0,079934383	1,1698E-07
Contig117-snap.28	0,208152097	1,17864E-07
Contig113-snap.53	0,247973868	1,36443E-07
Contig97-snap.4	0,147278628	1,45928E-07
Contig10-snap.379	0,054318219	1,45928E-07
Contig596-snap.1	0	4,02173E-07
Contig87-snap.105	0,174699817	4,65774E-07
Contig11-snap.483	0,028543182	9,35917E-07
Contig129-snap.4	0,254733393	1,25038E-06
Contig147-snap.12	0,066336651	1,63658E-06
Contig1-snap.88	0,063084964	2,10043E-06
Contig102-snap.20	0,143834334	2,52546E-06
Contig351-snap.3	0,083092956	2,72689E-06
Contig8-snap.30	0,006196976	4,8697E-06
Contig143-snap.4	0,237189163	9,43974E-06
Contig61-snap.159	0,029406523	1,26452E-05
Contig14-snap.382	0,224699684	1,69382E-05
Contig57-snap.107	0,031562165	1,87804E-05
Contig6-snap.122	0,12688206	3,25359E-05
Contig66-snap.69	0,097884891	5,78653E-05
Contig32-snap.276	0,147143937	8,44083E-05
Contig56-snap.180	0,179479379	8,54968E-05
Contig113-snap.52	0,333262293	0,000095418

Contig109-snap.22	0,206883429	9,54641E-05
Contig320-snap.3	0,132744133	9,54641E-05
Contig125-snap.27	0,240678638	9,63592E-05
Contig17-snap.49	0,232415791	0,00010668
Contig103-snap.29	0,103387953	0,00010668
Contig4-snap.211	0,091354525	0,00010668
Contig30-snap.226	0,055461483	0,00010668
Contig69-snap.22	0,005980327	0,00010668
Contig5-snap.274	0,228739908	0,000110519
Contig10-snap.436	0,051785787	0,000132014
Contig36-snap.257	0,006023259	0,000176584
Contig100-snap.48	0,354495692	0,000207246
Contig538-snap.2	0,103939073	0,000303722
Contig90-snap.13	0,288595358	0,000325322
Contig11-snap.43	0,254805796	0,000365236
Contig17-snap.264	0,156744856	0,000505174
Contig75-snap.112	0,013192301	0,000517447
Contig0-snap.381	0,064646228	0,000553292
Contig9-snap.313	0,201031015	0,000585007
Contig141-snap.25	0,135514581	0,000604639
Contig33-snap.23	0,382247773	0,000625135
Contig105-snap.26	0,045746019	0,000705992
Contig110-snap.55	0,025046451	0,000725377
Contig1-snap.299	0,148843693	0,000733087
Contig41-snap.114	0,182167816	0,000758377
Contig2-snap.318	0,060444295	0,000792405
Contig127-snap.54	0,079514953	0,000864763
Contig2-snap.275	0,09453681	0,000987442
Contig43-snap.58	0,292072817	0,00104124
Contig124-snap.25	0,084121594	0,0010463
Contig30-snap.268	0,346519873	0,00112257
Contig127-snap.25	0,290278575	0,00113623
Contig14-snap.198	0	0,00119696
Contig14-snap.67	0,136411767	0,00125167
Contig176-snap.15	0,337937885	0,00156484
Contig77-snap.126	0,235315784	0,00159015
Contig20-snap.87	0,165081459	0,00162149
Contig62-snap.7	0,149554166	0,00197536
Contig32-snap.157	0,077255422	0,00201161
Contig30-snap.201	0,221253165	0,00221731
Contig105-snap.6	0,276779692	0,00236551
Contig61-snap.89	0,337659253	0,00247332
Contig180-snap.9	0,020522354	0,00251249
Contig746-snap.1	0,230706411	0,0026016
Contig55-snap.82	0,198706366	0,00266865
Contig31-snap.216	0,4009516	0,00270048
Contig13-snap.374	0,342130826	0,0027383
Contig138-snap.6	0,012526177	0,00284796
Contig115-snap.3	0,390363481	0,00333557
Contig25-snap.92	0,233240464	0,00333557
Contig316-snap.1	0,061844967	0,00333557
Contig638-snap.1	0,223393637	0,00345627
Contig100-snap.5	0,351983572	0,00355141
Contig226-snap.2	0,133744364	0,00360474
Contig23-snap.196	0,19687475	0,00377964

Contig11-snap.474	0,274038405	0,00394852
Contig68-snap.24	0,218887276	0,00394852
Contig11-snap.260	0,404208061	0,00409407
Contig50-snap.44	0,395749656	0,00440543
Contig11-snap.210	0,116315882	0,0046836
Contig18-snap.93	0,23959837	0,00475155
Contig31-snap.69	0,406788275	0,00505112
Contig11-snap.183	0,185316083	0,00516887
Contig30-snap.188	0,086845807	0,00516887
Contig102-snap.8	0,117734578	0,00532036
Contig14-snap.349	0,036243598	0,00547608
Contig2-snap.317	0,067416241	0,00638273
Contig12-snap.221	0,254394608	0,00642965
Contig43-snap.22	0,276962009	0,00698537
Contig89-snap.78	0,156075934	0,00698537
Contig11-snap.402	0,201710767	0,00709599
Contig11-snap.150	0,313196501	0,00714069
Contig9-snap.131	0,015545922	0,00724048
Contig0-snap.344	0,443513523	0,00790813
Contig61-snap.10	0,159160032	0,00790813
Contig2-snap.327	0,403664886	0,00791615
Contig10-snap.289	0,091353259	0,00809759
Contig8-snap.280	0,437052956	0,00843321
Contig30-snap.63	0,290153855	0,00874019
Contig11-snap.7	0,168225697	0,00892375
Contig14-snap.267	0,177325264	0,00917801
Contig14-snap.68	0,255069093	0,00926488
Contig97-snap.37	0,214714273	0,00937072
Contig75-snap.2	0,309684268	0,00969665
Contig35-snap.117	0,259160904	0,00993981
Contig99-snap.45	0,199891634	0,00996932
Contig14-snap.384	0,016946252	0,0100429
Contig75-snap.45	0,128483945	0,0103225
Contig33-snap.111	0,090981057	0,0103225
Contig35-snap.18	0,296694482	0,01052
Contig10-snap.340	0,304746171	0,0105511
Contig5-snap.72	0,017931252	0,0106252
Contig56-snap.84	0,313781021	0,0107445
Contig104-snap.11	0,041949284	0,0107445
Contig1160-snap.1	0	0,012323
Contig5-snap.325	0,248281728	0,0124433
Contig43-snap.55	0,349024448	0,012506
Contig50-snap.120	0,193104006	0,012506
Contig10-snap.254	0,24399441	0,012591
Contig25-snap.48	0,045720025	0,0128824
Contig61-snap.126	0,219836066	0,0140299
Contig272-snap.1	0,139846883	0,0143238
Contig6-snap.268	0,396328879	0,0143824
Contig22-snap.178	0,220331856	0,0143824
Contig34-snap.10	0,046566943	0,0143824
Contig103-snap.59	0,276860281	0,0145896
Contig145-snap.29	0,397611117	0,0149171
Contig119-snap.50	0,019156529	0,0149171
Contig11-snap.241	0,212106391	0,0149967
Contig103-snap.51	0,335020202	0,0156301

Contig13-snap.56	0,174639281	0,0156301
Contig87-snap.122	0,301683981	0,0160403
Contig40-snap.66	0,043539541	0,0170466
Contig20-snap.196	0,063252223	0,0172997
Contig7-snap.348	0,039360436	0,0192332
Contig139-snap.33	0,234516283	0,0199627
Contig60-snap.12	0,047230087	0,0199857
Contig61-snap.81	0,23069042	0,0202204
Contig11-snap.296	0,053070355	0,0207815
Contig68-snap.73	0,203165874	0,0214741
Contig103-snap.99	0,29197161	0,0218902
Contig46-snap.15	0,121971839	0,0218902
Contig8-snap.184	0,090620421	0,0218902
Contig529-snap.1	0,188650784	0,0221346
Contig11-snap.151	0,086109129	0,0224133
Contig138-snap.5	0,24235101	0,0226078
Contig31-snap.142	0,185674809	0,0226078
Contig57-snap.69	0,099234804	0,0226078
Contig125-snap.44	0,33974636	0,0226978
Contig255-snap.2	0,028524591	0,0228273
Contig71-snap.30	0,112669583	0,0229579
Contig81-snap.40	0,02201911	0,0229579
Contig14-snap.47	0,375631512	0,0233194
Contig23-snap.104	0,222588351	0,0246983
Contig31-snap.62	0,128226824	0,0249605
Contig98-snap.66	0,436568517	0,0268217
Contig11-snap.319	0,30534455	0,0268217
Contig14-snap.63	0,159719238	0,0268217
Contig130-snap.24	0,060521015	0,0268217
Contig4-snap.213	0,182392713	0,0275784
Contig8-snap.141	0,117972295	0,0275784
Contig56-snap.69	0,179478135	0,0284166
Contig75-snap.4	0,177300683	0,0284317
Contig296-snap.2	0,034001919	0,0284782
Contig70-snap.8	0,158220671	0,0291303
Contig79-snap.18	0,217012492	0,0297596
Contig32-snap.76	0,032265138	0,0297596
Contig14-snap.86	0,35259893	0,0301426
Contig419-snap.1	0,234708175	0,0301426
Contig45-snap.121	0,171517775	0,0306335
Contig10-snap.456	0,239975662	0,0315463
Contig19-snap.51	0,065352218	0,0315463
Contig39-snap.128	0	0,0315463
Contig25-snap.107	0,149760597	0,0315887
Contig24-snap.271	0,461224163	0,0316623
Contig85-snap.22	0,032946522	0,0318677
Contig26-snap.36	0,180418602	0,0327456
Contig39-snap.102	0,372419366	0,0328329
Contig123-snap.1	0,101530142	0,0328329
Contig17-snap.252	0,023531384	0,0328329
Contig139-snap.55	0,165925784	0,0333581
Contig14-snap.33	0,025719208	0,0333581
Contig17-snap.112	0,245363065	0,0335256
Contig145-snap.30	0,408220348	0,0335616
Contig1-snap.82	0,226306511	0,0364589

Contig14-snap.357	0,069649171	0,0364589
Contig10-snap.373	0,048384877	0,0364589
Contig28-snap.217	0,374417559	0,0365082
Contig14-snap.311	0,3900227	0,0379509
Contig97-snap.126	0,178337252	0,0379509
Contig27-snap.188	0,105757362	0,0379509
Contig31-snap.323	0,429086376	0,039204
Contig26-snap.33	0,139935121	0,0394386
Contig47-snap.162	0,041426565	0,0394386
Contig26-snap.105	0,035200507	0,0396762
Contig69-snap.9	0	0,0396762
Contig59-snap.151	0,395831958	0,0399193
Contig23-snap.122	0,057827919	0,0409057
Contig68-snap.82	0,026065584	0,0414377
Contig145-snap.27	0,473931349	0,0420894
Contig30-snap.228	0,272855683	0,0420894
Contig14-snap.100	0,196356873	0,0422089
Contig49-snap.25	0,139910874	0,0422089
Contig18-snap.193	0	0,0422089
Contig144-snap.39	0,138325592	0,0427174
Contig71-snap.22	0,045734605	0,0429852
Contig32-snap.91	0,299299132	0,04327
Contig15-snap.71	0,505167594	0,0436495
Contig97-snap.107	0,346027835	0,0436495
Contig5-snap.67	0,280077889	0,0436495
Contig26-snap.72	0,27336681	0,0436495
Contig18-snap.260	0,158129671	0,0436495
Contig24-snap.174	0,075086117	0,0436495
Contig73-snap.30	0,044867357	0,0436495
Contig123-snap.25	0,196818809	0,0440327
Contig14-snap.199	0,233918845	0,044093
Contig140-snap.28	0,444649356	0,0451409
Contig126-snap.11	0,028468889	0,0451409
Contig10-snap.426	0,087819188	0,0471901
Contig17-snap.161	0,065427457	0,0478031
Contig14-snap.418	0,044978208	0,0478031
Contig17-snap.45	0,428022932	0,0485581
Contig31-snap.287	0,108101616	0,0485581
Contig8-snap.357	0,485051555	0,0487759
Contig627-snap.1	0,29613358	0,0490452
Contig100-snap.50	0,400163088	0,0493838
Contig0-snap.323	0,052822998	0,0493838

Supplementary Table 2: List of gene specific primers of *lsy-12* 3' and 5' RACE

CDNA END	PRIMER	OLIGO
3'	Co6GSP2	GCCGTGTTTGTCGCCGCAGTACGCGAGA
	Co6NGSP2	GAGGGCGCGAGCAGCAGCAATGAGGACG
	Co6.1GSP2	GAAATCGCGGCGGACACGGGCATCTCTC
	Co6.1NSP2	GGCGCTCGGGATGCTCGTCAAGAGCGAG
	Co6.2GSP2	GCTAAATTTTGGCATGGCCCCTCACTCG
	Co6.2NGSP2	GCGGCGGTATGCAGTCCACGCCGGGCAG
5'	Co6GSP1	GTACTTGAGGCAGAACTCGCAGATGTAC
	Co6NGSP1	GATAGGGCGCGGTGAACCACGTCTCCAT
	Co6.1GSP1	CCTCATATGCCGCCCACTGGTCCTGCGT
	Co6.1NGSP1	GCGTCGGCTCGTCACTGGGCGGCATCGA

Supplementary Table 3: List of primers used for as-*eud-1* transcript identification

Primer	Oligo
Co10F3	GGAAGACTTCCGCAAGAAGCATGC
Co10R6	CTCGAGTGTTCATTCCTCAGGACATTG
Co10F4	AGGGCCGAGTGGGCTACAAGGG
Co10R5	CCTACTACATCTCCACGCAGTGATC
CoasFn	GAAGAACAAAACACACGGAGAAG
Co10asRn	ACTACCGAAAGACGAGACTACAATG

Supplementary Table 4: List of antibodies used in this study

Antibody	Host	Type	Company	Dilution	Cat. #
Alpha tubulin	Mouse	mAb	SIGMA ALDRICH	1:100	F22168
H3K4me3	Mouse	mAb	Diagenenode	1:1000	C15200152
H3K4me2	Rabbit	pAb	Diagenenode	1:1000	C15410035
H3K4me1	Mouse	mAb	Diagenenode	1:1000	Mab-150-050
H3K9ac	Mouse	mAb	Diagenenode	1:1000	Mab-185-050
H3K27ac	Mouse	mAb	Diagenenode	1:1000	C15200184
H2Bub	Mouse	mAb	Active Motif	1:1000	39623, 39624
H2Aub	Mouse	mAb	Millipore	1:2000	05-678
H4K20me1	Rabbit	pAb	Abcam	1:1000	9051

Research

Young genes have distinct gene structure, epigenetic profiles, and transcriptional regulation

Michael S. Werner, Bogdan Sieriebriennikov, Neel Prabh, Tobias Loschko, Christa Lanz, and Ralf J. Sommer

Department of Evolutionary Biology, Max Planck Institute for Developmental Biology, 72076 Tübingen, Germany

Species-specific, new, or "orphan" genes account for 10%–30% of eukaryotic genomes. Although initially considered to have limited function, an increasing number of orphan genes have been shown to provide important phenotypic innovation. How new genes acquire regulatory sequences for proper temporal and spatial expression is unknown. Orphan gene regulation may rely in part on origination in open chromatin adjacent to preexisting promoters, although this has not yet been assessed by genome-wide analysis of chromatin states. Here, we combine taxon-rich nematode phylogenies with Iso-Seq, RNA-seq, ChIP-seq, and ATAC-seq to identify the gene structure and epigenetic signature of orphan genes in the satellite model nematode *Pristionchus pacificus*. Consistent with previous findings, we find young genes are shorter, contain fewer exons, and are on average less strongly expressed than older genes. However, the subset of orphan genes that are expressed exhibit distinct chromatin states from similarly expressed conserved genes. Orphan gene transcription is determined by a lack of repressive histone modifications, confirming long-held hypotheses that open chromatin is important for new gene formation. Yet orphan gene start sites more closely resemble enhancers defined by H3K4mel, H3K27ac, and ATAC-seq peaks, in contrast to conserved genes that exhibit traditional promoters defined by H3K4me3 and H3K27ac. Although the majority of orphan genes are located on chromosome arms that contain high recombination rates and repressive histone marks, strongly expressed orphan genes are more randomly distributed. Our results support a model of new gene origination by rare integration into open chromatin near enhancers.

[Supplemental material is available for this article.]

Gene regulation is a highly orchestrated process that includes transcription factor binding sites (TFBSs), noncoding RNAs, histone modifications, and chromatin structure (Voss and Hager 2014). The identification and mechanism of these molecular factors have been revealed for several conserved gene networks leading toward a better understanding of development and disease. But how new genes, also referred to as orphan or taxon-restricted, acquire this complex architecture is unknown. For the increasing number of identified new genes that provide important biological function (Burki and Kaessmann 2004; Cai et al. 2008; Rosso et al. 2008; Chen et al. 2010, 2013b; Reinhardt et al. 2013; Mayer et al. 2015; Santos et al. 2017), the evolutionary path from origin to integration into gene networks depends on their precise transcriptional regulation (Carelli et al. 2016). Yet in the majority of cases, it is unclear how even the most fundamental *cis*-regulatory elements like promoter and termination sequences are obtained (Tautz and Domazet-Lošo 2011; Long et al. 2013). Orphan genes can originate de novo or by duplication, recombination, or horizontal gene transfer into preexisting regulatory architecture (Betrán and Long 2003; Kaessmann et al. 2009; Li et al. 2009; Kaessmann 2010; Chen et al. 2012b; McLysaght and Hurst 2016), but the extent to which this occurs is limited by the potential to disrupt the genes already there (Vinckenbosch et al. 2006). In the few cases in which integration has been observed, the presence of nearby regulatory sequences was largely detected by proximity, or sequence homology with known promoters, CpG islands, or TFBSs (Carvunis et al. 2012; Abrusán 2013; Ruiz-Orera et al. 2015; Li et al. 2016). Given these constraints, the contribution of preexisting regulatory architecture to new gene transcription is still unknown and, with functional genomic information (e.g., chromatin states and enhancers), could potentially be large. Indeed, a recent analysis of mammalian ChIP-seq data sets found 51% of expressed mouse retrogenes (mRNAs that are reverse transcribed and inserted into the genome) exhibit robust H3K4 trimethylation (Carelli et al. 2016), and transcription of the new gene *QQS* in *Arabidopsis thaliana* is inversely correlated with DNA methylation at 5′ transposable elements (Silveira et al. 2013), suggesting an important role for chromatin regulation in new gene transcription. We sought to use the rich taxonomic resources of nematodes to first identify young and old genes, and then observe their regulatory architecture by several genome-wide approaches.

The diplogastrid nematode *Pristionchus pacificus* can be found in a necromenic relationship with beetles, but has been developed in the laboratory as a satellite model for comparative studies to *C. elegans* (Fig. 1A–D; Sommer and Streit 2011; Sommer and McGaughran 2013). More recent genetic analysis of dimorphic mouth-forms (Fig. 1E–G) has led to *P. pacificus* emerging as an important model system for phenotypic plasticity in its own right (Bento et al. 2010; Ragsdale et al. 2013; Kieninger et al. 2016; Serobyan et al. 2016). In addition to the vast taxonomic diversity and corresponding genomes of other nematode species, the recent high-quality chromosome-scale genome (Rödelsperger et al. 2017) and reverse genetic tools (Witte et al. 2015) in *P. pacificus* provide a

Corresponding author: ralf.sommer@tuebingen.mpg.de
Article published online before print. Article, supplemental material, and publication date are at http://www.genome.org/cgi/doi/10.1101/gr.234872.118. Freely available online through the *Genome Research* Open Access option.

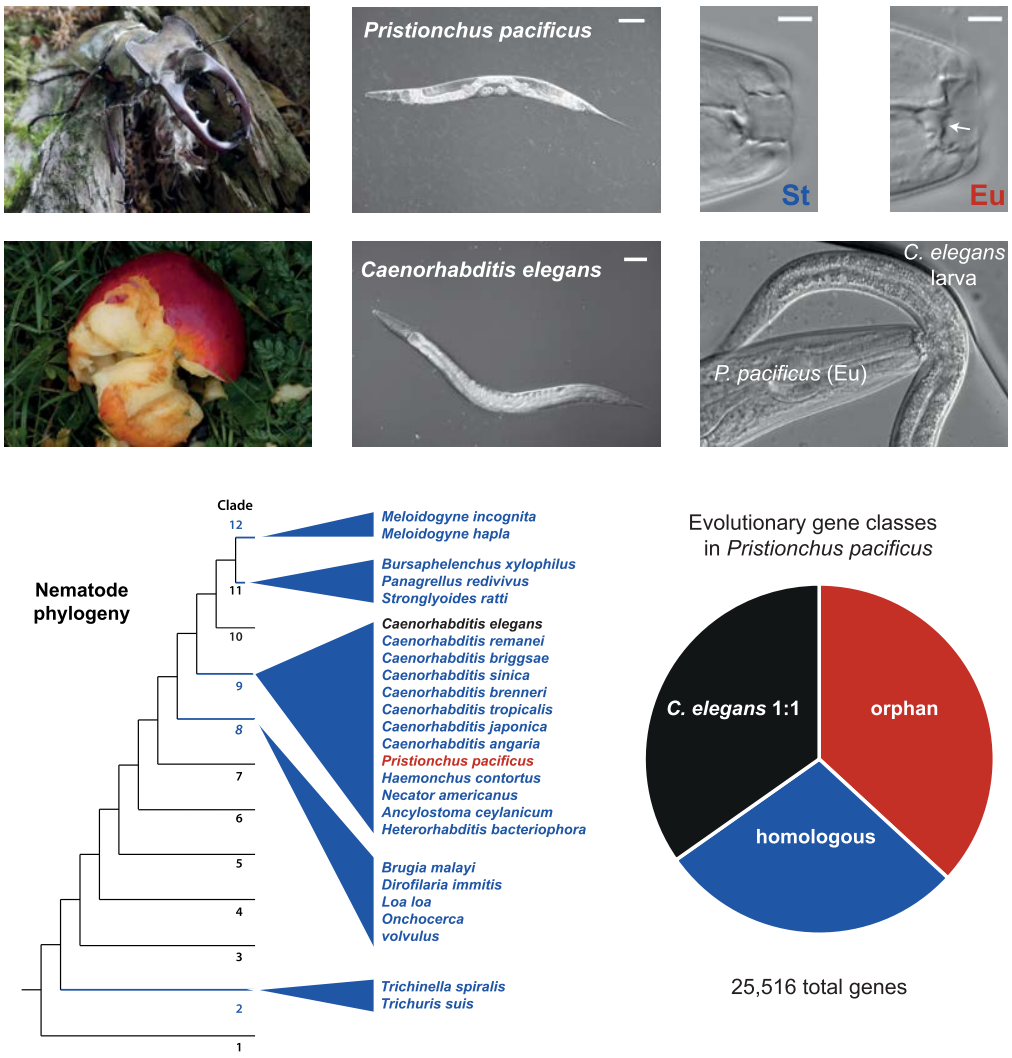

Figure 1. Comparison of *Pristionchus pacificus* and *Caenorhabditis elegans* and phylogenetic relationship. (*A*,*B*). *P. pacificus* is often found in a necromenic relationship with insect hosts, preferentially scarab beetles, in the dormant dauer state. When the beetle dies, worms exit the dauer stage to feed on bacteria that bloom on the decomposing carcass. (*C*,*D*) *C. elegans*, the classic nematode model organism, is often found in leaf detritus and rotting fruits. Example rotting apple photo taken by M.S.W. (*E*–*G*) *P. pacificus* has become an important model for developmental (phenotypic) plasticity. Adults can adopt (*E*) a narrow mouth form with one tooth (stenostomatous [St]) that makes them strict bacterial feeders. However, the "boom-and-bust" life cycle creates significant competition for resources, and under crowded conditions adults can develop an alternative mouth form (*F*) with a wider buccal cavity and an extra tooth (eurystomatous [Eu]) that allows them to prey on other nematodes. (*G*) Shown here is a eurystomatous *P. pacificus* preying on a *C. elegans* larva. (*H*) A schematic phylogeny of nematodes that was generated based on the publications of Holterman et al. (2017) and Van Megen et al. (2009). (*I*) Breakdown of *P. pacificus* genes by evolutionary category: One-to-one orthology with *C. elegans* (*C. elegans* 1:1) is the most conserved, followed by genes sharing homology with at least one gene from the 24 other nematodes (homologous), and finally genes that are only found in *Pristionchus* (orphan). All categories were defined by BLASTP homology (*e*-value ≤0.001) (Methods).

robust framework for studying new genes (Baskaran et al. 2015; Prabh and Rödelsperger 2016). Here, we probe the gene structure, expression, and regulatory architecture of *P. pacificus* evolutionary gene classes with long-read Pacific Biosciences (PacBio) transcript sequencing (Iso-Seq), traditional high-depth RNA sequencing (RNA-seq), and chromatin immunoprecipitation (ChIP-seq) of six histone post-translational modifications and assay for transposon-accessible chromatin (ATAC-seq). In addition to our findings, the data sets collected provide the first epigenomic map in *P. pacificus*, which is only the second comprehensive chromatin state annotation in nematodes, creating a resource for future functional and comparative studies.

Results

Partitioning of *P. pacificus* genes into evolutionary classes

The first *P. pacificus* draft genome published in 2008 (Dieterich et al. 2008) had a large number of genes with undetectable homology. Although the confidence in these gene predictions was initially low, every subsequent refinement of both the genome and gene annotation continually detected 20%–40% of genes that appear as new, orphan, or taxon-restricted (Sinha et al. 2012; Baskaran et al. 2015; Baskaran and Rödelsperger 2015; Prabh and Rödelsperger 2016). Using our most recent chromosome-scale PacBio genome (Rödelsperger et al. 2017) and 24 other nematode species, we

reevaluated the relative abundance of evolutionary gene classes (Fig. 1H). We defined the most highly conserved genes as having 1:1 orthology with *C. elegans* (BLASTP *e*-value ≤ 0.001), which is estimated to have diverged from *P. pacificus* between 60 to 90 million years ago (Cutter 2008; Rota-Stabelli et al. 2013; Hedges et al. 2015). We also defined an intermediate conserved class as "homologs" if they display homology with at least one gene in the other 24 nematode species (Methods)—which could represent either relatively young genes or old genes that have been lost. Finally, we define "orphan" genes as having no homology with genes in the other 24 queried species. The resulting partition of genes approximates the "30% rule" of new gene composition (Fig. 1I; Khalturin et al. 2009). We then applied several genomic approaches to molecularly characterize each evolutionary gene class.

Characterization of gene structure by long-read RNA sequencing (Iso-Seq)

We sought to improve the overall gene annotation in *P. pacificus* and then characterize the genetic structure of each evolutionary gene class using PacBio Iso-Seq on mixed-developmental stage RNA (Supplemental Methods; Supplemental Fig. S1A–C). After alignment, we obtained 640,664 reads with a median insert size of 1363 nucleotides (Supplemental Fig. S1D). Despite low read depth compared to conventional RNA-seq, our Iso-Seq data covered 17,307 genes (68% of genes in the reference annotation "El Paco") (Rödelsperger et al. 2017).

Relative to the current reference annotation, Iso-Seq identified a tighter distribution of gene lengths (median Iso-Seq = 1452 compared to median reference = 1599, $P < 2.2 \times 10^{-16}$, Wilcoxon rank-sum test) (Fig. 2A). This difference appears to be due to a more narrow distribution of exons, with 96.5% of Iso-Seq gene annotations containing between 1 and 20 exons, compared to 85.7% for the reference annotation ($P = <2.2 \times 10^{-16}$, Wilcoxon rank-sum test) (Fig. 2B). The tighter distribution is also more consistent with the highly curated gene annotation of *C. elegans* in which 98.0% of genes contain between 1 and 20 exons (Supplemental Fig. S1E,F; Deutsch and Long 1999). This potential improvement in accuracy appears to result from fragmentation of excessively long gene predictions into distinct transcripts (for example, see Supplemental Fig. S1G).

Long-read Iso-Seq also provides more robust identification of isoforms, which are historically difficult to assemble from standard short-read RNA sequencing (Conesa et al. 2016). Approximately half (50.6%) of expressed genes in *P. pacificus* exhibit greater than one isoform, and roughly a third (30.9%) exhibit greater than three isoforms (Supplemental Fig. S1H,I). However, some of these transcripts could be artifacts biased by incomplete coverage of 5′ ends.

Hence, we conservatively defined alternatively spliced isoforms as transcripts with the same start and stop coordinates, but differential exon inclusion or exclusion, intron retention, or differential splice site. Under this classification we observed 3861 (24%) of expressed genes exhibit alternative splicing in *P. pacificus* (Fig. 2C), similar to the ~25% of genes estimated in *C. elegans* (Ramani et al. 2011). As an example, we highlight gene *ummS259-11.10-mRNA*, where the majority of Iso-Seq reads (17/19) cover the entire transcript yielding eight isoforms, in stark contrast to standard short-read sequencing, which rarely covers more than three exons per read (Fig. 2D). Collectively, a tighter distribution of transcript lengths and exon numbers, and diversity of isoforms, suggests that Iso-Seq improves the quality and quantity of gene annotation in *P. pacificus*.

Among evolutionary gene classes, most *C. elegans* 1:1 orthologs (88%), and approximately half of homologous and orphan genes (46% and 56%, respectively) exhibit Iso-Seq coverage, demonstrating that our Iso-Seq data are sensitive enough to detect thousands of transcripts from each evolutionary gene class (Fig. 2E). We also performed Iso-Seq on rRNA-depleted "total RNA" (Supplemental Methods) to assess whether young genes are un-, or under-polyadenylated, which is typical of noncoding RNAs (Derrien et al. 2012). We found a similar percent coverage from the direct and total RNA methods (Fig. 2E,F) and a consistent polyadenylation read bias for all gene classes (Fig. 2G–I). Hence most young genes, or at least transcribed young genes, are polyadenylated. Because polyadenylation is an important component of transcriptional and translational regulation (Proudfoot et al. 2002; Proudfoot 2011), this argues that most young genes have retained, or already acquired, 3′ termination and processing sequence architecture.

We then used our Iso-Seq annotation to characterize gene length and exon number between evolutionary gene classes. Consistent with other systems (Ruiz-Orera et al. 2015; Stein et al. 2018), we found a strong bias of *C. elegans* 1:1 orthologs to be longer and contain more exons than homologs, which in turn were longer and contained more exons than orphan genes ($P = <2.2 \times 10^{-16}$, Wilcoxon rank-sum test) (Fig. 2J,K). The intermediate gene structure of intermediate conserved genes (homologs) is also consistent with a transitional evolutionary path between young and old genes proposed by Carvunis et al. (2012) (Abrusán 2013; Neme and Tautz 2013). In the following sections we seek to characterize and compare the chromatin regulation of young versus old genes.

The *P. pacificus* epigenome

To identify regulatory regions and expression levels of orphan, homolog, and *C. elegans* 1:1 orthologs, we performed two to three replicates of ChIP-seq on nine histone modifications and two replicates of RNA-seq in *P. pacificus* adults, and two replicates of ATAC-seq on mixed-stage cultures (Supplemental Fig. S2; Supplemental Table S3; Supplemental Methods). All data sets showed good correlations between biological replicates (Pearson's correlation between 0.70–0.93 for ChIP-seq, 0.88 for ATAC-seq, and 0.98 for gene FPKMs in RNA-seq) (Supplemental Fig. S3). We identified enriched regions (i.e., peaks) for each replicate of ChIP-seq and ATAC-seq using MACS2 (Methods; Supplemental Table S1; Zhang et al. 2008). H2Bub, H3K9ac, and H3K79me2 exhibited <50% peak reproducibility and were excluded from further analysis (Supplemental Fig. S4A). The majority of remaining samples exhibited >70% overlap between replicates, except for H3K9me3 (54% reproducibility). However, H3K9me3 is a broadly distributed histone modification that is challenging for peak-finding software (Wang et al. 2013), and although most H3K9me3 antibodies are of low specificity (Nishikori et al. 2012; Hattori et al. 2013), they can nevertheless distinguish constitutive versus facultative heterochromatin (Trojer and Reinberg 2007).

We also performed ATAC-seq for identifying regions of open chromatin (Buenrostro et al. 2013). Although the standard protocol led to reproducible peaks, initially we could not identify nucleosomal read density, perhaps suggesting a difficulty of obtaining higher resolution fragments from highly differentiated and heterogeneous cell populations. Yet the new Omni-ATAC method (Corces et al. 2017) yielded nucleosomal and subnucleosomal read densities (Supplemental Fig. S2E), which we used for subsequent analysis.

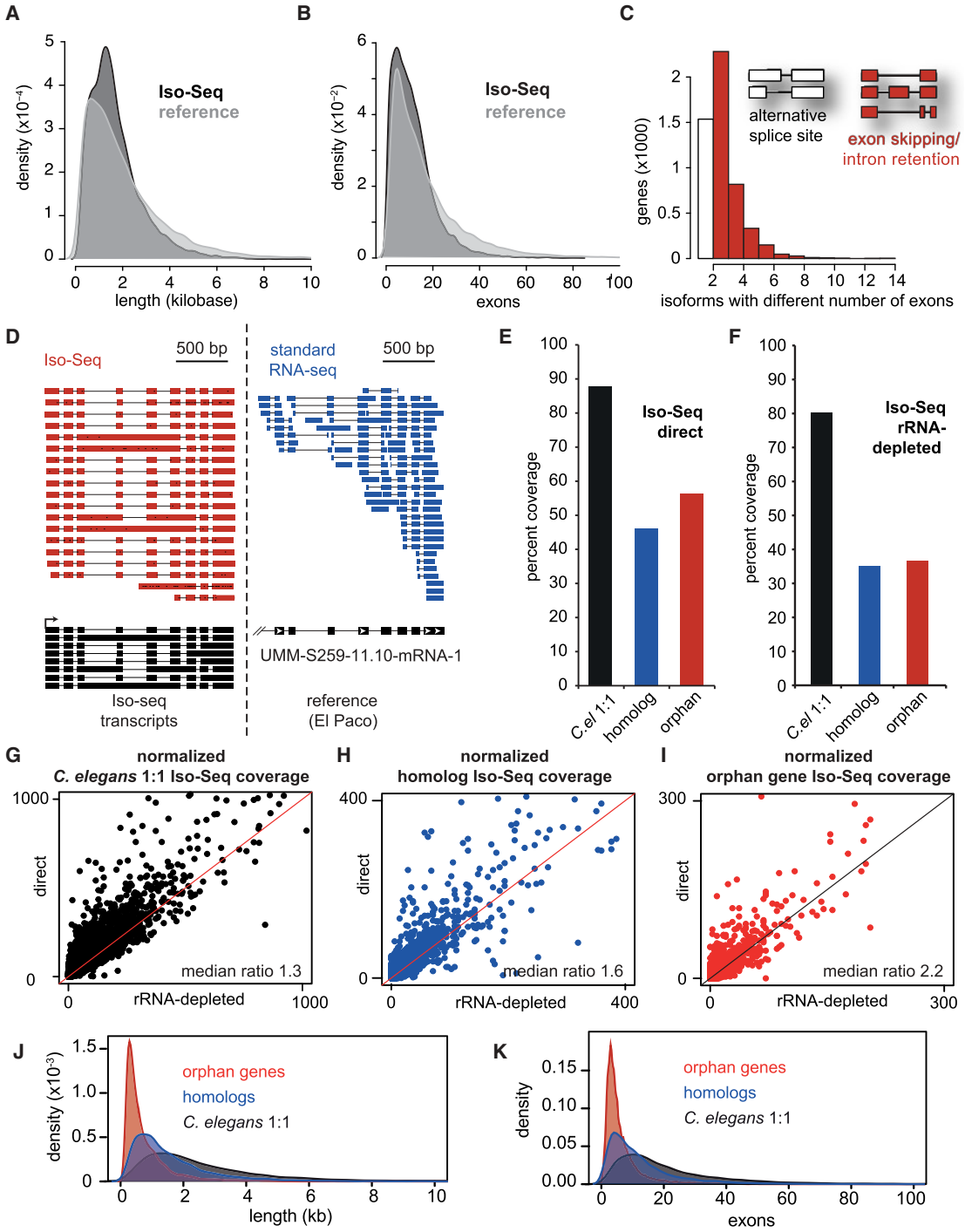

Figure 2. Long-read RNA sequencing (Iso-Seq) improves gene annotation, identifies alternative splicing, and can distinguish different evolutionary gene classes by gene structure. (*A*) Density distribution of cDNA gene lengths between the El Paco reference (gray) and Iso-Seq annotation (black). The Iso-Seq annotation was derived from guided assembly using StringTie (Pertea et al. 2016; Methods), and plots were created using the density function in R. (*B*) Density distribution of exons per gene between El Paco reference and Iso-Seq annotations. Method and color scheme are similar to *A*. (*C*) Alternatively spliced isoforms, defined as having multiple detected isoforms with the same start and stop coordinates. The white column represents genes containing isoforms that have the same exon–intron structure but different splice sites, and red columns represent genes containing isoforms with different numbers of exons due to intron retention or exon inclusion/exclusion. (*D*) Example locus of Iso-Seq reads compared to standard short-read RNA-seq. Also shown are Iso-Seq-assembled isoforms compared to the single reference gene umm-S259-11.10-mRNA-1, visualized using Integrated Genome Viewer (IGV). (*E,F*) Percent coverage of evolutionary gene classes by Iso-Seq with either the "direct" method (*E*) or rRNA-depleted "total RNA" (*F*). (*G–I*) Iso-Seq coverage per gene of each evolutionary class in direct (*y*-axis) compared to total (*x*-axis). Coverage was determined by BEDTools, and median ratios of direct/total RNA are presented. Lines (slope = 1, *y* intercept = 0) represent equal coverage between methods. (*J,K*) Similar density distributions of cDNA length and exon number as in *A* and *B*, but for the three evolutionary gene classes.

We clustered the six high-confidence histone marks and Omni-ATAC-seq data using a hidden Markov model (ChromHMM) (Ernst and Kellis 2012) into eight chromatin states (Fig. 3A). Each chromatin state is enriched in histone modifications that define specific functional domains, such as actively transcribed regions, heterochromatin, and regulatory loci. We assigned putative chromatin state annotations based on established classifications (Supplemental Table S2; Fig. 3B; Ernst et al. 2011; Rada-Iglesias et al. 2011). We find that, at least at the whole-animal level, approximately half (57%) of the genome is repressed, approximately a fifth (16%) represents actively transcribed genes, and more than a quarter (27%) is regulatory (including 6785 promoters, 13,648 active enhancers, and 3853 "poised" enhancers) (Fig. 3C).

Next, we verified that histone marks are enriched at the center of promoters and active enhancer annotations, and we performed a de novo motif search (Fig. 3D–G; Heinz et al. 2010). Both promoters (30.6%) and enhancers (22.2%) were enriched in a recognition sequence for MBP1, a yeast transcriptional activator that controls cell-cycle progression (Koch et al. 1993). There is weak homology (BlastP, $e = 2 \times 10^{-4}$) with MBP1 in *P. pacificus* (UMM-S233-5.4-mRNA-1), and in the future it will be interesting to see if this gene is also involved in cell-cycle control. There were also notable differences between enhancers and promoters, including binding site matches to human homeobox, *Drosophila* GAGA, and eukaryotic GATA transcription factors, demonstrating the precision of promoter and enhancer annotations, and hinting at the existence of deeply conserved regulatory elements.

As expected, promoter annotations were strongly enriched at the 5′ end of genes (Fig. 3H). There was also another peak near the 3′ end of genes. Enhancers were also enriched at both 5′ and 3′ ends, although they are more evenly distributed throughout gene bodies. The existence of promoter/enhancer elements at the 3′ ends of genes has been observed in other species, and although their functions are still unclear, there are several reports supporting promoter-3′-end chromatin looping to facilitate successive rounds of transcription and enforce directionality (O'Sullivan et al. 2004; Lainé et al. 2009; Grzechnik et al. 2014; Werner et al. 2017).

To verify that our chromatin states correlate with a dynamically regulated gene, we looked at *Ppa-pax-3*, which our laboratory has shown to be expressed in early juvenile stages but is repressed during development (Yi and Sommer 2007). Indeed, we found *Ppa-pax-3* is in a large H3K27me3-repressed domain in adults (Fig. 3I). However, we also noticed two putative enhancers after the first exon and 3′ end, perhaps suggesting preparation for activation in developing embryos. Collectively, these data represent the first genome-wide annotation of chromatin regulation in *P. pacificus* and, to our knowledge, represents only the second comprehensive data set in nematodes.

Chromatin regulation corresponds to gene expression

We extended the previous single gene example to genome-wide high-depth RNA-seq and binned the adult transcriptome into four expression categories (Fig. 4A), then assessed the chromatin states of each. As predicted, gene bodies (exons and introns) of the highest expressed categories (groups 1 and 2) exhibited enrichment in chromatin states designated as "transcriptional transition" and "elongation." Conversely, repressive chromatin states were virtually absent from genes in the top two categories. In contrast, the two lowest expression categories (groups 3 and 4) exhibited proportionally greater enrichment in repressive chromatin states and decreased enrichment in transcriptional transition and elongation states (Fig. 4B). Although there was a minor enrichment in promoter chromatin states at 5′ ends and 5′ UTRs among high versus low expression categories, there was a larger difference in repressive chromatin states, especially at the 5′ ends. There was also an increase in enhancer enrichment at 5′ ends and 5′ UTRs in the low expression categories, perhaps reflecting a "poised" chromatin state that is reactive to environmental influence. Although promoters and enhancers exhibit a relatively small portion of the genome (15.6%), they comprise the majority of intergenic regions (Fig. 4B), hinting at a large and mostly unexplored regulatory circuitry in the compact nematode genome.

Chromatin regulation of evolutionary gene classes

Next, we assessed the chromatin states of evolutionary gene classes. *C. elegans* 1:1 orthologs resembled the highest expression categories (groups 1 and 2), whereas conserved and orphan genes more closely resembled the lower expression categories (groups 3 and 4) (Fig. 4C–E). These histone patterns reflect the higher expression of *C. elegans* 1:1 orthologs compared to less conserved gene classes (Fig. 4F). Nevertheless, we noticed a significant number of orphan and homologous expressed gene outliers (Fig. 4F) and wondered whether their chromatin signatures resembled that of expressed *C. elegans* 1:1 orthologs. Here, we found differences. Specifically, strongly expressed (groups 1 and 2) orphan and homologous genes, which represent only 9.3% and 12.8% of their respective categories, broadly resembled the general chromatin state pattern of their classes except for having reduced repressive histone marks (Fig. 4G–I). Second, chromatin states 3 and 4, representing transcriptional transition and elongation, are more highly represented in *C. elegans* 1:1 orthologs compared to expressed orphan and conserved genes. Third, *C. elegans* 1:1 orthologs exhibit little to no signature of active enhancers (chromatin state 1) at their 5′ ends or 5′ UTRs, which are instead dominated by the promoter chromatin state consisting of H3K4me3 and H3K27ac. However, expressed homologous and orphan genes exhibited both promoter and enhancer enrichment at their 5′ ends and 5′ UTRs, and orphan genes, in particular, exhibited greater enrichment in enhancer versus promoter chromatin states.

To investigate this difference more closely, we examined the distribution of histone ChIP-seq and ATAC-seq around the 5′ ends of each evolutionary class. Whereas expressed *C. elegans* 1:1 ortholog TSSs are dominated by H3K4me3 and H3K27ac, expressed orphan and homologous genes exhibit comparatively stronger enrichment of H3K4me1 and ATAC-seq (Fig. 4J). Specifically, *C. elegans* 1:1 orthologs exhibit an average 5′ H3K4me3/H3K4me1 ratio of 10.1, compared to 2.4 for homologs and 1.4 for orphan genes. Furthermore, although 54% of expressed *C. elegans* 1:1 ortholog 5′ ends are within 1 kb of an annotated promoter, only 27% of expressed homologous genes and 21% of expressed orphan genes are in similar proximity to promoters ($P < 2.2 \times 10^{-16}$, Wilcoxon rank-sum test) (Fig. 5A). Conversely, 46% of expressed homologous and orphan gene TSSs are within 1 kb of active and poised enhancers, compared to 33% of expressed *C. elegans* 1:1 ortholog TSSs ($P < 2.2 \times 10^{-16}$, Wilcoxon rank-sum test for both comparisons) (Fig. 5B). Importantly, the expression of groups 1 and 2 orphan and homologous genes are actually higher than *C. elegans* 1:1 orthologs ($P < 2.2 \times 10^{-16}$, Wilcoxon rank-sum test) (Supplemental Fig. S5), demonstrating that their chromatin architecture is independent of the general correlation with expression. There are two key points from these results. First, the transcription of young genes appears to depend on the absence of repressive

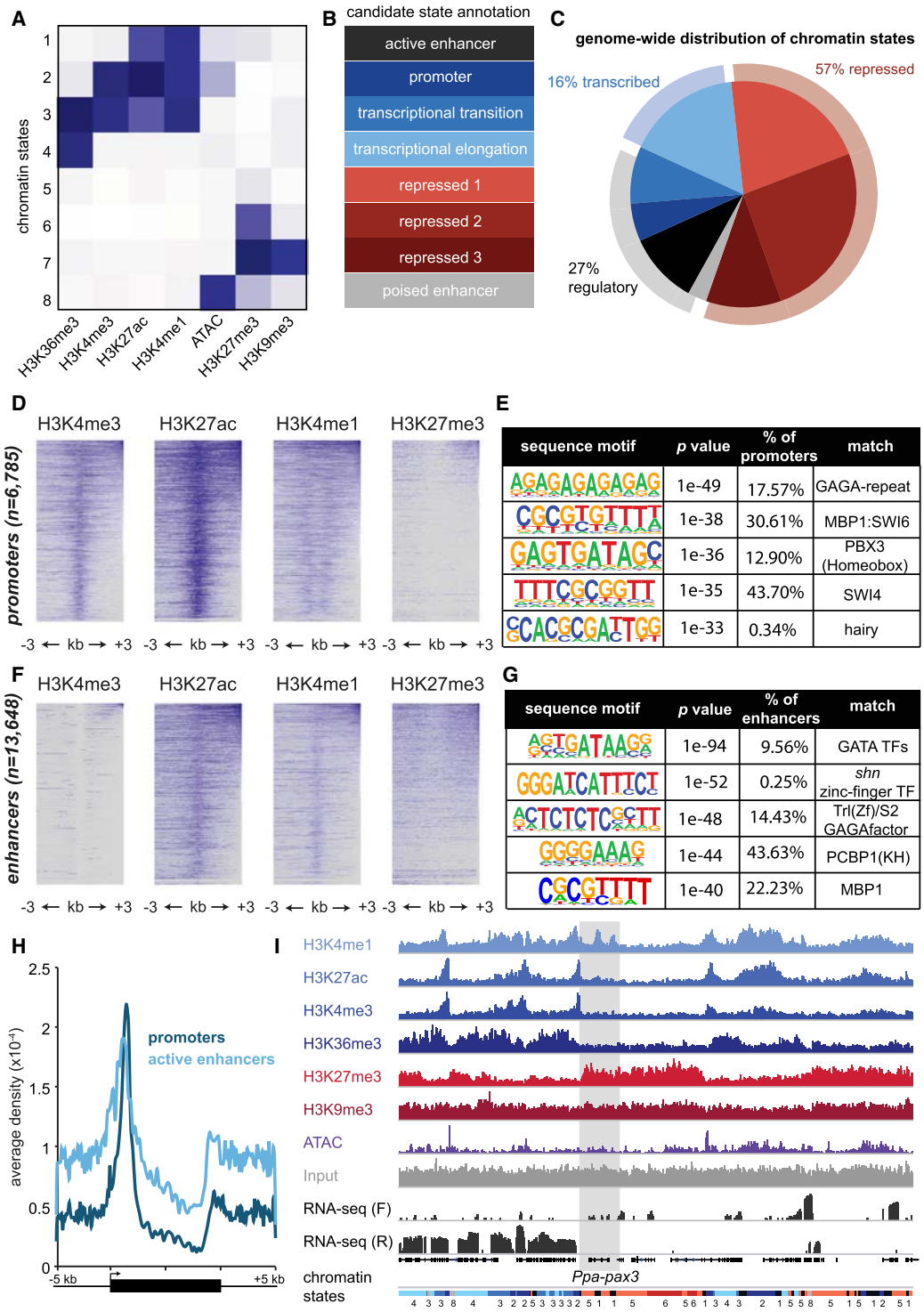

Figure 3. The epigenome of *Pristionchus pacificus*. (*A*) Chromatin states determined through a hidden Markov model (ChromHMM) clustered by histone modifications and ATAC-seq, normalized by coverage. Darker blue represents greater enrichment. (*B*) Candidate annotation of each chromatin state according to ENCODE/modENCODE data sets (Ernst et al. 2011; Roadmap Epigenomics Consortium et al. 2015). Repressive chromatin states are divided into three categories according to standard definitions of constitutive (repressed 3) and facultative (repressed 1 and 2) heterochromatin. Poised enhancers are defined according to previous annotations of loci containing H3K27me3 and DNase sensitivity. (*C*) Genome-wide distribution of chromatin states, and further clustering into three categories: repressive, transcribed, or regulatory. (*D*) Heatmap of indicated histone modifications for promoter chromatin states, in which each line represents a single 6-kb locus centered on the promoter. Heatmap matrices were generated in HOMER, clustered from highest to lowest enrichment, and plotted in R. (*E*) Position weight matrices of de novo sequence motifs in promoters, queried using HOMER. The table also includes the percentage of promoters containing motif, *P*-value, and matches to known transcription factors. (*F*,*G*) Similar to *D*,*E*, but for enhancer chromatin states. (*H*) Average density plots of promoter (dark blue) and enhancer (light blue) locations relative to gene bodies, extended 5 kb in each direction from their 5′ and 3′ ends. Density values measured using HOMER and plotted in Excel. (*I*) Epigenomic data of histone modification ChIP-seq, ATAC-seq, and RNA-seq surrounding the *Ppa-pax3* gene. Input is included as a reference, and chromatin state annotations are included at the *bottom* matching the colors in *C*. ChIP-seq and ATAC-seq coverage are autoscaled per sample, and RNA-seq forward (F) and reverse (R) read coverage is in log-scale.

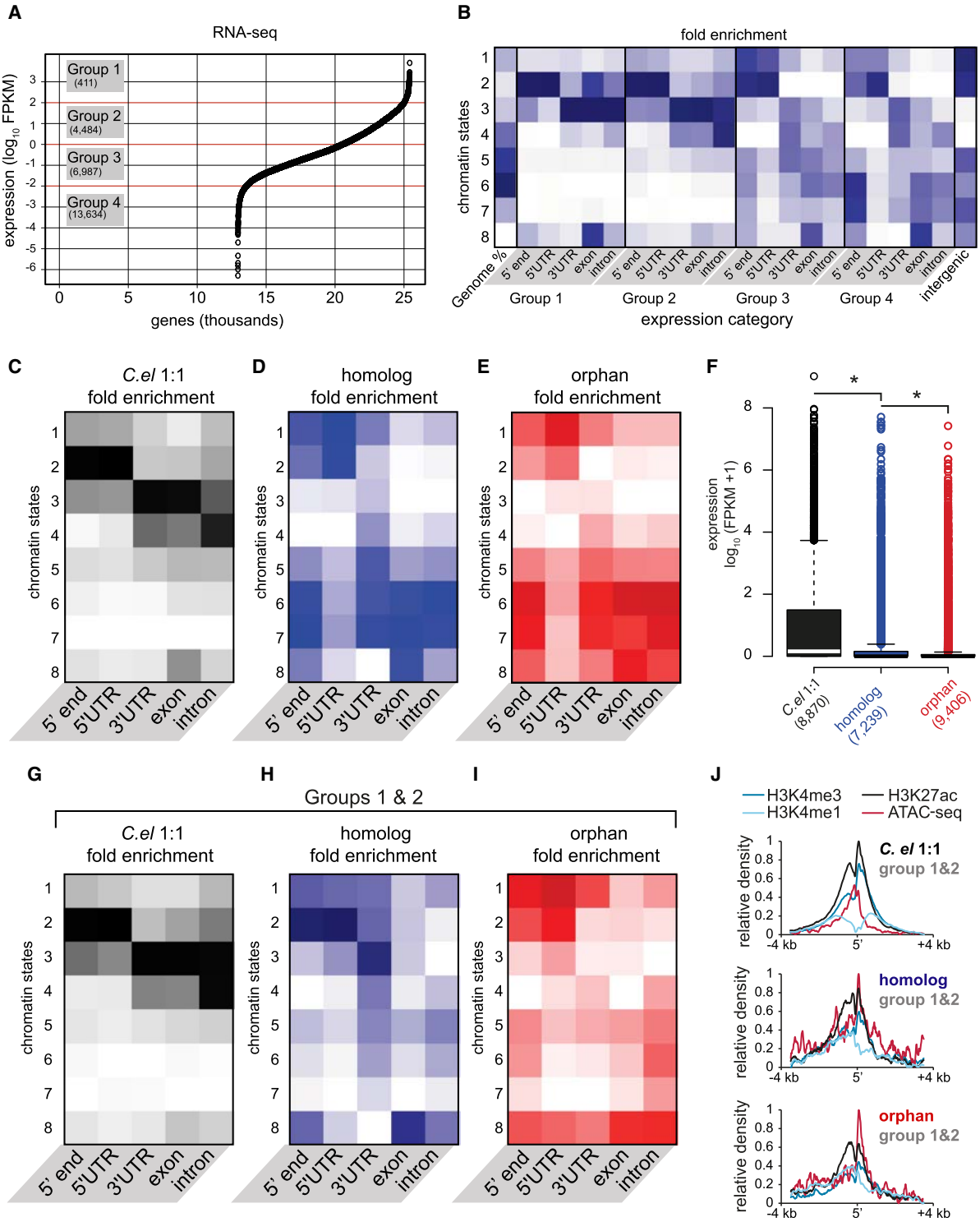

Figure 4. Chromatin states correlate with expression, but expressed young genes exhibit distinct profiles. (*A*) Average expression (FPKM) from two biological replicates of RNA-seq, plotted for each gene from highest to lowest along the *x*-axis. Expression categories were binned according to approximate inflection points. (*B*) Chromatin state enrichment of each expression category broken down by genetic element (i.e., TSSs, UTRs, exons, and introns). (*C–E*) Similar to *B*, but for each evolutionary gene class. (*F*) Expression of each evolutionary gene class determined from average RNA-seq FPKMs: (*) *P*-value <0.05, Welch's *t*-test (two-tailed). (*G–I*) Similar to *B–E*, but only for highly expressed (groups 1 and 2) genes belonging to each category. (*J*) Normalized average densities of H3K4me3, H3K4me1, H3K27ac, and ATAC-seq over a 7-kb window centered at 5′ ends. Densities were measured in HOMER and normalized to the highest and lowest values in each gene class.

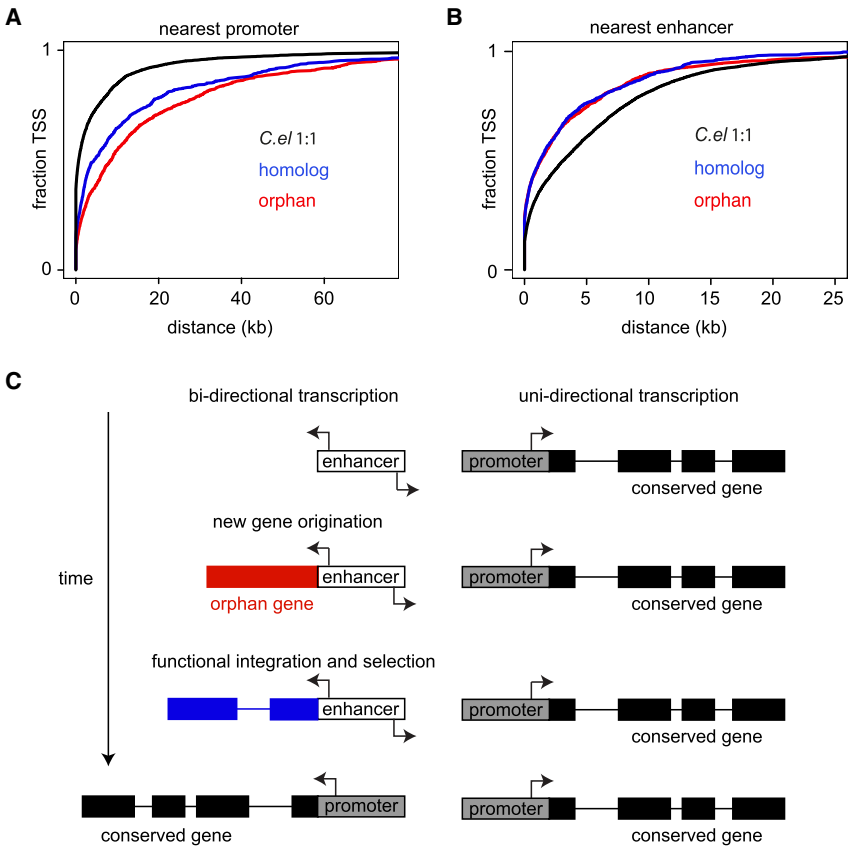

Figure 5. Distance of promoters and enhancers to evolutionary gene classes. (*A*) Distance cumulative frequency distribution of the nearest promoter, or (*B*) enhancer (active and poised) to transcription start sites (TSSs) from each evolutionary gene category. (*C*) Model of new gene transcriptional regulation. Enhancers exhibit bidirectional transcription, which can lead to de novo gene expression, or expression of duplications/insertions. If the new gene provides a useful function, selection will occur on not only protein function, but also the gene structure leading to more exons, and on regulatory elements to provide more temporal or spatial control, and more or less transcription. Ultimately, evolution on enhancer sequences will convert it to a traditional promoter.

heterochromatin, demonstrating a widely held but unconfirmed theory for the requirement of open chromatin in new gene expression. Second, the 5′ end of expressed young genes, especially orphan genes, resemble enhancers rather than canonical promoters.

Genomic position affects chromatin regulation of evolutionary gene classes

Finally, we analyzed the general pattern of chromatin marks and evolutionary gene classes at the chromosomal level (Fig. 6). We observed strong patterns of activating marks in the center of autosomes II–V and the repressive mark H3K27me3 on the chromosome arms. Conversely the X Chromosome was highly enriched in both repressive marks H3K27me3 and H3K9me3. These patterns have been observed in *C. elegans* (Liu et al. 2011), and they correspond to general patterns in nematodes of dense clusters of conserved genes and low recombination rates in the center of chromosomes, and species-specific genes and high recombination rates in the chromosome arms (Coghlan 2005). However, Chromosome I in *P. pacificus* is an exception to other autosomes, in which we observed two bands of activating marks instead of one. Recent analysis suggests that roughly half of *P. pacificus* Chromosome I is homologous with *C. elegans* Chromosome X, and the other half is homologous with Chromosome V (Rödelsperger et al. 2017). The *P. pacificus* chromosome pattern was viewed as ancestral because this organization is also found in the distantly related nematode *Bursaphelenchus xylophilus*. However, the bipartite presence of histone modifications and conserved genes hints at an ancient chromosomal fusion from an even earlier origin, or frequent and repeated chromosomal fission and fusion events.

The chromosome-scale distribution of evolutionary gene classes was consistent with histone modification patterns. Specifically, *C. elegans* 1:1 orthologs, which are strongly expressed, are enriched in the active histone mark chromosome centers. Conversely, the lower expressed homologous and orphan genes are enriched in the chromosome arms, which contain higher recombination rates and a greater density of repressive histone marks. However, these patterns are lost when controlling for expression. Highly transcribed (groups 1 and 2) orphan and homologous genes were more randomly distributed throughout chromosomes, if not slightly biased to be closer toward the centers (Fig. 6). This genome-wide perspective also supports the model that location into open chromatin is a critical factor for origination, or at least transcription, of new genes.

Discussion

Here, we combine the first chromatin state analysis in *P. pacificus* with taxon-rich nematode phylogenies to analyze the transcriptional regulation of young genes. We identified eight chromatin states that partition the genome into varying levels of repression, transcription, or regulatory elements. Expressed young genes were found in open chromatin states, supporting a widely held model of new gene origination. To our surprise, however, young gene 5′ ends are more similar to enhancers than traditional promoters. We also analyzed young gene transcript structure by long-read Iso-Seq, which revealed a unique signature for each evolutionary gene class. Finally, a bipartite pattern of active histone marks in Chromosome I provides molecular evidence of an ancient chromosomal fusion event ~180 million years ago. The ability to probe more than 20,000 high-confidence promoters and enhancers will be a valuable resource for future mechanistic studies, especially when combined with the powerful array of genetic, phylogenetic, and ecological tools recently available to *P. pacificus*.

The origin and subsequent regulation of orphan genes is a widely debated topic that has garnered several theoretical models. Among these are that orphan genes can be transcribed by integrating into open chromatin, or near gene promoters, effectively hijacking their regulatory sequences and thereby mitigating the need to evolve them de novo (Kaessmann et al. 2009;

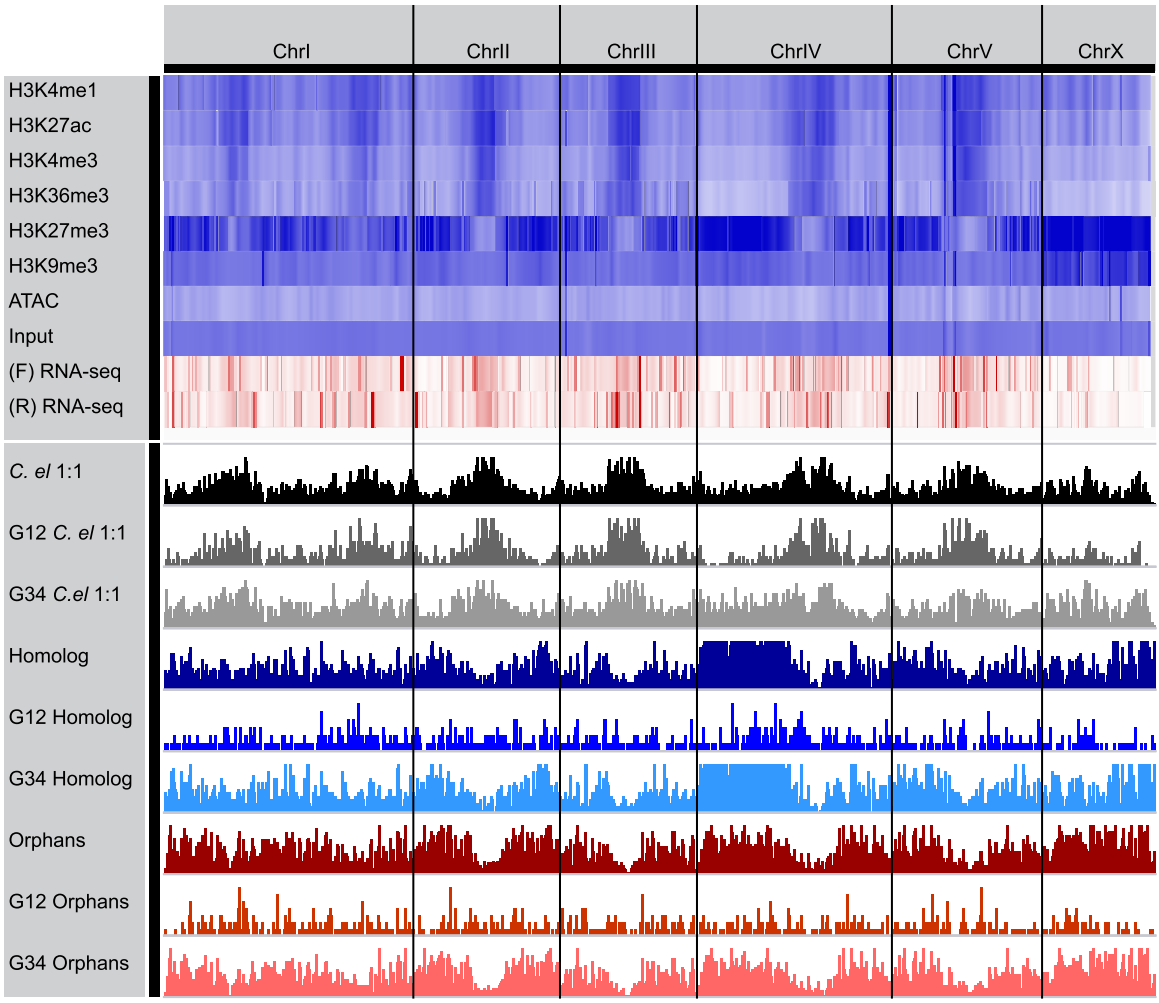

Figure 6. Chromosome-wide distribution of histone modifications reveals distinct patterns for evolutionary gene classes and a double-band pattern on Chr I. Genome-wide patterns of histone modifications from ChIP-seq and ATAC-seq presented as a heatmap with increasing abundance from white to blue, and white to red for RNA-seq (normalized by depth). Also plotted are gene densities of each evolutionary class binned by expressed (groups 1 and 2) or transcriptionally repressed (groups 3 and 4) for each class.

Kaessmann 2010; Tautz and Domazet-Lošo 2011; Chen et al. 2012a,b; Long et al. 2013; McLysaght and Hurst 2016). This model was supported by analyzing the position of transcribed retrogenes in the human genome (Vinckenbosch et al. 2006); however, it was also demonstrated that such integration is often deleterious to the host genes. Indeed, a recent analysis found only ~14% of mammalian retrogenes utilized preexisting promoters (Carelli et al. 2016). Nevertheless, to date very few tests of these predictions have been performed beyond retrogenes, and the identities of *cis*-regulatory elements have traditionally been inferred through spatial proximity to genes or known regulatory sequences like TFBSs and CpG islands (Betrán and Long 2003; Carvunis et al. 2012; Chen et al. 2012b; Ni et al. 2012; Ruiz-Orera et al. 2015; Li et al. 2016). The phylogenetic diversity of nematode genomes and our recent chromosome-scale genome (Rödelsperger et al. 2017) allowed us to query all orphan genes in *P. pacificus*, including but not limited to retrogenes. By applying ChIP-seq and ATAC-seq, we could then interrogate the functional *P. pacificus* genome, including *cis* and *trans* enhancers, and up to eight different chromatin states. The data presented herein support a model of orphan gene integration into open chromatin near enhancers preferentially over promoters.

Enhancers were originally thought of as inactive DNA elements that harbor TFBSs (Wasylyk 1988); however, over the last decade, research from several laboratories has shown that enhancers exhibit bidirectional transcription by RNA polymerase (Chen et al. 2013a; Andersson et al. 2014; Lam et al. 2014). Now there is a growing consensus that enhancers and promoters are similar regulatory elements (Andersson et al. 2015; Kim and Shiekhattar 2015), but promoters have evolved additional sequences to enforce directionality (Grzechnik et al. 2014) or increased expression. Indeed, promoters can even function as enhancers for other genes (Engreitz et al. 2016). Under this paradigm, we propose a model whereby a new gene that originates near an enhancer, and is adaptive, will eventually acquire more sophisticated regulatory architecture, thereby transitioning the enhancer into a promoter (Fig. 5C). This model is complimentary to "proto-promoters" proposed by the Kaessmann laboratory for 8%–9% of rat expressed retrogenes that have H3K4me3 enrichment in rats but H3K4me1 enrichment in syntenic nonexpressed regions in

mouse (Carelli et al. 2016). However, here we show that proximity of new genes to enhancers correlates with and presumably drives their transcription, and we extend this argument beyond retrogenes as a general feature of new genes. If these transcripts prove functional, then selection can convert the enhancer to a promoter. This model potentially solves two problems faced by new genes: (1) expression via origination near enhancers, and (2) introduction near enhancers, especially *trans* enhancers, as opposed to promoters, does not require exchange or competition with the preexisting gene landscape. Nevertheless, we caution that such interpretation is speculative at this point, and examining and then experimentally manipulating H3K4me1/3 at syntenic loci in closely related strains and species is necessary to test these hypotheses.

In principle, this model could operate regardless of the method of new gene origination (de novo, duplication and divergence, or retrotransposition). Transcripts from enhancers or lncRNA promoters generally exhibit less splicing, 3′ processing, and polyadenylation relative to protein coding genes (Derrien et al. 2012) and are often digested by the nuclear exosome (Schlackow et al. 2017). In de novo gene evolution, mutations that recruit sequence-specific splicing factors or 3′ processing factors such as CPSF73 could stabilize enhancer transcripts allowing for their translation and potential functionalization. In some cases, a de novo gene that is acting as a functional ncRNA, referred to as "moonlighting," could lead to greater expression and a greater window of time to accrue such mutations (Jalali et al. 2016). New genes formed by duplication and insertion, or retrotransposition near an enhancer, could similarly be transcribed, but without the parental regulatory architecture. In this new genomic context, the gene will likely be expressed in different developmental stages or tissues, possibly providing new functions. Although misregulation of genes often coincides with deleterious effects and disease (Lee and Young 2013), in this case, the parental gene is still maintained and operating under normal control, while the copied gene is freed, within limits (Geiler-Samerotte et al. 2011), to explore neofunctionalization.

Compared to the current reference annotation (El Paco), our Iso-Seq annotation identified shorter genes with fewer exons. The distribution was more similar to *C. elegans* gene structures. Nevertheless, we note that there are still substantially more genes in *P. pacificus* with more than 10 exons compared to *C. elegans* (Supplemental Fig. S1F), arguing that further refinement is still required (although an evolutionary divergence in gene length is formally possible). We also explored the genetic structure of young versus old genes. Orphan genes displayed the shortest gene lengths and fewest exons, and *C. elegans* 1:1 orthologs were the longest and contained the most exons. The result that homologs appear to be intermediate in length and exon number is consistent with a transitional path between old and young genes (Carvunis et al. 2012; Abrusán 2013), but whether this indicates divergence from old genes or de novo evolution from young genes is unknown, likely reflecting examples of both. Iso-Seq also identified that almost a quarter (24%) of expressed genes in *P. pacificus* have multiple isoforms. Although a subset of observed alternative splicing events can be attributed to splicing errors (Pickrell et al. 2010), there are important examples of alternative isoforms that affect diverse biological processes (Baralle and Giudice 2017). Whether the multiplicity of transcripts observed here are differentially expressed during development or in different environmental conditions, and ultimately if they are functional, will be the focus of future experiments.

Iso-Seq of polyadenylated transcripts and rRNA-depleted total RNA demonstrated that most young genes are polyadenylated. In mammals, noncoding RNAs are un- or underpolyadenylated (Derrien et al. 2012), arguing that most new genes in *P. pacificus* represent coding transcripts. However, retrogene transcripts that contain their polyadenylation "scar" in the genome may be transcribed directly with a poly(A) tail, and thus appear as polyadenylated regardless of whether they have been pseudogenized or not. Nevertheless, our interpretation that they are mostly coding is consistent with a previous investigation of orphan genes in *P. pacificus* that found appreciable peptide coverage from mass spectrometry and evidence of negative selection (Prabh and Rödelsperger 2016). Beyond orphan genes, comparing polyadenylated and total RNA Iso-Seq data sets should also be valuable for investigating gene structures of long noncoding RNAs (lncRNAs), including antisense ncRNAs that have been shown to affect phenotypic plasticity in *P. pacificus* (Serobyan et al. 2016).

Genome-wide, we found most young genes are present in chromosome arms where recombination and repressive chromatin in nematodes is the highest (The *C. elegans* Sequencing Consortium 1998; Coghlan 2005). However, the ∼10% of young genes that are highly transcribed (expression groups 1 and 2) were more randomly distributed. Thus, although recombination in the arms appears to be a furnace for new gene generation, most of these genes are repressed (expression groups 3 and 4) and have a higher barrier for functionalization. This pattern highlights several unresolved questions. In particular, does the presence in open chromatin reflect rare recombination events or de novo origination? Further, are these transcribed new genes "born" into open chromatin and serve as a template for evolution, or have they already acquired nascent function and their presence in open chromatin is a result of translocation to increase their expression? Additional functional genomic comparisons and synteny analysis may shed light on these questions.

At chromosome-scale resolution, we observed a double-banding of active histone marks on Chromosome I, in contrast to all other autosomes in both *P. pacificus* and *C. elegans* (Liu et al. 2011). Based on previous phylogeny and synteny analyses (Rödelsperger et al. 2017), we propose this pattern is a remnant from a fusion event that occurred prior to the split between *Diplogasterida* and *Tylenchida*, estimated at ∼180 million years ago (Cutter 2008; Hedges et al. 2015). Then more recently, this portion broke off in the *Caenorhabditis* lineage. This interpretation parsimoniously explains the long-standing conundrum that Chromosome V in *C. elegans* has unusual chromosome "arm-like" characteristics, including relatively high recombination rates and a low density of conserved genes (Barnes et al. 1995; The *C. elegans* Sequencing Consortium 1998; Parkinson et al. 2004). In essence, it looks like a chromosome arm because it is, or more precisely, was, prior to breaking off. If true, the remarkable stability of histone mark patterns suggests that chromatin organization per se could serve as a molecular fossil of past genomic rearrangements. Perhaps probing chromatin structure in conjunction with recombination rates could provide a historical record of genome evolution in other nematodes and organisms.

Methods

Evolutionary gene classification

Nematode phylogenies were schematically drawn using data downloaded and analyzed from Holterman et al. (2017) and van

Megen et al. (2009). Evolutionary gene classes were defined in a tiered process. First, we defined conserved genes by BLASTP and TBLASTN analyses; we performed all pairwise searches of *P. pacificus* proteins as query against 24 nematode protein sets as target, and the proteins of each of the 24 nematodes as query against *P. pacificus* proteins as target. One BLASTP hit ($e < 10^{-3}$) in any of these 48 comparisons, or one TBLASTN hit ($e < 10^{-5}$) using *P. pacificus* proteins as query against any of the 24 nematode species genomes was enough to classify a gene in *P. pacificus* as conserved. Any gene that did not fit these criteria was defined as a *P. pacificus* "orphan gene." Within the conserved gene class, we then defined 1:1 orthologs as having the best reciprocal BLASTP hit ($e \leq 10^{-3}$) between *C. elegans* and *P. pacificus* (sorted by *e*-value, and raw scores were used to break ties). Conserved genes that were not in this 1:1 ortholog class but were previously identified by homology in at least one of the 24 nematodes species, were defined as "homologous genes." We kept the *e*-value cutoff relatively "high" because of the large phylogenetic distance between *C. elegans* and *P. pacificus*, and hence more conservative with respect to our orphan gene lists.

Nematode synchronization and collection

P. pacificus (PS312) cultures for ChIP-, ATAC-, and RNA-seq were synchronized with bleach and grown on agar to young adults following Werner et al. (2017) (Supplemental Methods). Worm pellets were flash-frozen until processing. For Iso-Seq, we used mixed-developmental stage (egg, J2, and J4/young adult) RNA at equimolar ratios.

Native histone ChIP-seq

Native (non-cross-linked) chromatin immunoprecipitation (ChIP) of histone post-translational modifications was performed by combining nematode nuclear isolation (Steiner et al. 2012) with native ChIP (Brand et al. 2008). Coprecipitated DNA was PCR-amplified and converted to Illumina libraries using the TruSeq Nano kit (Illumina) and sequenced on a HiSeq 3000. See Supplemental Methods for the detailed protocol.

ATAC-seq

Omni-ATAC-seq was performed on mixed-stage purified nuclei following the Corces et al. (2017) protocol, with a few modifications (Supplemental Methods) and sequenced on an Illumina HiSeq 3000.

Iso-Seq

RNA was extracted from different developmental time points separately using TRIzol Reagent (Invitrogen), then after the quality control, equal amounts of RNA from different time points were pooled. cDNA synthesis of "direct" Iso-Seq was performed directly using SMARTer PCR cDNA Synthesis Kit (Clontech Laboratories), and "total RNA" was first rRNA-depleted with Ribo-Zero rRNA Removal Kit (Human/Mouse/Rat) (Illumina), then in vitro polyadenylated with Poly(A) Polymerase (New England Biolabs). Direct and rRNA-depleted cDNA were converted into SMRTbell libraries following the guidelines provided by Pacific Biosciences. SMRT Link software version 4.0.0 (Pacific Biosciences) was used to convert subreads to circular consensus sequences and identify full-length nonchimeric reads, which were mapped to the El Paco genome using GMAP (Wu and Watanabe 2005). See Supplemental Methods for the detailed protocol.

RNA-seq

Whole-animal young adult (64–68 h post-bleaching) frozen pellets were freeze-thawed 3× in TRIzol Reagent (Invitrogen) before purification, converted to sequencing libraries with the NEBNext Ultra Directional RNA-seq for Illumina kit, and sequenced on a HiSeq 3000. See Supplemental Methods for the detailed protocol.

Bioinformatics

All sequencing data were mapped to the El Paco genome assembly (Rödelsperger et al. 2017) using GMAP (Wu and Watanabe 2005) for Iso-Seq, Bowtie 2 (Langmead and Salzberg 2012) for ChIP- and ATAC-seq, and HISAT2 (Kim et al. 2015) for RNA-seq. Peaks were obtained by MACS2 (Zhang et al. 2008), and only samples containing 50% overlap between replicates were kept. Overlapping peaks were merged using BEDTools (Supplemental Table S1; Quinlan and Hall 2010). Coverage plots were calculated using BEDTools or HOMER (Heinz et al. 2010) with merged replicate files, and plotted in R (R Core Team 2016). Chromatin states were obtained with ChromHMM (Ernst and Kellis 2012) using merged replicate input files. Distances to nearest promoter or enhancers were performed with BEDTools. See Supplemental Methods for the detailed procedure of all bioinformatic steps.

Data access

Raw and processed data sets from this study have been submitted to the European Nucleotide Archive (ENA; https://www.ebi.ac.uk/ena) under accession number PRJEB24584.

Acknowledgments

We thank current members of the Sommer laboratory and Dr. Talia Karasov for thoughtful critique of experiments, results, and interpretations. This study was funded by the Max Planck Society.

Author contributions: M.S.W. and R.J.S. conceived and designed all experiments. M.S.W. conducted ChIP- and ATAC-seq with assistance from T.L.; M.S.W, B.S., and C.L. performed Iso-Seq; N.P. conducted phylogenetic analysis and prepared evolutionary gene category data sets; M.S.W. performed all bioinformatic analysis. M.S.W. wrote the manuscript with assistance from R.J.S.

References

Abrusán G. 2013. Integration of new genes into cellular networks, and their structural maturation. *Genetics* **195:** 1407–1417.

Andersson R, Gebhard C, Miguel-Escalada I, Hoof I, Bornholdt J, Boyd M, Chen Y, Zhao X, Schmidl C, Suzuki T, et al. 2014. An atlas of active enhancers across human cell types and tissues. *Nature* **507:** 455–461.

Andersson R, Sandelin A, Danko CG. 2015. A unified architecture of transcriptional regulatory elements. *Trends Genet* **31:** 426–433.

Baralle FE, Giudice J. 2017. Alternative splicing as a regulator of development and tissue identity. *Nat Rev Mol Cell Biol* **18:** 437–451.

Barnes TM, Kohara Y, Coulson A, Hekimi S. 1995. Meiotic recombination, noncoding DNA and genomic organization in *Caenorhabditis elegans*. *Genetics* **141:** 159–179.

Baskaran P, Rödelsperger C. 2015. Microevolution of duplications and deletions and their impact on gene expression in the nematode *Pristionchus pacificus*. *PLoS One* **10:** e0131136.

Baskaran P, Rödelsperger C, Prabh N, Serobyan V, Markov GV, Hirsekorn A, Dieterich C. 2015. Ancient gene duplications have shaped developmental stage-specific expression in *Pristionchus pacificus*. *BMC Evol Biol* **15:** 185.

Bento G, Ogawa A, Sommer RJ. 2010. Co-option of the hormone-signalling module dafachronic acid–DAF-12 in nematode evolution. *Nature* **466:** 494–497.

Betrán E, Long M. 2003. *Dntf-2r*, a young Drosophila retroposed gene with specific male expression under positive Darwinian selection. *Genetics* **164:** 977–988.
Brand M, Rampalli S, Chaturvedi CP, Dilworth FJ. 2008. Analysis of epigenetic modifications of chromatin at specific gene loci by native chromatin immunoprecipitation of nucleosomes isolated using hydroxyapatite chromatography. *Nat Protoc* **3:** 398–409.
Buenrostro JD, Giresi PG, Zaba LC, Chang HY, Greenleaf WJ. 2013. Transposition of native chromatin for fast and sensitive epigenomic profiling of open chromatin, DNA-binding proteins and nucleosome position. *Nat Methods* **10:** 1213–1218.
Burki F, Kaessmann H. 2004. Birth and adaptive evolution of a hominoid gene that supports high neurotransmitter flux. *Nat Genet* **36:** 1061–1063.
The *C. elegans* Sequencing Consortium. 1998. Genome sequence of the nematode *C. elegans*: a platform for investigating biology. *Science* **282:** 2012–2018.
Cai J, Zhao R, Jiang H, Wang W. 2008. *De novo* origination of a new protein-coding gene in *Saccharomyces cerevisiae*. *Genetics* **179:** 487–496.
Carelli FN, Hayakawa T, Go Y, Imai H, Warnefors M, Kaessmann H. 2016. The life history of retrocopies illuminates the evolution of new mammalian genes. *Genome Res* **26:** 301–314.
Carvunis AR, Rolland T, Wapinski I, Calderwood MA, Yildirim MA, Simonis N, Charloteaux B, Hidalgo CA, Barbette J, Santhanam B, et al. 2012. Proto-genes and *de novo* gene birth. *Nature* **487:** 370.
Chen S, Zhang YE, Long M. 2010. New genes in *Drosophila* quickly become essential. *Science* **330:** 1682–1685.
Chen S, Ni X, Krinsky BH, Zhang YE, Vibranovski MD, White KP, Long M. 2012a. Reshaping of global gene expression networks and sex-biased gene expression by integration of a young gene. *EMBO J* **31:** 2798–2809.
Chen S, Spletter M, Ni X, White KP, Luo L, Long M. 2012b. Frequent recent origination of brain genes shaped the evolution of foraging behavior in *Drosophila*. *Cell Rep* **1:** 118–132.
Chen RA, Down TA, Stempor P, Chen QB, Egelhofer TA, Hillier LW, Jeffers TE, Ahringer J. 2013a. The landscape of RNA polymerase II transcription initiation in *C. elegans* reveals promoter and enhancer architectures. *Genome Res* **23:** 1339–1347.
Chen S, Krinsky BH, Long M. 2013b. New genes as drivers of phenotypic evolution. *Nat Rev Genet* **14:** 645–660.
Coghlan A. 2005. Nematode genome evolution. In *WormBook* (ed. The *C. elegans* Research Community). doi: 10.1895/wormbook.1.15.1, http://www.wormbook.org.
Conesa A, Madrigal P, Tarazona S, Gomez-Cabrero D, Cervera A, McPherson A, Szcześniak MW, Gaffney DJ, Elo LL, Zhang X, et al. 2016. A survey of best practices for RNA-seq data analysis. *Genome Biol* **17:** 13.
Corces MR, Trevino AE, Hamilton EG, Greenside PG, Sinnott-Armstrong NA, Vesuna S, Satpathy AT, Rubin AJ, Montine KS, Wu B, et al. 2017. An improved ATAC-seq protocol reduces background and enables interrogation of frozen tissues. *Nat Methods* **14:** 959–962.
Cutter AD. 2008. Divergence times in *Caenorhabditis* and *Drosophila* inferred from direct estimates of the neutral mutation rate. *Mol Biol Evol* **25:** 778–786.
Derrien T, Johnson R, Bussotti G, Tanzer A, Djebali S, Tilgner H, Guernec G, Martin D, Merkel A, Knowles DG, et al. 2012. The GENCODE v7 catalog of human long noncoding RNAs: analysis of their gene structure, evolution, and expression. *Genome Res* **22:** 1775–1789.
Deutsch M, Long M. 1999. Intron–exon structures of eukaryotic model organisms. *Nucleic Acids Res* **27:** 3219–3228.
Dieterich C, Clifton SW, Schuster LN, Chinwalla A, Delehaunty K, Dinkelacker I, Fulton L, Fulton R, Godfrey J, Minx P, et al. 2008. The *Pristionchus pacificus* genome provides a unique perspective on nematode lifestyle and parasitism. *Nat Genet* **40:** 1193–1198.
Engreitz JM, Haines JE, Perez EM, Munson G, Chen J, Kane M, McDonel PE, Guttman M, Lander ES. 2016. Local regulation of gene expression by lncRNA promoters, transcription and splicing. *Nature* **539:** 452–455.
Ernst J, Kellis M. 2012. ChromHMM: automating chromatin-state discovery and characterization. *Nat Methods* **9:** 215–216.
Ernst J, Kheradpour P, Mikkelsen TS, Shoresh N, Ward LD, Epstein CB, Zhang X, Wang L, Issner R, Coyne M, et al. 2011. Mapping and analysis of chromatin state dynamics in nine human cell types. *Nature* **473:** 43–49.
Geiler-Samerotte KA, Dion MF, Budnik BA, Wang SM, Hartl DL, Drummond DA. 2011. Misfolded proteins impose a dosage-dependent fitness cost and trigger a cytosolic unfolded protein response in yeast. *Proc Natl Acad Sci* **108:** 680–685.
Grzechnik P, Tan-Wong SM, Proudfoot NJ. 2014. Terminate and make a loop: regulation of transcriptional directionality. *Trends Biochem Sci* **39:** 319–327.
Hattori T, Taft JM, Swist KM, Luo H, Witt H, Slattery M, Koide A, Ruthenburg AJ, Krajewski K, Strahl BD, et al. 2013. Recombinant antibodies to histone post-translational modifications. *Nat Methods* **10:** 992–995.
Hedges SB, Marin J, Suleski M, Paymer M, Kumar S. 2015. Tree of life reveals clock-like speciation and diversification. *Mol Biol Evol* **32:** 835–845.
Heinz S, Benner C, Spann N, Bertolino E, Lin YC, Laslo P, Cheng JX, Murre C, Singh H, Glass CK. 2010. Simple combinations of lineage-determining transcription factors prime *cis*-regulatory elements required for macrophage and B cell identities. *Mol Cell* **38:** 576–589.
Holterman M, Karegar A, Mooijman P, van Megen H, van den Elsen S, Vervoort MTW, Quist CW, Karssen G, Decraemer W, Opperman CH, et al. 2017. Disparate gain and loss of parasitic abilities among nematode lineages. *PLoS One* **12:** e0185445.
Jalali S, Gandhi S, Scaria V. 2016. Navigating the dynamic landscape of long noncoding RNA and protein-coding gene annotations in GENCODE. *Hum Genomics* **10:** 35.
Kaessmann H. 2010. Origins, evolution, and phenotypic impact of new genes. *Genome Res* **20:** 1313–1326.
Kaessmann H, Vinckenbosch N, Long M. 2009. RNA-based gene duplication: mechanistic and evolutionary insights. *Nat Rev Genet* **10:** 19–31.
Khalturin K, Hemmrich G, Fraune S, Augustin R, Bosch TC. 2009. More than just orphans: Are taxonomically-restricted genes important in evolution? *Trends Genet* **25:** 404–413.
Kieninger MR, Ivers NA, Rödelsperger C, Markov GV, Sommer RJ, Ragsdale EJ. 2016. The nuclear hormone receptor NHR-40 acts downstream of the sulfatase EUD-1 as part of a developmental plasticity switch in *Pristionchus*. *Curr Biol* **26:** 2174–2179.
Kim TK, Shiekhattar R. 2015. Architectural and functional commonalities between enhancers and promoters. *Cell* **162:** 948–959.
Kim D, Langmead B, Salzberg SL. 2015. HISAT: a fast spliced aligner with low memory requirements. *Nat Methods* **12:** 357–360.
Koch C, Moll T, Neuberg M, Ahorn H, Nasmyth K. 1993. A role for the transcription factors Mbp1 and Swi4 in progression from G1 to S phase. *Science* **261:** 1551–1557.
Lainé JP, Singh BN, Krishnamurthy S, Hampsey M. 2009. A physiological role for gene loops in yeast. *Genes Dev* **23:** 2604–2609.
Lam MT, Li W, Rosenfeld MG, Glass CK. 2014. Enhancer RNAs and regulated transcriptional programs. *Trends Biochem Sci* **39:** 170–182.
Langmead B, Salzberg SL. 2012. Fast gapped-read alignment with Bowtie 2. *Nat Methods* **9:** 357–359.
Lee TI, Young RA. 2013. Transcriptional regulation and its misregulation in disease. *Cell* **152:** 1237–1251.
Li L, Foster CM, Gan Q, Nettleton D, James MG, Myers AM, Wurtele ES. 2009. Identification of the novel protein QQS as a component of the starch metabolic network in Arabidopsis leaves. *Plant J* **58:** 485–498.
Li ZW, Chen X, Wu Q, Hagmann J, Han TS, Zou YP, Ge S, Guo YL. 2016. On the origin of de novo genes in *Arabidopsis thaliana* populations. *Genome Biol Evol* **8:** 2190–2202.
Liu T, Rechtsteiner A, Egelhofer TA, Vielle A, Latorre I, Cheung M-S, Ercan S, Ikegami K, Jensen M, Kolasinska-Zwierz P, et al. 2011. Broad chromosomal domains of histone modification patterns in *C. elegans*. *Genome Res* **21:** 227–236.
Long M, VanKuren NW, Chen S, Vibranovski MD. 2013. New gene evolution: Little did we know. *Annu Rev Genet* **47:** 307–333.
Mayer MG, Rödelsperger C, Witte H, Riebesell M, Sommer RJ. 2015. The orphan gene *dauerless* regulates dauer development and intraspecific competition in nematodes by copy number variation. *PLoS Genet* **11:** e1005146.
McLysaght A, Hurst LD. 2016. Open questions in the study of *de novo* genes: what, how and why. *Nat Rev Genet* **17:** 567–578.
Neme R, Tautz D. 2013. Phylogenetic patterns of emergence of new genes support a model of frequent *de novo* evolution. *BMC Genomics* **14:** 117.
Ni X, Zhang YE, Nègre N, Chen S, Long M, White KP. 2012. Adaptive evolution and the birth of CTCF binding sites in the *Drosophila* genome. *PLoS Biol* **10:** e1001420.
Nishikori S, Hattori T, Fuchs SM, Yasui N, Wojcik J, Koide A, Strahl BD, Koide S. 2012. Broad ranges of affinity and specificity of anti-histone antibodies revealed by a quantitative peptide immunoprecipitation assay. *J Mol Biol* **424:** 391–399.
O'Sullivan JM, Tan-Wong SM, Morillon A, Lee B, Coles J, Mellor J, Proudfoot NJ. 2004. Gene loops juxtapose promoters and terminators in yeast. *Nat Genet* **36:** 1014–1018.
Parkinson J, Mitreva M, Whitton C, Thomson M, Daub J, Martin J, Schmid R, Hall N, Barrell B, Waterston RH, et al. 2004. A transcriptomic analysis of the phylum Nematoda. *Nat Genet* **36:** 1259–1267.
Pertea M, Kim D, Pertea GM, Leek JT, Salzberg SL. 2016. Transcript-level expression analysis of RNA-seq experiments with HISAT, StringTie and Ballgown. *Nat Protoc* **11:** 1650–1667.
Pickrell JK, Pai AA, Gilad Y, Pritchard JK. 2010. Noisy splicing drives mRNA isoform diversity in human cells. *PLoS Genet* **6:** e1001236.
Prabh N, Rödelsperger C. 2016. Are orphan genes protein-coding, prediction artifacts, or non-coding RNAs? *BMC Bioinformatics* **17:** 226.
Proudfoot NJ. 2011. Ending the message: poly(A) signals then and now. *Genes Dev* **25:** 1770–1782.

Proudfoot NJ, Furger A, Dye MJ. 2002. Integrating mRNA processing with transcription. *Cell* **108:** 501–512.
Quinlan AR, Hall IM. 2010. BEDTools: a flexible suite of utilities for comparing genomic features. *Bioinformatics* **26:** 841–842.
R Core Team. 2016. *R: a language and environment for statistical computing*. R Foundation for Statistical Computing, Vienna, Austria. https://www.R-project.org/.
Rada-Iglesias A, Bajpai R, Swigut T, Brugmann SA, Flynn RA, Wysocka J. 2011. A unique chromatin signature uncovers early developmental enhancers in humans. *Nature* **470:** 279–283.
Ragsdale EJ, Müller MR, Rödelsperger C, Sommer RJ. 2013. A developmental switch coupled to the evolution of plasticity acts through a sulfatase. *Cell* **155:** 922–933.
Ramani AK, Calarco JA, Pan Q, Mavandadi S, Wang Y, Nelson AC, Lee LJ, Morris Q, Blencowe BJ, Zhen M, et al. 2011. Genome-wide analysis of alternative splicing in *Caenorhabditis elegans*. *Genome Res* **21:** 342–348.
Reinhardt JA, Wanjiru BM, Brant AT, Saelao P, Begun DJ, Jones CD. 2013. *De novo* ORFs in Drosophila are important to organismal fitness and evolved rapidly from previously non-coding sequences. *PLoS Genet* **9:** e1003860.
Roadmap Epigenomics Consortium, Kundaje A, Meuleman W, Ernst J, Bilenky M, Yen A, Heravi-Moussavi A, Kheradpour P, Zhang Z, Wang J, et al. 2015. Integrative analysis of 111 reference human epigenomes. *Nature* **518:** 317–330.
Rödelsperger C, Meyer JM, Prabh N, Lanz C, Bemm F, Sommer RJ. 2017. Single-molecule sequencing reveals the chromosome-scale genomic architecture of the nematode model organism *Pristionchus pacificus*. *Cell Rep* **21:** 834–844.
Rosso L, Marques AC, Weier M, Lambert N, Lambot MA, Vanderhaeghen P, Kaessmann H. 2008. Birth and rapid subcellular adaptation of a hominoid-specific CDC14 protein. *PLoS Biol* **6:** e140.
Rota-Stabelli O, Daley AC, Pisani D. 2013. Molecular timetrees reveal a Cambrian colonization of land and a new scenario for ecdysozoan evolution. *Curr Biol* **23:** 392–398.
Ruiz-Orera J, Hernandez-Rodriguez J, Chiva C, Sabidó E, Kondova I, Bontrop R, Marqués-Bonet T, Albà MM. 2015. Origins of *de novo* genes in human and chimpanzee. *PLoS Genet* **11:** e1005721.
Santos ME, Le Bouquin A, Crumière AJJ, Khila A. 2017. Taxon-restricted genes at the origin of a novel trait allowing access to a new environment. *Science* **358:** 386–390.
Schlackow M, Nojima T, Gomes T, Dhir A, Carmo-Fonseca M, Proudfoot NJ. 2017. Distinctive patterns of transcription and RNA processing for human lincRNAs. *Mol Cell* **65:** 25–38.
Serobyan V, Xiao H, Namdeo S, Rödelsperger C, Sieriebriennikov B, Witte H, Röseler W, Sommer RJ. 2016. Chromatin remodelling and antisense-mediated up-regulation of the developmental switch gene *eud-1* control predatory feeding plasticity. *Nat Commun* **7:** 12337.
Silveira AB, Trontin C, Cortijo S, Barau J, Del Bem LE, Loudet O, Colot V, Vincentz M. 2013. Extensive natural epigenetic variation at a *de novo* originated gene. *PLoS Genet* **9:** e1003437.
Sinha A, Sommer RJ, Dieterich C. 2012. Divergent gene expression in the conserved dauer stage of the nematodes *Pristionchus pacificus* and *Caenorhabditis elegans*. *BMC Genomics* **13:** 254.
Sommer RJ, McGaughran A. 2013. The nematode *Pristionchus pacificus* as a model system for integrative studies in evolutionary biology. *Mol Ecol* **22:** 2380–2393.
Sommer RJ, Streit A. 2011. Comparative genetics and genomics of nematodes: genome structure, development, and lifestyle. *Ann Rev Genet* **45:** 1–20.
Stein JC, Yu Y, Copetti D, Zwickl DJ, Zhang L, Zhang C, Chougule K, Gao D, Iwata A, Goicoechea JL, et al. 2018. Genomes of 13 domesticated and wild rice relatives highlight genetic conservation, turnover and innovation across the genus *Oryza*. *Nat Genet* **50:** 285–296.
Steiner FA, Talbert PB, Kasinathan S, Deal RB, Henikoff S. 2012. Cell-type-specific nuclei purification from whole animals for genome-wide expression and chromatin profiling. *Genome Res* **22:** 766–777.
Tautz D, Domazet-Lošo T. 2011. The evolutionary origin of orphan genes. *Nat Rev Genet* **12:** 692–702.
Trojer P, Reinberg D. 2007. Facultative heterochromatin: Is there a distinctive molecular signature? *Mol Cell* **28:** 1–13.
van Megen H, van den Elsen S, Holterman M, Karssen G, Mooyman P, Bongers T, Holovachov O, Bakker J, Helder J. 2009. A phylogenetic tree of nematodes based on about 1200 full-length small subunit ribosomal DNA sequences. *Nematology* **11:** 927–950.
Vinckenbosch N, Dupanloup I, Kaessmann H. 2006. Evolutionary fate of retroposed gene copies in the human genome. *Proc Natl Acad Sci* **103:** 3220–3225.
Voss TC, Hager GL. 2014. Dynamic regulation of transcriptional states by chromatin and transcription factors. *Nat Rev Genet* **15:** 69–81.
Wang J, Lunyak VV, Jordan IK. 2013. BroadPeak: a novel algorithm for identifying broad peaks in diffuse ChIP-seq datasets. *Bioinformatics* **29:** 492–493.
Wasylyk B. 1988. Enhancers and transcription factors in the control of gene expression. *Biochim Biophys Acta* **951:** 17–35.
Werner MS, Sullivan MA, Shah RN, Nadadur RD, Grzybowski AT, Galat V, Moskowitz IP, Ruthenburg AJ. 2017. Chromatin-enriched lncRNAs can act as cell-type specific activators of proximal gene transcription. *Nat Struct Mol Biol* **24:** 596–603.
Witte H, Moreno E, Rödelsperger C, Kim J, Kim JS, Streit A, Sommer RJ. 2015. Gene inactivation using the CRISPR/Cas9 system in the nematode *Pristionchus pacificus*. *Dev Genes Evol* **225:** 55–62.
Wu TD, Watanabe CK. 2005. GMAP: a genomic mapping and alignment program for mRNA and EST sequences. *Bioinformatics* **21:** 1859–1875.
Yi B, Sommer RJ. 2007. The *pax-3* gene is involved in vulva formation in *Pristionchus pacificus* and is a target of the Hox gene *lin-39*. *Development* **134:** 3111–3119.
Zhang Y, Liu T, Meyer CA, Eeckhoute J, Johnson DS, Bernstein BE, Nusbaum C, Myers RM, Brown M, Li W, et al. 2008. Model-based Analysis of ChIP-Seq (MACS). *Genome Biol* **9:** R137.

Received January 24, 2018; accepted in revised form September 5, 2018.

Young genes have distinct gene structure, epigenetic profiles, and transcriptional regulation

Michael S. Werner, Bogdan Sieriebriennikov, Neel Prabh, et al.

Genome Res. 2018 28: 1675-1687 originally published online September 19, 2018
Access the most recent version at doi:10.1101/gr.234872.118

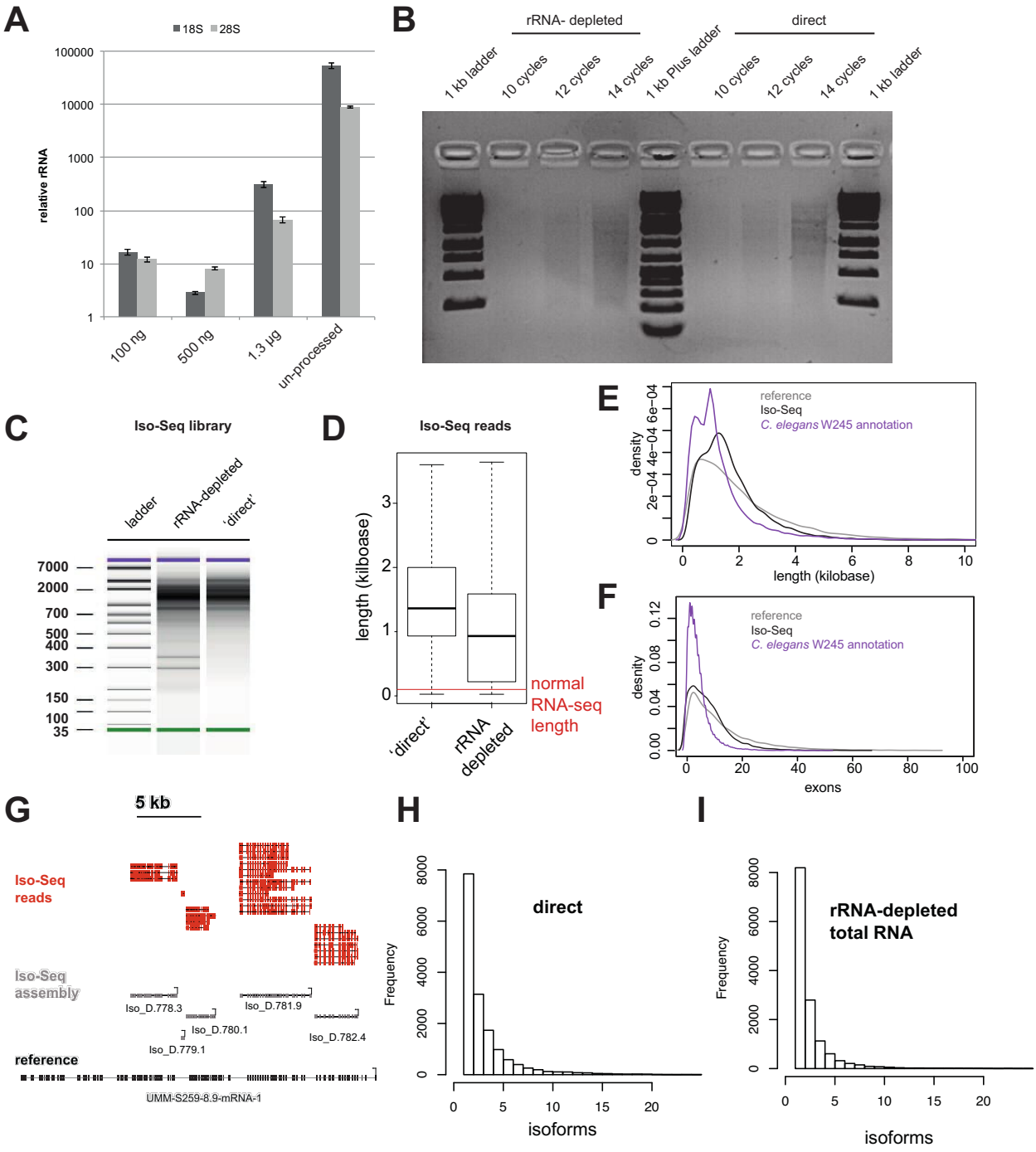

Supplemental Figure S1. Iso-seq methodology and quality control. (*A*) qPCR of rRNA (18 and 28S) from rRNA-depleted or un-processed cDNA, normalized to *Ppa-cdc-42*. Y-axis is the ratio of $2^{\Delta Ct}$ in log10-scale, and error bars represent the propagated standard deviation of four technical replicates. Based on this analysis, 500 ng of RNA input was used for Iso-seq rRNA-depletion with the Ribo-Zero rRNA removal kit (Human/Mouse/Rat) (Illumina), which yielded a 1,105-fold decrease in 28S and 19,383-fold decrease in 18S rRNA. (*B*) Agarose gel of Iso-seq library with indicated number of cycles, which was used to determine the appropriate cycle number without over-amplification (12 cycles). (*C*) Bioanalyzer trace of Iso-seq libraries showing size distribution (bp). (*D*) Actual read-length distribution of Iso-seq sequences (kb). Red line indicates standard RNA-seq read length of 0.1 kb. (*E*) Density distribution of gene length, and (*F*) exon number for *P. pacificus* reference (El Paco), Iso-seq 'direct', and *C. elegans* Ref-seq gene annotations, produced in R using the density function. (*G*) Example locus comparing the direct Iso-seq annotation that includes five genes, to the reference annotation that has one long gene, and accompanying Iso-seq reads. (*H*) Frequency distribution of isoform number from direct and total Iso-seq. Isoform annotations determined from Stringtie assembly.

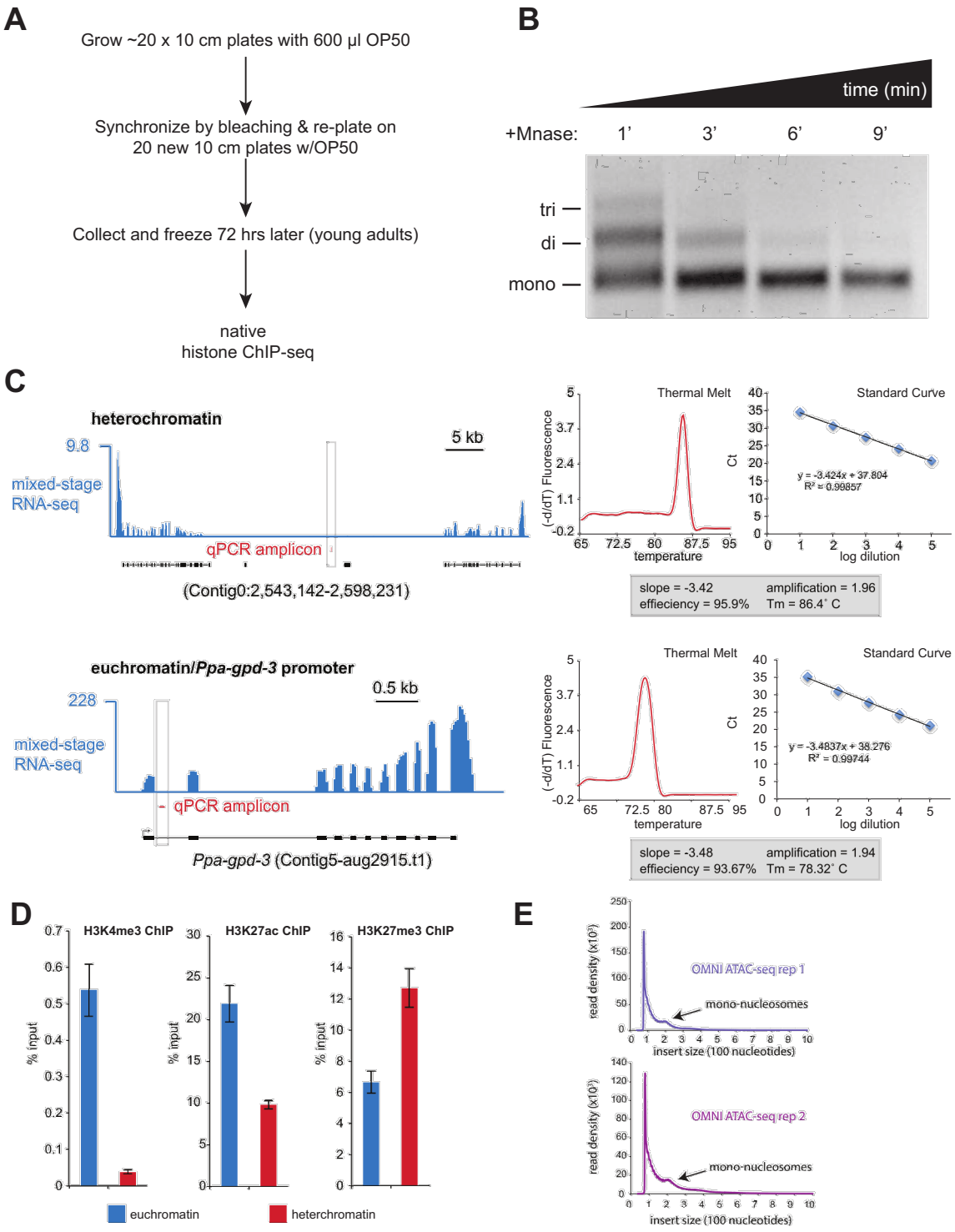

Supplemental Figure S2. ChIP and ATAC-seq methodology and quality control. (*A*) Strategy for biological sample collection and processing. (*B*) Mnase digestion of purified native nuclei results in time-dependent nucleosome fragmentation. Shown is an agarose gel of purified DNA incubated at 37° C for the indicated times with MNase (NEB). We chose 5 min. for subsequent chromatin fragmentation. (*C*) Genomic loci of qPCR Primers (Supplemental Table S3) used for verifying ChIP-seq specificity. The heterochromatin pair was designed in a gene 'desert' devoid of RNA-seq expression, and the euchromatin primer pair was designed near the *Ppa-gpd-3/gapdh* promoter. Also shown are thermal melts and a 5-log titration to demonstrate primer specificity, assessed on a LightCycler 480 (Roche). RNA-seq reads and coordinates apply to the Hybrid 1 Genome (http://pristionchus.org/download/), and genes correspond to the Augustus 2013 annotation. (*D*) ChIP-qPCR with indicated antibodies shows specificity of histone marks for euchromatin (H3K4me3, H3K27ac) and heterochromatin (H3K27me3) enrichment. Data is presented as percent input ($100x2^{\Delta Ct}$). (*E*) Sequencing read density of OMNI ATAC by size for two replicates. Reads less than 100 nucleoties are considered sub-nucleosomal integration events (Buenrostro et al., 2013).

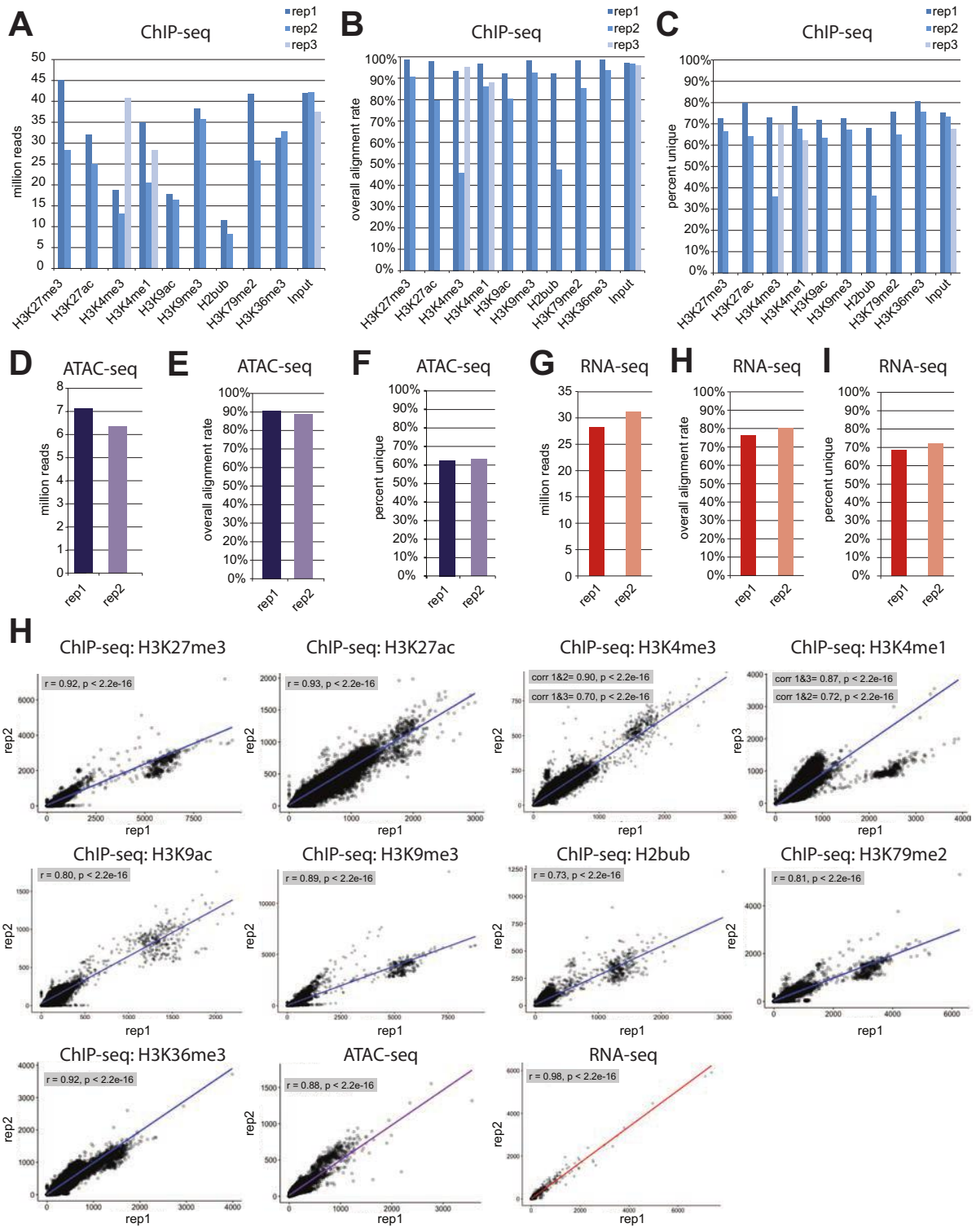

Supplemental Figure S3. ChIP-, ATAC-, and RNA-sequencing quality control. (*A*) Sequencing depth (millions of reads) for ChIP-seq biological replicates for each antibody. (*B*) Overall alignment, and (*C*) percent unique reads for each ChIP-seq sample. Note H3K4me1 and H3K4me3 have three replicates, while the other samples have two. (*D-I*) Similar to (*A-C*) but for ATAC-seq and RNA-seq replicates. Alignments and read mapping statistics were obtained with Bowtie2 (Langmead B, Salzberg S., 2012) for ChIP and ATAC-seq, and HISAT2 (Kim et al., 2015) for RNA-seq. (*H*) Pearson correlations of biological replicate coverage for each data set across 600 bp sliding windows, coverage calculated using 'genomecov' in Bedtools and pearson correlations calculated and plotted in R.

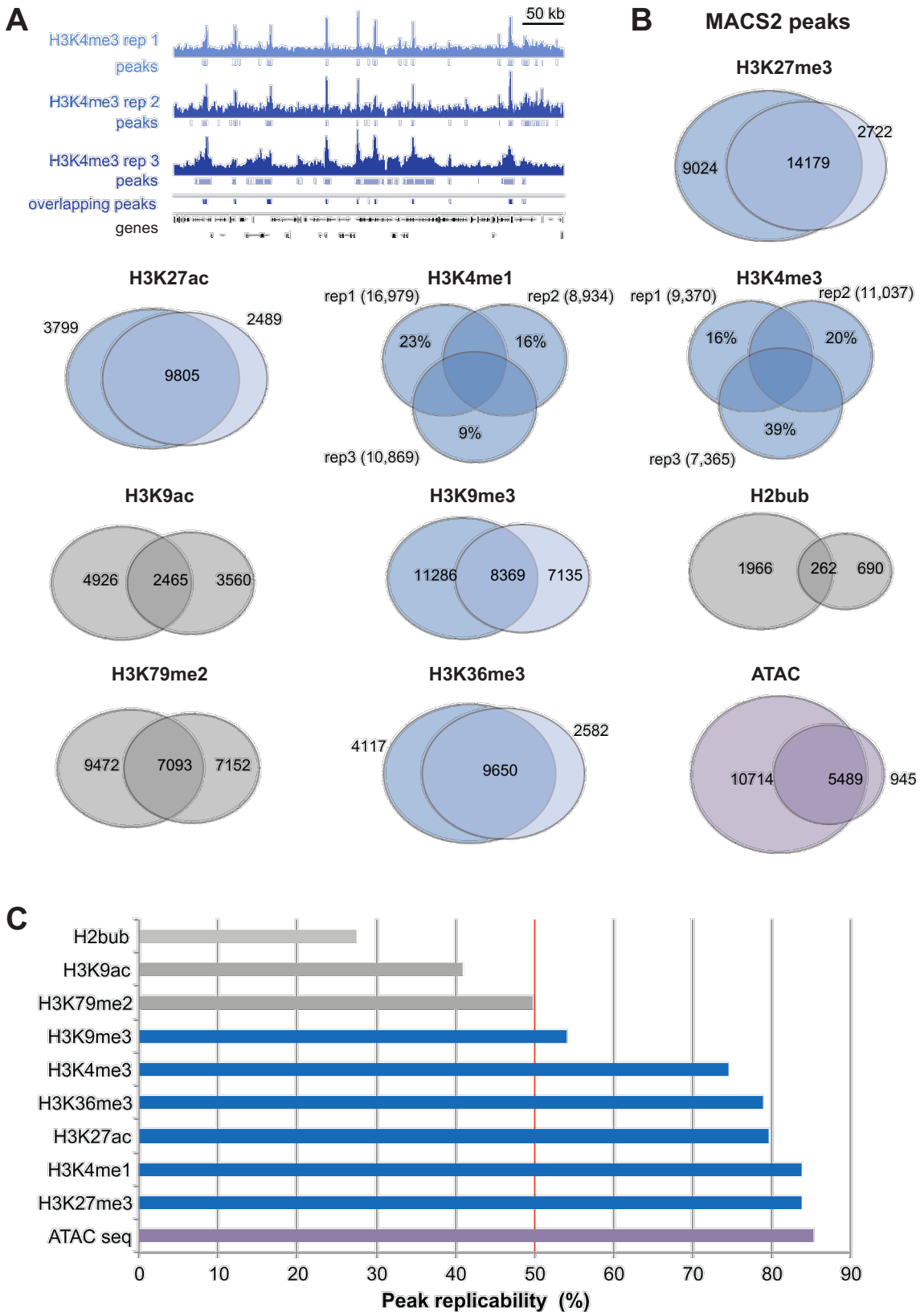

Supplemental Figure S4. ChIP-, ATAC-, and RNA-seq peak overlaps between replicates. (*A*) Ex. of H3K4me3 replicate coverage over a defined interval in Integrated Genome Viewer (IGV). (*B*) Overlap of MACS2 peaks between biological replicates of ChIP-, ATAC-, and RNA-seq. Venn diagrams produced in R. Only peaks detected in both data sets are reported in Supplemental Table S1. Peak replicability = percent overlap of merged overlapping peaks relative to the smaller data set for samples with two replicates, or average overlap with at least one other replicate for samples with three repliclicates. H2bub, H3K9ac, and H3K79me2 fall below a 50% threshold, and were excluded from further analysis.

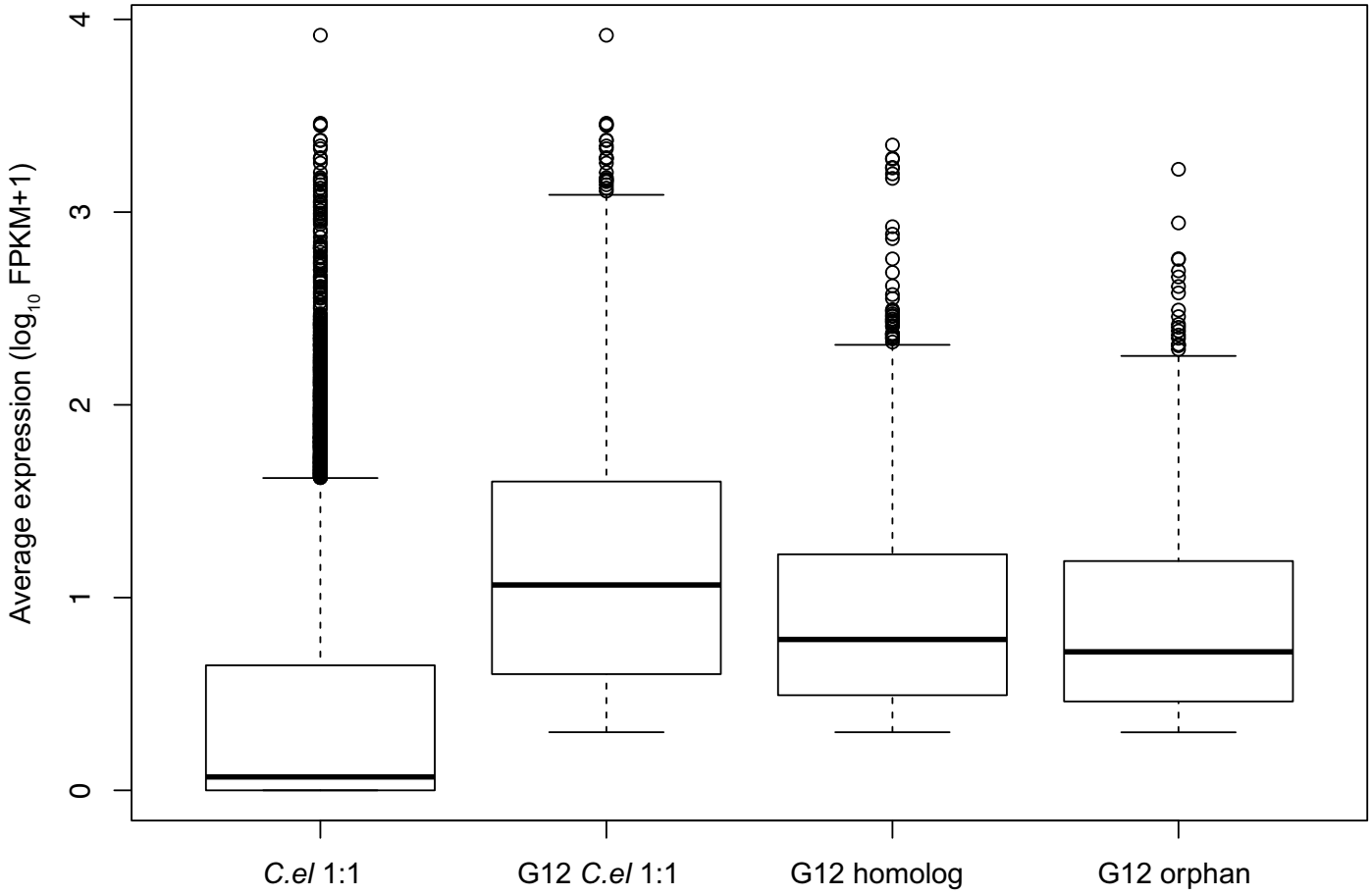

Supplemental Figure S5. Expression of group 1 and 2 genes are similar between different evolutionary gene classes, and higher than overall C. elegans 1:1 orthologs. Average FPKM of genes within group 1 and 2 for each evolutionary gene category. Importantly, genes in orphan and homolog groups 1 and 2 are higher than overall *C. elegans* 1:1 orthologs, despite a substantial difference in chromatin states, and overall *C. elegans* 1:1 orthologs exhibit similar chromatin state patterns to group 1 and 2 *C. elegans* 1:1 orthologs (Fig. 4C,G).

Supplemental Methods

Young genes have distinct gene structure, epigenetic profiles, and transcriptional regulation

Michael S. Werner[1], Bogdan Sieriebriennikov[1], Neel Prabh[1], Tobias Loschko[1], Christa Lanz[1] and Ralf J. Sommer[1]

Nematode synchronization and growth for ChIP-, ATAC-, and RNA-seq

P. pacificus were grown for three healthy generations on OP50 bacteria. Then, to increase homozygosity, a single worm was passaged to 10 x 10 cm plates. After 5 days, 15-20 worms were split to 100 x 10 cm plates spotted with 700 µl OP50 and grown 5-6 days (at 7 days the presence of too many late stage J1s that are still resistant to bleach prevents consistent synchronization). Worms were washed with water into 50 ml conical tubes, and bleach-treated (10 minutes, 30% NaOH/bleach)(Stiernagle 2006) to isolate eggs and J1 larva. Eggs-J1 were then filtered through a 140 µM nylon net (Millipore) to remove carcasses, then centrifuged 500 x g, 1 minute to pellet. The pellet was washed by removing supernatant with a pipette and re-suspending in 3 ml M9, then re-centrifuged 500 x g, 30-60 seconds. Supernatant was removed, and the egg-J1 pellet was re-suspended in 100 µl M9 buffer x the number of plates grown (i.e. 20 ml for 200 plates). Eggs-J1 were added drop-wise to new 10 cm agar plates (100 µl each) spotted with 700 µl OP50 and grown to young adults (approximately 64 hours).

ChIP-seq

Most antibodies used conformed to the ChIP-Seq guidelines outlined by ENCODE/modENCODE (Landt et al. 2012). Specifically, we applied three levels of quality control: (1) immunoblot specificity (primary evidence) from previous work in the lab (Serobyan et al. 2016) or the manufacturer (Diagenode or abcam), except for H3K9ac and H3K36me3, (2) expected annotation enrichment (i.e. H3K4me3/H3K27ac overlap with each other and at promoters), and (3) independent biological replication of each antibody (see below). Note, ChIP with H4K20me1 and H2AZ.2 antibodies did not successfully co-precipitate sufficient DNA for library preparation (Supplemental Fig. 2F). A list of antibodies used is provided in Supplemental Table 3. Two to three independent biological replicates of native ChIP-seq of histone modifications in *P. pacificus* were performed by a combination of native ChIP (Brand et al. 2008) with nematode nuclear isolation (Steiner et al. 2012), with the exception that we did not observe

an increase in specificity with hydroxyapatite purification, and therefore this step was not used. We first disrupted the worm cuticle using liquid nitrogen and mortar and pestle adapted from Steiner et al., 2012, followed by resuspension in 10 ml nuclei purification buffer (NPB: 10 mM Tris at pH 7.5, 40 ml NaCl, 90 mM KCl, 2 mM EDTA, 0.5 mM EGTA, 0.2 mM DTT, 0.5 mM PMSF, 0.5 mM spermidine, 0.25 mM spermine, 0.1% Triton X-100). Cells were lysed by applying 30-50 strokes of dounce-homoginization, then cell and cuticle debris were removed by slow centrifugation (100 x g, 2 minutes, room temperature). Nuclei in the supernatant were purified over a 7.5 ml sucrose cushion (10 mM Hepes, pH 7.5, 30 % w/v sucrose, 1.5 mM $MgCl_2$) for 12 minutes, 4° C, 1,300 x g. Then the sucrose cushion was removed by pipette, and nuclei were washed by resuspension in 1 ml NPB and centrifuged 10 minutes, 4° C, 1,300 x g. Nuclei concentration was assessed by A260 nanodrop absorption of a 1:10 dilution in NBP, then 1M $CaCl_2$ was added to 5 mM final concentration and incubated 37° C for 5 minutes to 'warm up' the sample, and then 0.015 µl MNase (NEB)/µg chromatin was added and incubated 37° C for six minutes to digest chromatin to predominately mono-nucleosomes (Supplemental Fig. S2B). Then 100 mM EGTA was added to 20 mM final concentration to stop the reaction, and 5 M NaCl was added drop-wise to 400 mM final concentration while vortexing on the lowest setting. Then nuclei were incubated 30 minutes 4° C with rotation to extract nucleosomes from nuclei, and centrifuged max speed, 4° C, 5 minutes to pellet nuclear debris. Resulting mono and di-nucleosomes in the supernatant were re-quantified by nanodrop, and diluted to 10-20 ng/µl in ChIP Buffer 1 (25 mM Tris pH 7.5, 5 mM $MgCl_2$, 100 mM KCl, 10% glycerol, 0.1% NP-40, 100 µM PMSF, 50 µg/ml BSA), and immunoprecipitated with histone modification-specific antibodies conjugated to 20 µl para-magnetic Dynabeads (Invitrogen) for 10 minutes. 2.5 µg of chromatin (~250-500 µl) was used as input per IP which is a typical amount from 20 x 10 cm plates, and 5 µg Ab were conjugated to 20 µl beads before hand per IP. Washing of IPs was performed for 1 minute with rotation at 4° C, followed by 1 minute magnetic separation, including three tube changes with the following buffers: 2x with 600 µl ChIP Buffer 2 (25 mM Tris pH 7.5, 5 mM

$MgCl_2$, 300 mM KCl, 10% glycerol, 0.1% NP-40, 100 µM PMSF, 50 µg/ml BSA), 1x with ChIP Buffer 3 (10 mM Tris pH 7.5, 250 mM LiCl, 1 mM EDTA, 0.5% Na-Deoxycholate, 0.5% NP-40, 100 µM PMSF, 50 µg/ml BSA), 1x with ChIP Buffer 1, and 1x with TE buffer. Immunoprecipated nucleosomes were eluted in 50 µl elution buffer (50 mM Tris pH 7.5, 1 mM EDTA, 1% SDS) 55° C for 5 minutes. Supernatant was transferred to a new tube and purified by adding 2 µl of 5 M NaCl (200 mM final), 1 µl of 500 mM EDTA (10 mM final), and 1 µl of 20 mg/ml Proteinase K (0.4 mg/ml final) and incubating 55° C for 2 hours, followed by 3 volumes of Ampure XP bead addition and purification, and elution in 50 µl TE buffer. Recovered DNA was verified for specificity by qPCR (Supplemental Fig. S2D), and then converted to Illumina sequencing libraries using a TruSeq Nano kit, and sequenced on an Illumina HiSeq 3000.

Iso-Seq

In order to increase representation of stage- and condition-specific transcripts, RNA used for the Iso-Seq experiment was collected from worms of different ages and grown in two different culture conditions, which are known to influence multiple aspects of nematode physiology, such as body morphology and development of feeding structures(Werner et al. 2017). First, eggs were synchronized by bleaching (see above, Stiernagle 2016). After bleach-synchronization, eggs were hatched in one of the two following conditions. Half of the eggs were added to 10 cm agar plates with Nematode Growth Medium (NGM) spotted with 1 mL of overnight culture of Escherichia coli OP50. Another half were transferred to 25 mL conical flasks with 10 mL of S-medium that contained re-suspended bacteria in the amount corresponding to 100 mL of an overnight culture with OD600 of 0.5. Flasks with liquid cultures were incubated on a shaking platform at 180 rpm. Worms were collected from both solid and liquid cultures at three time points - 24 h, 55-60 h and 75 h. Samples collected at 24 h contained a mixture of J2 and J3 (early juvenile stages) and samples collected at 55-60 h contained a mixture of J4 (late juvenile stage) and young adults. At 75 h, the majority of animals were gravid adults. They were

bleached as described above to extract embryos and J1 (egg-bound juvenile stage). RNA was extracted from all samples separately using TRIzol Reagent (Invitrogen) including 3x freeze-thaw cycles, and chloroform, and RNA was purified from the aqueous phase using RNA Clean and Concentrator kit (Zymo Research). Extracted RNA was quantified using Nanodrop One C (Thermo Scientific) and quality was verified using capillary electrophoresis performed on Bioanalyzer 2100 in combination with RNA 6000 Nano Kit (Agilent Technologies). After the quality control step, equal amounts of RNA from different time points were pooled. Two separate pools were made for worms grown on agar plates and in the liquid medium. 1 ug of RNA was taken from each pool and first-strand cDNA synthesis was performed using SMARTer PCR cDNA Synthesis Kit (Clontech Laboratories). These cDNA samples were labelled as "direct" and presumably only contained cDNA reverse-transcribed from polyadenylated transcripts. Another 4 ug of RNA was taken from each pool and split into "rRNA-depleted" and "control" samples. The "rRNA-depleted" samples were purified from ribosomal RNA (rRNA) using Ribo-Zero rRNA Removal Kit (Human/Mouse/Rat) (Illumina) and both samples were *in vitro* polyadenylated using E. coli Poly(A) Polymerase (New England Biolabs) to enrich the polyA RNA profile for transcripts that are not, or under-polyadenylated *in vivo*. cDNA synthesis was performed as described above, and the efficiency of rRNA depletion was verified by comparing relative abundances of rRNA in the "rRNA-depleted" and the "control" samples using real-time quantitative PCR (qPCR)(Supplemental Fig. S1A). Primers targeted 18S rRNA, 28S rRNA and a reference gene *Ppa-cdc-42*(Schuster and Sommer 2012), and qPCR was performed on a LightCycler 480 Instrument using LightCycler 480 SYBR Green I Master (Roche). "Direct" and "rRNA-depleted" cDNA was further converted into SMRTbell libraries following the guidelines provided by Pacific Biosciences. In short, cDNA was amplified by PCR using PrimeSTAR GXL Polymerase (Clontech Laboratories). Optimal number of cycles (12 cycles) was identified based on band intensity and size distribution of amplification products run on a 1% agarose gel (Supplemental Fig. S1B). Amplified cDNA was repaired from damage

using SMRTbell Damage Repair Kit-SPv3 (Pacific Biosciences) and ligated to sequencing adapters, followed by exonuclease treatment using SMRTbell Template Prep Kit 1.0-SPv3. Optional size selection step was omitted. Libraries were sequenced on the Sequel System using Sequel Binding Kit 2.0, Sequel Sequencing Kit 2.0, Sequencing Primer v3 and Sequel SMRT Cell 1M v2 Trays (Pacific Biosciences). Each sample ("direct" and "rRNA-depleted" for liquid culture, "direct" and "rRNA-depleted" for agar plates) was run on two SMRT Cells in separate runs, totaling to 2 trays of 4 SMRT Cells. The following parameters were used for library loading and sequencing: MagBead loading at 20 pM (first run) or 30 pM (second run), 120 min immobilization, 120 min pre-extension, 600 min movie. Sequencing of one SMRT Cell containing "rRNA-depleted" sample for agar plates failed as a result of a manufacturing defect. The rest of SMRT Cells produced the sequencing output of 2.1-4.3 Gb each with mean polymerase read length of 17-25 kb. SMRT Link software version 4.0.0 (Pacific Biosciences) was used to convert subreads to circular consensus sequences and identify full-length non-chimeric reads.

ATAC-seq

To obtain regions of open chromatin we followed the omni-ATAC protocol (Corces et al. 2017) with purified worm nuclei from ≥15 µl of worm pellet. After the Iodixanol centrifugation, a 200 µl nuclear band was mixed with 1 ml ATAC-RSB/0.1% Tween-20 solution, and centrifuged 10 minutes, 500 x g, 4°C. Typically a pellet was not visible at this stage, however 12.5 µl was pipetted from the bottom of the tube and used for the transposon reaction. The duration and amount of transposase enzyme were the same as described in the Corces et al. protocol. After purification, ATAC libraries were size-selected using a BluePippin (Sage Science), and sequenced on site on an Illumina HiSeq3000. Technical replicates of each biological replicate were prepared with different illumina adapters, and after mapping the resulting .bam files were merged.

153

154 **Bioinformatic data analysis**

155 Iso-Seq reads were mapped to the El Paco assembly of the *P. pacificus* genome (Rödelsperger
156 et al. 2017) using GMAP (Wu and Watanabe 2005). Reads of the same samples from different
157 sequencing runs were merged, sorted and indexed using SAMtools (Li et al. 2009)(2009). Gene
158 annotations were derived from Stringtie (Pertea et al. 2016) using guided assembly ('-G' option)
159 with the El Paco reference for both 'direct' and 'rRNA-depleted total RNA'. Gene annotations
160 were then compared to El Paco for gene length and exon number using the density function in
161 R. Isoforms were assessed by converting .gtf annotations to .bed with a constant numerical 5th
162 column (1000), then parsing overlapping transcripts using BEDTools merge and performing
163 'sum' on the 5th column, and selecting genes that had greater than 1000 in this column.
164 Isoforms with the same start and stop coordinates were selected (again using BEDTools merge
165 and selecting genes with 'distinct' coordinates = 1), and a histogram of distinct coordinates was
166 plotted in R. Iso-Seq coverage of evolutionary gene classes was assessed by BEDTools
167 coverage, and density of exons and gene lengths was determined as before with the entire
168 annotation, but broken down by class.

169 For ChIP- and ATAC-seq, Illumina Fastq reads were aligned to the El Paco reference
170 genome (Rödelsperger et al. 2017) using Bowtie 2. The output .bam files were converted to
171 .sam using samtools and peaks were called independently for each biological replicate with
172 MACS2 (macs2 callpeak --broad -t Ab.bam -c Input.bam -f BAMPE -g 15e7 -n Ab_BP -B -m 2
173 50) (Supplementary Fig. S3). Input samples were processed and sequenced identically for each
174 biological replicate, and used as background control in MACS2 analysis. For duplicate data,
175 overlapping BroadPeaks were merged to create a genome-wide histone peak data set, and for
176 triplicate data (H3K4me1 and H3K4me3) we performed a multiIntersect (BEDTools), which
177 identified 6,081 H3K4me3 and 6,720 H3K4me1 locations that exhibited a peak in each of the
178 three replicates (Supplemental Table S1, ex. Supplemental Fig. S4A). To assess replicability

between duplicate data, we determined the fraction of overlapping peaks compared to the total amount of peaks (displayed as a weighted Venn Diagram in Supplemental Fig. S4B). For triplicate data we determined overlapping peaks for each sample with either of the other two samples, and for simplicity displayed the percent unique per replicate as an un-weighted Venn Diagram (weighted Venn Diagrams for three samples are mathematically impossible)(Supplemental Fig. S4B). Most of the Ab ChIP-seq and ATAC-seq replicates exhibited between 70-90% replicability of the smaller (fewer peaks) sample for duplicate data, or the average for triplicate data (Supplemental Fig. S4C). We set a minimum threshold of ≥50% overlap, which led to the removal of H2bub (27.5% overlap), H3K9ac (40.9% overlap), and H3K79me2 (49.8% overlap) data from further analysis. Although H3K9me3 exhibits relatively poor reproducibility to the other remaining samples (54% compared to >70%), we chose to keep it as 1) its broad distribution can make peak calling challenging, and 2) although H3K9me3 antibodies are generally less specific (Nishikori et al. 2012; Hattori et al. 2013), ChIP-seq data sets from multiple samples and organisms suggest it can still provide relevant information to distinguish facultative vs. constitutive heterochromatin (Trojer and Reinberg 2007).

Mapped replicate reads were normalized by coverage (depth x alignment rate) using samtools sub-sampling (samtools view –h –b –s), then combined using samtools 'merge' for chromatin state annotation with ChromHMM (Ernst and Kellis 2012) with a strict Poisson threshold (-strictthresh) and bin center (-center) options in 'BinarizeBam', and eight chromatin states (LearnModel binarized_files std_out 8 gene__assembly). Candidate state annotations were derived from previous observations in other organisms (Ernst et al. 2011; ENCODE Project Consortium 2012; Zentner et al. 2011; Consortium et al. 2015). Heatmaps of promoters and enhancers for different histone marks were made in R with combined replicate .bams using 'Pheatmap' from a matrix of per locus densities created in HOMER using 'annotatePeaks' -ghist. Rows were clustered from high to low densities, and colored from high to low log2(coverage)+1, the same scale was used for per mark for both promoters and enhancers. Sequence motifs

found in promoters and enhancers were obtained from HOMER using 'findMotifs' with standard options, and data presented are from a *de novo* motif search. Genomic loci presented are derived from Integrated Genome Viewer (IGV) images of combined replicate .bam files. Density of histone and ATAC-seq reads across the TSS of each evolutionary gene class were calculated in HOMER using combined .bams of replicates, and normalized by the high and low values from each data set. Meta-gene profiles of promoter and active enhancer locations relative to gene-bodies (+/-20 percent from 'slopBed') were obtained using the HOMER tool 'makeMetaGeneProfile.pl'.

Stranded RNA-seq data from two biological adult replicates were prepared by NEBNext Ultra Directional RNA-seq for Illumina kits, and mapped to El Paco using HISAT2 with standard parameters. Average expression (FPKM) from the two biological replicates of the reference gene annotation or evolutionary gene classes was determined by Stringtie and Ballgown(Pertea et al. 2016), and plotted in R by gene count. Expression groups were binned according to approximate inflection points. Distances in base pairs between evolutionary gene class TSSs to the nearest promoter (chromatin state 2) or enhancer (chromatin states 1 and 8) were obtained with the 'closestBed' function from BEDTools, and ordered and plotted in R in kilobase (kb).

Supplemental References

Brand M, Rampalli S, Chaturvedi C-P, Dilworth FJ. 2008. Analysis of epigenetic modifications of chromatin at specific gene loci by native chromatin immunoprecipitation of nucleosomes isolated using hydroxyapatite chromatography. *Nat Protoc* **3**: 398–409.

Consortium RE, Kundaje A, Meuleman W, Ernst J, Bilenky M, Yen A, Heravi-Moussavi A, Kheradpour P, Zhang Z, Wang J, et al. 2015. Integrative analysis of 111 reference human epigenomes. *Nature* **518**: 317–330.

Corces MR, Trevino AE, Hamilton EG, Greenside PG, Sinnott-Armstrong NA, Vesuna S, Satpathy AT, Rubin AJ, Montine KS, Wu B, et al. 2017. An improved ATAC-seq protocol reduces background and enables interrogation of frozen tissues. *Nat Methods* **14**: 959–962.

ENCODE Project Consortium. 2012. An integrated encyclopedia of DNA elements in the human genome. *Nature* **489**: 57–74.

Ernst J, Kellis M. 2012. ChromHMM: automating chromatin-state discovery and characterization. *Nat Methods* **9**: 215–216.

Ernst J, Kheradpour P, Mikkelsen TS, Shoresh N, Ward LD, Epstein CB, Zhang X, Wang L, Issner R, Coyne M, et al. 2011. Mapping and analysis of chromatin state dynamics in nine human cell types. *Nature* **473**: 43–49.

Hattori T, Taft JM, Swist KM, Luo H, Witt H, Slattery M, Koide A, Ruthenburg AJ, Krajewski K, Strahl BD, et al. 2013. Recombinant antibodies to histone post-translational modifications. *Nat Methods* **10**: 992–995.

Landt SG, Marinov GK, Kundaje A, Kheradpour P, Pauli F, Batzoglou S, Bernstein BE, Bickel P, Brown JB, Cayting P, et al. 2012. ChIP-seq guidelines and practices of the ENCODE and modENCODE consortia. *Genome Res* **22**: 1813–1831.

Nishikori S, Hattori T, Fuchs SM, Yasui N, Wojcik J, Koide A, Strahl BD, Koide S. 2012. Broad Ranges of Affinity and Specificity of Anti-Histone Antibodies Revealed by a Quantitative Peptide Immunoprecipitation Assay. *Journal of Molecular Biology* **424**: 391–399.

Pertea M, Kim D, Pertea GM, Leek JT, Salzberg SL. 2016. Transcript-level expression analysis of RNA-seq experiments with HISAT, StringTie and Ballgown. *Nat Protoc* **11**: 1650–1667.

Rödelsperger C, Meyer JM, Prabh N, Lanz C, Bemm F, Sommer RJ. 2017. Single-Molecule Sequencing Reveals the Chromosome-Scale Genomic Architecture of the Nematode Model Organism Pristionchus pacificus. *Cell Rep* **21**: 834–844.

Schuster LN, Sommer RJ. 2012. Expressional and functional variation of horizontally acquired cellulases in the nematode Pristionchus pacificus. *Gene* **506**: 274–282.

Serobyan V, Xiao H, Namdeo S, Rödelsperger C, Sieriebriennikov B, Witte H, Röseler W, Sommer RJ. 2016. Chromatin remodelling and antisense-mediated up-regulation of the developmental switch gene eud-1 control predatory feeding plasticity. *Nat Commun* **7**: 12337.

Steiner FA, Talbert PB, Kasinathan S, Deal RB, Henikoff S. 2012. Cell-type-specific nuclei purification from whole animals for genome-wide expression and chromatin profiling. *Genome Res* **22**: 766–777.

Stiernagle T. 2006. *Maintenance of C. elegans, WormBook, ed. The C. elegans Research Community*. WormBook.

Trojer P, Reinberg D. 2007. Facultative Heterochromatin: Is There a Distinctive Molecular Signature? *Mol Cell* **28**: 1–13.

Werner MS, Sieriebriennikov B, Loschko T, Namdeo S, Lenuzzi M, Dardiry M, Renahan T, Sharma DR, Sommer RJ. 2017. Environmental influence on Pristionchus pacificus mouth form through different culture methods. *Sci Rep* **7**: 7207.

Wu TD, Watanabe CK. 2005. GMAP: a genomic mapping and alignment program for mRNA and EST sequences. *Bioinformatics* **21**: 1859–1875.

271 Zentner GE, Tesar PJ, Scacheri PC. 2011. Epigenetic signatures distinguish multiple classes of
272 enhancers with distinct cellular functions. *Genome Res* **21**: 1273–1283.

273 2009. The Sequence Alignment/Map format and SAMtools. **25**: 2078–2079.
274 http://eutils.ncbi.nlm.nih.gov/entrez/eutils/elink.fcgi?dbfrom=pubmed&id=19505943&retmod
275 e=ref&cmd=prlinks.

276

The Role of DAF-21/Hsp90 in Mouth-Form Plasticity in *Pristionchus pacificus*

Bogdan Sieriebriennikov,[1] Gabriel V. Markov,[1,2] Hanh Witte,[1] and Ralf J. Sommer*,[1]

[1]Department of Evolutionary Biology, Max Planck Institute for Developmental Biology, Tübingen, Germany

[2]CNRS, UMR 8227, Integrative Biology of Marine Models, Station Biologique de Roscoff, Sorbonne Universités, UPMC University of Paris 06, Roscoff, France

***Corresponding author:** E-mail: ralf.sommer@tuebingen.mpg.de.

Associate editor: Ilya Ruvinsky

Abstract

Phenotypic plasticity is increasingly recognized to facilitate adaptive change in plants and animals, including insects, nematodes, and vertebrates. Plasticity can occur as continuous or discrete (polyphenisms) variation. In social insects, for example, in ants, some species have workers of distinct size classes while in other closely related species variation in size may be continuous. Despite the abundance of examples in nature, how discrete morphs are specified remains currently unknown. In theory, polyphenisms might require robustness, whereby the distribution of morphologies would be limited by the same mechanisms that execute buffering from stochastic perturbations, a function attributed to heat-shock proteins of the Hsp90 family. However, this possibility has never been directly tested because plasticity and robustness are considered to represent opposite evolutionary principles. Here, we used a polyphenism of feeding structures in the nematode *Pristionchus pacificus* to test the relationship between robustness and plasticity using geometric morphometrics of 20 mouth-form landmarks. We show that reducing heat-shock protein activity, which reduces developmental robustness, increases the range of mouth-form morphologies. Specifically, elevated temperature led to a shift within morphospace, pharmacological inhibition of all Hsp90 genes using radicicol treatment increased shape variability in both mouth-forms, and CRISPR/Cas9-induced *Ppa-daf-21/Hsp90* knockout had a combined effect. Thus, Hsp90 canalizes the morphologies of plastic traits resulting in discrete polyphenism of mouth-forms.

Key words: **plasticity, canalization, robustness, heat-shock proteins, *Pristionchus pacificus*.**

Article

Introduction

Developmental (phenotypic) robustness, often referred to as canalization, describes the property of organisms to produce an unchanged phenotype despite environmental perturbations (Wagner 2005). Heat-shock proteins of the Hsp90 family have been implicated in developmental robustness and were shown to act through Piwi proteins (Gangaraju et al. 2011). They are thought to have two potential functions in this context: first, they might suppress stochastic phenotypic variation and second, they are thought to facilitate unchanged development in the presence of mutations, rendering such mutations cryptic (Rutherford 2003; Siegal and Leu 2014). Hsp90 was shown to buffer phenotypic variation in diverse organisms, such as *Drosophila*, *Arabidopsis*, and cavefish, indicating that chaperone function is conserved throughout multicellular organisms (Rutherford and Lindquist 1998; Queitsch et al. 2002; Rohner et al. 2013). Despite the fact that heat-shock proteins are recognized to provide a molecular mechanism for developmental robustness, many conceptual issues are still controversially discussed in literature (Siegal and Leu 2014). In the following, we mainly use the term "developmental robustness" and investigate its relationship to plasticity.

On the surface, it appears that developmental robustness is an opposing evolutionary constraint to phenotypic variation. However, it has been proposed that developmental robustness facilitates morphological evolution because buffered phenotypic variation may be subsequently revealed and become a substrate for natural selection, a theory that is still contentious. This concept is similar to theories regarding the contribution of phenotypic plasticity as a pulse of morphological adaptation (Susoy et al. 2015). In phenotypic (developmental) plasticity, a single genotype can produce distinct phenotypes in response to environmental conditions. This ability is argued to facilitate evolutionary change by allowing more flexible adaptation and providing additional substrate for selection (Pigliucci and Hayden 2001; West-Eberhard 2003). When conditions ultimately favor the fixation of one morph over the other, built-up genetic variation allowed by having two options is released to one morph, leading to rapid evolution as seen in nematodes (Susoy et al. 2015).

The conceptual difficulty in studying the interplay between developmental robustness and plasticity lies in plasticity being viewed as sensitivity and robustness as insensitivity to the environment. Still, both developmental robustness and plasticity are essential systemic features of organisms and both have been speculated to accelerate evolutionary change (West-Eberhard 2003; Wagner 2005). Here, we use an example of discrete plasticity (polyphenism) in clonally propagating

nematodes to overcome existing conceptual and practical limitations for addressing the relationship between the two phenomena.

The nematode *Pristionchus pacificus* is a distant relative of *Caenorhabditis elegans* and has been developed as a laboratory model for comparative and evolutionary studies (Sommer 2015). It shares with *C. elegans* its hermaphroditic mode of reproduction resulting in isogenic lines and the availability of forward and reverse genetic, genomic and transgenic tools (Sommer and McGaughran 2013). In addition, *P. pacificus* is an omnivorous feeder that predates on other nematodes and generates feeding structures consisting of moveable teeth that occur in two alternative morphs (Bento et al. 2010): adult animals develop into either "narrow-mouthed" stenostomatous (St) or "wide-mouthed" eurystomatous (Eu) morphs after an irreversible decision in postembryonic development. St animals have a narrow stoma and a flint-like dorsal tooth, whereas the ventrosublateral tooth is replaced by a cuticular ridge with a minute denticle (fig. 1*A* and *B*) . In contrast, Eu animals have a broad stoma with a claw-like dorsal tooth and a hooked right ventrosublateral tooth (fig. 1*C* and *D*). Although Eu animals can kill and feed on nematode prey, St animals are strict microbial feeders under laboratory conditions (Wilecki et al. 2015).

Importantly, the two described phenotypes in *P. pacificus* are discrete. Varying the levels of environmental factors, such as applying a gradient of pheromone concentrations, never results in formation of intermediate mouth-forms, but instead shifts the ratio between the numbers of Eu and St individuals (Bose et al. 2012). This indicates that the developmental switch leading to the formation of one or the other morph operates in a threshold-dependent manner and that the polyphenism has a discontinuous reaction norm (see hypothetical representation in fig. 2). Consequently, the Eu:St ratio is subject to apparent stochasticity. Under standard laboratory conditions, the proportion of Eu animals in the wild-type strain RS2333 varies between 70% and 90% (Ragsdale et al. 2013; Serobyan et al. 2013; Susoy and Sommer 2016). Together, the discreteness and simultaneous production of both morphs make mouth-form polyphenism in *P. pacificus* a unique study system to investigate whether the same mechanism that guards development against stochastic perturbations is involved in maintaining polyphenisms.

Thus, we set out to determine whether heat-shock proteins, which were shown to act as capacitors of morphological evolution, play a role in the execution of correct mouth-forms in *P. pacificus*. In theory, four different scenarios are possible (fig. 2). First, as a null hypothesis, interference with heat-shock proteins might not affect mouth-form plasticity. Second, elimination of developmental robustness might lead to the occurrence of intermediate mouth-forms, resulting in one continuous distribution of morphologies and thus, the disappearance of the polyphenism (fig. 2*C* and *D*). Such a finding would suggest that the presence of the alternative mouth-forms requires developmental robustness. Alternatively, the elimination of developmental robustness might third, shift (fig. 2*E*) or fourth, expand the respective distribution of morphologies (fig. 2*F*), without eliminating the polyphenism. To distinguish between these partially overlapping scenarios, we applied geometric morphometrics approaches to detect such changes in the mouth shape of *P. pacificus*, which was subjected to conditions known to affect developmental buffering, ranging from a generic stress, such as exposure to elevated temperatures, to knock-out of a specific gene encoding Hsp90. We observed two kinds of predicted changes, shift and expansion of the distribution of morphologies, and conclude that Hsp90 activity canalizes mouth-form plasticity in *P. pacificus*.

Results

Investigation of the robustness of a polyphenic trait requires formal proof that shape variation of individual morphs is limited and that they are indeed discrete. To validate if mouth morphology in *P. pacificus* satisfies these criteria, we used geometric morphometric analysis of 20 landmarks in the stoma (fig. 1*E*) (Ragsdale and Baldwin 2010; Susoy, et al. 2015). In short, their coordinates were measured and then centered, rotated and scaled, resulting in Procrustes alignment that was used to conduct principal component analysis (PCA) (Dryden and Mardia 1998; Mitteroecker et al. 2004). Ordination of sets of landmarks representing individual *P. pacificus* RS2333 wild-type animals resulted in distinct distributions of morphologies for Eu and St animals without any overlap, thus representing a baseline to study the relationship between plasticity and robustness (fig. 1*F*).

To examine a potential role of heat-shock proteins in the execution of the Eu and St morphs, we analyzed the effect of elevated temperature on mouth morphology, as such treatment compromises the heat-shock machinery (Rutherford and Lindquist 1998). Animals reared at 28 °C, the highest temperature at which *P. pacificus* RS2333 continuously reproduces (Leaver et al. 2016), displayed evidently abnormal mouth morphology, represented as a shift within morphospace in relation to control conditions (fig. 3*A*). Morphological disparity estimated as sum of variances increased in comparison to the control group, but the change was small and, in case of Eu animals, not statistically significant (fig. 3*B*). Importantly, both mouth-forms were still clearly distinguishable, and thus the discreteness of the polyphenism remained clearly visible. Even though elevated temperature presumably produces a very general stress, this result provided the first indication that heat-shock proteins may be involved in limiting the distribution of mouth morphologies in *P. pacificus* and justified application of a more specific treatment.

Next, we used pharmacological inhibition with radicicol to reduce Hsp90 function in a targeted manner, as it was previously applied in *Drosophila*, *Arabidopsis* and cave fish (Rutherford and Lindquist 1998; Queitsch et al. 2002; Rohner et al. 2013). Like in heat-stress treatment, many animals exhibited abnormal mouth morphology. However, the most pronounced effect detected through morphometric analysis was not a shift within morphospace, as seen in temperature treatment, but an increase in shape variability, evident from almost 2-fold significant increase in morphological

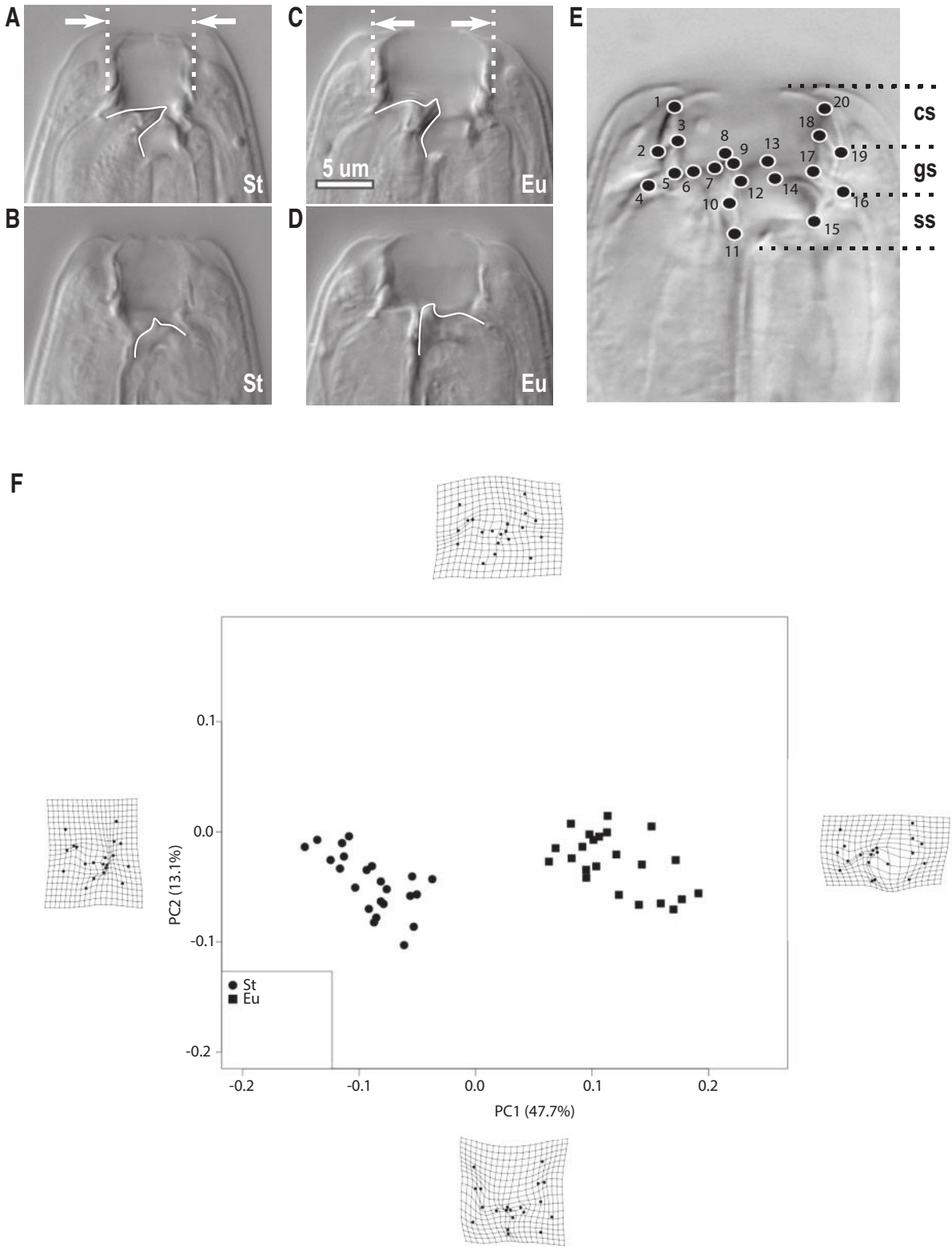

Fig. 1. Mouth dimorphism in *Pristionchus* nematodes. (*A*) St morph, view in sagittal (median) plane. Stoma is narrow and dorsal tooth is flint-shaped. (*B*) St morph, view in right parasagittal plane. Cuticularization of the right ventrosublateral part of stegostom is represented by a ridge with a minute denticle. (*C*) Eu morph, view in sagittal (median) plane. Stoma is wide and dorsal tooth is claw-shaped. Scale bar equally applies to images A–D. (*D*). Eu morph, view in right parasagittal plane. The right ventrosublateral part of stegostom contains a hooked tooth. (*E*). Landmarks in the stoma, which were used for geometric morphometric analysis (see supplementary table 1, Supplementary Material online for their detailed description). cs, cheilostom; gs, gymnostom; ss, stegostom; (*F*) PCA ordination of sets of landmarks in Eu and St animals, which shows clear separation of the two morphs. Each point represents one individual. Deformation grids depict differences between the shape coordinates of the corresponding extreme ends of the PC1 and PC2 axes and the mean shape of all specimens.

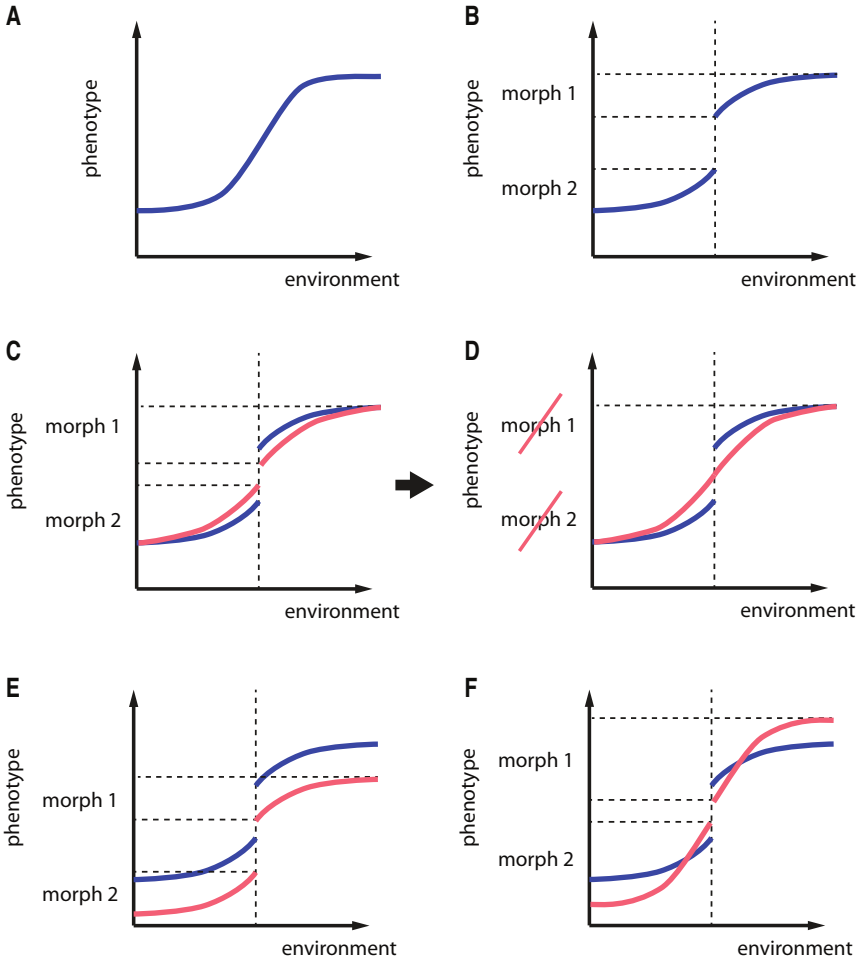

Fig. 2. Hypothetical scenarios of change in reaction norm of a dimorphic trait upon reduction of developmental robustness through suppression of heat-shock protein activity. (*A*) Reaction norm of a continuous trait. (*B*) Reaction norm of a polyphenic trait (i.e., plastic trait with discrete phenotypes). (*C*) Occurrence of individuals with intermediate phenotypes leading to narrowing the gap between the two morphs. (*D*) Extreme case of C, whereby the two reaction norms merge and polyphenism is negated. (*E*) Shift in reaction norms. (*F*) Expansion of reaction norms without loss of polyphenism.

disparity (fig. 3*A* and *B*). However, the distributions of morphologies in St and Eu animals are still fully separated. This finding suggested that Hsp90 proteins limit the range of possible mouth morphologies in *P. pacificus* from stochastic variation.

Next, we validated the previous finding by knocking out an Hsp90-encoding gene. In *C. elegans*, three genes encode Hsp90-type proteins, all of which have *P. pacificus* 1:1 orthologs (fig. 4*A*). *enpl-1* encodes an endoplasmic reticulum associated chaperone orthologous to GRP94, whereas *trap-1* is the ortholog of mitochondrial Hsp75/TRAP1 in vertebrates (Johnson 2012). The only Hsp90 gene that was identified in genetic screens in *C. elegans* is *daf-21* (Thomas et al. 1993; Birnby et al. 2000). It is required for larval development, chemosensory behavior and has a **da**uer **f**ormation **c**onstitutive (Daf-c) phenotype when mutated. DAF-21 has the highest sequence similarity to the *Drosophila* protein *Hsp83*, which has been identified as capacitor for morphological evolution (Rutherford and Lindquist 1998). Using CRISPR/Cas9 engineering we targeted exon 2 of *Ppa-daf-21* and were able to isolate a mutant strain (*tu519*) with a 10 bp insertion, representing a presumptive "loss-of-function" allele (fig. 4*B*). *Ppa-daf-21(tu519)* mutant animals are not Daf-c, but they are small, clear, locomotion-defective, vulvaless, and sterile (fig. 4*C* and *D*); therefore, cultures can only be kept as heterozygous carriers. These pleiotropic phenotypes of *Ppa-daf-21* mutant animals are consistent with the pleiotropy observed in flies (Rutherford and Lindquist 1998). The comparison between *Cel-daf-21* and *Ppa-daf-21* mutant phenotypes reveals multiple similarities, such as sterility, locomotion defects and abnormal gonad development, but also important differences, such as the absence of the Daf-c phenotype in *P. pacificus*. This observation follows the principal of developmental systems drift, which has previously been seen in vulva formation and dauer development between these two nematodes (Wang and Sommer 2011; Sommer and Mayer 2015).

With regard to mouth-form polyphenism, homozygous mutant animals exhibit severely distorted mouth morphologies (fig. 3*C*), an observation supported by a considerable shift within morphospace and a significant increase in morphological disparity (fig. 3*D* and *E*). Although a classification of

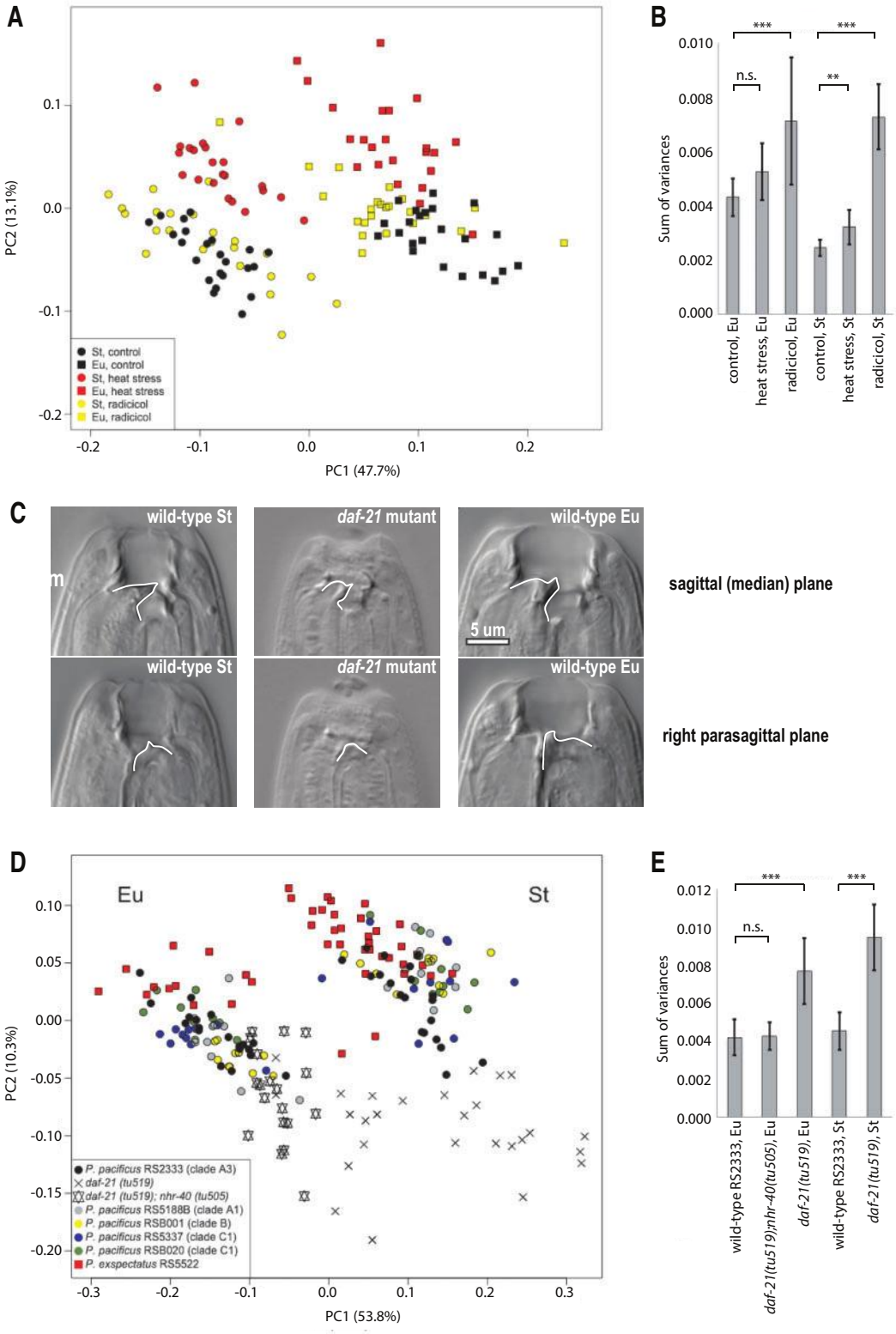

Fig. 3. Change in mouth morphology of *P. pacificus* upon impediment of function of heat-shock proteins. (*A*) PCA ordination of sets of landmarks representing control individuals (identical to the ones depicted in fig. 1*F*) and individuals exposed to heat stress and treatment by radicicol, a pharmacological inhibitor of Hsp90. (*B*) Morphological disparity in different groups shown in the PCA ordination in panel A. Error bars show SD. n.s., not significant (*P*-value $>$ 0.05); **P-value $<$ 0.01; ***P-value $<$ 0.001. (*C*) An example of distorted mouth in a *Ppa-daf-21/Hsp90* mutant, alongside a St and a Eu wild-type animal. Scale bar applies to all six images. (*D*) PCA ordination of sets of landmarks from the laboratory *P. pacificus* strain RS2333, the *Ppa-daf-21* and *daf-21; nhr-40* mutants, four wild isolates of *P. pacificus* and a wild isolate of *P. exspectatus*. (*E*) Morphological disparity in wild-type *P. pacificus* and *daf-21* mutant. Error bars show SD. n.s., not significant (*P*-value $>$ 0.05), ***P value $<$ 0.001.

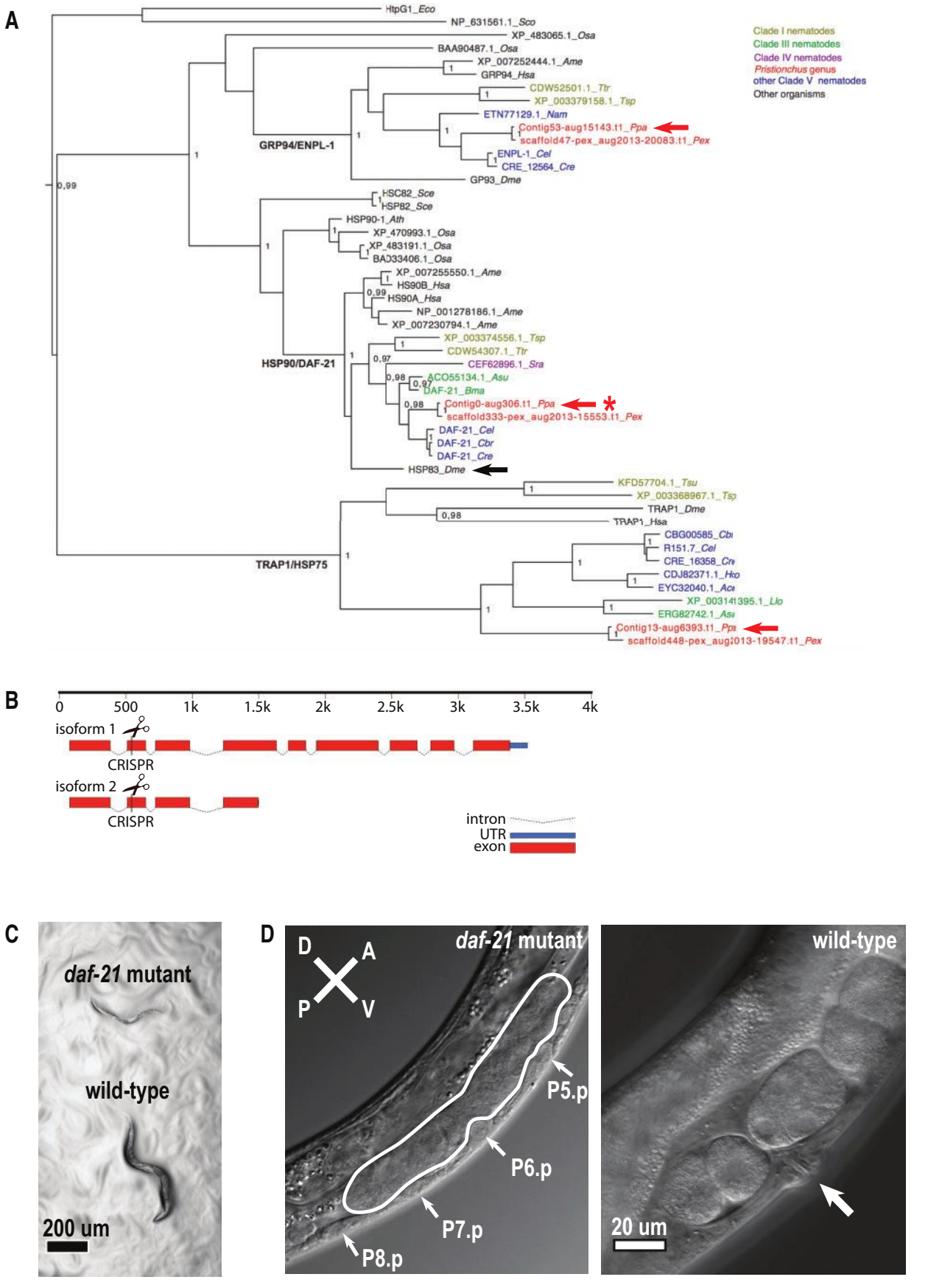

FIG. 4. *daf-21/Hsp90* knockout in *P. pacificus*. (*A*) Maximum likelihood tree of Hsp90 homologs in animals. Black arrow indicates the *D. melanogaster* protein used in previous studies (Rutherford and Lindquist 1998). Red arrows show predicted proteins in *P. pacificus*. Ppa-DAF-21 is marked with an asterisk. Branch support values under 0.97 are considered not significant and were thus removed from the tree.

animals into Eu and St morphs was still possible, morphologies were severely affected and some individuals displayed combined characteristics of different morphs to a certain degree (e.g., narrow mouth, like in St, and hooked right ventrosublateral tooth, like in Eu). The data shown in figures 3*D* and *E* indicate that the *Ppa-daf-21* knockout led to a shift within morphospace and an increase in shape variability and thus a combined effect when compared to temperature and radicicol treatments. Therefore, reducing the activity of HSP90-type proteins indeed affects the distribution of morphologies of both mouth-forms, indicating that developmental robustness is required for the discreteness of the polyphenism. Finally, it is worth noting that *Ppa-daf-21* mutant animals show altered ratios of Eu:St animals. Specifically, we found that 52% of *Ppa-daf-21* animals were Eu, while wild-type RS2333 had 90% Eu individuals ($n = 21$, $\chi^2 = 7.47$, $P = 0.006$).

Next, we wanted to know if the knockout of *Ppa-daf-21* still affects mouth morphology when one of the morphs is fixed and no dimorphism occurs. We crossed *daf-21(tu519)* with *nhr-40 (tu505)*, a mutant that produces only Eu individuals (Kieninger et al. 2016), and performed morphometric analysis on the *daf-21(tu519);nhr-40(tu505)* double mutant. The distribution of morphologies in such animals was still distinct from that of wild-type individuals (fig. 3*D*); however, mouth shape of the double mutant was less diverged from the wild type than mouth shape of the *daf-21* single mutant. Interestingly, no significant increase in morphological disparity was observed in double mutants, in contrast to the single mutant (fig. 3*E*). Together, these findings demonstrate that limiting a polyphenic trait to one morph also limits the amount of variation that can be released when Hsp90 activity is reduced.

Finally, capacitance theory suggests that a temporary decrease in buffering by heat–shock proteins (e.g., during stress) could expose cryptic morphological variants to selection, which would accompany microevolutionary processes and/or speciation (Rutherford and Lindquist 1998; Rutherford 2003; Hermisson and Wagner 2004; Paaby and Rockman 2014). Therefore, we set out to determine if the amount of morphological change induced by the mutation in *Ppa-daf-21* is similar to existing morphological divergence among various wild isolates of *P. pacificus* and between *P. pacificus* and its sister species *P. exspectatus* (Kanzaki et al. 2012; Rodelsperger et al. 2014). We compared *P. pacificus* RS2333 and *Ppa-daf-21* mutants with four wild isolates that cover the complete worldwide diversity of *P. pacificus* and with one strain of *P. exspectatus* (fig. 3*D*). Morphologies of most *P. pacificus* strains demonstrated considerable overlap, but some of them (e.g., Eu RSB020 and RSB001) showed apparent divergence. As expected, *P. exspectatus* appeared the most distinct from the rest of wild isolates, but it still retained some overlap with *P. pacificus*. Importantly, *Ppa-daf-21* mutants occupied a region within the morphospace as distant from wild-type *P. pacificus* RS2333 as regions occupied by *P. pacificus* RS2333 and *P. exspectatus* are from each other. This finding demonstrates that the amount of morphological change buffered by Hsp90 is on the same scale as the degree of morphological divergence across examined wild isolates. Thus, concealed morphological variation associated with diverging lineages is within the canalization function of Hsp90 proteins.

Discussion

We used alternative mouth morphologies in the isogenic nematode *P. pacificus* as a model to link developmental plasticity and robustness at the molecular mechanistic level. Although both plasticity and robustness have long been discussed as important principles of evolution, little was known about their relationship to each other. This has changed largely by the work of Lindquist and co-workers, who provided a molecular basis for developmental robustness by showing a link to Hsp90 proteins (Rutherford and Lindquist 1998). Still, it is inherently difficult to examine the interplay with plasticity because robustness and plasticity represent opposite systemic features of organisms and are often contrasted.

We predicted four possibilities for how reaction norm of a dimorphic trait may change once buffering from stochastic variation is released (fig. 2). We observed two kinds of change when heat-shock protein activity was impeded in *P. pacificus*. Specifically, incubation at an elevated temperature led to a shift within morphospace, pharmacological inhibition produced increased variation of both morphs, and mutation in the *daf-21/Hsp90* gene had combined effects. Thus, the main conclusion of our study is that heat–shock protein activity, which provides developmental robustness, canalizes the exact morphologies of mouth-forms in *P. pacificus*.

There are two possible reasons why the applied treatments affected morphology in different ways. First, these treatments interfere with a different number and types of molecular factors. Specifically, the mutation in *Ppa-daf-21* has a targeted effect, whereas the pharmacological inhibition is assumed to

Fig. 4 Continued

See supplementary table 1, Supplementary Material online for the list of accession numbers of sequences used and supplementary figure 1, Supplementary Material online for sequences of the *P. pacificus* proteins. (*B*) Inferred gene structure of *Ppa-daf-21*. CRISPR/Cas9 mutation was introduced in the second exon, which interferes with both identified isoforms. (*C* and *D*). Pleiotropic effects of the *Ppa-daf-21* knockout. (*C*) On the top, a homozygous mutant. Such animals are small and clear. On the bottom, a normally looking heterozygous or genetically wild-type individual from the same brood. (*D*) On the left, a seven-day-old homozygous mutant. Mid-body region, sagittal plane. The gonad is underdeveloped. Proximal part of the gonad is encircled (distal parts are not visible in this plane). Vulva is absent, as vulval precursor cells (marked with arrows) do not develop into the functional organ during postnatal development and can be still observed in adults. On the right, a 4-day-old wild-type individual. The gonad is fully developed and the uterus is filled with eggs. The slit of the vulva is marked with an arrow. The scale bar applies to both images. D, dorsal side; V, ventral side; P, posterior end; A, anterior end.

interfere with all proteins of the Hsp90 family, and the molecular effects of heat stress are arguably very diverse. Second, different treatments presumably influence Hsp90 proteins to a different extent, with a null mutation producing potentially the strongest effect. Generally, our data are consistent with the second and potentially sufficient explanation. Still, the possibility remains that the underlying mechanism involves complex machinery consisting of multiple molecular players.

In addition to this, the role of Hsp90 in mouth-form plasticity may go beyond its generic chaperone function (Arbeitman and Hogness 2000). This protein may be directly involved in the development of certain mouth structures, as any mutation in the gene network underlying mouth development may be expected to increase morphological variability of the mouth (Bergman and Siegal 2003). However, during the first genetic screens for mutations affecting mouth-form, only few mutants were identified, which had defects in the development of substructures of the teeth. In contrast, many mutants were found that alter mouth-form ratios (Ragsdale et al. 2013; Serobyan et al. 2016). It is worth noting that all these mutations did not increase shape variability of the whole mouth. Also, the nematode mouth is a heterogeneous structure formed by tissues of different developmental origin (Ragsdale and Baldwin 2010), so it is unlikely that a mutation affecting the development of one mouth component would increase the morphological variability of the complete organ. Nevertheless, the direct involvement of heat-shock proteins in mouth morphogenesis is possible and awaits future analysis.

We tested if interfering with Hsp90 function still has an effect on mouth shape when one of the morphs is fixed and no dimorphism occurs. The *daf-21; nhr-40* double mutants, which only produce Eu animals, were less diverged from the wild type than single *daf-21* mutants were and less variable than Eu individuals were of the single mutant strain. Together, this shows that once a polyphenic trait is constrained to one morph, the amount of variation released upon impediment of the Hsp90 system is also limited. This finding is consistent with the idea that simultaneous utilization of multiple developmental pathways by polyphenic traits provides space for additional morphological variants (West-Eberhard 2003).

The phenotypic effects described in this study were observed in an isogenic background. It is important to note that the isogenicity of *P. pacificus* allows a clear disentanglement of the role of Hsp90 as a suppressor of stochastic phenotypic variation from its involvement in buffering from mutations (Siegal and Bergman 2002). We speculate that the cause of increased phenotypic variation was either sensitization to microenvironmental changes or stochastic noise in gene regulatory networks. Given current information, it is impossible to determine which of the two possibilities is more likely. To our knowledge, this study is the first of its kind in self-fertilizing hermaphroditic animals, which arguably achieve a higher degree of isogenicity than gonochoristic species, such as *Drosophila* or cavefish.

Finally, there is a long-standing prediction that an erratic decrease in buffering capacity may release morphological variants that can subsequently undergo natural selection (Rutherford and Lindquist 1998; Rutherford, 2003). Strictly speaking, a proof that this has occurred in nature may be unachievable. Instead, we tested if the buffering capacity of Hsp90 system is sufficient to harbor the degree of variation that is actually seen across different strains and species of *Pristionchus*. We saw that mouth shape in the *daf-21/Hsp90* mutant is equally diverged from its background wild type strain *P. pacificus* RS2333 as the rest of strains and species tested are from each other. Therefore, our results indicate that morphological variation associated with diverging lineages and speciation is within the canalization capacity of Hsp90.

Materials and Methods

Nematode Cultures

For experiments with elevated temperature and radicicol, *P. pacificus* strain RS2333 was used. For comparison of wild isolates, *P. pacificus* strains RS5188B, RSB001, RS5337, and RSB020 and *P. exspectatus* strain RS5522 were used. Before each experiment, all *P. pacificus* strains were cultured for at least three generations at 20 °C on NGM plates (Stiernagle 2016) and fed *ad libitum* with *Escherichia coli* OP50. *Pristionchus exspectatus* did not produce Eu animals on *E. coli* OP50, so it was cultured on *Brevibacillus sp.* isolated from a contaminated culture where Eu *P. exspectatus* were seen.

Geometric Morphometrics Analysis

Worms were mounted on microscope slides on 4% agar pads containing 0.3% NaN_3. Animals were turned right side up and covered with a cover slip. Correct positioning of the head was verified by checking if amphid openings were seen close to the central axis. Animals were examined using a 100x/1.4 oil objective. A stack image of the head region was taken, and coordinates of 20 landmarks in XY plane were recorded using FIJI software (Schindelin et al. 2012). Detailed descriptions of landmarks are available in supplementary table 1, Supplementary Material online. Procrustes alignment and PCA were done in R using geomorph package (Adams and Otarola-Castillo 2013; R Development Core Team 2013). Sum of variances was calculated using the MATLAB package MDA (Guide MUs 1998; Navarro 2003). Four first PC axes were retained for the calculations. Rarefaction was done to correct for differences in sample size. Bootstrapping with 10,000 replicates was performed to calculate means and SDs of sum of variances. Bootstrapping with 100,000 replicates was done to estimate two-tailed *P*-values in pairwise comparisons.

Incubation at Elevated Temperature

A non-starved plate with many eggs was taken and vermiform stages were washed away with S-medium (Stiernagle 2016). Then, 1 ml of S-medium was added to the plate and eggs were gently scraped off using a glass cell spreader. Egg suspension was collected in a 1.5 ml tube, centrifuged for 30 s in a table-top centrifuge and washed with S-medium two times. The resulting egg suspension was transferred to a

staining block. Eggs containing pre-comma stage embryos were selected using a stereomicroscope and one egg was transferred to each well of a 96-well plate containing 200 µl S-medium with 1% w/v frozen and thawed *E. coli* OP50 and 0.5% DMSO. The plate was sealed with a paraffin film and placed in an incubator set to 28 °C. Animals were collected for analyses upon reaching maturity (4 days).

Radicicol Treatment

Worms were grown in the same way as described earlier but at 20 °C. Radicicol (Sigma-Aldrich) was dissolved in DMSO and then added to S-medium to the final concentration of 15 µg/ml radicicol and 0.5% DMSO. Solution containing no radicicol and 0.5% DMSO was used as control.

CRISPR/Cas9 Knock Out

As a first step, we searched for homologs of Hsp90 in *P. pacificus* genome. Protein sequences were retrieved from Genbank and the http://pristionchus.org databases. Alignment was done using MUSCLE (Edgar 2004). Conserved sites were manually selected using SeaView (Gouy et al. 2010). Phylogenetic trees were inferred using PhyML (Guindon and Gascuel 2003) with the LG G substitution model. Branch support values were assessed using the approximate likelihood ratio test (Anisimova and Gascuel 2006). Ppa-DAF-21 was identified as the closest homolog of *Drosophila melanogaster* Hsp83 protein, which was knocked out in earlier studies (Rutherford and Lindquist 1998). Exon 2 of the *Ppa-daf-21* gene was selected as CRISPR/Cas9 target due to high sequence conservation. To verify if the mutation in this locus would interfere with the function of the protein product, we performed Rapid Amplification of cDNA Ends experiment and identified two isoforms both containing the targeted exon. Therefore, we concluded that targeting exon 2 should produce a strong "reduction-of-function" or even a null allele. Upon designing a sgRNA, BLASTn was done to confirm the absence of off-target sites. We followed the protocol of Witte et al. (Witte et al. 2015) to induce a mutation in the genetic background of the *P. pacificus* RS2333 strain. Progeny of a heterozygous mutant animal were singled out, allowed to lay eggs and the mutated locus was sequenced. After repeating this for several generations, we did not obtain any fertile homozygous mutants. To eliminate the need to sequence each generation, we checked for a characteristic phenotype or a set of phenotypes associated with homozygous mutants. We singled out 40 offspring of a heterozygous animal, tracked their development for 5 days and then sequenced the *daf-21* locus. Although some heterozygous or genetically wild type animals stopped their development at an unidentifiable larval stage, most of them developed into wild-type looking animals. Only homozygous mutants developed a characteristic complex of Small, Clear, Sick and Uncoordinated phenotypes.

Comparison of *Ppa-daf-21* Mutant with Wild Isolates

Before the experiment, multiple adult offspring of a heterozygous *Ppa-daf-21* mutant were singled out on a NGM plate seeded with 400 µl *E. coli* OP50. As expected, around two-third of these animals produced some progeny with a complex of phenotypes characteristic of *Ppa-daf-21* homozygous mutants. These animals were used to conduct morphometric analysis as described earlier. However, oftentimes the mouth shape was distorted so severely that it was not possible to measure the coordinates of landmarks 1, 2, 19, and 20. Hence, these landmarks were excluded from the analysis. Wild isolates were grown on NGM plates with 400 µl of bacteria and young adults were used for morphometric analysis. Landmarks 1, 2, 19, and 20 were also excluded to make wild isolate individuals comparable to *Ppa-daf-21* mutants.

Supplementary Material

Supplementary data are available at *Molecular Biology and Evolution* online.

Acknowledgments

We thank Dr Vladislav Susoy for advice on experimental design and discussion of the results and Dr Natsumi Kanzaki for morphological expertise. We are also grateful to Dr Michael Werner and Dr James Lightfoot, Tess Renahan, and four anonymous reviewers for critical reading of the article. The work was funded by the Max Planck Society.

References

Adams DC, Otarola-Castillo E. 2013. geomorph: an R package for the collection and analysis of geometric morphometric shape data. *Methods Ecol Evol* 4:393–399.

Anisimova M, Gascuel O. 2006. Approximate likelihood-ratio test for branches: a fast, accurate, and powerful alternative. *Syst Biol* 55:539–552.

Arbeitman MN, Hogness DS. 2000. Molecular chaperones activate the Drosophila ecdysone receptor, an RXR heterodimer. *Cell* 101:67–77.

Bento G, Ogawa A, Sommer RJ. 2010. Co-option of the hormone-signalling module dafachronic acid-DAF-12 in nematode evolution. *Nature* 466:494–499.

Bergman A, Siegal ML. 2003. Evolutionary capacitance as a general feature of complex gene networks. *Nature* 424:549–552.

Birnby DA, Link EM, Vowels JJ, Tian H, Colacurcio PL, Thomas JH. 2000. A transmembrane guanylyl cyclase (DAF-11) and Hsp90 (DAF-21) regulate a common set of chemosensory behaviors in *Caenorhabditis elegans*. *Genetics* 155:85–104.

Bose N, Ogawa A, von Reuss SH, Yim JJ, Ragsdale EJ, Sommer RJ, Schroeder FC. 2012. Complex small-molecule architectures regulate phenotypic plasticity in a nematode. *Angew Chem Int Ed Engl* 51:12438–12443.

Dryden IL, Mardia KV. 1998. Statistical shape analysis. Chichester: J. Wiley.

Edgar RC. 2004. MUSCLE: a multiple sequence alignment method with reduced time and space complexity. *BMC Bioinformatics* 5:1–19.

Gangaraju VK, Yin H, Weiner MM, Wang JQ, Huang XA, Lin HF. 2011. Drosophila Piwi functions in Hsp90-mediated suppression of phenotypic variation. *Nat Genet* 43:153–158.

Gouy M, Guindon S, Gascuel O. 2010. SeaView version 4: a multiplatform graphical user interface for sequence alignment and phylogenetic tree building. *Mol Biol Evol* 27:221–224.

Guide MUs. 1998. The mathworks. Inc. Vol. 5, p. 333. Natick, MA.

Guindon S, Gascuel O. 2003. A simple, fast, and accurate algorithm to estimate large phylogenies by maximum likelihood. *Syst Biol* 52:696–704.

Hermisson J, Wagner GP. 2004. The population genetic theory of hidden variation and genetic robustness. *Genetics* 168:2271–2284.

Johnson JL. 2012. Evolution and function of diverse Hsp90 homologs and cochaperone proteins. *Biochim Biophys Acta Mol Cell Res* 1823:607–613.

Kanzaki N, Ragsdale EJ, Herrmann M, Mayer WE, Sommer RJ. 2012. Description of three *Pristionchus* species (Nematoda: Diplogastridae) from Japan that form a cryptic species complex with the model organism *P. pacificus*. *Zool Sci* 29:403–417.

Kieninger MR, Ivers NA, Rodelsperger C, Markov GV, Sommer RJ, Ragsdale EJ. 2016. The nuclear hormone receptor NHR-40 acts downstream of the sulfatase EUD-1 as part of a developmental plasticity switch in *Pristionchus*. *Curr Biol* 26:2174–2179.

Leaver M, Kienle S, Begasse ML, Sommer RJ, Hyman AA. 2016. A locus in *Pristionchus pacificus* that is responsible for the ability to give rise to fertile offspring at higher temperatures. *Biol Open* 5: 1111–1117.

Mitteroecker P, Gunz P, Bernhard M, Schaefer K, Bookstein FL. 2004. Comparison of cranial ontogenetic trajectories among great apes and humans. *J Hum Evol* 46:679–697.

Navarro N. 2003. MDA: a MATLAB-based program for morphospace-disparity analysis. *Comput Geosci* 29:655–664.

Paaby AB, Rockman MV. 2014. Cryptic genetic variation: evolutioń s hidden substrate. *Nat Rev Genet* 15:247–258.

Pigliucci M, Hayden K. 2001. Phenotypic plasticity is the major determinant of changes in phenotypic integration in Arabidopsis. *New Phytologist* 152:419–430.

Queitsch C, Sangster TA, Lindquist S. 2002. Hsp90 as a capacitor of phenotypic variation. *Nature* 417:618–624.

R Development Core Team. 2016. R: A language and environment for statistical computing. R Foundation for Statistical Computing, Vienna, Austria. URL: https://www.R-project.org/.

Ragsdale EJ, Baldwin JG. 2010. Resolving phylogenetic incongruence to articulate homology and phenotypic evolution: a case study from Nematoda. *Proc Royal Soc B* 277:1299–1307.

Ragsdale EJ, Muller MR, Rodelsperger C, Sommer RJ. 2013. A developmental switch coupled to the evolution of plasticity acts through a sulfatase. *Cell* 155:922–933.

Rodelsperger C, Neher RA, Weller AM, Eberhardt G, Witte H, Mayer WE, Dieterich C, Sommer RJ. 2014. Characterization of genetic diversity in the nematode *Pristionchus pacificus* from population-scale resequencing data. *Genetics* 196:1153–1165.

Rohner N, Jarosz DF, Kowalko JE, Yoshizawa M, Jeffery WR, Borowsky RL, Lindquist S, Tabin CJ. 2013. Cryptic variation in morphological evolution: HSP90 as a capacitor for loss of eyes in cavefish. *Science* 342:1372–1375.

Rutherford SL, Lindquist S. 1998. Hsp90 as a capacitor for morphological evolution. *Nature* 396:336–342.

Rutherford SL. 2003. Between genotype and phenotype: Protein chaperones and evolvability. *Nat Rev Genet* 4:263–274.

Schindelin J, Arganda-Carreras I, Frise E, Kaynig V, Longair M, Pietzsch T, Preibisch S, Rueden C, Saalfeld S, Schmid B, et al. 2012. Fiji: an open-source platform for biological-image analysis. *Nat Methods* 9:676–682.

Serobyan V, Ragsdale EJ, Muller MR, Sommer RJ. 2013. Feeding plasticity in the nematode *Pristionchus pacificus* is influenced by sex and social context and is linked to developmental speed. *Evol Dev* 15:161–170.

Serobyan V, Xiao H, Rödelsperger C, Namdeo S, Röseler W, Witte H, Sommer RJ. 2016. Chromatin remodeling and antisense-mediate up-regulation of the developmental switch gene *eud-1* control predatory feeding plasticity. *Nat Commun* 7:12337.

Siegal ML, Leu J-Y. 2014. On the nature and evolutionary impact of phenotypic robustness mechanisms. *Annu Rev Ecol Evol Syst* 45:496–517.

Siegal ML, Bergman A. 2002. Waddington's canalizationrevisited: developmental stability and evolution. *Proc Natl Acad Sci U S A* 99:10528–10532.

Sommer RJ. 2015. Nematoda. In: Wanninger A, editor. Evolutionary developmental biology of Invertebrates. Heidelberg: Springer. p. 15–34.

Sommer RJ, McGaughran A. 2013. The nematode *Pristionchus pacificus* as a model system for integrative studies in evolutionary biology. *Mol Ecol* 22:2380–2393.

Sommer RJ, Mayer MG. 2015. Towards a synthesis of developmental biology with evolutionary theory and ecology. *Ann Rev Cell DevBiol* 31:453–471.

Stiernagle T. 2016. Maintenance of C. elegans. In: The *C. elegans* Research Community, editor. WormBook. URL: http://www.wormbook.org

Susoy V, Ragsdale EJ, Kanzaki N, Sommer RJ. 2015. Rapid diversification associated with a macroevolutionary pulse of developmental plasticity. *Elife* 4:e05463.

Susoy V, Sommer RJ. 2016. Stochastic and conditional regulation of nematode mouth-form dimorphisms. *Front Ecol Evol* 4:23.

Thomas JH, Birnby DA, Vowels JJ. 1993. Evidence for parallel processing of sensory information controlling dauer formation in *Caenorhabditis elegans*. *Genetics* 134:1105–1117.

Wagner A. 2005. Robustness, evolvability, and neutrality. *Febs Lett* 579:1772–1778.

Wang X, Sommer RJ. 2011. Antagonism of LIN-17/Frizzled and LIN-18/Ryk in nematode vulva induction reveals evolutionary alterations in core developmental pathways. *PLoS Biol* 9:e1001110.

West-Eberhard MJ. 2003. Developmental plasticity and evolution. Oxford; New York: Oxford University Press.

Wilecki M, Lightfoot JW, Susoy V, Sommer RJ. 2015. Predatory feeding behaviour in Pristionchus nematodes is dependent on phenotypic plasticity and induced by serotonin. *J Exp Biol* 218:1306–1313.

Witte H, Moreno E, Rodelsperger C, Kim J, Kim JS, Streit A, Sommer RJ. 2015. Gene inactivation using the CRISPR/Cas9 system in the nematode *Pristionchus pacificus*. *Dev Gen Evol* 225:55–62.

SFig 1. Sequences of identified Hsp90 homologs in *P. pacificus*.

STable 1. Description of landmarks used for geometric morphometric analysis.

STable 2. Accession numbers for sequences used to build the tree in Fig. 3.

Supplementary figure 1

> Contig0-aug306.t1

MAEEQFAFQAEIAQLMSLIINTFYSNKEIFLRELVSNASDALDKIRYQALTEPSELDSGKELYIKITPNKAEKTLTIFDSGI
GMTKADLVNNLGTIAKSGTKAFMEALQAGADISMIGQFGVGFYSAFLVADKVVVTSKHNDDDCHVWESSAGGSF
TVKTVNDPEVTRGTKITMHIKEDQIEYLEERKIKEIIKKHSQFIGYPIKLVVEKEREKEVEDDEADEEKEEKKEGEVENVG
EDEDADKKNEKKTKKIKEKYTEDEELNKQKPIWTRNPDDISNEEYAEFYKSLSNDWEDHLAVKHFSVEGQLEFRALLY
VPQRAPFDLFENKKAKNSIKLYVRRVFIMENCDELMPEYLNFVRGVVDSEDLPLNISREMLQQSKILKVIRKNLVKKCI
ELFEEIAEDKDNFKKFYEHFGKNLKLGIHEDSTNRKKLADFLRYSSSTSGEEVTSLKDYVSRMKENQSQIYYITGESKDA
VANSAFVERVRKGGFEVLYMVDPIDEYCVQQLKEYDGKKLVSVTKEGLELPTSEEQKKKFEEDKVKFENLCKAVKDIL
EKKVEKVAVSERLVSSPCCIVTSEYGWSANMERIMKAQALRDSSTMGYMAAKKHLEINPDHAIIKTLAERVEADKND
KTVKDLVNLLFETALLSSGFTLEDPTQHASRIFRMIKLGLDINEEDEEENLPSGSGVSSDAPKVEGAAEDASRMEEVD*

> Contig13-aug6393.t1

MRSVRSLSRLSRVLSTQIPSARTVQVRLISASPRVLSSSASSTQPERREFQAETAKLLDIVAKSLYSDSEVFVRELISNSSD
AIEKRRLANLDSGESHNGEIKITVDEAKNTIVFQDNGIGMTKDELVSYLGTIAHSGSKAFVQENAEKAENVIGQFGVG
FYSAFMVADRVEVRTRKVGEQSGIQWMWNGGNSYEMSEGVETPEGTTILIHLKKGDAELYAQFLRMKDIIEKYSYF
VSAPIILNEERVNSLNAIWTANPKEVTSDQHDQFFAQLTRMHHPHLQQDRPAYYIHYKADSPLSIRSIMYIPSHRVSQ
MEFATQGEEYGLSLYARRVLIKAKAKELLPKYLRFVIGVVDCEDIPLNLSREMLQNDPVVTKLRRVLTDKILGFFVQQ
MKKDPIKYNDIYKNINLYLKEGIVLEPEQNVKEDIARLLQLETSNSRAGTMTSLTDYISRMQEGQKDIYYMYAPSRQL
AESSPYLEVVKGEGKEVLFLLDPADEVVFLSLGQFKGHNLVSVEKWAEKAEDKTEDKKDERGDKKELYDWVKNTLGS
VNEVKASRRASEHPAMISVQTEMGAARHFLRVGETKGNEHLAFLKPTLHLHLNHPVTEGLLKLRKTDPKTAQLLLEQ
VTVDAL*

> Contig53-aug15143.t1

MTREYCKRGGTNKRRVANAAREAWCALIGRAFCQFSSSFVGVVYSYPTSALGKTEEDFSSSAFIPSSYVLAEDEVEDT
KPAKGTDTEAIQREEDAIKIDGLSGAEVKKLRESAEKHEFQAEVNRMMKLIINSLYRNKEIFLRELISNASDALDKIRLLS
LTNPEVLKATDDMSIKIKCDKEARTLSITDTGVGMTKKDLMNNLGTIARSGTSEFLSKLLDSSTNSETQQDLIGQFGV
GFYSTFLVADRVVVTTKNNDDDQYIWESDSASYTIVKDPRGATLKRGTEITLYLKEEALDFLETKTLENLVHKYSQFINF
NIFQWASKTEEVEEEVEEEEKSEKEDGAVEEEAEKKTKKVQKTTWDWDRVNNVKPIWMRKSAEVEDAEYEDFYKS
VTKDSEKPLAHVHFTAEGEVSFKSILYVPKKSPNDMFQNYGKIMENIKLYVRRVFITDDFNDMMPKYLSFIRGIVDSD
DLPLNVSRENLQQHKLLKVIKKKLVRKVLDMLKKLDGEKFDEFWKEFSTNIKLGVMEDPSNRMRLAKLLRFFSSADAE
KQTTLSAYIERMKDKQEAIFYVAGTSRKEVEQSPFVERLLAKGYEVLFLTEPVDEYCIQAMPEFDGKKFQNVAKEGLNI
DDGEKAKEAQKELEEAFKPLTTWLKENGLKDKIEKAVMSQRLVKTPSALVASSYGWSANMERIMKSQAYAKAKDPT
QDFYMSQKKTLELNPRHPVIKELLKRVESDAEDAKAKFTAQLLFDTATLRSGFSIQDQVEFAERIESILKQSIDVDASA
QVEEEQHIEEDAEEEKKEESEETTVEEEHTEL*

Supplementary table 1

Nr.	Morphological description	Landmark type
1	Anteriormost point of cheilostom on the D side	homologous
2	Posteriormost point of cheilostom on the D side	homologous
3	Anteriormost point of gymnostom on the D side	homologous
4	Posteriormost point of gymnostom on the D side	homologous
5	Anteriormost point of prostegostom on the D side	homologous
6	Extreme point of the concave part of the D surface of the D tooth	sliding
7	Extreme point of convex part of the D surface of the D tooth	sliding
8	Tip of the D tooth	homologous
9	Opening of the D pharyngeal gland	homologous
10	Extreme point of the convex part of the V surface of the D tooth	sliding
11	Junction point between the D tooth and the RVSL tooth/ridge	homologous
12	D base point of the hook of the RVSL tooth or of denticle of the RVSL ridge	sliding
13	Tip of the hook of the RVSL tooth or of denticle of the RVSL ridge	homologous
14	V base point of the hook of the RVSL tooth or of the denticle on the RVSL ridge	sliding
15	V base point of the RVSL tooth/ridge	homologous
16	Posteriormost point of gymnostom on the V side	homologous
17	Anteriormost point of prostegostom on the V side	homologous
18	Anteriormost point of gymnostom on the V side	homologous
19	Posteriormost point of cheilostom on the V side	homologous
20	Anteriormost point of cheilostom on the D side	homologous

D = dorsal
V = ventral
RVSL = right ventrosublateral

Supplementary table 2

Accession number	Name	Species
NP_415006.1	HtpG1	*Escherichia coli (Eco)*
NP_631561.1	-	*Streptomyces coelicor (Sco)*
XP_483065.1	-	*Oryza sativa (Osa)*
BAA90487.1	-	*Oryza sativa (Osa)*
XP_007252444.1	-	*Astyanax mexicanus (Ame)*
NP_003290.1	GRP94	*Homo sapiens (Hsa)*
CDW52501.1	-	*Trichuris trichiura (Ttr)*
XP_003379158.1	-	*Trichinella spiralis (Tsp)*
ETN77129.1	-	*Necator americanus (Nam)*
Contig53-aug15143.t1	-	*Pristionchus pacificus (Ppa)*
scaffold47-pex_aug2013-20083.t1		*Pristionchus exspectatus (Pex)*
NP_001255536.1	ENPL-1	*Caenorhabditis elegans (Cel)*
XP_003107918.1	CRE_12564	*Caenorhabditis remanei (Cre)*
NP_651601.1	GP93	*Drosophila melanogaster (Dme)*
P15108.4	HSC82	*Saccharomyces cerevisiae (Sce)*
CAA97961.1	HSP82	*Saccharomyces cerevisiae (Sce)*
1908431A	HSP90-1	*Arabidopsis thaliana (Ath)*
XP_470993.1	-	*Oryza sativa (Osa)*
XP_483191.1	-	*Oryza sativa (Osa)*
BAD33406.1	-	*Oryza sativa (Osa)*
XP_007255550.1	-	*Astyanax mexicanus (Ame)*
P08238.4	HSP90B	*Homo sapiens (Hsa)*
P07900.5	HSP90A	*Homo sapiens (Hsa)*
NP_001278186.1	-	*Astyanax mexicanus (Ame)*
XP_007230794.1	-	*Astyanax mexicanus (Ame)*
XP_003374556.1	-	*Trichinella spiralis (Tsp)*
CDW54307.1	-	*Trichuris trichiura (Ttr)*
CEF62896.1	-	*Strongyloides ratti (Sra)*
ACO55134.1	-	*Ascaris suum (Asu)*
CDP96098.1	DAF-21	*Brugia malayi (Bma)*
Contig0-aug306.t1	DAF-21	*Pristionchus pacificus (Ppa)*
scaffold333-pex_aug2013-15553.t1		*Pristionchus exspectatus (Pex)*
NP_506626.1	DAF-21	*Caenorhabditis elegans (Cel)*
XP_002637777.1	DAF-21	*Caenorhabditis briggsae (Cbr)*
XP_003102316.1	DAF-21	*Caenorhabditis remanei (Cre)*
NP_523899.1	HSP83	*Drosophila melanogaster (Dme)*
KFD57704.1	-	*Trichuris suis (Tsu)*
XP_003368967.1	-	*Trichinella spiralis (Tsp)*
AAD29307.2	TRAP1	*Drosophila melanogaster (Dme)*
NP_057376.2	TRAP1	*Homo sapiens (Hsa)*
CAP22043.2	CBG00585	*Caenorhabditis briggsae (Cbr)*
NP_741220.2	R151.7	*Caenorhabditis elegans (Cel)*
XP_003093981.1	CRE_16358	*Caenorhabditis remanei (Cre)*
CDJ82371.1	-	*Haemonchus contortus (Hco)*
EYC32040.1	-	*Ancylostoma ceylianicum (Ace)*
XP_003141395.1	-	*Loa loa (Llo)*
ERG82742.1	-	*Ascaris suum (Asu)*
Contig13-aug6393.t1	-	*Pristionchus pacificus (Ppa)*
scaffold448-pex_aug2013-19547.t1	-	*Pristionchus exspectatus (Pex)*

frontiers in Genetics

REVIEW
published: 11 September 2018
doi: 10.3389/fgene.2018.00382

Developmental Plasticity and Robustness of a Nematode Mouth-Form Polyphenism

*Bogdan Sieriebriennikov and Ralf J. Sommer**

Max Planck Institute for Developmental Biology, Department of Integrative Evolutionary Biology, Tübingen, Germany

In the last decade, case studies in plants and animals provided increasing insight into the molecular mechanisms of developmental plasticity. When complemented with evolutionary and ecological analyses, these studies suggest that plasticity represents a mechanism facilitating adaptive change, increasing diversity and fostering the evolution of novelty. Here, we summarize genetic, molecular and evolutionary studies on developmental plasticity of feeding structures in nematodes, focusing on the model organism *Pristionchus pacificus* and its relatives. Like its famous cousin *Caenorhabditis elegans*, *P. pacificus* reproduces as a self-fertilizing hermaphrodite and can be cultured in the laboratory on *E. coli* indefinitely with a four-day generation time. However, in contrast to *C. elegans*, *Pristionchus* worms show more complex feeding structures in adaptation to their life history. *Pristionchus* nematodes live in the soil and are reliably found in association with scarab beetles, but only reproduce after the insects' death. Insect carcasses usually exist only for a short time period and their turnover is partially unpredictable. Strikingly, *Pristionchus* worms can have two alternative mouth-forms; animals are either stenostomatous (St) with a single tooth resulting in strict bacterial feeding, or alternatively, they are eurystomatous (Eu) with two teeth allowing facultative predation. Laboratory-based studies revealed a regulatory network that controls the irreversible decision of individual worms to adopt the St or Eu form. These studies revealed that a developmental switch controls the mouth-form decision, confirming long-standing theory about the role of switch genes in developmental plasticity. Here, we describe the current understanding of *P. pacificus* mouth-form regulation. In contrast to plasticity, robustness describes the property of organisms to produce unchanged phenotypes despite environmental perturbations. While largely opposite in principle, the relationship between developmental plasticity and robustness has only rarely been tested in particular study systems. Based on a study of the Hsp90 chaperones in nematodes, we suggest that robustness and plasticity are indeed complementary concepts. Genetic switch networks regulating plasticity require robustness to produce reproducible responses to the multitude of environmental inputs and the phenotypic output requires robustness because the range of possible phenotypic outcomes is constrained. Thus, plasticity and robustness are actually not mutually exclusive, but rather complementary concepts.

Keywords: ***Pristionchus pacificus*, developmental plasticity, robustness, switch genes, Hsp chaperones, *Caenorhabditis elegans***

OPEN ACCESS

Edited by:
Jean-Michel Gibert,
Centre National de la Recherche Scientifique (CNRS), France

Reviewed by:
Adrienne H. K. Roeder,
Cornell University, United States
Morris Maduro,
University of California, Riverside, United States

***Correspondence:**
Ralf J. Sommer
ralf.sommer@tuebingen.mpg.de

Specialty section:
This article was submitted to Epigenomics and Epigenetics, a section of the journal Frontiers in Genetics

Received: *20 July 2018*
Accepted: *27 August 2018*
Published: *11 September 2018*

Citation:
Sieriebriennikov B and Sommer RJ (2018) Developmental Plasticity and Robustness of a Nematode Mouth-Form Polyphenism. Front. Genet. 9:382. doi: 10.3389/fgene.2018.00382

INTRODUCTION

Phenotypic plasticity is a feature of development whereby identical genotypes generate different phenotypes upon perception of environmental input (West-Eberhard, 2003). Examples of plasticity are ubiquitous and in extreme cases the alternative phenotypes produced are discrete, such as the various caste systems in social insects (Abouheif and Wray, 2002). However, the evolutionary significance of phenotypic plasticity is still widely debated. One view is that plasticity hampers evolution by enabling adaptation without genetic assimilation (Price et al., 2003). Conversely, the so called "flexible stem hypothesis" suggests a possibility that a phase of plasticity may be an obligatory step in the evolution of novel traits, whereby their expression remains conditional in the beginning before it becomes fully integrated into the development and fixed (Gibert, 2017). It is unknown in how many instances the origination of novel traits has followed this pattern, because careful phylogenetic studies of novel traits using the comparative method are scarce. Nonetheless, plasticity may increase evolutionary change through the simultaneous employment of multiple developmental pathways. Since every alternative pathway is only expressed in a fraction of the population or in a limited number of generations, selective constraints are relaxed and mutations can accumulate more quickly, thereby accelerating evolution (West-Eberhard, 2005; Susoy et al., 2015). Together, this makes phenotypic plasticity an important concept in both developmental and evolutionary biology.

Another fundamental feature of development is robustness, which is defined as the ability to generate identical phenotypes in the face of environmental perturbations and genetic variation (Wagner, 2005). Apart from the obvious role in maintaining the function of the organism under challenging conditions, robustness is argued to accelerate evolution by enabling accumulation of cryptic variation, which can be subsequently released and become material for selection (Rutherford and Lindquist, 1998; de Visser et al., 2003). Since the definition of plasticity entails sensitivity to the environment, whereas the definition of robustness entails insensitivity to it, the two phenomena are often contrasted. And yet, both plasticity and robustness have been suggested to accelerate evolution by releasing selective constraints – plasticity through conditional expression and robustness through concealing mutations from the forces of selection. This enigmatic relationship prompts the question if the two phenomena may, in fact, be complementary rather than opposing.

Much of the discussion on the significance of plasticity and robustness for evolutionary change is based on theoretical arguments. In contrast, few experimental case studies address the molecular, genetic, and developmental mechanisms underlying these phenomena. Even more importantly, only a few experimental studies have investigated the potential crosstalk between plasticity and robustness simultaneously in the same study system. This is surprising as arguably knowledge about the mechanisms of plastic development can help address the interplay between plasticity and robustness in a more nuanced way than simply contrasting the two phenomena. The existence of a genetic control of plasticity and, therefore, the involvement of developmental switch gene networks and the execution gene network as separate developmental modules has long been debated (Bradshaw, 1965; Schlichting and Pigliucci, 1993; West-Eberhard, 2003). Developmental switches are genes that can change the developmental trajectory (Mather and de Winton, 1941; Ptashne et al., 1980). They do so by activating one or the other set of genes required for an alternative developmental pathway – sets, which we refer to as execution gene networks. For example, feminizing transcription factors *Sex-lethal* and *tra-1* act as developmental switches in *Drosophila* and *Caenorhabditis elegans*, respectively, because the level of their activity determines whether the animal will develop as a male or as a female/hermaphrodite. The targets of these switch genes are gene execution networks that generate traits typical of one or the other sex (Hodgkin, 1987; Bell et al., 1988). In this example, the developmental choice is mandatory and determined chromosomally, but studies on the genetic regulation of plasticity also confirmed the long-standing prediction about the involvement of switch genes in plastic development (for recent comprehensive reviews, see Fielenbach and Antebi, 2008; Projecto-Garcia et al., 2017; Sommer et al., 2017) (**Figure 1A**). Therefore, we suggest that the question of robustness of plastic traits can be addressed at two levels and that indeed robustness and plasticity are complementary concepts. First, genetic switch networks regulating plasticity require robustness to produce reproducible responses to the multitude of environmental inputs. Second, the phenotypic output requires robustness because the range of possible phenotypic outcomes is constrained. In the following we concentrate on a case study in a nematode, which explores the interplay between plasticity and robustness.

GENETICS OF PLASTICITY: CONTINUOUS VS. DISCRETE PHENOTYPES

In theory, the relationship between plasticity and robustness can be interrogated in any organism, however, some experimental systems possess features which greatly facilitate such studies. These features are, first, availability of isogenic lines, which simplify the genetics of the study system, and second, discreteness of alternative phenotypes. Specifically, studying genetically uniform individuals offers the possibility to unambiguously separate plasticity from polymorphisms generated by different genetic variants. As for the ability to generate discrete, as opposed to continuous, alternative phenotypes, such an ability potentially allows a sharper contrast between a constrained phenotypic distribution and conditions when developmental buffering is impaired and atypical phenotypes are produced.

More importantly, the hypothesis that genetic switch networks and phenotype execution networks are separate developmental modules whose robustness is provided by different mechanisms can only be explicitly tested in organisms in which impairment of the binary switches can be disentangled from expansion or displacement of the phenotypic distribution. Although a series of developmental switches is thought to underlie both

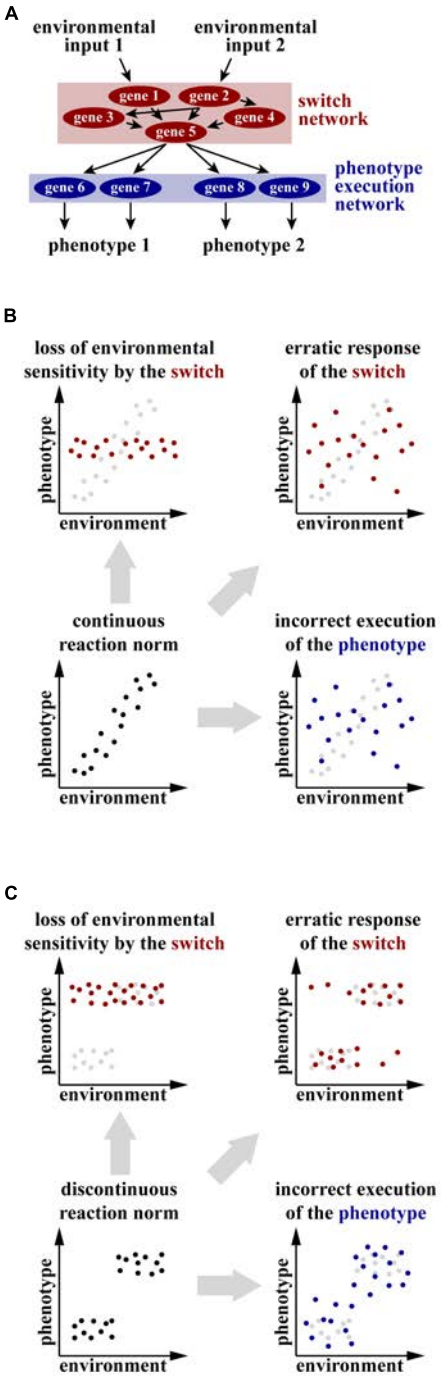

FIGURE 1 | (A) Conceptual mechanism of the genetic regulation of plastic development. Environmental inputs are processed and integrated by a network of genes, referred to as switch genes. The switch network takes a decision to activate one of the alternative developmental programs and passes the signal down to a genetic network that executes the selected phenotype. **(B,C)** Hypothetical scenarios of change in the reaction norm of a continuously **(B)** or discontinuously **(C)** plastic trait in the conditions when the switch network or the phenotype execution network is impaired. The original distribution of phenotypes is shown in black in the foreground or gray in the background, altered distribution resulting from impairment of the switch network is shown in red and altered distribution resulting from incorrect execution of the phenotype is shown in blue.

continuous and discontinuous distributions of plastic phenotypes (West-Eberhard, 2003), phenotypic changes resulting from the manipulation of the switch and of the structural genes can be interpreted in different ways depending on the distribution of phenotypes. In the case of continuous traits, inactivation of genes channeling and integrating environmental inputs (the switch network) can either constrain the phenotypic distribution through a decrease in sensitivity to an inducing signal, or make it more variable as a consequence of improper integration of various environmental signals (**Figure 1B**). At the same time, tampering with the gene network executing the phenotype will also increase the variance of the phenotypic distribution (**Figure 1B**). Thus, developmental perturbations at the same level can potentially lead to different phenotypic outcomes, while manipulating different gene networks can lead to similar change. Together, this obscures the potential interplay between plasticity and robustness when continuously plastic traits are studied.

In contrast, manipulation of the switch and the execution networks will change the phenotypic distribution of discrete traits in a different manner. Interfering with the switch network will only affect the distribution of individual phenotypes *between* the discrete clusters, whereby the most extreme case would be the absence of individuals from some clusters (corresponding, e.g., to a loss of a morph). However, the distribution of phenotypes *within* the clusters is expected to be constant (**Figure 1C**). In contrast, loss of robustness of the gene network executing the phenotype is expected to affect the phenotypic distribution *within* the clusters (**Figure 1C**). Thus, only using organisms exhibiting discrete plasticity as a study model allows falsification of the hypothesis that plastic traits require robustness of both the switch and the execution gene network.

THE STUDY SYSTEM: *Pristionchus pacificus* MOUTH-FORM PLASTICITY

The nematode *Pristionchus pacificus* is a dimorphic species that belongs to the same order as the classical model *C. elegans* and shares its amenability to genetic manipulation, as well as the hermaphroditic mode of reproduction, which enables creation of isogenic lines (Sommer and McGaughran, 2013). Depending on the culture conditions, genetically identical individuals of *P. pacificus* can develop into two morphs – eurystomatous (Eu) (literally "wide-mouthed") and stenostomatous (St) ("narrow-mouthed") morphs. Eu animals possess a wide buccal cavity with two hooked teeth, which worms can use to kill other nematodes (**Figures 2A,B**). In contrast, the buccal cavity in St animals is narrow, the dorsal tooth is flint-shaped and the right ventrosublateral tooth is reduced to a cuticular ridge with a minute denticle (**Figure 2C**), which precludes killing, leaving such animals as obligatory microbial grazers (Bento et al., 2010; Wilecki et al., 2015). The decision on mouth-form development is taken during larval development and is irreversible in the adult stage (Serobyan et al., 2013). The developmental decision is influenced by the presence of pheromones, diet composition and the state of the culture medium (solid vs. liquid) (Bose et al., 2012; Sanghvi et al., 2016; Werner et al., 2017) (**Figure 2D**).

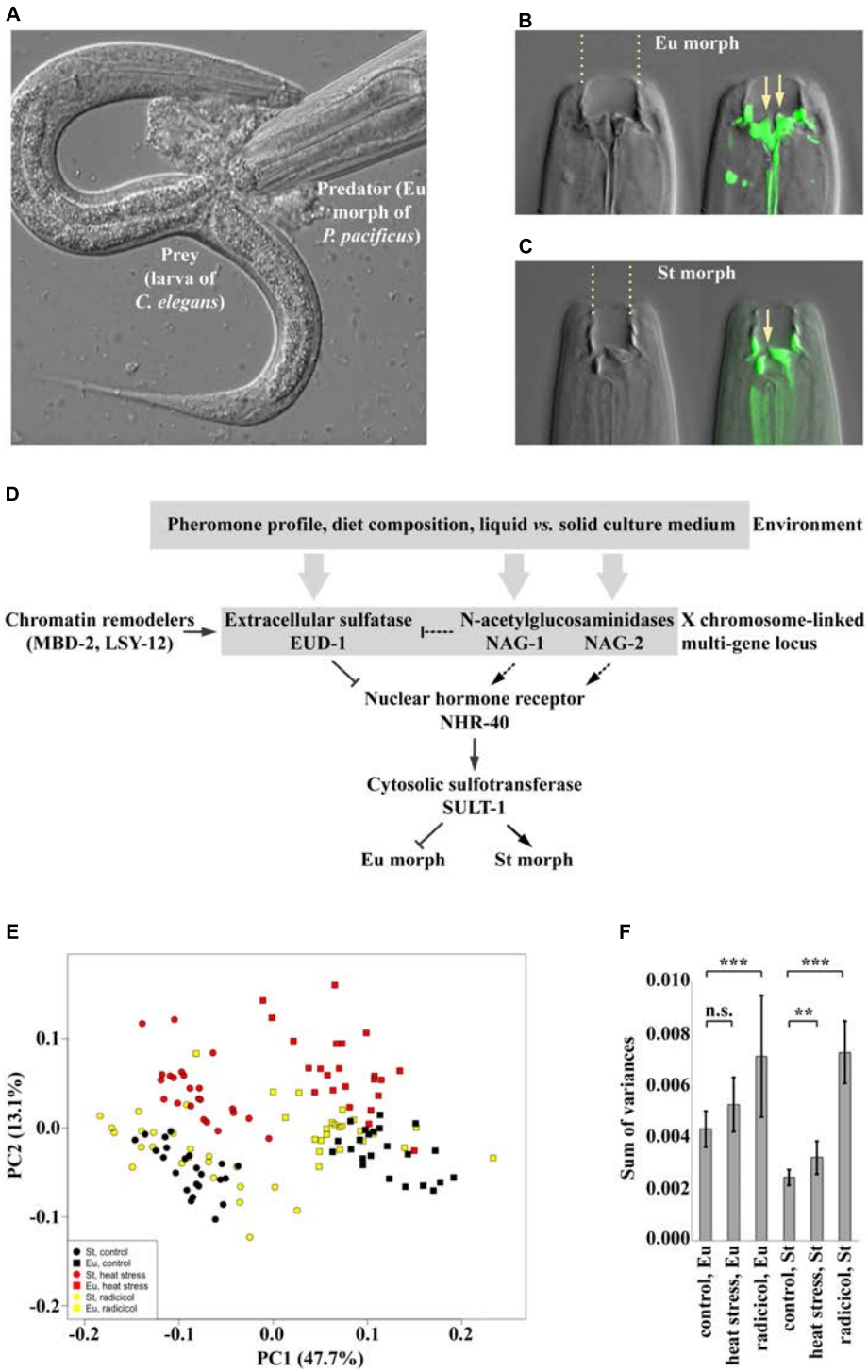

FIGURE 2 | (A) The eurystomatous morph of *P. pacificus* devouring a larva of *C. elegans*. **(B,C)** The mouth of the eurystomatous **(B)** and of the stenostomatous **(C)** morph. On the left, differential interference contrast (DIC) image. On the right, overlay of the DIC image and an image of fluorescein-stained cuticle at the base of the buccal cavity, which includes teeth. Arrows point at the tips of teeth. **(D)** Current model of the regulation of mouth-form plasticity in *P. pacificus*. The genes shown are part of the switch network, i.e., mutations in these genes only change the frequencies of alternative phenotypes in the population. **(E,F)** Phenotypic effects caused by impairment of Hsp90 heat shock proteins, which are known to provide robustness to phenotype execution networks. In these conditions, both morphs are still produced but the morphologies are abnormal. **(E)** PCA ordination of sets of landmarks representing control individuals and individuals exposed to heat stress and treatment by radicicol, a pharmacological inhibitor of Hsp90. **(F)** Morphological disparity within different groups shown in the PCA ordination in panel **E**. Error bars show *SD*. n.s., not significant (P-value > 0.05); $^{**}P$-value < 0.01; $^{***}P$-value < 0.001. Panels E and F reproduced from Sieriebriennikov et al. (2017).

Importantly, changing environmental conditions only alters the ratio between the phenotypes in populations, whereas intermorphs are extremely scarce. Together, these conditions make *P. pacificus* mouth-form plasticity an ideal study system to investigate the genetics, molecular biology and epigenetics of developmental plasticity and, building on the availability of such mechanistic insight, the potential relationship between plasticity and robustness.

Recent studies on the genetics of mouth-form plasticity in *P. pacificus* began to elucidate how the developmental decision is controlled. Forward and reverse genetic experiments implicated a locus on the X chromosome in switching between phenotypes (**Figure 2D**). This locus contains three functionally relevant genes, which are expressed in sensory and interneurons and which affect the phenotype ratio in the opposite manner. Specifically, the gene *eud-1* encodes an extracellular sulfatase and promotes the Eu morph, whereas *nag-1* and its paralog *nag-2* encode α-N-acetylgalactosaminidases, which additively promote the St morph (Ragsdale et al., 2013; Sieriebriennikov et al., 2018). Furthermore, the chromatin remodelers MBD-2, a methyl binding protein, and LSY-12, a histone acetyltransferase regulate *eud-1* levels (Serobyan et al., 2016; Serobyan and Sommer, 2017). The downstream transcription factor in the switch network is NHR-40, and the cytosolic sulfotransferase SULT-1 presumably acts downstream of *nhr-40* (Kieninger et al., 2016; Namdeo et al., 2018). Similar to manipulating environmental conditions, the manipulation of genes in this switch network only affects the ratio between the alternative morphs produced, but the morphologies of individual morphs remain intact. For example, *eud-1* mutant animals are all-St, whereas *nag-1 nag-2* double mutants are all-Eu. It is important to note that the current information on the genetic network is likely to be incomplete for several potential reasons. For example, genes that are part of the execution network might have essential functions earlier in development and as such, would go unnoticed in genetic screens as their phenotype would be lethal. Nonetheless, this genetic network for *P. pacificus* mouth-form plasticity provides a genetic and molecular platform for studying environmental influences, the evolution of plasticity and its relationship with robustness.

ROBUSTNESS OF DEVELOPMENTAL SWITCHES

We suggested that plastic traits require the robustness of the switch network and of the network producing the phenotype (**Figure 1A**). The switch network integrates all the relevant environmental signals and takes the developmental decision, during which it faces several challenges. First, multiple contradictory environmental inputs can be perceived simultaneously. For example, the pheromone *dasc#1* induces the Eu morph in *P. pacificus*, whereas consumption of the yeast *Cryptococcus albidus* represses it (Bose et al., 2012; Sanghvi et al., 2016). Additionally, the developmental decision is often not taken instantaneously. Instead, the environmental signals accumulate over a prolonged time period, such as in *P. pacificus*, in which crowding has influence on the mouth-form ratio during all larval instars after hatching (Serobyan et al., 2013). Finally, development is inherently noisy and the precision of developmental decision-making processes, such as morphogen gradients, is generally limited (Gregor et al., 2007). Therefore, the ability to generate reproducible responses to multiple and potentially contradicting environmental inputs, while staying insensitive to noise, is crucial for developmental switches.

Such an ability is believed to be an intrinsic property of the architecture of gene regulatory networks (Masel and Siegal, 2009), with known examples in both vertebrates and invertebrates. For instance, the ecdysone receptor EcR in *Drosophila* positively regulates its own transcription and small fluctuations in ecdysone level or spontaneous transcriptional bursts could lead to a premature self-amplifying response (Herranz and Cohen, 2010). This is prevented by a negative feedback loop between EcR and microRNA miR-14. When the level of ecdysone is low, miR-14 represses the expression of the *EcR* gene, which ensures that EcR does not self-activate and remains poised for response to the elevated level of the hormone (Varghese and Cohen, 2007). An additional example is the circuit regulating neuronal subtype specification in mice in response to Sonic Hedgehog signaling, dissection of which revealed a network that consists of the transcription factors Olig2, Nkx2.2, and Pax6 connected with feedback and feedforward loops (Balaskas et al., 2012). Experiments with knockout lines and *in silico* modeling showed that negative feedback loops in the network provide robustness to small signal fluctuations, such that the network can respond to the morphogen by generating a highly reproducible pattern despite developmental noise (Gregor et al., 2007).

In *P. pacificus*, a phenomenon dependent on the robustness of the switch network during the regulation of mouth-form plasticity is the stochasticity of the phenotypic output. Although the phenotypic implementation of plasticity in this species is binary under normal circumstances, and as such intermediate morphs are extremely rare, there is apparent stochasticity as to which morph is finally adopted by an individual. The proportion of Eu morphs on agar plates under standard laboratory conditions fluctuates between 70 and 98%, even though all animals are genetically identical and grow in the same environment (Ragsdale et al., 2013; Werner et al., 2017). This pattern is consistent with the theoretical expectation of the phenotypic distribution produced by erratic action of the switch network (**Figure 1C**).

It is possible that such stochasticity is adaptive and represents a bet-hedging strategy – as the developmental decision is irreversible, it may be advantageous to always have some individuals of the underrepresented morph in the population in case the environmental conditions change more rapidly than a new generation can grow and develop suitable phenotypes (Losick and Desplan, 2008; Susoy and Sommer, 2016). In general, bet-hedging strategies are well-known in microbes that often face unpredictable environments (Veening et al., 2008). While the exact mechanism of how such stochasticity is generated is unknown, the gene regulatory network regulating plasticity may be susceptible to noise or it may even have a special mechanism to convert noise into phenotypic response. For example, cells forming sensory organ precursors in *Drosophila* are randomly

selected from a field of equipotent cells due to noisy expression of the transcription factor Senseless, followed by lateral inhibition of the neighboring cells (Jafar-Nejad et al., 2003). In such cases, sensitivity to developmental noise may be advantageous for the organism.

The alternative view is that the response of the gene network is robust to noise and the apparent stochasticity in the phenotypic outcome results from environmental micro-heterogeneity. Indeed, there are known examples of seemingly stochastic plastic outputs when the environmental conditions approach the so called "neutral point," i.e., a set of conditions near the threshold zone of responsiveness (Nijhout, 1975; Emlen, 1996; West-Eberhard, 2003). In such a case, reactiveness to the environment is still robust, but only a fraction of organisms happens to experience the amount of combined inducing signal above the threshold value. However, given our current knowledge it is difficult to disentangle between the two scenarios. Therefore, additional studies are needed to demonstrate if mechanisms converting developmental noise to stochastic phenotypic output exist in *P. pacificus*. Nevertheless, the seemingly stochastic action of the switch network does not lead to the production of intermediate morphologies, corroborating our expectation that studying discontinuous plasticity allows to disentangle the robustness of the switch network and the robustness of the phenotype.

ROBUSTNESS OF THE PHENOTYPE

Several mechanisms were suggested to buffer the development of both invariable and plastic traits against stochastic environmental and genetic variation. The best studied mechanism is provided by heat shock proteins of the Hsp90 family. A naive idea that chaperones maintain normal functioning of cells because they can refold proteins destabilized by weakly deleterious mutations or by environmental influences prompted a wave of experiments in various organisms, which showed that cryptic variation is indeed uncovered once the Hsp90 function is compromised (Rutherford and Lindquist, 1998; Queitsch et al., 2002; Rohner et al., 2013). Interestingly, subsequent studies provided evidence that the role of Hsp90 proteins may be more complex than simply exhibiting chaperone activity. Namely, they were implicated in the regulation of piRNA production, which in turn may silence deleterious gene variants (Gangaraju et al., 2011). Further research in yeast, animals and plants demonstrated that complementary mechanisms also exist. For example, the prion form [PSI^{+}] of the translation release factor Sup35 in *Saccharomyces* yeasts allows stop codon readthrough and thus releases the cryptic genetic variation accumulated in the 3′ untranslated regions of genes (Masel and Griswold, 2009). In *C. elegans*, the remarkable reproducibility of the division pattern of seam cells (epidermal stem cells) is provided by the action of a basic helix-loop-helix (bHLH) transcription factor LIN-22 (Katsanos et al., 2017). In *Arabidposis*, robust timing and positioning of organs on the stem is generated by a common action of two hormone-based fields (Besnard et al., 2014). In addition to studies on single genes, simulations of complex gene networks, followed by large-scale mutant screens, demonstrated that functional knockdowns of 5% of all genes in *S. cerevisiae* decrease phenotypic robustness (Bergman and Siegal, 2003; Levy and Siegal, 2008; Bauer et al., 2015). Studies of developmental stability in recombinant inbred lines in *Arabidopsis thaliana* also unraveled multiple quantitative trait loci (QTL) associated with robustness against genetic and environmental variation (Hall et al., 2007; Fu et al., 2009). Nevertheless, heat shock proteins remain the best studied capacitors of morphological variation to date. Importantly, the emergence of aberrant phenotypes after developmental buffering by Hsp90 is alleviated was observed in laboratory populations of *Drosophila* and *Arabidopsis*, which are nearly isogenic (Rutherford and Lindquist, 1998; Queitsch et al., 2002). This indicates that not only cryptic genetic variation, but also environmental micro-heterogeneity and developmental noise are likely sources of stochastic variation buffered by heat shock proteins.

The proposed independence of the phenotypic buffering from the action of the switch suggests that the inhibition of the Hsp90 machinery in *P. pacificus* should lead to a change in the distribution of mouth morphologies, whereby the Eu and St morphs could nevertheless still be distinguishable even if distorted (**Figure 1C**). To visualize the extent of morphological differences between individuals, morphologies can be quantified using geometric morphometric analysis. As expected, in *P. pacificus* and other dimorphic species of the same nematode family, the Eu and St morphs form separate clusters in the morphospace with no overlap (Susoy et al., 2015). In accordance with the prediction, manipulation of Hsp90 activity through life-long exposure to elevated temperature, pharmacological inhibition or knockout of the Hsp90-encoding gene *daf-21* increased the morphological variation of the Eu and St morphs in *P. pacificus* (Sieriebriennikov et al., 2017) (**Figures 2E,F**). Specifically, rearing animals at the highest sublethal temperature displaced the distribution of the mouth morphologies in the morphospace, an effect that was observable in both morphs. In contrast, applying the pharmacological inhibitor of Hsp90 function induced expansion of morphology distributions without any evident shift. Finally, *daf-21*/Hsp90 knockout generated using CRISPR/Cas9 resulted in a combined effect, whereby the distribution of morphologies was displaced in the morphospace and morphological disparity was increased (**Figures 2E,F**). These observations demonstrate that the mechanism that provides developmental buffering against genetic and environmental perturbations acts to canalize the development of the discrete morphs in *P. pacificus*. Importantly, although some treated animals exhibited intermediate morphologies, most individuals could still be classified into Eu and St. Additionally, introduction of the *daf-21*/Hsp90 mutation in the Eu-constitutive *nhr-40* mutant line did not lead to the appearance of St animals, but only increased the morphological variation of the Eu morphs (Sieriebriennikov et al., 2017). This finding strongly supports the hypothesis that the two types of robustness of plastic traits described here – robustness of environmental responsiveness and robustness of phenotypic output – are provided by at least partially non-overlapping mechanisms.

CONCLUSION

In summary, the *P. pacificus* mouth-form polyphenism allows two major conclusions with regard to the relationship of plasticity and robustness. First, we propose that robustness and plasticity are complementary rather than opposing phenomena. Second, we argue that knowledge about the mechanisms of plastic development enables formulation of testable hypotheses about the interplay between plasticity and robustness. Specifically, separation between the developmental switch gene network and the gene network executing the selected phenotype (**Figure 1A**) strongly suggests that plastic traits require robustness at two levels. Firstly, the switch network must generate a robust response to the multitude of environmental inputs despite developmental noise and other stochastic perturbations. Secondly, the execution network must generate a robust phenotypic outcome within a constrained range of possible phenotypes.

To demonstrate how these questions can be addressed, we use an example of a self-fertilizing nematode that exhibits a discrete plasticity of feeding structures. In *P. pacificus*, manipulation of culture conditions or introduction of mutations in the switch network only influences the ratio between the morphs and not the alternative morphologies themselves, supporting the long-standing prediction that the switch genetic network is developmentally independent from the network involved in building the morphologies. We discuss the phenomenon of apparent stochasticity of morph ratios in fixed culture conditions, which was previously suggested to be a bet-hedging strategy, and propose that it may be linked to limited robustness of the switch network to developmental noise. Importantly, such stochasticity only affects the morph ratios and not the morphology. Further, we discuss experiments in which developmental buffering by Hsp90 was compromised, which changed the distribution of morphologies of both morphs. Yet, both morphs were still produced even though their ratio was somewhat shifted. Together, these observations corroborate our hypothesis that robustness of the switch and robustness of the execution network are provided by at least partially non-overlapping mechanisms.

While our knowledge of plastic development of the feeding structures in *P. pacificus* is far from being complete, the approaches discussed here pave the way to reconcile plasticity and robustness. Both phenomena are suggested to promote evolution and more mechanistic studies are necessary to elucidate the genetic and physical basis of their interaction. Therefore, we would like to encourage similar studies in other models, which will verify our conceptualizations and provide new insight into addressing the relationship between plasticity and robustness, and their role in evolution.

AUTHOR CONTRIBUTIONS

BS and RS conceived and wrote the manuscript.

FUNDING

The authors were financially supported by the Max Planck Society.

ACKNOWLEDGMENTS

We would like to thank Dr. Michael Werner and Ms. Sara Wighard for their comments on the manuscript.

REFERENCES

Abouheif, E., and Wray, G. A. (2002). Evolution of the gene network underlying wing polyphenism in ants. *Science* 297, 249–252. doi: 10.1126/science.1071468

Balaskas, N., Ribeiro, A., Panovska, J., Dessaud, E., Sasai, N., Page, K. M., et al. (2012). Gene regulatory logic for reading the sonic hedgehog signaling gradient in the vertebrate neural tube. *Cell* 148, 273–284. doi: 10.1016/j.cell.2011.10.047

Bauer, C. R., Li, S., and Siegal, M. L. (2015). Essential gene disruptions reveal complex relationships between phenotypic robustness, pleiotropy, and fitness. *Mol. Syst. Biol.* 11:773. doi: 10.15252/msb.20145264

Bell, L. R., Maine, E. M., Schedl, P., and Cline, T. W. (1988). *Sex-lethal*, a *Drosophila* sex determination switch gene, exhibits sex-specific RNA splicing and sequence similarity to RNA binding proteins. *Cell* 55, 1037–1046. doi: 10.1016/0092-8674(88)90248-6

Bento, G., Ogawa, A., and Sommer, R. J. (2010). Co-option of the hormone-signalling module dafachronic acid-DAF-12 in nematode evolution. *Nature* 466, 494–499. doi: 10.1038/nature09164

Bergman, A., and Siegal, M. L. (2003). Evolutionary capacitance as a general feature of complex gene networks. *Nature* 424, 549–552. doi: 10.1038/nature01765

Besnard, F., Refahi, Y., Morin, V., Marteaux, B., Brunoud, G., Chambrier, P., et al. (2014). Cytokinin signalling inhibitory fields provide robustness to phyllotaxis. *Nature* 505, 417–421. doi: 10.1038/nature12791

Bose, N., Ogawa, A., von Reuss, S. H., Yim, J. J., Ragsdale, E. J., Sommer, R. J., et al. (2012). Complex small-molecule architectures regulate phenotypic plasticity in a nematode. *Angew. Chem. Int. Ed. Engl.* 51, 12438–12443. doi: 10.1002/anie.201206797

Bradshaw, A. D. (1965). "Evolutionary significance of phenotypic plasticity in plants," in *Advances in Genetics*, eds E. W. Caspari and J. M. Thoday (Cambridge, MA: Academic Press), 115–155.

de Visser, J. A. G. M., Hermisson, J., Wagner, G. P., Ancel Meyers, L., Bagheri-Chaichian, H., Blanchard, J. L., et al. (2003). Perspective: evolution and detection of genetic robustness. *Evolution* 57, 1959–1972. doi: 10.1111/j.0014-3820.2003.tb00377.x

Emlen, D. J. (1996). Artificial selection on horn length-body size allometry in the horned beetle *Onthophagus acuminatus* (Coleoptera: Scarabaeidae). *Evolution* 50, 1219–1230. doi: 10.1111/j.1558-5646.1996.tb02362.x

Fielenbach, N., and Antebi, A. (2008). *C. elegans* dauer formation and the molecular basis of plasticity. *Genes Dev.* 22, 2149–2165. doi: 10.1101/gad.1701508

Fu, J., Keurentjes, J. J. B., Bouwmeester, H., America, T., Verstappen, F. W. A., Ward, J. L., et al. (2009). System-wide molecular evidence for phenotypic buffering in *Arabidopsis*. *Nat. Genet.* 41, 166–167. doi: 10.1038/ng.308

Gangaraju, V. K., Yin, H., Weiner, M. M., Wang, J. Q., Huang, X. A., and Lin, H. F. (2011). *Drosophila* Piwi functions in Hsp90-mediated suppression of phenotypic variation. *Nat. Genet.* 43, 153–158. doi: 10.1038/ng.743

Gibert, J.-M. (2017). The flexible stem hypothesis: evidence from genetic data. *Dev. Genes Evol.* 227, 297–307. doi: 10.1007/s00427-017-0589-0

Gregor, T., Tank, D. W., Wieschaus, E. F., and Bialek, W. (2007). Probing the limits to positional information. *Cell* 130, 153–164. doi: 10.1016/j.cell.2007.05.025

Hall, M. C., Dworkin, I., Ungerer, M. C., and Purugganan, M. (2007). Genetics of microenvironmental canalization in *Arabidopsis thaliana*. *Proc. Natl. Acad. Sci. U.S.A.* 104, 13717–13722. doi: 10.1073/pnas.0701936104

Herranz, H., and Cohen, S. M. (2010). MicroRNAs and gene regulatory networks: managing the impact of noise in biological systems. *Genes Dev.* 24, 1339–1344. doi: 10.1101/gad.1937010

Hodgkin, J. (1987). A genetic analysis of the sex-determining gene, *tra-1*, in the nematode *Caenorhabditis elegans*. *Genes Dev.* 1, 731–745. doi: 10.1101/gad.1.7.731

Jafar-Nejad, H., Acar, M., Nolo, R., Lacin, H., Pan, H., Parkhurst, S. M., et al. (2003). Senseless acts as a binary switch during sensory organ precursor selection. *Genes Dev.* 17, 2966–2978. doi: 10.1101/gad.1122403

Katsanos, D., Koneru, S. L., Mestek Boukhibar, L., Gritti, N., Ghose, R., Appleford, P. J., et al. (2017). Stochastic loss and gain of symmetric divisions in the *C. elegans* epidermis perturbs robustness of stem cell number. *PLoS Biol.* 15:e2002429. doi: 10.1371/journal.pbio.2002429

Kieninger, M. R., Ivers, N. A., Rödelsperger, C., Markov, G. V., Sommer, R. J., and Ragsdale, E. J. (2016). The nuclear hormone receptor NHR-40 acts downstream of the sulfatase EUD-1 as part of a developmental plasticity switch in *Pristionchus*. *Curr. Biol.* 26, 2174–2179. doi: 10.1016/j.cub.2016.06.018

Levy, S. F., and Siegal, M. L. (2008). Network hubs buffer environmental variation in *Saccharomyces cerevisiae*. *PLoS Biol.* 6:e264. doi: 10.1371/journal.pbio.0060264

Losick, R., and Desplan, C. (2008). Stochasticity and cell fate. *Science* 320, 65–68. doi: 10.1126/science.1147888

Masel, J., and Griswold, C. K. (2009). The strength of selection against the yeast prion [PSI+]. *Genetics* 181, 1057–1063. doi: 10.1534/genetics.108.100297

Masel, J., and Siegal, M. L. (2009). Robustness: mechanisms and consequences. *Trends Genet.* 25, 395–403. doi: 10.1016/j.tig.2009.07.005

Mather, K., and de Winton, D. (1941). Adaptation and counter-adaptation of the breeding system in primula. *Ann. Bot.* 5, 297–311. doi: 10.1093/oxfordjournals.aob.a087394

Namdeo, S., Moreno, E., Rödelsperger, C., Baskaran, P., Witte, H., and Sommer, R. J. (2018). Two independent sulfation processes regulate mouth-form plasticity in the nematode *Pristionchus pacificus*. *Development* 145:dev166272. doi: 10.1242/dev.166272

Nijhout, H. F. (1975). A threshold size for metamorphosis in the tobacco hornworm, *Manduca sexta* (L.). *Biol. Bull.* 149, 214–225. doi: 10.2307/1540491

Price, T. D., Qvarnström, A., and Irwin, D. E. (2003). The role of phenotypic plasticity in driving genetic evolution. *Proc. Biol. Sci.* 270, 1433–1440. doi: 10.1098/rspb.2003.2372

Projecto-Garcia, J., Biddle, J. F., and Ragsdale, E. J. (2017). Decoding the architecture and origins of mechanisms for developmental polyphenism. *Curr. Opin. Genet. Dev.* 47, 1–8. doi: 10.1016/j.gde.2017.07.015

Ptashne, M., Jeffrey, A., Johnson, A. D., Maurer, R., Meyer, B. J., Pabo, C. O., et al. (1980). How the lambda repressor and cro work. *Cell* 19, 1–11. doi: 10.1016/0092-8674(80)90383-9

Queitsch, C., Sangster, T. A., and Lindquist, S. (2002). Hsp90 as a capacitor of phenotypic variation. *Nature* 417, 618–624. doi: 10.1038/nature749

Ragsdale, E. J., Müller, M. R., Rödelsperger, C., and Sommer, R. J. (2013). A developmental switch coupled to the evolution of plasticity acts through a sulfatase. *Cell* 155, 922–933. doi: 10.1016/j.cell.2013.09.054

Rohner, N., Jarosz, D. F., Kowalko, J. E., Yoshizawa, M., Jeffery, W. R., Borowsky, R. L., et al. (2013). Cryptic variation in morphological evolution: HSP90 as a capacitor for loss of eyes in cavefish. *Science* 342, 1372–1375. doi: 10.1126/science.1240276

Rutherford, S. L., and Lindquist, S. (1998). Hsp90 as a capacitor for morphological evolution. *Nature* 396, 336–342. doi: 10.1038/24550

Sanghvi, G. V., Baskaran, P., Röseler, W., Sieriebriennikov, B., Rödelsperger, C., and Sommer, R. J. (2016). Life history responses and gene expression profiles of the nematode *Pristionchus pacificus* cultured on *Cryptococcus* yeasts. *PLoS One* 11:e0164881. doi: 10.1371/journal.pone.0164881

Schlichting, C. D., and Pigliucci, M. (1993). Control of phenotypic plasticity via regulatory genes. *Am. Nat.* 142, 366–370. doi: 10.1086/285543

Serobyan, V., Ragsdale, E. J., Müller, M. R., and Sommer, R. J. (2013). Feeding plasticity in the nematode *Pristionchus pacificus* is influenced by sex and social context and is linked to developmental speed. *Evol. Dev.* 15, 161–170. doi: 10.1111/ede.12030

Serobyan, V., and Sommer, R. J. (2017). Developmental systems of plasticity and trans-generational epigenetic inheritance in nematodes. *Curr. Opin. Genet. Dev.* 45, 51–57. doi: 10.1016/j.gde.2017.03.001

Serobyan, V., Xiao, H., Namdeo, S., Rödelsperger, C., Sieriebriennikov, B., Witte, H., et al. (2016). Chromatin remodelling and antisense-mediated up-regulation of the developmental switch gene *eud-1* control predatory feeding plasticity. *Nat. Commun.* 7:12337. doi: 10.1038/ncomms12337

Sieriebriennikov, B., Markov, G. V., Witte, H., and Sommer, R. J. (2017). The role of DAF-21/Hsp90 in mouth-form plasticity in *Pristionchus pacificus*. *Mol. Biol. Evol.* 34, 1644–1653. doi: 10.1093/molbev/msx106

Sieriebriennikov, B., Prabh, N., Dardiry, M., Witte, H., Röseler, W., Kieninger, M. R., et al. (2018). A developmental switch generating phenotypic plasticity is part of a conserved multi-gene locus. *Cell Rep.* 23, 2835.e4–2843.e4. doi: 10.1016/j.celrep.2018.05.008

Sommer, R. J., Dardiry, M., Lenuzzi, M., Namdeo, S., Renahan, T., Sieriebriennikov, B., et al. (2017). The genetics of phenotypic plasticity in nematode feeding structures. *Open Biol.* 7:160332. doi: 10.1098/rsob.160332

Sommer, R. J., and McGaughran, A. (2013). The nematode *Pristionchus pacificus* as a model system for integrative studies in evolutionary biology. *Mol. Ecol.* 22, 2380–2393. doi: 10.1111/mec.12286

Susoy, V., Ragsdale, E. J., Kanzaki, N., and Sommer, R. J. (2015). Rapid diversification associated with a macroevolutionary pulse of developmental plasticity. *Elife* 4:e05463. doi: 10.7554/eLife.05463

Susoy, V., and Sommer, R. J. (2016). Stochastic and conditional regulation of nematode mouth-form dimorphisms. *Front. Ecol. Evol.* 4:23. doi: 10.3389/fevo.2016.00023

Varghese, J., and Cohen, S. M. (2007). microRNA miR-14 acts to modulate a positive autoregulatory loop controlling steroid hormone signaling in *Drosophila*. *Genes Dev.* 21, 2277–2282. doi: 10.1101/gad.439807

Veening, J.-W., Smits, W. K., and Kuipers, O. P. (2008). Bistability, epigenetics, and bet-hedging in bacteria. *Annu. Rev. Microbiol.* 62, 193–210. doi: 10.1146/annurev.micro.62.081307.163002

Wagner, A. (2005). Robustness, evolvability, and neutrality. *FEBS Lett.* 579, 1772–1778. doi: 10.1016/j.febslet.2005.01.063

Werner, M. S., Sieriebriennikov, B., Loschko, T., Namdeo, S., Lenuzzi, M., Dardiry, M., et al. (2017). Environmental influence on *Pristionchus pacificus* mouth form through different culture methods. *Sci. Rep.* 7:7207. doi: 10.1038/s41598-017-07455-7

West-Eberhard, M. J. (2003). *Developmental Plasticity and Evolution*. New York, NY: Oxford University Press.

West-Eberhard, M. J. (2005). Developmental plasticity and the origin of species differences. *Proc. Natl. Acad. Sci. U.S.A.* 102(Suppl. 1), 6543–6549. doi: 10.1073/pnas.0501844102

Wilecki, M., Lightfoot, J. W., Susoy, V., and Sommer, R. J. (2015). Predatory feeding behaviour in *Pristionchus* nematodes is dependent on phenotypic plasticity and induced by serotonin. *J. Exp. Biol.* 218, 1306–1313. doi: 10.1242/jeb.118620

Conflict of Interest Statement: The authors declare that the research was conducted in the absence of any commercial or financial relationships that could be construed as a potential conflict of interest.

Conserved nuclear receptors controlling a novel plastic trait in nematodes target rapidly evolving genes

Bogdan Sieriebriennikov, Shuai Sun, James W. Lightfoot, Hanh Witte, Eduardo Moreno, Christian Rödelsperger, Ralf J. Sommer*

*corresponding author

Developmental plasticity was shown to act through switch genes, but little is known about the gene regulatory networks on which environmental signals impinge. Knowledge about the composition of these networks is crucial for understanding how novel environments shape development and evolution. Here, we elucidated the gene regulatory network controlling the development of environmentally-induced predatory morphs in the nematode *Pristionchus pacificus* and explored the evolutionary dynamics of associated genes. We found that two conserved nuclear hormone receptors regulate a small set of 24 target genes. These genes have no orthologs in *Caenorhabditis elegans* and likely result from lineage-specific expansions. Furthermore, they show extreme redundancy, as revealed by systematic CRISPR/Cas9 knockouts and expression studies. Strikingly, all tested target genes are expressed in a single cell, the dorsal pharyngeal gland cell, whose morphological remodeling accompanied the evolution of teeth and predation. Our study links rapid gene evolution with morphological innovations associated with plasticity.

Keywords

Developmental plasticity, nuclear hormone receptors, *Pristionchus pacificus*, switch genes, Astacins, evolutionary novelty.

Introduction

Developmental plasticity is the ability to generate different phenotypes in response to environmental input [1]. As a result, even genetically identical individuals may develop distinct phenotypes, the most extreme example being castes in social insects [2]. Developmental plasticity is ubiquitous and attracting considerable attention in the context of adaptation to climate change [3–6] and as a facilitator of evolutionary novelty [7–11]. However, the role of plasticity in evolution has been contentious [6,12] because the genetic and epigenetic underpinnings of plastic traits have long remained elusive. Nonetheless, recent studies have begun to elucidate associated molecular mechanisms in insects and nematodes [13–16]. Ultimately, the identification of gene regulatory networks (GRN) controlling plasticity will provide an understanding of development in novel environments and enable testing theories about the long-term evolutionary significance of plasticity.

The free-living nematode *Pristionchus pacificus* has recently been established as a model to study plasticity [13]. These worms can develop two alternative mouth forms, called the eurystomatous (Eu) and the stenostomatous (St) mouth forms, respectively. Eu morphs have a large buccal cavity and two large opposed teeth enabling predation on other nematodes, while St morphs have a smaller buccal cavity and one tooth limiting their diet to microbial sources [17,18] (Fig. 1A-C, SFig. 1A). The wild-type *P. pacificus* strain PS312 preferentially forms the Eu morph in standard culture conditions on agar plates, but becomes predominantly St in liquid culture [19]. Additionally, nematode-derived modular metabolites excreted by adult animals induce the predatory Eu morph [20,21]. A forward genetic screen identified the sulfatase gene *eud-1* as a developmental switch confirming long-standing predictions that plastic traits are regulated by binary switches [18]. Subsequent studies implicated several other enzyme-encoding genes, such as *nag-1*, *nag-2*, *sult-1/seud-1* in regulating mouth-form plasticity [22–25]. Additionally, the chromatin modifier genes *lsy-12* and *mbd-2* influence *eud-1* expression [26]. In contrast, only one transcription factor, the nuclear hormone receptor (NHR) NHR-40, was so far found to regulate mouth-form fate [27], and no downstream targets have been identified (Fig. 1D). Here, we leveraged the power of suppressor screen genetics to identify the conserved nuclear hormone receptor NHR-1 as a second transcription factor controlling mouth-form development. Strikingly, transcriptomic profiling revealed that NHR-40 and NHR-1 have only 24 common targets. Their systematic CRISPR/Cas9 knockouts and expression analysis indicated extreme functional redundancy and showed that they are expressed in a single pharyngeal gland cell, g1D. This cell has undergone extreme morphological remodeling in nematode evolution, which is associated with the emergence of teeth and predatory feeding. Interestingly, *nhr-1* and *nhr-40* are well conserved, whereas all target genes are rapidly evolving and have no orthologs in *C. elegans*. This study enhances the understanding of the GRN regulating mouth-form plasticity, elucidates the evolutionary dynamics of underlying genes and links morphological innovations with rapid gene evolution.

Results and Discussion

Suppressor screen in *nhr-40* identifies another NHR gene regulating mouth-form development

Suppressor screens are a powerful tool to discover new genetic players [28]. We therefore conducted a suppressor screen in the mutant background of *nhr-40*, which is the most downstream gene in the current GRN controlling *P. pacificus* mouth-form plasticity and encodes a transcription factor [27]. We mutagenized *nhr-40(tu505)* worms, which are all-Eu, and isolated one allele, *tu515*, that had a no-Eu phenotype (Fig 1E, Table 1). The phenotype was fully penetrant both, in the presence of *nhr-40(tu505)* and after outcrossing, *i.e.* Eu animals were never observed under any culture condition. Thus, *tu515* represents a novel factor influencing the mouth-form ratio. Interestingly, however, *tu515* mutants also exhibited abnormal mouth morphology (Fig. 1A, SFig. 1A). While wild-type Eu animals have a large right ventrosublateral tooth with a hook, wild-type St animals have a cuticular ridge with a minute denticle instead. In contrast, in *tu515* mutants, the size and shape of this structure ranged from an enlarged ridge to a reduced tooth with a small hook. Additionally, the size and curvature of the dorsal tooth, and the width of the mouth in *tu515* mutants was variable, although the overall morphology resembled that of the St morph. It is important to note that *tu515* is the first mutation that simultaneously leads to the absence of one morph and morphological defects. Thus, the corresponding gene may be involved in mouth-form determination and differentiation.

To map *tu515*, we performed bulk segregant analysis. We examined the list of non-synonymous and nonsense mutations within the candidate region on the X chromosome (SFig. 2B, STable 1) and discovered a non-synonymous mutation in another NHR-encoding gene, *nhr-1*. The substitution changed the sequence of a highly conserved FFRR motif within the DNA recognition helix [29] to FFRW, which may cause the loss of DNA-binding activity. We performed the following experiments to verify that *nhr-1* is the suppressor of *nhr-40(tu505)*. First, we created *nhr-1* mutants using CRISPR/Cas9 by generating frameshift mutations at the beginning of the ligand-binding domain (LBD). The resulting alleles *tu1163* and *tu1164* exhibited an all-St phenotype and the same morphological abnormalities as *tu515* (Fig. 1A, SFig. 1A, Table 1). Second, we crossed the *tu1163* and *tu515* mutants and established that *tu1163/tu515* trans-heterozygotes were all-St showing that the two mutants do not complement each other (Table 1). Third, we overexpressed the complementary DNA (cDNA) of *nhr-1* driven by the *nhr-1* promoter region in the *nhr-1(tu1163)* mutant background and obtained an almost complete rescue (Table 1). Fourth, we crossed *nhr-1(tu1163)* with *nhr-40(tu505)* and observed a highly penetrant all-St phenotype in double mutant animals, similar to the phenotype of *tu515 nhr-40(tu505)* mutants (Table 1). Taken together, frameshift alleles of *nhr-1* and the original suppressor allele *tu515* exhibit the same phenotype, do not complement each other, and have identical epistatic interactions with *nhr-40(tu505)*. Therefore, *nhr-1* is the suppressor of *nhr-40(tu505)*.

Reverse genetic analysis of *nhr-40* results in all-stenostomatous mutants

The available alleles of *nhr-1* and *nhr-40* have opposite phenotypes with regard to mouth-form frequency, resulting in all-St and all-Eu animals, respectively. This is surprising because NHRs often form heterodimers [30], in which case *loss-of-function* phenotypes of interacting partners

are identical. Two different hypotheses could explain our observations. First, *nhr-1* and *nhr-40* may indeed have different functions. Second, the three available alleles of *nhr-40* (*tu505, iub6, iub5*), all of which are non-synonymous substitutions outside of the DNA-binding domain (DBD) [27], may represent *gain-of-function* alleles. Our previous analysis had suggested that these alleles are *loss-of-function* based on the phenotype of *nhr-40* overexpression, which resulted in all-St animals [27]. However, we recently realized that in *C. elegans*, overexpression of *Cel-nhr-40* and *loss of function* of *Cel-nhr-40* induced by RNAi and a deletion mutation all cause similar developmental defects [31]. Therefore, we generated nonsense alleles of *nhr-40* in *P. pacificus* using CRISPR/Cas9.

We introduced mutations in two different locations (Fig. 2A). The alleles *tu1418* and *tu1419* truncate the DBD. The *tu1420* allele contains a frameshift at the beginning of the LBD while leaving the DBD intact. We phenotyped the newly obtained mutants in liquid S-medium, which represses the Eu morph, and on agar plates, which induces it [19]. All frameshift alleles had a completely penetrant all-St phenotype in both culture conditions, which is opposite to the original ethyl methanesulfonate (EMS) alleles (Table 1). Additionally, we created a *null* allele, *tu1423*, which contains a 13 kb deletion or rearrangement of the locus (SFig. 2A). This *null* allele also had a completely penetrant all-St phenotype (Table 1). To eliminate the possibility that the phenotype of the EMS mutants was caused by random mutations outside *nhr-40*, we introduced a nucleotide substitution identical to *iub6* via homology-directed repair (Fig. 2A). Indeed, the two resulting alleles, *tu1421* and *tu1422*, had an all-Eu phenotype, identical to that of *iub6* and other EMS alleles, and opposite to that of the frameshift alleles (Table 1). Thus, frameshift mutations in DBD, LBD, and the deletion/rearrangement of the entire gene have an opposite phenotype to that of the three non-synonymous substitutions. We conclude that *tu505, iub6, iub5, tu1421* and *tu1422* are *gain-of-function* alleles.

NHR-40 and NHR-1 interact post-transcriptionally

In GRNs, transcription factors may activate or repress each other transcriptionally [32–36], or alternatively, they may interact at the post-transcriptional level. The latter includes indirect interactions, such as independent binding to the same promoters [37], or ligand-mediated interactions [38]. To distinguish if *nhr-1* and *nhr-40* interact at the transcriptional or post-transcriptional level, we analyzed the transcriptomes of wild type, *nhr-1 loss-of-function*, *nhr-40 loss-of-function* and *nhr-40 gain-of-function* mutants at two developmental stages (Fig. 3A). RNA collected from J2-J4 larvae is enriched with transcripts expressed at the time of mouth-form determination, while RNA collected from J4 larvae and adults is enriched with transcripts expressed at the time of mouth-form differentiation [39]. We found that at both time points, *nhr-40* transcript levels were not affected by *loss of function* of *nhr-1*. Similarly, *nhr-1* transcript levels were not affected by *loss of function* of *nhr-40*, although they were slightly, but not significantly increased in *nhr-40 gain of function* (Fig. 2B). Thus, at the transcriptional level, both *nhr* genes remain unaffected by the *loss of function* of the other *nhr* gene. Therefore, NHR-40 and NHR-1 may interact at the post-transcriptional level.

***nhr-40* and *nhr-1* are expressed at the site of polyphenism with limited co-localization**

Next, we wanted to determine the expression pattern of *nhr-1* and *nhr-40* and test if they were co-expressed. We took three complementary approaches to establish the expression pattern of *nhr-1*. First, we created transcriptional reporters comprising the presumptive promoter

region upstream of the potential start site in the second exon fused with TurboRFP or Venus. The resulting expression pattern was broad with the strongest expression in the head, including both, muscle and gland cells of the pharynx, and what may be the hypodermal and arcade cells (Fig. 2D, SFig. 1B). Second, we performed antibody staining against an HA epitope tag in the *nhr-1* rescue line described above. We observed a similar expression pattern that was predictably localized to the nuclei (Fig. 2C). Finally, we used CRISPR/Cas9 to "knock in" an HA tag in the endogenous *nhr-1* locus at the C-terminus of the coding sequence. Antibody staining against HA revealed a similar expression pattern but with a weaker signal due to the lower number of copies of endogenous DNA (SFig. 1C). Together, these results show that NHR-1 localizes to nuclei of multiple cells in the head region, with strong expression in pharyngeal muscle cells, which presumably secrete structural components of the teeth.

To explore whether NHR-40 and NHR-1 are expressed in overlapping tissues, we created a double reporter line, in which the *nhr-40* promoter is fused to TurboRFP and the *nhr-1* promoter to Venus. We observed a strong and consistent expression of *nhr-40* in the head. Specifically, it localized to the pharyngeal muscle cells and cells whose cell body position is consistent with them being arcade or hypodermal cells (Fig. 2D, SFig. 1D). *nhr-40* and *nhr-1* signals co-localized in a subset of presumptive hypodermal and arcade cells, and in the pharyngeal muscles. In contrast, only *nhr-1* was expressed in the dorsal pharyngeal gland cell g1D (Fig. 2D, SFig. 1D,E). In summary, the expression of *nhr-40* is more restricted than the expression of *nhr-1*, and the two genes display limited co-localization.

Suppressor screen in *nhr-1* failed to identify downstream target genes

The experiments described above established that two NHR-type transcription factors control mouth-form plasticity in *P. pacificus*. We speculate that NHR-40 and NHR-1 regulate a set of target genes, which execute the developmental decision and generate alternative phenotypes. To identify such downstream target genes, we performed genetic and transcriptomic analyses. In the first attempt, we conducted two suppressor screens in the *nhr-1(tu1163)* mutant background. In total, we screened approximately four times more gametes than in our first suppressor screen, but we isolated no all-Eu lines. There are three explanations for this result. First, functional *nhr-1* may be essential for the Eu morph. Second, the number of downstream targets may be small, and a considerably larger screen is required to identify them. Third, the downstream targets may be redundant, and multiple genes may need to be inactivated to change the phenotype. Therefore, we took an alternative approach and identified targets of NHR-40 and NHR-1 through transcriptomic profiling.

Common transcriptional targets of NHR-40 and NHR-1 encode extracellular proteins expressed during mouth-form differentiation

We analyzed the full list of genes differentially expressed between the wild type and mutant samples from the experiments described above. Given the pleiotropic action of NHR-40 and NHR-1, we applied the following selection criteria. We only retained genes whose expression at either of the two examined time points simultaneously changed in one direction in the *loss of function* mutants of *nhr-1* and *nhr-40*, and in the opposite direction in the *gain of function* mutants of *nhr-40* (Fig. 3A). Strikingly, only 24 genes, provided in Table 2, satisfied these criteria, whereby the expression of 23 of them was reduced in the *loss-of-function* mutants (Table 2). We hypothesized that if the making of cuticularized mouthparts involves these

genes, they must encode extracellular proteins, and their expression is likely to be biased towards the time of mouth-form differentiation. To verify the extracellular function of the target proteins, we predicted signal peptides and compared the list of targets with the genome-wide pattern. Indeed, we found that the targets of NHR-40 and NHR-1 are significantly enriched with genes containing signal peptides (Fig. 3B). To examine a potential temporal expression bias, we compared the wild-type transcriptomes at the time of mouth-form determination and mouth-form differentiation. While most genes in the genome (51%) showed uniform expression at the two time points, 23 of the 24 targets of NHR-40 and NHR-1 where more highly expressed at the time of mouth-form differentiation (Fig. 3B). Surprisingly, we also observed a third trend in our data set. While only 12% of all genes in the genome are located on the X chromosome, 15 of the 24 targets of NHR-40 and NHR-1 were X-linked (Fig. 3B). It is worth noting that *nhr-40* and *nhr-1* themselves, and also the multigene locus comprising *eud-1, nag-1* and *nag-2*, are located on the X chromosome, although the biological meaning of this phenomenon remains currently unclear. In summary, the downstream targets of NHR-40 and NHR-1 are enriched with genes that are X-linked, encode extracellular proteins, and are more highly expressed at the time of mouth-form differentiation.

To explore the potential functions of the NHR-40 and NHR-1 targets, we used information about their annotated protein domains. Surprisingly, 12 of the 24 genes contain an Astacin domain (Table 2). Astacins are secreted or membrane-anchored Zinc-dependent endopeptidases, first described in the crayfish *Astacus astacus* [40]. Of the 40 genes present in *C. elegans*, only *dpy-31, nas-6* and *nas-7* have known functions, whereby mutations in these genes result in abnormal cuticle synthesis [41,42]. Another five of the 24 NHR targets encode a CAP (**c**ysteine-rich secretory proteins, **a**ntigen 5, and **p**athogenesis-related 1) domain (Table 2), which is contained in extracellular proteins with diverse functions [43,44,45], including the proteolytic modification of extracellular matrix [46]. Two genes belong to the glycoside hydrolases family 18 (Table 2), which includes chitinases and chitinase-like proteins [47] that may modify the cuticle, as chitin is the main component of the cuticle in nematodes [48]. Finally, the NHR target list includes an unannotated protein, PPA30108 (Table 2), which contains multiple GGX repeats, where X is F or R. Intriguingly, a similar sequence repeat has been proposed to facilitate the formation of elastic fibers by structural proteins of spider silk [49,50]. Thus, the examination of the coding sequences and domain composition of the targets of NHR-40 and NHR-1 shows that most of them encode enzymes that may directly modify the cuticle, and one gene encoding what may be an elastic structural protein.

A duodecuple Astacin mutant has no detectable phenotype

Next, we tested if mutations in the identified genes affected mouth-form frequency or morphology. We therefore performed systematic CRISPR/Cas9 knockout experiments of the 23 genes downregulated in the *loss-of-function* mutants. To compensate for potential redundancy between paralogous genes encoding identical domains, we produced lines in which all such genes are inactivated simultaneously. For example, rather than generating 12 strains with mutations affecting single Astacin-encoding genes, we produced a duodecuple mutant line, in which we sequentially knocked out all 12 genes (Table 1). We phenotyped the mutants both on agar plates and in liquid S-medium. However, we detected no significant change in mouth-form frequencies and no recapitulation of the morphological defects of *nhr-1*. Similarly, we produced a quintuple CAP mutant and double chitinase mutants and observed no change in mouth-form frequency or morphology (Table 1). We speculate that extreme

redundancy of the factors involved may cause this observation. For instance, even though we mutagenized 12 Astacin-encoding genes, more than 50 such genes in the genome remain unaffected. Similarly, in the phenotypic screen of Astacin genes in *C. elegans*, a mutant allele of *nas-7* had no phenotype, and its function was only elucidated because it happened to enhance the phenotype of a weakly penetrant allele of *nas-6* [42]. Alternatively, it is also possible that some examined genes function in other tissues unrelated to mouth morphology. Therefore, we next studied the spatial expression of selected downstream target genes.

Downstream targets genes are expressed in the same pharyngeal gland cell

We selected six of the 12 Astacin genes, one chitinase gene, one CAP gene, and the gene bearing similarity to spider silk proteins, and created transcriptional reporters by fusing their promoters with TurboRFP. Strikingly, all reporter lines showed expression in the same single cell, the dorsal pharyngeal gland cell g1D (Fig. 3C). In contrast, we found no expression in the pharyngeal muscles or other expression foci of *nhr-40* and *nhr-1*. Thus, all analyzed targets are co-expressed with *nhr-1* in g1D (Fig. 3C, SFig. 1E). Unfortunately, physical ablation of g1D was not possible given its large size. Depending on the laser intensity, g1D-ablated animals either retained residual g1D activity as revealed by the expression of a selected transcriptional reporter or exhibit severe developmental abnormalities, similar to g1D-ablated *C. elegans* [51].

The recent reconstruction of the pharyngeal gland cell system of *P. pacificus* [52] revealed that the cell body of g1D is located at the posterior end of the pharynx. It sends a long process through the entire pharynx to the anterior tip where it connects, via a short duct in the cuticle, to a channel in the dorsal tooth which opens into the buccal cavity (Fig. 3C). Importantly, the process of g1D is surrounded by pharyngeal muscle cells. Therefore, we hypothesize that the enzymes excreted from g1D act on the structural components that are themselves secreted by the pharyngeal muscles.

Expansion of the pharyngeal gland cells is concomitant with the emergence of teeth

The expression of the targets of NHR-40 and NHR-1 in g1D is remarkable, because g1D is the site of a major evolutionary innovation in the family Diplogastridae, to which *P. pacificus* belongs. The pharynx in free-living nematodes of the order Rhabditida and the outgroup [53] family Teratocephalidae is divided into two parts. The anterior part, called the corpus, is muscular, and in some lineages it ends with a dilation, called the median bulb. The posterior part, called the postcorpus, is divided into a narrow isthmus and a dilation, called the terminal bulb, which contains muscle cells and three to five gland cells. The terminal bulb contains muscular valves that form a specialized cuticular structure called the grinder, which helps fragment food particles [54] (Fig. 4). Phylogenetic reconstruction indicates that the outgroup Teratocephalidae, and the rhabditid families Cephalobidae and Rhabditidae retained the ancestral character states, whereby they have a grinder, but no teeth [55–57]. In contrast, Diplogastridae have no grinder, but they have concomitantly gained teeth at the base of the family [7,58]. The acquisition of teeth and the loss of the grinder were accompanied by the reduction of the muscle cells in the postcorpus, and an expansion of three gland cells g1D, g1VL, and g1VR, one in each sector of the trilaterally symmetrical pharynx [52,58] (Fig. 4). While the exact role of pharyngeal gland cells in *C. elegans* and other nematodes has remained elusive [54], we speculate that the functional remodeling of g1D, in which the target genes of

NHR-40 and NHR-1 are expressed, may be a prerequisite for the formation of teeth and the evolution of predation. Therefore, we finally wanted to investigate the evolutionary dynamics of the identified genes expressed in this cell.

Conserved transcription factors regulate fast-evolving target genes

To investigate if the morphological lineage-specific evolutionary innovation in *P. pacificus* and the Diplogastridae is associated with taxonomically restricted genes, we reconstructed the phylogeny of NHR genes and their identified targets. This is an important evolutionary question as recent genomic studies involving deep taxon sampling revealed high evolutionary dynamics of novel gene families in *Pristionchus*, with only one third of all genes having 1:1 orthologs between *P. pacificus* and *C. elegans* [59]. First, we reconstructed the phylogeny of NHR genes. We identified similar numbers of NHR genes in the genomes of *P. pacificus* and *C. elegans* - 254 and 266 genes, respectively. In the phylogenetic tree (Fig. 5A), most clades contained genes from predominantly or exclusively one of the two species. These genes likely result from lineage-specific duplications and losses, a phenomenon commonly seen in nematode gene families [60]. Strikingly, however, *nhr-40* and *nhr-1* belonged to one of the few clades that contained a mixture of genes from both species, with many genes displaying a 1:1 orthology relationship. Indeed, the *P. pacificus* and *C. elegans* copies of *nhr-40* and *nhr-1* showed 1:1 orthology with 100% bootstrap support (Fig. 5A). Importantly, *nhr-40* and *nhr-1* are also extremely closely related to each other (Fig. 5A). Thus, in the overall context of NHR evolution, *nhr-40* and *nhr-1* are closely related duplicates that have been conserved since the divergence of *P. pacificus* and *C. elegans*.

The conservation of *nhr-40* and *nhr-1* is in stark contrast to the evolutionary dynamics of their downstream targets. To reconstruct the phylogenies of the Astacin, CAP and chitinase genes (Fig. 5B-D), we used functional domains rather than complete genes to facilitate the alignment of genes with different domain architectures. Similar to the case of NHRs, all three gene families exhibit strong signatures of lineage-specific expansions. Strikingly, all target genes containing Astacin, CAP and chitinase domains belonged to such lineage-specific clades (Fig. 5B-D). These findings suggest that the targets of NHR-40 and NHR-1 undergo rapid turnover and exhibit high evolutionary dynamics. This is further supported by the phylogeny of CAP genes within the genus *Pristionchus*. Specifically, the five targets identified in *P. pacificus* clustered separately from the homologs in the early branching species *P. fissidentatus* with 94% bootstrap support (Fig. 5E). Thus, two conserved NHRs target rapidly evolving downstream genes of multiple gene families. We speculate that the striking co-expression of the target genes results from the ancient regulatory linkage between the NHRs and the promoters of the ancestral target genes. Such divergent evolutionary dynamics of transcription factors and their downstream targets might represent general features of GRNs.

Conclusions

In this study, we elucidated the GRN controlling predatory *vs.* non-predatory plasticity in *P. pacificus*, thereby expanding the molecular understanding of plasticity. We uncovered novel factors at two regulatory levels, which allowed linking rapid gene evolution with morphological innovations associated with plasticity. First, we found that NHR-40 and NHR-1 regulate the mouth-form decision and the latter also affects mouth morphology. The significance of this finding is the co-option of two conserved transcription factors for regulating a novel trait given that teeth and the associated predatory behavior are an evolutionary novelty of *P. pacificus* and its relatives. The opposite mouth-form phenotypes of *loss-of-function* and *gain-of-function* mutations in *nhr-40* are reminiscent of the role of *daf-12*, another *nhr* gene, in controlling dauer plasticity in *C. elegans* [61]. Thus, the two known examples of nematode plasticity both involve NHRs as key regulators. It is important to note that except for DAF-12, no single NHR has been de-orphanized and therefore, the identification of their potential ligands may reveal additional layers of regulation. Indeed, recent studies in both, *P. pacificus* and *C. elegans* suggested that cytosolic sulfotransferases may regulate NHRs by modifying their ligands [23,24,62].

Second, the transcriptomic analysis of *nhr-1* and *nhr-40* mutants revealed an unexpectedly small number of downstream targets, which enabled a systematic analysis of their function and expression. Both, the absence of phenotypes in duodecuple and quintuple mutants and the restricted expression of all tested genes in the same cell g1D, are compatible with extreme redundancy. Such redundancy might result from features of genome evolution that are common to nematodes and other animals. Studies over the last decade revealed that nematode genomes are gene-rich and exhibit high rates of gene birth and death [59,63,64]. In particular, enzyme-encoding genes are subject to such evolutionary dynamics [60]. Therefore, genes in GRNs consisting of signaling pathways, transcription factors and their downstream targets may undergo different dynamics that will at least in part be shaped by the position in the network. Consistent with this idea, many genes encoding proteins of signal transduction and their terminal transcription factors are highly conserved across animals [65–67]. In this study, we complement this knowledge by showing that the downstream targets of such transcription factors are indeed fast evolving genes. Future studies are required to fully understand their dynamics and the relative contribution of adaptive and non-adaptive processes in shaping their evolution.

Methods

Maintenance of worm cultures and genetic crosses

Stock cultures of all strains used in this study were reared at room temperature (20-25°C) on nematode growth medium (NGM) (1.7% agar, 2.5 g/L tryptone, 3 g/L NaCl, 1 mM $CaCl_2$, 1 mM $MgSO_4$, 5 mg/L cholesterol, 25 mM KPO_4 buffer at pH 6.0) in 6 cm Petri dishes, as outlined in the *C. elegans* maintenance protocol [68]. *Escherichia coli* OP50 was used as food source. Bacteria were grown overnight at 37°C in L Broth (10 g/L tryptone, 5 g/L yeast extract, 5 g/L NaCl, pH adjusted to 7.0), and 400 µL of the overnight culture was pipetted on NGM agar plates and left for several days at room temperature to grow bacterial lawns. *P. pacificus* were passed on these lawns and propagated by passing various numbers of mixed developmental stages. To cross worms, agar plates were spotted with 10 µL of the *E. coli* culture, and five to six males and one or two hermaphrodites were transferred to the plate and allowed to mate. Males were removed after two days of mating.

Mouth form phenotyping

We phenotyped worms in two culture conditions. Rearing *P. pacificus* on solid NGM induces the Eu morph and facilitates identification of Eu-deficient (all-St) phenotypes. Conversely, growing worms in liquid S-medium (5.85 g/L NaCl, 1 g/L K_2HPO_4, 6 g/L KH_2PO_4, 5 mg/L cholesterol, 3 mM $CaCl_2$, 3 mM $MgSO_4$, 18.6 mg/L disodium EDTA, 6.9 mg/L $FeSO_4$•$7H_2O$, 2 mg/L $MnCl_2$•$4H_2O$, 2.9 mg/L $ZnSO_4$•$7H_2O$, 0.25 mg/L $CuSO_4$•$5H_2O$ and 10 mM Potassium citrate buffer at pH 6.0) represses the Eu morph and facilitates identification of Eu-constitutive (all-Eu) phenotypes [19,68]. As food source, S-medium contained *E. coli* OP50 in the amount corresponding to 100 mL of an overnight culture with OD_{600} 0.5 per 10 mL of medium. We started phenotyping by isolating eggs from stock culture plates, which contained large numbers of gravid hermaphrodites and eggs deposited on the agar surface [68]. To isolate eggs, we washed worms and eggs from plates with water, and incubated them in a mixture of 0.5 M NaOH and household bleach at 1:5 final dilution for 10 min with regular vortexing to disintegrate vermiform stages. Remaining eggs were pelleted at 1,300 g for 30 sec, washed with 5 mL of water, pelleted again, resuspended in water and pipetted on agar plates or into S-medium. Agar plates were left at room temperature (20-25°C) for 3-5 days and 25 mL Erlenmeyer flasks with liquid medium were shaken at 22°C, 180 rpm for 4-6 days. Adult hermaphrodites were immobilized on 5% Noble Agar pads with 0.3% NaN_3 added as an anesthetic, and examined using differential interference contrast (DIC) microscopy. Animals that had a large right ventrosublateral tooth, curved dorsal tooth, and the anterior tip of the promesostegostom posterior to the anterior tip of the gymnostom plate were classified as Eu morphs. Animals that did not exhibit these three characters simultaneously were classified as St morphs, although there was a distinction between the morphology of *nhr-1* mutants and of other all-St mutants (SFig. 1A).

CRISPR/Cas9 mutagenesis

We followed the previously published protocol for *P. pacificus* [69] with subsequently introduced modifications [70]. All target-specific CRISPR RNAs (crRNAs) were designed to target 20 bp upstream of the protospacer adjacent motifs (PAMs). We purchased crRNAs and universal trans-activating CRISPR RNA (tracrRNA) from Integrated DNA Technologies (Alt-R product

line). 10 µL of the 100 uM stock of crRNA was combined with 10 µL of the 100 uM stock of tracrRNA, denatured at 95°C for 5 min, and allowed to cool down to room temperature and anneal. The hybridization product was combined with Cas9 protein (purchased from New England Biolabs or Integrated DNA Technologies) and incubated at room temperature for 5 min. The mix was diluted with Tris-EDTA buffer to a final concentration of 18.1 µM for the RNA hybrid and 2.5 µM for Cas9. When site-directed mutations were introduced via homology-directed repair, a ssDNA oligo template designed on the same strand as the gRNA was included in the mix at a final concentration of 4 µM. The diluted mixture was injected in the gonad rachis of approximately one day old adult hermaphrodites. Eggs laid by injected animals within a 12-16 h period post injection were recovered, and the F1 progeny were singled out upon reaching maturity. After F1 animals have laid eggs, they were placed in 10 µL of single worm lysis buffer (10 mM Tris-HCl at pH 8.3, 50 mM KCl, 2.5 mM $MgCl_2$, 0.45% NP-40, 0.45% Tween 20, 120 µg/ml Proteinase K), frozen and thawed once, and incubated in a thermocycler at 65°C for 1 h, followed by heat deactivation of the proteinase at 95°C for 10 min. The resulting lysate was used as a template in subsequent PCR steps. Where possible, molecular lesions at the crRNA target sites were detected by melting curve analysis on a LightCycler 480 Instrument II (Roche) of PCR amplicons obtained using LightCycler 480 High Resolution Melting Master (Roche). Presence of mutations in candidate amplicons was further verified by Sanger sequencing. Alternatively, PCR was done using Taq PCR Master Mix (Qiagen) and all the F1 were Sanger sequenced. To detect large rearrangements, we conducted whole genome re-sequencing of lines for which no PCR amplicon containing the crRNA target site could be obtained. For most such lines, we extracted genomic DNA using GenElute Mammalian Genomic DNA Miniprep Kit (Merck), whereby we modified the tissue digestion step by raising the Proteinase K concentration to 2 mg/mL, and prepared next-generation sequencing (NGS) libraries using Nextera DNA Flex Library Prep Kit (Illumina). For the *nhr-40* null mutant line, we followed a recently introduced cost-effective alternative procedure [71] with several modifications. Single worms were placed in 10 µL water, and frozen and thawed 3 times in liquid nitrogen. Then, we added 10 µL 2x single worm lysis buffer (20 mM Tris-HCl at pH 8.3, 100 mM KCl, 5 mM $MgCl_2$, 0.9% NP-40, 0.9% Tween 20, 240 µg/ml Proteinase K) and incubated the tubes in a thermocycler at 65°C for 1 h. After a clean-up using HighPrep beads (MagBio Genomics), DNA was eluted in 7 µL Tris buffer at pH 8.0. 100 pg of DNA was diluted with water to the total volume of 9 µL, mixed with 2 µL 5X TAPS-DMF buffer (50 mM TAPS at pH 8.5, 25 mM $MgCl_2$, 50% DMF) and 1 µL Tn5 transposase from Nextera DNA Library Prep Kit (Illumina) diluted beforehand 1:25 in dialysis buffer (100 mM HEPES at pH 7.2, 0.2 M NaCl, 0.2 mM EDTA, 0.2% Triton X-100, 20% glycerol). The mixture was incubated for 14 min at 55°C. Tagmented DNA was amplified using Q5 HotStart High-Fidelity DNA Polymerase (New England Biolabs) for 14 cycles, whereby adapters and indices were added as primer overhangs, and size-selected for 250–550 bp fragments using HighPrep beads (MagBio Genomics). NGS libraries prepared using both methods were sequenced in a paired-end run of a HiSeq 3000 machine (Illumina). Reads were mapped to the El Paco assembly of the *P. pacificus* genome [72] using Bowtie 2 (ver. 2.3.4.1) [73]. We visually inspected read coverage in the loci of interest using IGV [74] to identify the precise regions in which coverage was close to zero.

EMS mutagenesis

To induce heritable mutations in *P. pacificus*, we incubated a mixture of J4 larvae and young adults in M9 buffer (3 g/L KH_2PO_4, 6 g/L Na_2HPO_4, 5 g/L NaCl, 1 mM $MgSO_4$) with 47 mM

ethyl methanesulfonate (EMS) for 4 h [75]. Subsequently, the worms were allowed to recover on agar plates with bacteria (see above), and 40-120 actively moving J4 larvae were singled out. After the animals have laid approximately 20 eggs, they were killed, and F1 progeny were allowed to develop and reach maturity. F1 animals (which contained heterozygous mutants) were then singled out, and F2 progeny (which contained a mixture of genotypes, including homozygous mutants) were allowed to develop until adulthood. In each F1 plate, we determined the mouth form in 5-10 F2 individuals using Discovery V20 stereomicroscope (Zeiss). If at least one individual appeared to have a mouth form different from that of the background strain, such an animal was transferred to a fresh plate and its progeny was screened again using DIC until we gained confidence that a homozygous line was isolated. In the screen for suppressors of *nhr-40*, we mutagenized *nhr-40(tu505)* worms, which are all-Eu, screened approximately 1,000 F1 plates, and isolated one all-St allele, *tu515*. In the screen for suppressors of *nhr-1*, we mutagenized *nhr-1(tu1163)* worms, which are all-St, screened approximately 3,800 F1 plates, but found no Eu individuals.

Mapping of tu515

We crossed the *tu515* mutant, produced in the background of the RS2333 strain (a derivative of the PS312 strain), to a highly-Eu wild type strain PS1843. The resulting males were crossed to a strain RS2089, which is a derivative of PS1843 containing a morphological marker mutation causing the Dumpy phenotype. The progeny were allowed to segregate and 100 all-St lines were established. Four individuals from each line were pooled and genomic DNA was extracted from the pool using the MasterPure Complete DNA and RNA Purification Kit (Epicentre). Additionally, genomic DNA was extracted from the *tu515* line. NGS libraries were prepared using Low Input Library Prep kit (Clontech) and sequenced on Illumina HiSeq3000. Raw Illumina reads of the *tu515* mutant and of a mapping panel were aligned to the El Paco assembly of the *P. pacificus* genome (strain PS312) [72] by the aln and sampe programs of the BWA software package (ver. 0.7.17-r1188) [76]. Initial mutations were called with the samtools (ver. 1.7) mpileup command [77]. The same program was used to measure PS312 allele frequencies in the mapping panel at variant positions with regard to whole genome sequencing data of the PS1843 strain [72]. SFig. 2B shows that large regions between the positions 5 Mb and 16 Mb of the *P. pacificus* chromosome X exhibit high frequency of the PS312 alleles (the mutant background) in the mapping panel. In total, 28 non-synonymous/nonsense mutations (STable 1) in annotated genes (El Paco gene annotations v1, Wormbase release WS268) were identified in the candidate interval by a previously described custom variant classification software [78].

Transgenesis

To identify putative promoter regions, which included 5' untranslated regions (UTR), we manually re-annotated the 5' ends of predicted genes of interest using RNA-seq data and the information about predicted signal peptides. The ATG codon preceding the signal peptide or the last ATG codon in the second exon was designated as the putative start codon. As a general rule, the promoter region included a sequence spanning from the 3' end of the closest upstream gene on the same strand to the start codon, but if the upstream neighbor gene was located further than 2 kb away, a 1.5-2 kb region upstream of the identified start codon was designated as the putative promoter. In the case of inverted tandem duplicates in the head-to-head orientation, the 5' end of the promoter region was approximately in the middle between

the start codons of the two genes. For the reporter constructs, we used the previously published coding sequences of TurboRFP [79] and Venus [27] fused with the 3' UTR of the ribosomal gene *rpl-23* [79]. For the *nhr-1* rescue construct, we used the native coding sequence, in which we replaced native introns with synthetic introns, fused with the native 3' UTR. As the latter fragment could not be amplified from genomic or complementary DNA in one piece, we purchased a corresponding gBlocks fragments (Integrated DNA Technologies).

Plasmids carrying reporter and rescue constructs were created by Gibson assembly using NEBuilder HiFi DNA Assembly Master Mix (New England Biolabs) or a homemade master mix [80]. Small modifications, such as deletions and insertions under 70 bp, were introduced using Q5 Site-Directed Mutagenesis kit (New England Biolabs). Injection mix for transformation was created by digesting the plasmid of interest, the marker plasmid carrying a tail-bound reporter *egl-20p::TurboRFP* (if applicable), and genomic DNA with FastDigest restriction enzymes (Thermo Fisher Scientific), whereby genomic DNA was cut with an enzyme(s) that had the same cutting site(s) as the enzyme(s) used to digest the plasmids. Digested DNA was purified using Wizard SV Gel and PCR Clean-Up system (Promega), and the components were mixed in the following ratios. Injection mixes with rescue constructs contained 1 ng/µL rescue construct, 10 ng/µL marker, and 50 ng/µL genomic DNA. Injection mixes with reporter constructs contained 10 ng/µL reporter construct, 10 ng/µL marker, and 60 ng/µL genomic DNA. The mix was injected in the gonad rachis of approximately 1 day old hermaphrodites, and their progeny was screened for fluorescent animals [79].

Antibody staining

We followed a previously published protocol [81] with minor modifications. Animals were washed from mature plates with phosphate-buffered saline (PBS) (137 mM NaCl, 2.7 mM KCl, 10 mM Na_2HPO_4, 1.8 mM KH_2PO_4 at pH 7.4), passed over a 5-20 µm nylon filter, concentrated at the bottom of a 2 mL tube and chilled on ice. We then added chilled fixative (15 mM Na-PIPES at pH 7.4, 80 mM KCl, 20 mM NaCl, 10 mM Na_2EGTA, 5 mM Spermidine-HCl, 2% paraformaldehyde, 40% MeOH), froze the worms in liquid nitrogen and thawed them on ice for 1-2 h with occasional inversion. Subsequently, the animals were washed twice with Tris-Triton buffer (100 mM Tris-HCl at pH 7.4, 1 mM EDTA, 1% Triton X-100), incubated in Tris-Triton buffer with 1% β-mercaptoethanol in a thermomixer at 600 rpm for 2 h at 37°C, washed once in borate buffer (25 mM H_3BO_3, 12.5 mM NaOH), incubated in borate buffer with 10 mM dithiothreitol in a thermomixer at 600 rpm for 15 min at room temperature, washed once in borate buffer, incubated in borate buffer with ~0.3% H_2O_2 in a thermomixer at 600 rpm for 15 min at room temperature, and washed once more in borate buffer. Next, the worms were washed three times with antibody buffer B (0.1% bovine serum albumin, 0.5% Triton X-100, 0.05% NaN_3, 1 mM EDTA in PBS) on a rocking wheel, incubated with a dye-conjugated antibody (Thermo Fisher Scientific, cat .# 26183-D550 and cat. # 26183-D488) diluted 1:25 in antibody buffer A (1% bovine serum albumin, 0.5% Triton X-100, 0.05% NaN_3, 1 mM EDTA in PBS) on a rocking wheel in the dark for 3 h at room temperature or overnight at 4°C, washed three times with antibody buffer B and mounted on slides in a 1:1 mixture of PBS and Vectashield (Vector Laboratories) with 1 µg/mL DAPI added. Slides were imaged using a Leica SP8 confocal microscope.

RNA-seq analysis

To obtain a sufficient number of eggs, we passed young adult hermaphrodites to new agar plates with 5-10 animals per plate. After their F1 progeny have laid eggs (5-6 days), they were bleached (see above), then resuspended in 400 µL water per starting plate, pipetted onto multiple fresh plates with 100 µL suspension per fresh plate and placed at 20°C. Animals were collected at 24 h (corresponding to J2 and J3 larvae), 48 h (J3 and J4 larvae) and 68 h (J4 instar larvae and young adults) post-bleaching by adding some water to the plates, scraping off the bacterial lawns with worms in them using disposable cell spreaders and passing the resulting suspension through a 5 µm nylon filter, which efficiently separated worms from bacteria. Worms were washed from the filter into 1.5 mL tubes, pelleted in a table-top centrifuge at the maximum speed setting, after which the supernatant was removed and 1 mL TRIzol (Invitrogen) was added to the worm pellets. Tubes were flash-frozen in liquid nitrogen and stored at -80°C for up to a month. To extract RNA, worms suspended in TRIzol were frozen and thawed three times in liquid nitrogen, debris were pelleted for 10-15 min at 14,000 rpm at 4°C, and 200 µL of chloroform was added to the supernatant. After vigorous vortexing and incubation at room temperature (20-25°C) for 5 min, tubes were rotated for 15 min at 14,000 rpm at 4°C. The aqueous phase was combined with an equal volume of 100% ethanol, RNA was purified using RNA Clean & Concentrator Kit (Zymo Research) and its integrity was verified using RNA Nano chips on the Bioanalyzer 2100 instrument (Agilent). To analyze the transcriptome at the time of mouth form determination, we combined 500 ng RNA isolated at 24 h with 500 ng RNA isolated at 48 h post-bleaching, and proceeded to make libraries using NEBNext Ultra II Directional RNA Library Prep Kit for Illumina (New England Biolabs). To analyze the transcriptome at the time of mouth form differentiation, we prepared libraries from 1 µg of RNA isolated at 68 h post-bleaching. Libraries were sequenced in two paired-end runs of a HiSeq 3000 machine, whereby we aimed at 10-20 mln reads per library. For wild type strain PS312, four biological replicates were collected at different time points. For the mutants, two replicates of two independent alleles were collected at two different time points, and these were treated as four biological replicates. Specifically, we sequenced the following alleles: *nhr-1(tu1163) loss-of-function, nhr-1(tu1164) loss-of-function, nhr-40(tu505) gain-of-function, nhr-40(iub6) gain-of-function, nhr-40(tu1418) loss-of-function, nhr-40(tu1423) null*. The last biological replicate of wild type PS312 and all replicates of the *nhr-40 loss-of-function/null* mutants were sequenced in a different run than the other samples. To ensure that batch effects were negligible, we additionally re-sequenced the first three replicates of wild type PS312 in the same run and verified that coordinates in PCA conducted using complete transcriptomes were minimally altered when comparing the same samples sequenced in the two runs. Reads were mapped to the El Paco assembly of the *P. pacificus* genome [72] using STAR (ver. 020201) [82]. Differential expression analysis was carried out in R (ver. 3.4.4) [83] using Bioconductor (ver. 3.6) [84] and DESeq2 (ver. 1.18.1) [85]. We applied an adjusted p-value cutoff of 0.05 and no fold change cutoff. Alignments and coverage were visualized in IGV [74].

Phylogenetic reconstructions

To identify NHR, CAP, and chitinase genes in the *C. elegans* genome, we retrieved the current version (PRJNA13758) of predicted proteins and domains from the http://wormbase.org website and selected genes that contained “IPR001628”, “CAP domain”, and “IPR001223” as predicted InterPro domains, respectively. The list of Astacin genes was taken from an earlier study [86] and the corresponding gene predictions were manually retrieved from the

http://wormbase.org website. To identify NHR, Astacin, CAP, and chitinase genes in the *P. pacificus* genome, we predicted domains in the El Paco v1 version of gene predictions [72] using HMMER (ver. 3.1b2) software in conjunction with the PFAM profile database [87] and selected genes that contained "PF00105", "Astacin", "CAP", and "PF00704" as predicted PFAM domains, respectively. Manual inspection of the retrieved NHR genes in *P. pacificus* revealed that many of the gene predictions represent fusion of multiple neighboring genes. Therefore, we used the information about the predicted domains, RNA-seq data generated in this study, and Illumina and PacBio RNA-seq datasets generated earlier [26,88,89] to manually reannotate the NHR gene predictions in *P. pacificus*. We submitted the improved annotations to http://wormbase.org and they will be released in due course. For the tree of CAP domains in *P. pacificus* and *P. fissidentatus*, we predicted domains in the Pinocchio versions of gene predictions for both genomes [59] and selected genes that contained "PF00188" as a predicted PFAM domain. In the case of NHR genes, complete sequences were aligned, while in the case of other gene families, functional domains extracted using HMMER (ver. 3.1b2) were aligned to facilitate the alignment of genes with divergent domain architecture. Alignments were done in MAFFT (ver. 7.310) [90] and maximum likelihood trees were built using RAxML (ver. 8.2.11) [91]. Protein-based trees were generated with the following parameters: -f a -m PROTGAMMAAUTO -N 100. In the case of CAP domains in *P. pacificus* and *P. fissidentatus*, we first generated a protein-based tree and identified a poorly resolved subtree containing the genes of interest. To increase the number of informative sites, we extracted corresponding nucleotide sequences, aligned them in MAFFT and built a tree in RAxML with the following parameters: -f a -m GTRCAT -N 100. Obtained phylogenetic trees were visualized using FigTree (ver. 1.4.2).

References

1. West-Eberhard, M. J. *Developmental plasticity and evolution*. (Oxford University Press, 2003).
2. Corona, M., Libbrecht, R. & Wheeler, D. E. Molecular mechanisms of phenotypic plasticity in social insects. *Curr Opin Insect Sci* **13**, 55–60 (2016).
3. Nicotra, A. B. *et al.* Plant phenotypic plasticity in a changing climate. *Trends Plant Sci.* **15**, 684–692 (2010).
4. Seebacher, F., White, C. R. & Franklin, C. E. Physiological plasticity increases resilience of ectothermic animals to climate change. *Nat. Clim. Chang.* **5**, 61 (2014).
5. Charmantier, A. *et al.* Adaptive phenotypic plasticity in response to climate change in a wild bird population. *Science* **320**, 800–803 (2008).
6. Oostra, V., Saastamoinen, M., Zwaan, B. J. & Wheat, C. W. Strong phenotypic plasticity limits potential for evolutionary responses to climate change. *Nat. Commun.* **9**, 1005 (2018).
7. Susoy, V., Ragsdale, E. J., Kanzaki, N. & Sommer, R. J. Rapid diversification associated with a macroevolutionary pulse of developmental plasticity. *Elife* **4**, e05463 (2015).
8. West-Eberhard, M. J. Developmental plasticity and the origin of species differences. *Proc. Natl. Acad. Sci. U. S. A.* **102 Suppl 1**, 6543–6549 (2005).
9. Corl, A. *et al.* The Genetic Basis of Adaptation following Plastic Changes in Coloration in a Novel Environment. *Curr. Biol.* **28**, 2970–2977.e7 (2018).
10. Wund, M. A., Baker, J. A., Clancy, B., Golub, J. L. & Foster, S. A. A test of the 'flexible stem' model of evolution: ancestral plasticity, genetic accommodation, and morphological divergence in the threespine stickleback radiation. *Am. Nat.* **172**, 449–462 (2008).
11. Levis, N. A. & Pfennig, D. W. Phenotypic plasticity, canalization, and the origins of novelty: Evidence and mechanisms from amphibians. *Semin. Cell Dev. Biol.* **88**, 80–90 (2019).
12. Ghalambor, C. K. *et al.* Non-adaptive plasticity potentiates rapid adaptive evolution of gene expression in nature. *Nature* **525**, 372–375 (2015).
13. Sommer, R. J. *et al.* The genetics of phenotypic plasticity in nematode feeding structures. *Open Biol.* **7**, 160332 (2017).
14. Projecto-Garcia, J., Biddle, J. F. & Ragsdale, E. J. Decoding the architecture and origins of mechanisms for developmental polyphenism. *Curr. Opin. Genet. Dev.* **47**, 1–8 (2017).
15. Opachaloemphan, C., Yan, H., Leibholz, A., Desplan, C. & Reinberg, D. Recent Advances in Behavioral (Epi)Genetics in Eusocial Insects. *Annu. Rev. Genet.* **52**, 489–510 (2018).
16. Moczek, A. P. *et al.* The role of developmental plasticity in evolutionary innovation. *Proc. Biol. Sci.* **278**, 2705–2713 (2011).
17. Bento, G., Ogawa, A. & Sommer, R. J. Co-option of the hormone-signalling module dafachronic acid-DAF-12 in nematode evolution. *Nature* **466**, 494–499 (2010).
18. Ragsdale, E. J., Müller, M. R., Rödelsperger, C. & Sommer, R. J. A Developmental Switch Coupled to the Evolution of Plasticity Acts through a Sulfatase. *Cell* **155**, 922–933 (2013).
19. Werner, M. S. *et al.* Environmental influence on *Pristionchus pacificus* mouth form through different culture methods. *Sci. Rep.* **7**, 7207 (2017).
20. Bose, N. *et al.* Complex small-molecule architectures regulate phenotypic plasticity in a

nematode. *Angew. Chem. Int. Ed Engl.* **51**, 12438–12443 (2012).
21. Werner, M. S., Claaßen, M. H., Renahan, T., Dardiry, M. & Sommer, R. J. Adult Influence on Juvenile Phenotypes by Stage-Specific Pheromone Production. *iScience* **10**, 123–134 (2018).
22. Sieriebriennikov, B. *et al.* A Developmental Switch Generating Phenotypic Plasticity Is Part of a Conserved Multi-gene Locus. *Cell Rep.* **23**, 2835–2843.e4 (2018).
23. Namdeo, S. *et al.* Two independent sulfation processes regulate mouth-form plasticity in the nematode *Pristionchus pacificus*. *Development* **145**, dev166272 (2018).
24. Bui, L. T., Ivers, N. A. & Ragsdale, E. J. A sulfotransferase dosage-dependently regulates mouthpart polyphenism in the nematode Pristionchus pacificus. *Nat. Commun.* **9**, 4119 (2018).
25. Bui, L. T. & Ragsdale, E. J. Multiple plasticity regulators reveal targets specifying an induced predatory form in nematodes. *Molecular Biology and Evolution* (2019). doi:10.1093/molbev/msz171
26. Serobyan, V. *et al.* Chromatin remodelling and antisense-mediated up-regulation of the developmental switch gene *eud-1* control predatory feeding plasticity. *Nat. Commun.* **7**, 12337 (2016).
27. Kieninger, M. R. *et al.* The Nuclear Hormone Receptor NHR-40 Acts Downstream of the Sulfatase EUD-1 as Part of a Developmental Plasticity Switch in *Pristionchus*. *Curr. Biol.* **26**, 2174–2179 (2016).
28. Hodgkin, J. Genetic suppression. in *WormBook* (2005).
29. Sluder, A. E., Mathews, S. W., Hough, D., Yin, V. P. & Maina, C. V. The nuclear receptor superfamily has undergone extensive proliferation and diversification in nematodes. *Genome Res.* **9**, 103–120 (1999).
30. Evans, R. M. & Mangelsdorf, D. J. Nuclear Receptors, RXR, and the Big Bang. *Cell* **157**, 255–266 (2014).
31. Brozová, E., Simecková, K., Kostrouch, Z., Rall, J. E. & Kostrouchová, M. NHR-40, a *Caenorhabditis elegans* supplementary nuclear receptor, regulates embryonic and early larval development. *Mech. Dev.* **123**, 689–701 (2006).
32. Mangan, S. & Alon, U. Structure and function of the feed-forward loop network motif. *Proc. Natl. Acad. Sci. U. S. A.* **100**, 11980–11985 (2003).
33. Macneil, L. T. & Walhout, A. J. M. Gene regulatory networks and the role of robustness and stochasticity in the control of gene expression. *Genome Res.* **21**, 645–657 (2011).
34. Bulcha, J. T. *et al.* A Persistence Detector for Metabolic Network Rewiring in an Animal. *Cell Rep.* **26**, 460–468.e4 (2019).
35. Abdusselamoglu, M. D., Eroglu, E., Burkard, T. R. & Knoblich, J. A. The transcription factor odd-paired regulates temporal identity in transit-amplifying neural progenitors via an incoherent feed-forward loop. *Elife* **8**, e46566 (2019).
36. Taylor-Teeples, M. *et al.* An *Arabidopsis* gene regulatory network for secondary cell wall synthesis. *Nature* **517**, 571–575 (2015).
37. Jaumouillé, E., Machado Almeida, P., Stähli, P., Koch, R. & Nagoshi, E. Transcriptional regulation via nuclear receptor crosstalk required for the *Drosophila* circadian clock. *Curr. Biol.* **25**, 1502–1508 (2015).
38. Anbalagan, M., Huderson, B., Murphy, L. & Rowan, B. G. Post-translational modifications of nuclear receptors and human disease. *Nucl. Recept. Signal.* **10**, e001 (2012).
39. Serobyan, V., Ragsdale, E. J., Müller, M. R. & Sommer, R. J. Feeding plasticity in the nematode *Pristionchus pacificus* is influenced by sex and social context and is linked to

753 developmental speed. *Evol. Dev.* **15**, 161–170 (2013).
754 40. Gomis-Rüth, F. X., Trillo-Muyo, S. & Stöcker, W. Functional and structural insights into
755 astacin metallopeptidases. *Biol. Chem.* **393**, 1027–1041 (2012).
756 41. Novelli, J., Ahmed, S. & Hodgkin, J. Gene interactions in *Caenorhabditis elegans* define
757 DPY-31 as a candidate procollagen C-proteinase and SQT-3/ROL-4 as its predicted
758 major target. *Genetics* **168**, 1259–1273 (2004).
759 42. Park, J.-O. *et al.* Characterization of the astacin family of metalloproteases in *C.*
760 *elegans*. *BMC Dev. Biol.* **10**, 14 (2010).
761 43. Li, Y. *et al.* Structural insights into the interaction of the conserved mammalian proteins
762 GAPR-1 and Beclin 1, a key autophagy protein. *Acta Crystallogr D Struct Biol* **73**, 775–
763 792 (2017).
764 44. Darwiche, R., Kelleher, A., Hudspeth, E. M., Schneiter, R. & Asojo, O. A. Structural and
765 functional characterization of the CAP domain of pathogen-related yeast 1 (Pry1)
766 protein. *Sci. Rep.* **6**, 28838 (2016).
767 45. Choudhary, V. & Schneiter, R. Pathogen-Related Yeast (PRY) proteins and members of
768 the CAP superfamily are secreted sterol-binding proteins. *Proc. Natl. Acad. Sci. U. S. A.*
769 **109**, 16882–16887 (2012).
770 46. Gibbs, G. M., Roelants, K. & O'Bryan, M. K. The CAP superfamily: cysteine-rich
771 secretory proteins, antigen 5, and pathogenesis-related 1 proteins - roles in
772 reproduction, cancer, and immune defense. *Endocr. Rev.* **29**, 865–897 (2008).
773 47. Henrissat, B. *et al.* Conserved catalytic machinery and the prediction of a common fold
774 for several families of glycosyl hydrolases. *Proc. Natl. Acad. Sci. U. S. A.* **92**, 7090–
775 7094 (1995).
776 48. Lints, R. & Hall, D. H. The cuticle. in *WormAtlas* (2009).
777 49. Tokareva, O., Jacobsen, M., Buehler, M., Wong, J. & Kaplan, D. L. Structure-function-
778 property-design interplay in biopolymers: spider silk. *Acta Biomater.* **10**, 1612–1626
779 (2014).
780 50. Guan, J., Vollrath, F. & Porter, D. Two mechanisms for supercontraction in *Nephila*
781 spider dragline silk. *Biomacromolecules* **12**, 4030–4035 (2011).
782 51. Smit, R. B., Schnabel, R. & Gaudet, J. The HLH-6 transcription factor regulates *C.*
783 *elegans* pharyngeal gland development and function. *PLoS Genet.* **4**, e1000222 (2008).
784 52. Riebesell, M. & Sommer, R. J. Three-dimensional reconstruction of the pharyngeal
785 gland cells in the predatory nematode *Pristionchus pacificus*. *Journal of Morphology*
786 **278**, 1656–1666 (2017).
787 53. van Megen, H. *et al.* A phylogenetic tree of nematodes based on about 1200 full-length
788 small subunit ribosomal DNA sequences. *Nematology* **11**, 927–950 (2009).
789 54. Altun, Z. F. & Hall, D. H. Alimentary System, Pharynx. in *WormAtlas* (2009).
790 55. Zhang, Y. C. & Baldwin, J. G. Ultrastructure of the postcorpus of the esophagus of
791 *Teratocephalus lirellus* (Teratocephalida) and its use for interpreting character evolution
792 in Secernentea (Nematoda). *Can. J. Zool.* **79**, 16–25 (2001).
793 56. Zhang Y. C. & Baldwin J. G. Ultrastructure of the post–corpus of *Zeldia punctata*
794 (Cephalobina) for analysis of the evolutionary framework of nematodes related to
795 *Caenorhabditis elegans* (Rhabditina). *Proceedings of the Royal Society of London.*
796 *Series B: Biological Sciences* **267**, 1229–1238 (2000).
797 57. Chiang, J.-T. A., Steciuk, M., Shtonda, B. & Avery, L. Evolution of pharyngeal behaviors
798 and neuronal functions in free-living soil nematodes. *J. Exp. Biol.* **209**, 1859–1873
799 (2006).
800 58. Zhang, Y. C. & Baldwin, J. G. Ultrastructure of the Esophagus of *Diplenteron* sp.

(Diplogasterida) to Test Hypotheses of Homology with Rhabditida and Tylenchida. *J. Nematol.* **31**, 1–19 (1999).
59. Prabh, N. *et al.* Deep taxon sampling reveals the evolutionary dynamics of novel gene families in *Pristionchus* nematodes. *Genome Res.* **28**, 1664–1674 (2018).
60. Markov, G. V., Baskaran, P. & Sommer, R. J. The same or not the same: lineage-specific gene expansions and homology relationships in multigene families in nematodes. *J. Mol. Evol.* **80**, 18–36 (2015).
61. Antebi, A., Yeh, W. H., Tait, D., Hedgecock, E. M. & Riddle, D. L. *daf-12* encodes a nuclear receptor that regulates the dauer diapause and developmental age in *C. elegans*. *Genes Dev.* **14**, 1512–1527 (2000).
62. Burton, N. O. *et al.* Neurohormonal signaling via a sulfotransferase antagonizes insulin-like signaling to regulate a *Caenorhabditis elegans* stress response. *Nat. Commun.* **9**, 5152 (2018).
63. Structure, Function and Evolution of The Nematode Genome. in *eLS* (ed. John Wiley & Sons, Ltd) **26**, 909 (John Wiley & Sons, Ltd, 2001).
64. Mitreva, M., Blaxter, M. L., Bird, D. M. & McCarter, J. P. Comparative genomics of nematodes. *Trends Genet.* **21**, 573–581 (2005).
65. Manning, G., Plowman, G. D., Hunter, T. & Sudarsanam, S. Evolution of protein kinase signaling from yeast to man. *Trends Biochem. Sci.* **27**, 514–520 (2002).
66. Goodrich, L. V., Johnson, R. L., Milenkovic, L., McMahon, J. A. & Scott, M. P. Conservation of the *hedgehog*/*patched* signaling pathway from flies to mice: induction of a mouse *patched* gene by Hedgehog. *Genes Dev.* **10**, 301–312 (1996).
67. Logan, C. Y. & Nusse, R. The Wnt signaling pathway in development and disease. *Annu. Rev. Cell Dev. Biol.* **20**, 781–810 (2004).
68. Stiernagle, T. Maintenance of *C. elegans* (February 11, 2006). in *WormBook* (ed. The C. elegans research community) (2016).
69. Witte, H. *et al.* Gene inactivation using the CRISPR/Cas9 system in the nematode *Pristionchus pacificus*. *Dev. Genes Evol.* **225**, 55–62 (2015).
70. Lightfoot, J. W. *et al.* Small peptide-mediated self-recognition prevents cannibalism in predatory nematodes. *Science* **364**, 86–89 (2019).
71. Zhou, S. *et al.* Characterization of a non-sexual population of *Strongyloides stercoralis* with hybrid 18S rDNA haplotypes in Guangxi, Southern China. *PLoS Negl. Trop. Dis.* **13**, e0007396 (2019).
72. Rödelsperger, C. *et al.* Single-Molecule Sequencing Reveals the Chromosome-Scale Genomic Architecture of the Nematode Model Organism *Pristionchus pacificus*. *Cell Rep.* **21**, 834–844 (2017).
73. Langmead, B. & Salzberg, S. L. Fast gapped-read alignment with Bowtie 2. *Nat. Methods* **9**, 357–359 (2012).
74. Robinson, J. T. *et al.* Integrative genomics viewer. *Nat. Biotechnol.* **29**, 24–26 (2011).
75. Pires-daSilva, A. *Pristionchus pacificus* protocols (March 14, 2013). in *WormBook* (ed. The C. elegans research community) (2013).
76. Li, H. & Durbin, R. Fast and accurate short read alignment with Burrows-Wheeler transform. *Bioinformatics* **25**, 1754–1760 (2009).
77. Li, H. *et al.* The Sequence Alignment/Map format and SAMtools. *Bioinformatics* **25**, 2078–2079 (2009).
78. Rae, R., Witte, H., Rödelsperger, C. & Sommer, R. J. The importance of being regular: *Caenorhabditis elegans* and *Pristionchus pacificus* defecation mutants are hypersusceptible to bacterial pathogens. *Int. J. Parasitol.* **42**, 747–753 (2012).

79. Schlager, B., Wang, X., Braach, G. & Sommer, R. J. Molecular cloning of a dominant roller mutant and establishment of DNA-mediated transformation in the nematode *Pristionchus pacificus*. *Genesis* **47**, 300–304 (2009).
80. OpenWetWare contributors. Gibson Assembly. *OpenWetWare* (2018). Available at: https://openwetware.org/mediawiki/index.php?title=Gibson_Assembly&oldid=1043969. (Accessed: 25th July 2018)
81. Bettinger, J. C., Lee, K. & Rougvie, A. E. Stage-specific accumulation of the terminal differentiation factor LIN-29 during *Caenorhabditis elegans* development. *Development* **122**, 2517–2527 (1996).
82. Dobin, A. *et al.* STAR: ultrafast universal RNA-seq aligner. *Bioinformatics* **29**, 15–21 (2013).
83. R Core Team. *R: A language and environment for statistical computing*. (R Foundation for Statistical Computing, 2016).
84. Gentleman, R. C. *et al.* Bioconductor: open software development for computational biology and bioinformatics. *Genome Biol.* **5**, R80 (2004).
85. Love, M. I., Huber, W. & Anders, S. Moderated estimation of fold change and dispersion for RNA-seq data with DESeq2. *Genome Biol.* **15**, 550 (2014).
86. Möhrlen, F., Hutter, H. & Zwilling, R. The astacin protein family in *Caenorhabditis elegans*. *Eur. J. Biochem.* **270**, 4909–4920 (2003).
87. Finn, R. D. *et al.* The Pfam protein families database: towards a more sustainable future. *Nucleic Acids Res.* **44**, D279–85 (2016).
88. Sinha, A., Langnick, C., Sommer, R. J. & Dieterich, C. Genome-wide analysis of trans-splicing in the nematode *Pristionchus pacificus* unravels conserved gene functions for germline and dauer development in divergent operons. *RNA* **20**, 1386–1397 (2014).
89. Werner, M. S. *et al.* Young genes have distinct gene structure, epigenetic profiles, and transcriptional regulation. *Genome Res.* **28**, 1675–1687 (2018).
90. Katoh, K. & Standley, D. M. MAFFT multiple sequence alignment software version 7: improvements in performance and usability. *Mol. Biol. Evol.* **30**, 772–780 (2013).
91. Stamatakis, A. RAxML version 8: a tool for phylogenetic analysis and post-analysis of large phylogenies. *Bioinformatics* **30**, 1312–1313 (2014).

Acknowledgments

We are grateful to Gabi Eberhardt and Tobias Loschko for their assistance with the mutagenesis screens. We also thank Dr. Adrian Streit, Metta Riebesell, Dr. Neel Prabh and Dr. Michael Werner for the discussion. The study was funded by the Max Planck Society, and S.S. was supported by the China Scholarship Council.

Author contributions

B.S. designed and performed all experiments with help from other authors, analyzed the data, and wrote the manuscript together with R.J.S.; S.S. designed and created reporter lines for Astacin genes, performed a suppressor screen in the *nhr-1* mutant background, and participated in mouth-form phenotyping; J.W.L. and E.M. generated *nhr-40* mutations using CRISPR/Cas9, J.W.L. additionally generated mutations in the downstream targets of NHR-1 and NHR-40; C.R. performed bulk segregant analysis; H.W. generated CRISPR/Cas9 mutants and transgenes; R.J.S. designed and supervised the study, and wrote the manuscript together with B.S.

Competing interests

The authors are not aware of any competing interests.

Materials & Correspondence

Correspondence and requests for materials should be addressed to R.J.S.

Figure legends

Fig. 1. Mouth-form plasticity in *P. pacificus*. (**A**) Mouth structure of wild-type eurystomatous (Eu) morph, wild-type stenostomatous (St) morph, *nhr-1* mutant, and *nhr-40* mutant. Unlabeled images in two focal planes are shown in SFig. 1A. (**B**) Scanning electron microscopy image of the mouth opening of the Eu morph. (**C**) The Eu morph devouring its prey. (**D**) Putative gene regulatory network controlling mouth-form plasticity in *P. pacificus*. (**E**) Design of the suppressor screen. D = dorsal, V= ventral, A = anterior, P = posterior, DT = dorsal tooth, RVSLT = right ventrosublateral tooth, RVSLR = right ventrosublateral ridge, EMS = ethyl methanesulfonate.

Fig. 2. Reverse genetics, transcriptomics and expression patterns of *nhr-40* and *nhr-1*. (**A**) Protein structure of NHR-40 in wild-type and mutant animals. (**B**) Expression levels of *nhr-40* and *nhr-1* in wild type and mutants as revealed by transcriptomic profiling. (**C**) Antibody staining against the HA epitope in an *nhr-1* rescue line. (**D**) Expression patterns of *nhr-40* and *nhr-1* transcriptional reporters in a double reporter line. TurboRFP (magenta) and Venus (green) channels are presented as maximum intensity projections. Co-expression results in white color. D = dorsal, V= ventral, A = anterior, P = posterior, N.S. = not significant.

Fig. 3. Target genes of NHR-40 and NHR-1. (**A**) Experimental setup of transcriptomics experiment and selection criteria to identify target genes. (**B**) Trends among target genes compared to genome-wide pattern. (**C**) Transmission electron microscopy reconstruction of the dorsal pharyngeal gland cell (g1D) [52] and expression patterns of transcriptional reporters for nine selected targets of NHR-40 and NHR-1. TurboRFP channel is presented as standard deviation projections. *lof* = *loss of function*, *gof* = *gain of function*, *** = $p<0.001$, D = dorsal, V= ventral, A = anterior, P = posterior.

Fig. 4. Evolution of pharynx morphology in the order Rhabditida.

Fig. 5. Evolution of *nhr-40*, *nhr-1*, and their target genes. Arrowheads point at the genes of interest. Protein-based trees of NHR genes (**A**), Astacin domains (**B**), chitinase domains (**C**), and CAP domains (**D**) in *P. pacificus* and *C. elegans*. (**E**) Nucleotide-based tree of the CAP domains from a poorly-resolved protein-based subtree of all predicted CAP domains in *P. pacificus* and *P. fissidentatus*.

Table 1. Mouth-form frequencies in wild type and mutant lines.

Table 2. List of targets of NHR-40 and NHR-1.

SFig. 1. Additional images. (**A**) The mouth of the wild-type eurystomatous (Eu) morph, wild-type stenostomatous (St) morph, *nhr-1* mutant, and *nhr-40* mutant in two focal planes. (**B**) Expression pattern of an *nhr-1* transcriptional reporter in a young larva. TurboRFP channel is presented as a maximum intensity projection. (**C**) Antibody staining against the HA epitope in a line, in which the tag was “knocked in” into the endogenous locus. Fluorescent channel is presented as a maximum intensity projection. (**D**) Expression patterns of *nhr-40* and *nhr-1* transcriptional reporters in a double reporter line. TurboRFP (magenta) and Venus (green) channels are presented as standard deviation and maximum intensity projections, respectively. Co-expression results in white color. (**E**) Expression patterns of *nhr-40* and *nhr-*

952 *1* transcriptional reporters in a double reporter line. TurboRFP is encoded as magenta, Venus
953 as green. Co-expression results in white color. D = dorsal, V= ventral, A = anterior, P =
954 posterior.
955
956 **SFig. 2.** Additional bioinformatic analyses. (**A**) Whole-genome re-sequencing and RNA-seq of
957 the *null* allele of *nhr-40*. (**B**) Bulk segregant analysis of the suppressor of *nhr-40(tu505)* with
958 the location of *nhr-1* marked with a dotted line. See STable 1 for the list of non-synonymous
959 and nonsense substitutions within the candidate region.
960
961 **STable 1.** List of non-synonymous and nonsense substitutions within the candidate region on
962 chromosome X identified through the bulk segregant analysis of the suppressor of *nhr-*
963 *40(tu505)*.

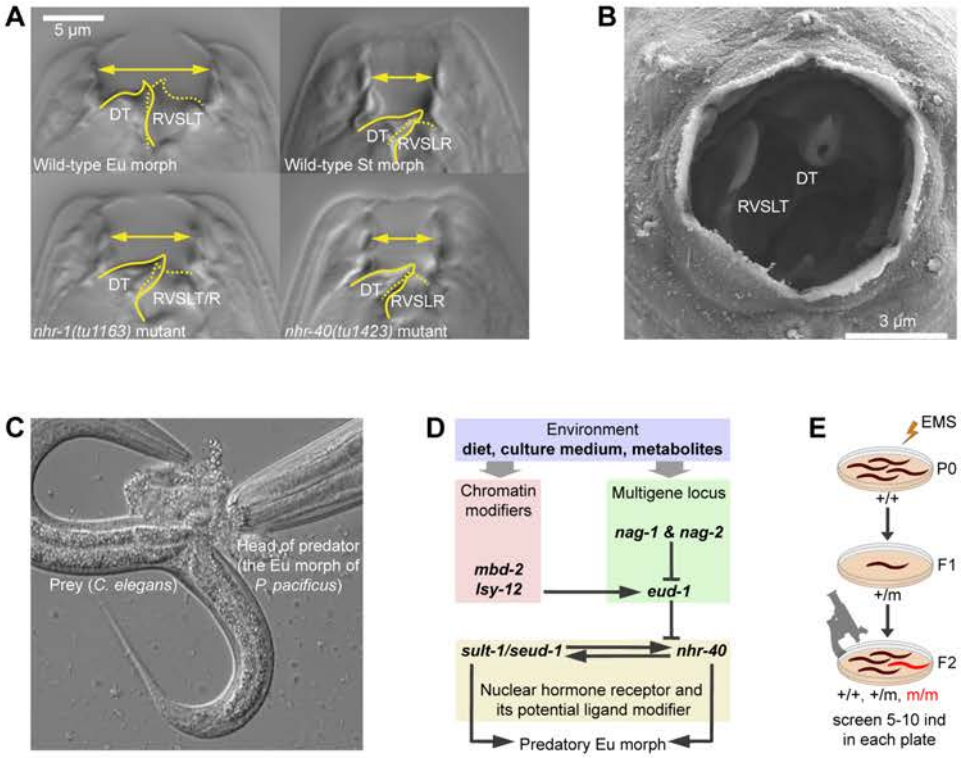

Fig. 1. Mouth-form plasticity in *P. pacificus*. (**A**) Mouth structure of wild-type eurystomatous (Eu) morph, wild-type stenostomatous (St) morph, *nhr-1* mutant, and *nhr-40* mutant. Unlabeled images in two focal planes are shown in SFig. 1A. (**B**) Scanning electron microscopy image of the mouth opening of the Eu morph. (**C**) The Eu morph devouring its prey. (**D**) Putative gene regulatory network controlling mouth-form plasticity in *P. pacificus*. (**E**) Design of the suppressor screen.
D = dorsal, V= ventral, A = anterior, P = posterior, DT = dorsal tooth, RVSLT = right ventrosublateral tooth, RVSLR = right ventrosublateral ridge, EMS = ethyl methanesulfonate.

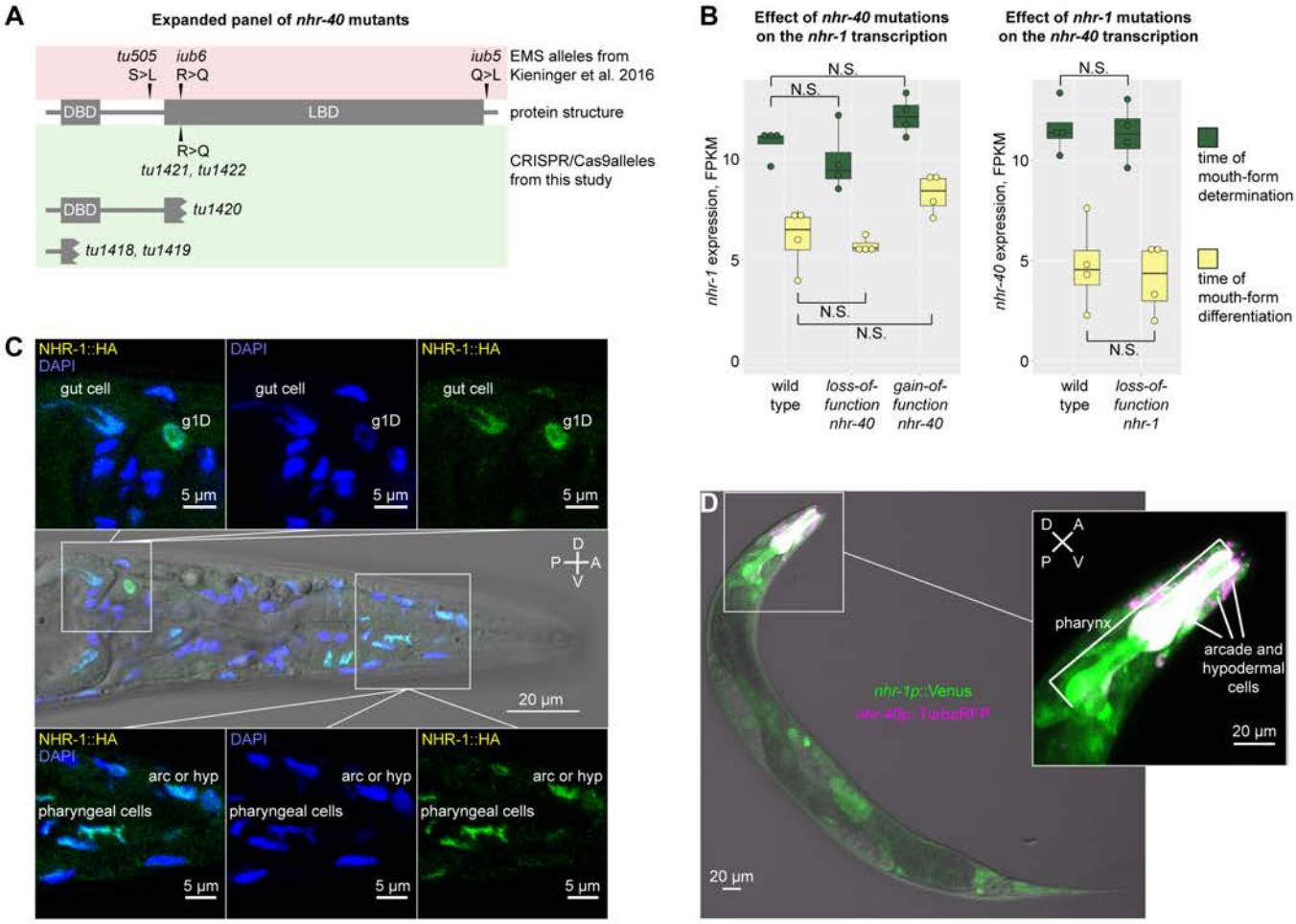

Fig. 2. Reverse genetics, transcriptomics and expression patterns of *nhr-40* and *nhr-1*. (**A**) Protein structure of NHR-40 in wild-type and mutant animals. (**B**) Expression levels of *nhr-40* and *nhr-1* in wild type and mutants as revealed by transcriptomic profiling. (**C**) Antibody staining against the HA epitope in an *nhr-1* rescue line. (**D**) Expression patterns of *nhr-40* and *nhr-1* transcriptional reporters in a double reporter line. TurboRFP (magenta) and Venus (green) channels are presented as maximum intensity projections. Co-expression results in white color.
D = dorsal, V= ventral, A = anterior, P = posterior, N.S. = not significant.

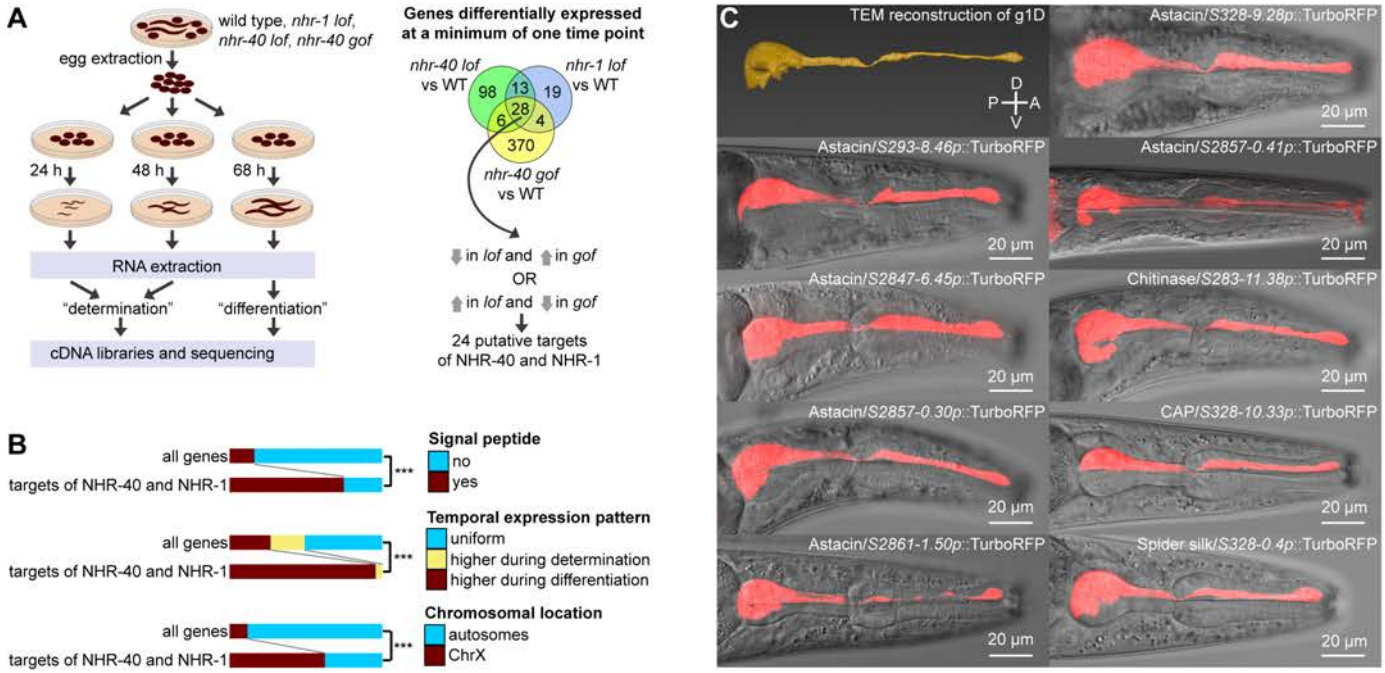

Fig. 3. Target genes of NHR-40 and NHR-1. (**A**) Experimental setup of transcriptomics experiment and selection criteria to identify target genes. (**B**) Trends among target genes compared to genome-wide pattern. (**C**) Transmission electron microscopy reconstruction of the dorsal pharyngeal gland cell (g1D) [52] and expression patterns of transcriptional reporters for nine selected targets of NHR-40 and NHR-1. TurboRFP channel is presented as standard deviation projections.
lof = loss of function, gof = gain of function, *** = p<0.001, D = dorsal, V= ventral, A = anterior, P = posterior.

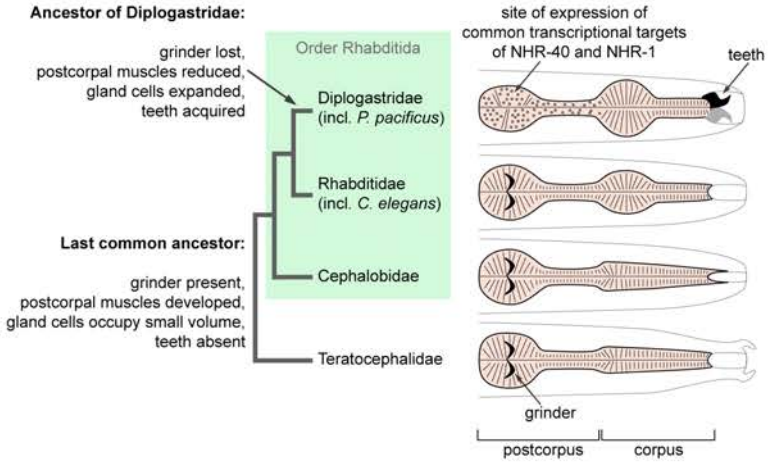

Fig. 4. Evolution of pharynx morphology in the order Rhabditida.

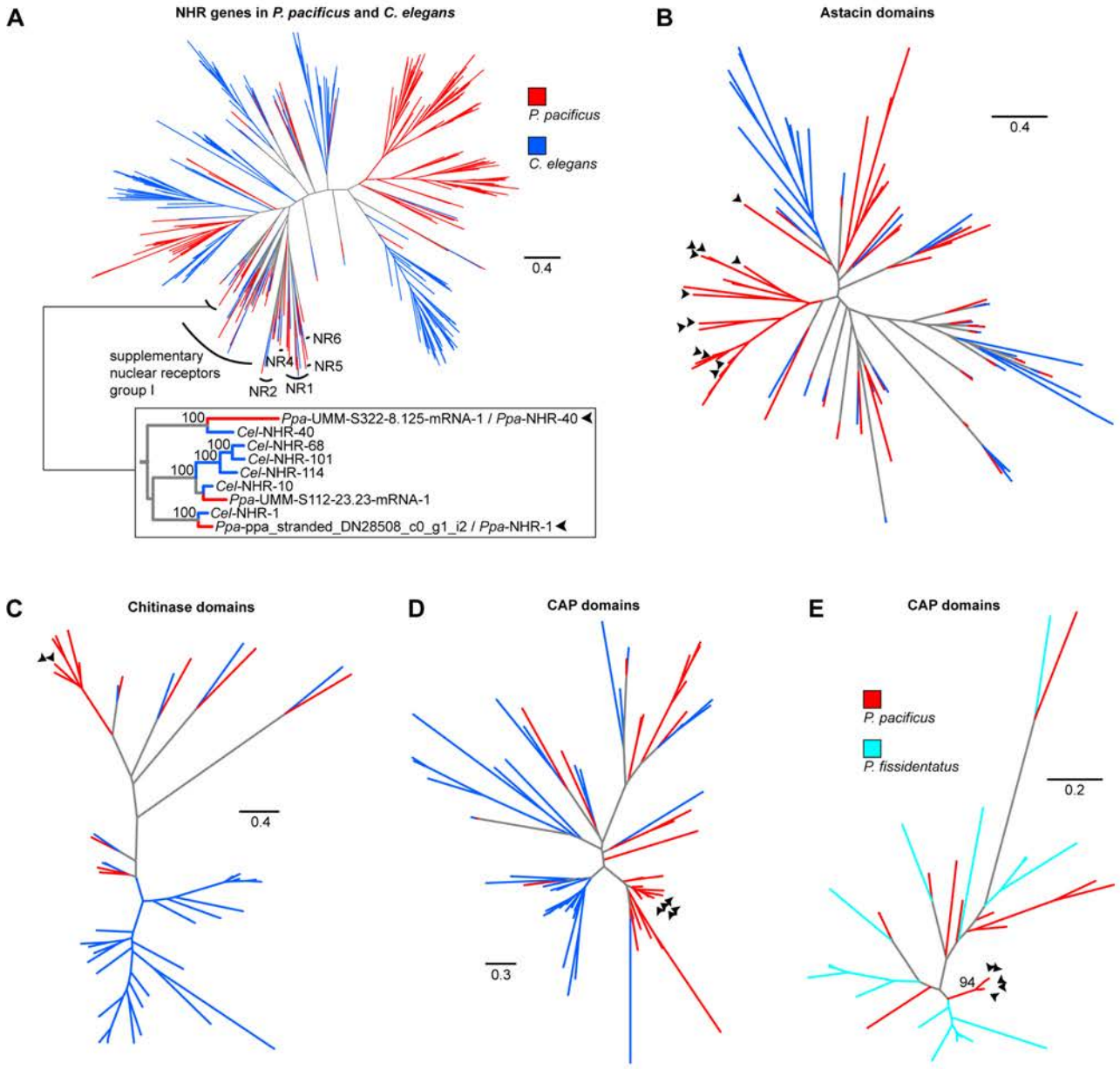

Fig. 5. Evolution of *nhr-40*, *nhr-1*, and their target genes. Arrowheads point at the genes of interest. Protein-based trees of NHR genes (**A**), Astacin domains (**B**), chitinase domains (**C**), and CAP domains (**D**) in *P. pacificus* and *C. elegans*. (**E**) Nucleotide-based tree of the CAP domains from a poorly-resolved protein-based subtree of all predicted CAP domains in *P. pacificus* and *P. fissidentatus*.

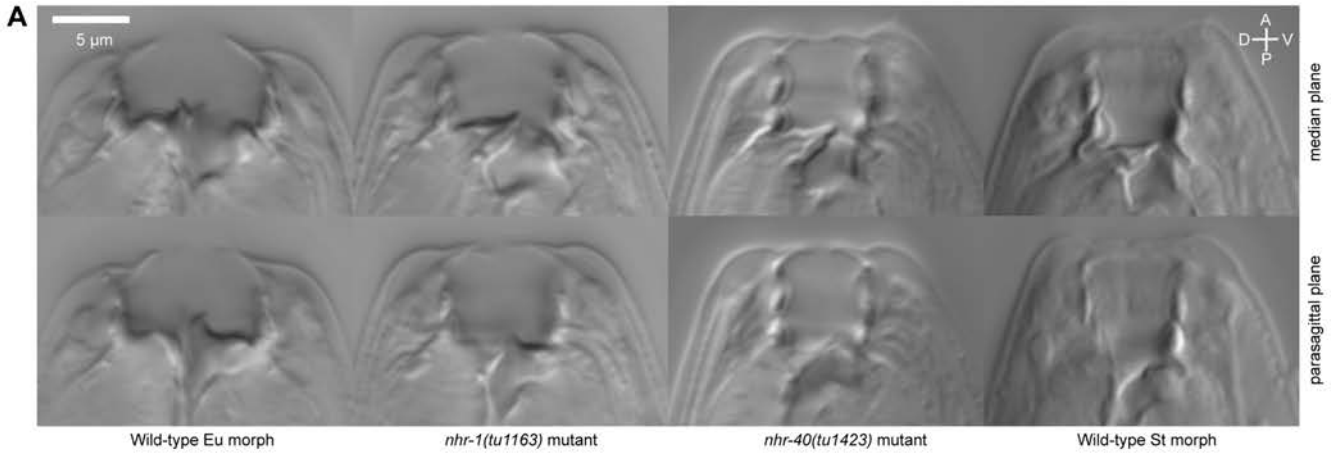
A
5 µm
A
D
V
P
median plane
parasagittal plane
Wild-type Eu morph
nhr-1(tu1163) mutant
nhr-40(tu1423) mutant
Wild-type St morph

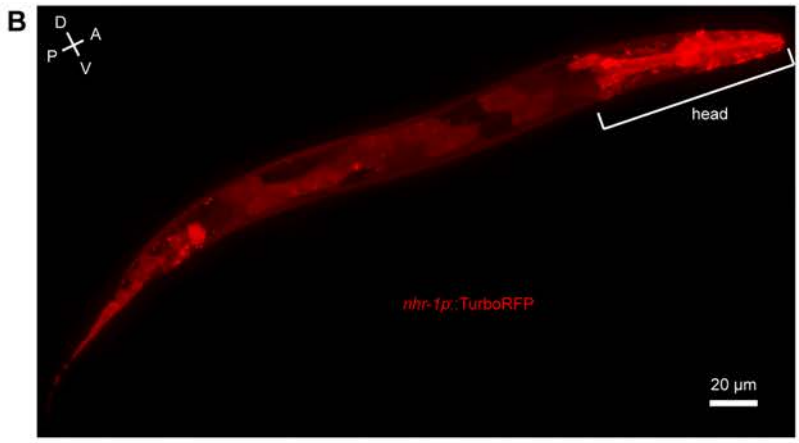
B
D
A
P
V
head
nhr-1p::TurboRFP
20 µm

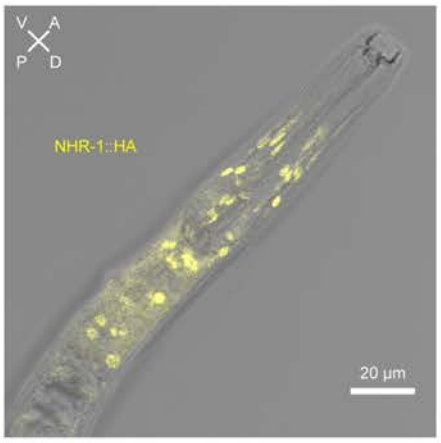
C
V
A
P
D
NHR-1::HA
20 µm

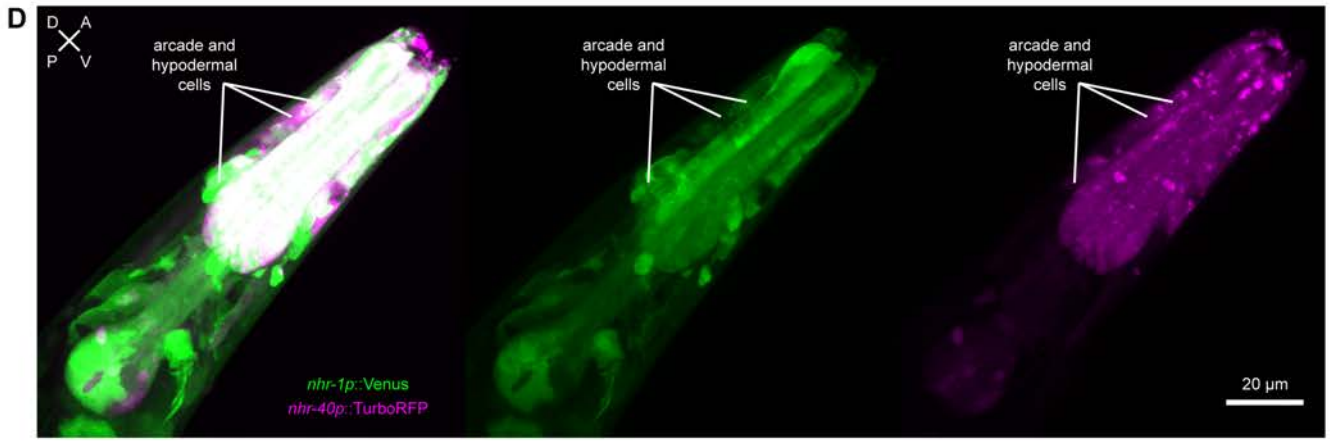
D
D
A
P
V
arcade and hypodermal cells
arcade and hypodermal cells
arcade and hypodermal cells
nhr-1p::Venus
nhr-40p::TurboRFP
20 µm

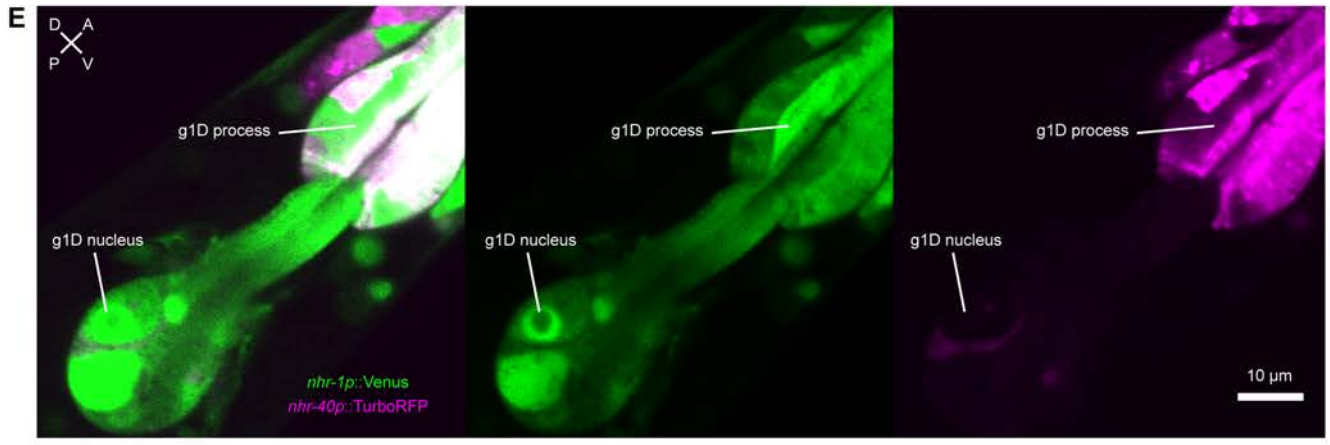
E
D
A
P
V
g1D process
g1D process
g1D process
g1D nucleus
g1D nucleus
g1D nucleus
nhr-1p::Venus
nhr-40p::TurboRFP
10 µm

SFig. 1.

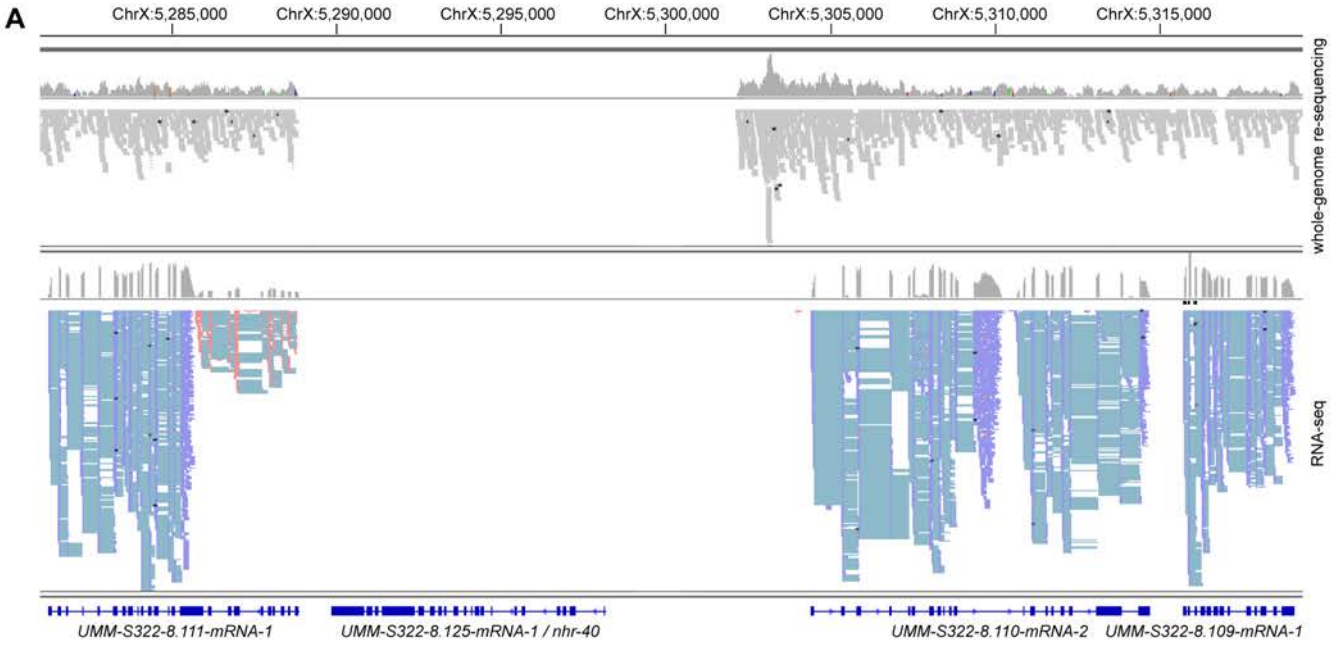
A
ChrX:5,285,000
ChrX:5,290,000
ChrX:5,295,000
ChrX:5,300,000
ChrX:5,305,000
ChrX:5,310,000
ChrX:5,315,000
whole-genome re-sequencing
RNA-seq
UMM-S322-8.111-mRNA-1
UMM-S322-8.125-mRNA-1 / nhr-40
UMM-S322-8.110-mRNA-2
UMM-S322-8.109-mRNA-1

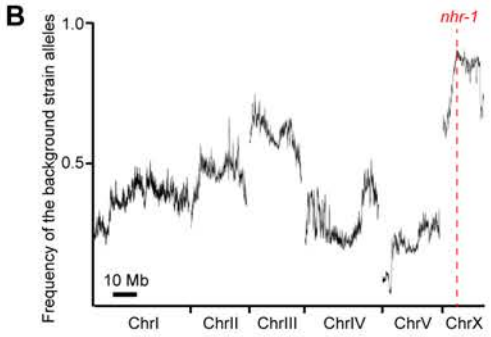
B
nhr-1
Frequency of the background strain alleles
1.0
0.5
10 Mb
ChrI
ChrII
ChrIII
ChrIV
ChrV
ChrX

SFig. 2.

Table 1

Medium	Genotype	Eu, %	N
NGM agar	wild type PS312	98	650
NGM agar	*nhr-40(tu505)*	100	100
NGM agar	*nhr-40(tu505) tu515*	0	136
NGM agar	*tu515*	0	136
NGM agar	*nhr-1(tu1163)*	0	133
NGM agar	*nhr-1(tu1164)*	0	140
NGM agar	*nhr-1(tu1163)/tu515*	0	70
NGM agar	*nhr-1(tu1163);tuEx305[nhr-1(+);egl-20p::TurboRFP]*	85	110
NGM agar	*nhr-1(tu1163);tuEx310[nhr-1(+);egl-20p::TurboRFP]*	86	112
NGM agar	*nhr-1(tu1163);tuEx328[nhr-1(+)::HA;egl-20p::TurboRFP]*	86	150
NGM agar	*nhr-40(tu505) nhr-1(tu1163)*	2	134
NGM agar	*nhr-40(tu1418)*	0	150
NGM agar	*nhr-40(tu1419)*	0	150
NGM agar	*nhr-40(tu1420)*	0	150
NGM agar	*nhr-40(tu1423)*	0	150
NGM agar	*nhr-40(iub6)*	100	100
NGM agar	*nhr-40(tu1421)*	100	150
NGM agar	*nhr-40(tu1422)*	100	100
NGM agar	*PPA03932(tu1259) PPA32730(tu1503);PPA05669(tu1316) PPA05618(tu1317) PPA21987(tu1329) PPA16331(tu1339) PPA27985(tu1340) PPA34430(tu1341) PPA20266(tu1385) PPA42924(tu1386);PPA05955(tu1481) PPA42525(tu1482)*	98	55
NGM agar	*tuDf6[PPA21912 PPA29522 PPA21910] tuDf7[PPA05611 PPA39470] tuDf8[PPA13058 PPA39735]*	94	50
NGM agar	*PPA04200(tu1213) PPA39293(tu1214)*	100	50
NGM agar	*PPA04200(tu1216) PPA39293(tu1217)*	100	50
NGM agar	*PPA27560(tu1475)*	100	51
NGM agar	*PPA27560(tu1476)*	100	53
NGM agar	*PPA30108(tu1230)*	100	50
NGM agar	*PPA30108(tu1231)*	100	50
NGM agar	*PPA30435(tu1477)*	100	48
NGM agar	*PPA30435(tu1478)*	98	54
NGM agar	*PPA38892(tu1473)*	100	50
NGM agar	*PPA38892(tu1474)*	100	50
S-medium	wild type PS312	5	850
S-medium	*nhr-40(tu505)*	100	150
S-medium	*nhr-40(tu1418)*	0	150
S-medium	*nhr-40(tu1419)*	0	150
S-medium	*nhr-40(tu1420)*	0	150
S-medium	*nhr-40(tu1423)*	0	150
S-medium	*nhr-40(iub6)*	100	150
S-medium	*nhr-40(tu1421)*	100	150
S-medium	*nhr-40(tu1422)*	100	150
S-medium	*PPA03932(tu1259) PPA32730(tu1503);PPA05669(tu1316) PPA05618(tu1317) PPA21987(tu1329) PPA16331(tu1339) PPA27985(tu1340) PPA34430(tu1341) PPA20266(tu1385) PPA42924(tu1386);PPA05955(tu1481) PPA42525(tu1482)*	32	50
S-medium	*tuDf6[PPA21912 PPA29522 PPA21910] tuDf7[PPA05611 PPA39470] tuDf8[PPA13058 PPA39735]*	19	100
S-medium	*PPA04200(tu1213) PPA39293(tu1214)*	0	50
S-medium	*PPA04200(tu1216) PPA39293(tu1217)*	4	50
S-medium	*PPA27560(tu1475)*	5	44
S-medium	*PPA27560(tu1476)*	24	54
S-medium	*PPA30108(tu1230)*	4	50
S-medium	*PPA30108(tu1231)*	0	50
S-medium	*PPA30435(tu1477)*	14	51
S-medium	*PPA30435(tu1478)*	8	53
S-medium	*PPA38892(tu1473)*	14	51
S-medium	*PPA38892(tu1474)*	0	46

Table 2

Chromosome	Wormbase WS268 Identifier	El Paco annotation v1 Identifier	Predicted PFAM domains	Log fold change, *nhr-1* vs. wild type, determination time point	Log fold change, *nhr-1* vs. wild type, differentiation time point	Log fold change, *nhr-40 loss-of-function* vs. wild type, determination time point	Log fold change, *nhr-40 loss-of-function* vs. wild type, differentiation time point	Log fold change, *nhr-40 gain-of-function* vs. wild type, determination time point	Log fold change, *nhr-40 gain-of-function* vs. wild type, differentiation time point
ChrX	*PPA05669*	*UMM-S328-9.28-mRNA-1*	Astacin	-6.240745897	-7.986635198	-7.210987982	-7.830279165	2.097757153	1.095985392
ChrIV	*PPA42525*	*UMM-S2847-7.46-mRNA-1*	Astacin	-4.841545383	-4.002165721	-7.839896476	-4.679957866	1.436839716	not significant
ChrIV	*PPA05955*	*UMM-S2847-6.45-mRNA-1*	Astacin	-4.032019323	-3.717834286	-6.639723524	-5.984683399	1.574571506	1.061560179
ChrX	*PPA05618*	*UMM-S328-7.47-mRNA-1*	Astacin	-3.574438844	-2.916374055	-7.745129989	-7.021294279	1.499309832	0.981934683
ChrX	*PPA16331*	*UMA-S293-8.46-mRNA-1*	Astacin	-2.699652128	-4.119198644	-3.460891813	-4.200736918	1.709937147	not significant
ChrX	*PPA39735*	*UMM-S328-10.33-mRNA-1*	CAP	-2.204596416	-2.494207229	-5.147759463	-5.268476177	1.413344404	not significant
ChrI	*PPA32730*	*UMM-S57-4.91-mRNA-1*	Astacin	-2.196833674	-1.648291234	-3.691078865	-3.030762239	1.685906094	0.781158675
ChrX	*PPA13058*	*UMM-S328-10.78-mRNA-1*	CAP	-2.072130667	-2.430015473	-4.777644344	-4.798862505	1.417106528	not significant
ChrIV	*PPA39293*	*UMM-S283-11.38-mRNA-1*	Glyco_hydro_18	-1.78798789	-1.00008438	-2.965102834	-1.920988766	0.91017037	not significant
ChrX	*PPA29522*	*UMM-S322-3.5-mRNA-1*	CAP	-1.619243845	not significant	-3.144502729	-1.482861278	0.989651252	not significant
ChrX	*PPA39470*	*UMM-S293-11.30-mRNA-1*	CAP	-1.535650433	-2.217536886	-4.429166678	-4.946006302	1.368183938	not significant
ChrX	*PPA21910*	*UMA-S322-3.38-mRNA-1*	CAP	-1.360420618	not significant	-2.333203285	-1.220283993	0.933478914	not significant
ChrIV	*PPA04200*	*UMM-S283-11.45-mRNA-1*	Glyco_hydro_18; MFS_1	-1.260777947	-0.790389646	-2.139628634	-1.317889252	0.858388553	not significant
ChrX	*PPA21987*	*UMA-S322-7.39-mRNA-1*	Astacin	-1.088820963	-1.133945969	-1.538108635	not significant	0.872393205	0.857569687
ChrX	*PPA27985*	*UMS-S2861-1.50-mRNA-1*	Astacin	-1.024169798	-1.594336612	-1.391792366	-1.82457695	0.856234189	0.920390529
ChrX	*PPA30108*	*UMS-S328-0.4-mRNA-1*		-0.947256862	-1.972768009	-1.664145426	-3.055683539	1.366224893	0.725689297
ChrII	*PPA27560*	*UMS-S10-46.25-mRNA-1*		not significant	-2.543527944	not significant	-1.495616763	1.576247265	not significant
ChrI	*PPA30435*	*UMM-S57-36.5-mRNA-1*	Lectin_C	not significant	-2.47831085	-6.394747605	-7.477473473	1.742988559	0.834485758
ChrX	*PPA34430*	*UMA-S2861-1.27-mRNA-1*	Astacin	not significant	-2.034806495	-1.356487112	-2.16601043	0.954950699	0.920888012
ChrX	*PPA38892*	*UMM-S250-3.76-mRNA-1*	ShK	not significant	-1.978289093	-1.766665626	-2.237851004	0.974981875	not significant
ChrX	*PPA20266*	*UMM-S2857-0.30-mRNA-1*	Astacin	not significant	-1.886347752	-1.391984972	-2.526477858	1.083601827	not significant
ChrX	*PPA42924*	*UMM-S2857-0.41-mRNA-1*	Astacin	not significant	-1.144915897	not significant	-1.729607349	0.848434069	not significant
ChrI	*PPA03932*	*UMM-S7-5.16-mRNA-1*	Astacin	not significant	-1.111093666	not significant	-1.621750021	1.106139077	0.751674205
ChrIV	*PPA06264*	*UMA-S2838-46.74-mRNA-1*	adh_short; KR; THF_DHG_CYH_C	not significant	2.240401693	not significant	2.955986944	-2.049582222	not significant

STable 1

Chromosome	Position	Ref allele	Mutant allele	Wormbase WS268 Identifier	El Paco annotation v1 Identifier	Putative *C. elegans* ortholog	Classification
ChrX	5699852	A	T	*PPA39635*	*UMM-S322-4.13-mRNA-1*		non-synonymous
ChrX	5753767	C	T	*PPA21915*	*UMM-S322-4.28-mRNA-1*	*nhr-1*	non-synonymous
ChrX	6299273	C	T	*PPA10517*	*UMM-S429-1.43-mRNA-1*	*glr-8*	non-synonymous
ChrX	6367712	A	C	*PPA40141*	*UMM-S429-2.95-mRNA-1*		non-synonymous
ChrX	6380013	A	T	*PPA05325*	*UMM-S429-2.97-mRNA-1*	*nep-17*	non-synonymous
ChrX	6402673	C	T	*PPA40146*	*UMM-S429-2.115-mRNA-1*		non-synonymous
ChrX	6443259	T	A	*PPA05313*	*UMM-S429-2.24-mRNA-1*	*K09E2.1*	non-synonymous
ChrX	6444545	G	C	*PPA05313*	*UMM-S429-2.24-mRNA-1*	*K09E2.1*	non-synonymous
ChrX	6957752	C	T	*PPA18712*	*UMM-S293-2.13-mRNA-1*	*sec-3*	non-synonymous
ChrX	7145062	C	T	*PPA39440*	*UMM-S293-4.13-mRNA-1*		non-synonymous
ChrX	7479342	T	A	*PPA18845*	*UMM-S293-7.70-mRNA-1*	*ZK470.2*	non-synonymous
ChrX	7479349	C	A	*PPA18845*	*UMM-S293-7.70-mRNA-1*	*ZK470.2*	non-synonymous
ChrX	7900717	A	G	*PPA09604*	*UMM-S293-11.35-mRNA-1*		non-synonymous
ChrX	8602408	C	T	*PPA45298*	*UMS-S328-6.31-mRNA-1*		non-synonymous
ChrX	8866724	C	T	*PPA39709*	*UMM-S328-3.19-mRNA-1*		non-synonymous
ChrX	9098848	T	G	*PPA30108*	*UMS-S328-0.4-mRNA-1*		non-synonymous
ChrX	9098849	T	A	*PPA30108*	*UMS-S328-0.4-mRNA-1*		nonsense
ChrX	9099400	A	G	*PPA30108*	*UMS-S328-0.4-mRNA-1*		non-synonymous
ChrX	9387377	C	T	*PPA07538*	*UMM-S419-3.4-mRNA-1*	*flp-11*	non-synonymous
ChrX	9894810	G	A	*PPA20385*	*UMM-S2857-8.19-mRNA-1*	*tap-1*	non-synonymous
ChrX	1.2E+07	C	T	*PPA03807*	*UMM-S2859-11.66-mRNA-3*		non-synonymous
ChrX	1.4E+07	A	T	*PPA39997*	*UMM-S398-3.15-mRNA-1*		non-synonymous
ChrX	1.4E+07	G	A	*PPA40003*	*UMM-S398-3.10-mRNA-1*		non-synonymous
ChrX	1.4E+07	G	A	*PPA40012*	*UMM-S398-4.109-mRNA-1*		non-synonymous
ChrX	1.4E+07	A	C	*PPA40020*	*UMM-S398-4.137-mRNA-1*	*gcy-36*	non-synonymous
ChrX	1.4E+07	A	G	*PPA42287*	*UMM-S2845-2.23-mRNA-1*		non-synonymous
ChrX	1.4E+07	A	T	*PPA42287*	*UMM-S2845-2.23-mRNA-1*		non-synonymous
ChrX	1.6E+07	A	G	*PPA42394*	*UMM-S2845-19.65-mRNA-1*		non-synonymous